Diffusive Gradients in Thin Films for Inorganic Arsenic Speciation and Electrothermal Atomic Absorption Spectrometry with a Coupled Microcolumn for Trace Metal Speciation

A thesis submitted in partial fulfillment of the requirements for the degree of

Doctor of Philosophy in Chemistry

at the

University of Canterbury

Christchurch

New Zealand

Jared G. Panther

August 2007

Abstract

This thesis is directed towards the development of the diffusive gradients in thin films (DGT) technique for the measurement of total dissolved As, and for As speciation measurements. In addition, a preliminary investigation of a novel laboratory-based method for measuring labile metal species was carried out; this method involved the coupling of a microcolumn of adsorbent with a standard electrothermal atomic absorption spectrometer.

An iron-oxide adsorbent was utilized for As measurements by DGT. The diffusion coefficients of inorganic As^{V} and As^{III} were measured through the polyacrylamide diffusive gel using both a diffusion cell and DGT devices. A variety of factors that may affect the measurement of total As by DGT were investigated. These factors, which included pH, anions, cations, fulvic acid, Fe^{III}-fulvic acid complexes, and colloidal Fe, may affect the adsorption of the As species to the iron-oxide, or may affect the diffusion coefficients of the individual As species.

The DGT method was further developed to selectively accumulate the As^{III} species in the presence of As^{V}. This was achieved by the placement of a negatively charged Nafion membrane at the front of the DGT device which slowed the diffusion of the negatively charged As^{V} species ($H_2AsO_4^-$) considerably, relative to the uncharged As^{III} species (H_3AsO_3). The effect that pH, anions, and cations may have on the selective accumulation of As^{III}, in the presence of As^{V}, was investigated. DGT devices without a Nafion membrane and with a Nafion membrane were deployed in natural waters to determine the total inorganic As and As^{III} concentrations, and to evaluate its performance.

A preliminary investigation of the coupling of a microcolumn of Chelex-100 resin with a standard electrothermal atomic absorption spectrometer was undertaken to establish its value as a laboratory-based speciation method. This involved the examination of various microcolumn materials to accommodate the Chelex-100 resin, and finding an appropriate buffer that could be used to buffer the Chelex-100 resin without interfering with the ETAAS measurement. Furthermore, factors that may affect the uptake of metal by the Chelex-100 resin, such as concentration of buffer in solution, ionic strength, and conditioning of the Chelex-100 resin, were investigated.

Acknowledgements

First, I would like to thank my supervisors, Alison Downard and Kip Powell, for their support, encouragement, and guidance during the course of this research. I greatly appreciate Alison and Kip's dedication to this project, and I am very grateful for the many hours they both spent reading this thesis. I also appreciate the time spent in this department with Dr Hao Zhang, who showed me the finer points of the DGT technique; this was very much appreciated.

I would like to thank the past and present members of the Downard research group for their friendship and support during the course of this research, and who have made my PhD experience an enjoyable one.

I would like to thank the technical staff of the chemistry department, who without their expertise much of this research would not have been possible. A special thanks goes to Sandy Ferguson, for keeping the very temperamental ETAAS behaving; Russell Gillard, for helping out with designing and making various components required for this research; and both Bruce Reid and Wayne MacKay, for always being available when issues relating to the clean room arose.

Financial assistance in the form of a Tertiary Education Commission Top Achiever Doctoral Scholarship and a Canterbury Scholarship, is gratefully acknowledged.

Lastly I would like to thank all my family and friends who have been very patient and understanding during my time at University, especially to Mum and Dad, who without their love, care, and financial assistance, it would not have been possible to complete this thesis.

Contents

Chapter 1: Introduction

Chapter 2: Experimental

Chapter 3: Investigation and optimization of hydride generation atomic absorption spectrometry for As determination

Chapter 4: Measurement of As^{V} and As^{III} diffusion coefficients through diffusive gels and membrane filters

Chapter 9 Conclusions and future work

Chapter 1

Introduction

1.1 Speciation

Speciation refers to the distribution of defined chemical species of an element in a system,[1] where a chemical species is a specific form of a chemical element.[1] The individual chemical forms in an environmental system may include simple inorganic species, organic complexes, and the element adsorbed to colloidal particles and/or particulate matter.[2] It is well established that a measure of the total element concentration is inadequate to predict the impact and behaviour that a metal or semi-metal has in biological or geochemical processes.[1, 2] The reactivity of an element is often related to the concentration of a single chemical species.[1, 2] For example, different chemical species can have varying toxicity effects, therefore analysis of a water sample for total element concentration is not sufficient to predict toxicity.[1, 2]

In many cases, the free metal is most toxic as this readily adsorbs on the surface of cell membranes.[2] Metal that is in labile complexes can also be bioavailable if dissociation occurs in the vicinity of the bio-membrane. In natural systems, only a small proportion of the total metal is generally present as the free ion, because metal ions form complexes with many organic and inorganic ligands. If these complexes are inert they will not contribute to the fraction of metal that is toxic.[1-3] Furthermore, lipid-soluble metal complexes can be very toxic as they can diffuse rapidly through a bio-membrane and transport metal species into the cell.[2] Similarly for some elements such as As and Cr, the toxicity depends on the particular form of the element (e.g. oxidation state). The inorganic As^{III} species is ~ 60 times more toxic than the inorganic As^{V} species, and these As species are ~ 100 to 400 times more toxic than organic forms of As.[3-5] For Cr, the Cr^{III} species is essential to animal life as it takes part in glucose metabolism, however Cr^{VI} is highly toxic and carcinogenic.[1]

It is clear that to predict the impact and behaviour that an element has in the environment, analytical methods must be used that provide information on individual species or fractions, without significantly disturbing the natural distribution of chemical species.

1.1.1 Speciation measurements

A variety of methods and techniques have been used to measure or isolate individual chemical species or operationally defined elemental fractions in environmental samples. These include, but are not limited to, the use of ion-selective electrodes (ISEs), anodic stripping voltammetry (ASV), cathodic stripping voltammetry (CSV), gel-integrated microelectrodes (GIMEs), use of chelating resins (in flow and batch systems), permeation liquid membranes (PLM), liquid chromatography (LC), gas chromatography (GC), capillary electrophoresis (CE), diffusive equilibrium in thin films (DET), and diffusive gradients in thin films (DGT).[1, 2, 6, 7]

Methods such as DGT, ASV, PLM, GIME, and the use of microcolumns containing adsorbents in flow manifolds, are all kinetic-based speciation techniques. In kinetic methods the important concept is complex lability: the concentration of kinetically labile metal in a sample is determined. These kinetic-based speciation methods involve different timescales and mechanisms for differentiating between labile and inert complexes. The discriminatory criterion between labile and inert species is the characteristic time-scale of the measurement in which the metal complex is permitted to dissociate. For DGT and flow systems utilizing adsorbents, the time-scale is between 5 and 10 min and 1 and 2 s, respectively; for ASV it is ~ 0.1 s.[7] These time-scales can be varied by changing appropriate parameters with each technique.

1.1.2 Sampling and storage in speciation studies

In many situations a sample is required to be collected on-site, stored, and then transported to the laboratory for analysis. It is the sampling and storage steps that are generally the most important for obtaining reliable speciation measurements. Failure to carry out these steps appropriately may result in analysis of non-representative samples due to chemical or physical changes, or adsorptive losses of particular species; contamination may also be a factor. These problems may result in speciation data that is unreliable. Therefore it is

necessary that sampling procedures are performed with an understanding of possible sources of contamination, analyte losses, and species transformation.

1.1.2.1 Sources of contamination

Contamination can arise during the collection of a sample. If sampling is being carried out from a boat, contamination from the boat itself can occur.[8] Discharges from an outboard motor or antifouling paints are possible sources of contamination, and airborne pollutants from the boat may also be a problem.[8] Sampling containers may be a source of contamination. Containers or bottles may include metal impurities which originate from the production process of the sampling vessel (e.g. use of catalyst, stabilizers, and dyes) and can be released during sample storage.[8-10] Containers may also include traces of metal from previous sample collection.[11] These contaminants can generally be removed by carefully acid-washing of the container or bottle prior to sample collection,[8] however the acid may damage the interior surface of the sampling vessel and increase its adsorptive capacity for metal ions.[8, 9] Furthermore, the acid-washing process might introduce contamination, either as a dissolved contaminant in the acid, or during any drying process.[9] In addition, the cap of bottles and containers may include rubber or metal inserts giving a further potential source of contamination.[9, 11] Contamination from filters and other analytical apparatus must also be considered.[8, 9, 12]

1.1.2.2 Potential changes in sample composition during storage

Species stability during storage is critical in obtaining reliable speciation data, as environmental samples are not usually analyzed immediately after sampling. The distribution of chemical species may change due to a variety of factors; which include: adsorption of species to container walls or suspended solids, microbial activity, coagulation of colloidal material, changes in temperature or pH, exposure to light, absorption of air components, and chemical reactions such as oxidation, reduction, volatilization, and precipitation.[11-14]

Glass containers exhibit ion-exchange properties and are generally not used to collect or store samples.[1, 8] Polymeric materials such as Teflon, polyethylene, polypropylene, and polycarbonate are more commonly used.[8, 15] Teflon and polyethylene show the lowest adsorptive losses.[8, 15]

Microbial activity during sample storage may significantly change the composition of the sample.[11, 12] The pH may decrease due to continual respiration of microorganisms, or increase due to photosynthesis; the concentrations of species may also vary as a result of direct uptake or release by microbes.[8, 12, 14] The change in pH can affect both the complexation and adsorptive behaviour of metals, rate of redox reactions, and may also cause metal precipitation.[8, 11] Methylation of particular species can also occur due to biological activity.[13] Addition of HNO_3 (and other preservation reagents) to samples can prevent adsorption of species to container walls and can inhibit growth and biological activity of microorganisms.[8, 11, 14] However this practice is not recommended for speciation studies as it may change the physical or chemical forms of the element. In addition, acidification may interfere with the analytical technique.[11]

The problems described above can be minimized by adopting appropriate handling and storage procedures without the need of adding preservatives. A suitable container should be chosen to avoid undesirable adsorption of chemical species to the walls. During transport, samples should not be exposed to light, and refrigeration is desirable.[11] Once returned to the laboratory, samples should be refrigerated at 4 ^{o}C and stored in the dark; this reduces the rate of chemical and biological processes.[6, 11] Filtration through a 0.45 μm pore size membrane filter is recommended to remove some bacteria and colloidal material.[6, 8] However, filtration can introduce additional problems. The effective pore size of the filter can change as it is becomes loaded with particles, and adsorption of species to the filtration apparatus or filter membrane itself can occur.[6] Furthermore, rupture of algal cells may be a problem if high pressures or vacuum are used for filtration; this can lead to changes in metal concentrations and an increase in dissolved organic matter in the filtrate.[6, 8] Lastly, it is essential that analyses of samples are carried out as soon as possible to limit the effects described above.

An alternative to using rigorous sampling and sample storage protocols is to use in-situ techniques to measure or fractionate chemical species.[6, 12] This relieves the problem of how to maintain the sample in its original state without disturbing the distribution of chemical species. In-situ methods include: electrochemical and optical sensors, dialysis, PLM, DET and DGT.[12]

1.2 Diffusive gradients in thin films (DGT)

The DGT technique is an in-situ analytical method that is designed to accumulate labile species in environmental systems.[12, 16-19] In a typical experiment, DGT devices are deployed in an environmental system (e.g. a river) for a time period ranging from days to months. The accumulation of chemical species occurs in-situ, however the species are not measured until the fractionated sample is returned to the laboratory for analysis by a suitable analytical technique. Since the first publication describing the use of DGT, by Davison and Zhang[16] in 1994, it has been applied to the accumulation of a variety of metals and semi-metals in waters, soils, and sediments, both under controlled laboratory conditions, and in field studies.[12, 16-33]

1.2.1 DGT theory

The DGT technique uses an adsorbent, usually immobilized in a polyacrylamide hydrogel (collectively called the binding gel), to adsorb analyte species from solution. The binding gel is separated from the bulk solution by a permeable gel (i.e. diffusive gel) that is well defined in terms of its thickness (Δg) and porosity (see Figure 1.1). Between the diffusive gel and the bulk solution is a diffusive boundary layer (DBL) of thickness δ. The transport of species from the bulk solution to the binding gel is by molecular diffusion through the diffusive gel and the DBL. The diffusive gel generally controls the overall rate of mass transport to the binding gel irrespective of the hydrodynamics of the bulk solution. Rapid and irreversible binding of analyte to the adsorbent ensures that a concentration gradient is quickly established between the bulk solution and the binding gel.

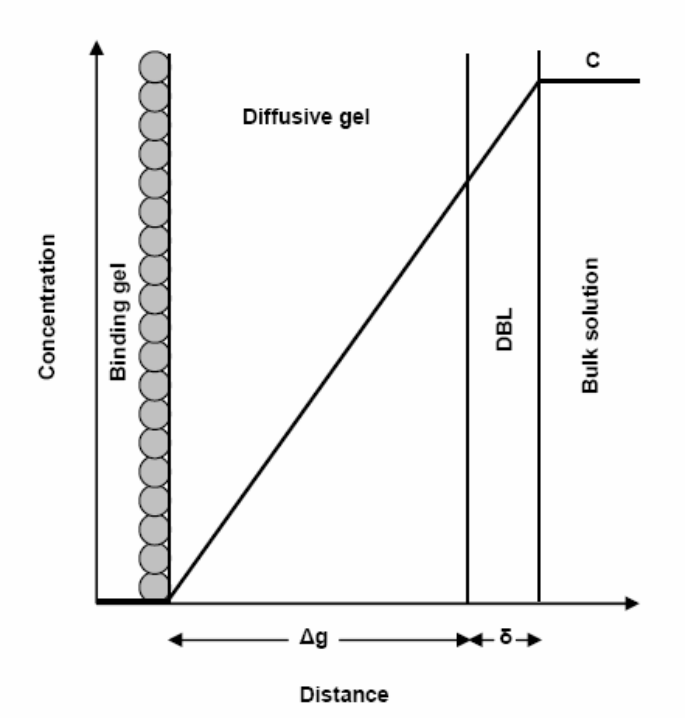

Figure 1.1 Schematic representation of the concentration gradient of a species through a DGT assembly as represented by the bold line (*C* is concentration; *Δg* and *δ* are the thicknesses of the diffusive gel and DBL, respectively). Figure adapted from Zhang *et al*.[25]

The DGT technique is based on Fick's first law of diffusion.[18] The flux, *F*, of a species to the binding gel is given by equation 1.1, where *D* is the species diffusion coefficient through the diffusive gel, *C* is the species concentration in the bulk solution, *C'* is the species concentration at the interface between the binding gel and diffusive gel, and *Δg* and *δ* are the thicknesses of the diffusive gel and DBL, respectively.

$$F = \frac{D(C - C')}{\Delta g + \delta} \qquad \textbf{(1.1)}$$

If the analyte binds rapidly to the adsorbent, *C'* is effectively zero (provided the adsorbent is not saturated), and assuming *δ* is negligibly small compared to *Δg* (which is generally assumed for well-mixed solutions), then equation 1.1 simplifies to equation 1.2.

$$F = \frac{DC}{\Delta g} \qquad \textbf{(1.2)}$$

The flux can also be determined from the mass, M, diffused through an area, A, after a given time, t (equation 1.3).

$$F = \frac{M}{At} \qquad \textbf{(1.3)}$$

Combining equations 1.2 and 1.3, and rearranging, gives equation 1.4. This equation is known as the DGT equation and is used to calculate the concentration of analyte in the bulk solution from the known values of Δg, D, A, the deployment time, t, and the mass of analyte accumulated on the binding gel, M.

$$C = \frac{M\Delta g}{DtA} \qquad \textbf{(1.4)}$$

At the completion of a DGT deployment, the binding gel and the diffusive gel are separated and the accumulated analyte is eluted from the binding gel. For metal ions this is usually achieved by using 1 to 2 mol L^{-1} HNO_3.[16, 18, 34] The concentration, C_e, of analyte in the eluent is then determined by an appropriate analytical technique. The accumulated mass, M, of analyte on the binding gel can then be calculated using equation 1.5, where V_e and V_g are the volumes of the eluent and binding gel, respectively, and E_f is the elution efficiency. The elution efficiency is important to consider as in some instances only a fraction of the analyte is removed from the binding gel (see sections 4.1.2.3 and 4.4.1 for a discussion about elution efficiencies).

$$M = \frac{C_e(V_e - V_g)}{E_f} \qquad \textbf{(1.5)}$$

A variety of adsorbents have been used with the DGT technique to bind the analyte of interest from solutions; for a brief discussion concerning the adsorbents that have been used in DGT, and the analytes that have been measured, see section 4.1.1. The polyacrylamide diffusive gels used in DGT are ~ 95 % water and generally have a 2 to 5 nm pore size.[16, 18] However by varying the amounts of reagent used to prepare the diffusive gels, pore sizes in the range of 1 to 20 nm can be prepared.[19] The diffusion coefficients of metal ions through the diffusive gel

are normally between 85 to 100 % of the diffusion coefficients in water;[18, 34-36] these values depend on the composition of the diffusive gel. The diffusion coefficients of hydrated metal ions through the diffusive gel are commonly in the range 4.5 to 8.0 x 10^{-6} cm^2 s^{-1} at 25 ^oC.[35, 37] However the diffusion coefficients of larger species such as metal-humate and metal-fulvate complexes are within the range 0.6 to 2.2 x 10^{-6} cm^2 s^{-1}.[35, 38, 39] For a discussion on the measurement of diffusion coefficients see section 4.1.2.

The diffusion coefficients of species in the diffusive gel are dependent on temperature due to changes in water viscosity.[18] The correction of diffusion coefficient values for temperatures other than 25 ºC can be carried out using equation 1.6,[18] where T is temperature (in ºC) and D_{25} and D_T are the diffusion coefficients at 25 ^oC and at any given temperature, respectively.

$$\log D_T = \frac{1.37023(T-25)+8.36\times10^{-4}(T-25)^2}{109+T} + \log\frac{D_{25}(273+T)}{298} \qquad \textbf{(1.6)}$$

The correction of diffusion coefficients for temperature is especially important for field applications as the temperature in the field can be significantly different to that in the laboratory under controlled conditions and may also vary during deployment.[17, 40, 41]

1.2.2 DGT assembly

For deployment in waters, the binding and diffusive gels are accommodated within a DGT device which is based on a simple piston design consisting of a backing cylinder and a front cap (Figure 1.2). The binding and diffusive gels are placed sequentially on top of the backing cylinder and a membrane filter is usually placed on top of the diffusive gel to protect it and prevent the adhesion of particles.[16] The membrane filter is generally treated as an extension of the diffusive layer.[16, 25, 35, 42] The front cap, which has an opening that allows species to diffuse from the bulk solution to the binding gel, is pushed down tightly onto the backing cylinder to hold the three layers firmly in place.

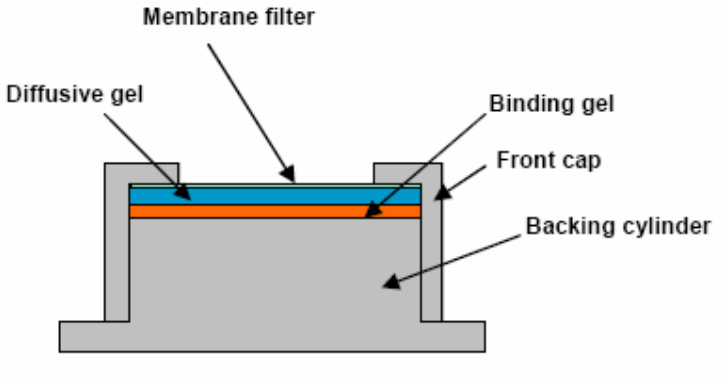

Figure 1.2 Schematic representation of a DGT device showing the placement of the binding gel, diffusive gel, and the membrane filter. Figure adapted from Zhang and Davison.[18]

1.2.3 Diffusive boundary layer

The DBL is a stationary region in the bulk solution that forms adjacent to the filter membrane surface of the DGT assembly. The transport of species through this layer is by diffusion, and not convection, hence it acts as an extension of the diffusive layer. The thickness of the DBL depends on the flow velocity in solution and the geometry of the DGT device.[34] When using DGT, the thickness of the DBL is generally considered to be negligible for well-mixed solutions in the laboratory, and fast flowing rivers, streams, and well-mixed seas and lakes.[12, 18, 35] However, in poorly-mixed waters, or when using a thin diffusive gel, it cannot be assumed that the DBL thickness is negligibly small relative to the diffusive gel thickness. Failure to account for a significant DBL thickness would result in an underestimation of the calculated concentration when using the DGT equation, (equation 1.4) and hence this would be a source of significant error. The magnitude of this error depends on both the thicknesses of the DBL and the diffusive gel.

When a significant DBL is present the measured mass, M, of analyte accumulated by DGT, is given by equation 1.7 which incorporates the DBL thickness, δ.[18] If δ is significant compared to Δg, a plot of M *vs*. $1/\Delta g$ will be non linear.[18] Therefore, the thickness of the DBL needs to be measured by deploying DGT devices with various diffusive gel thicknesses and plotting $1/M$ *vs*. Δg according to equation 1.8. This plot should be linear with a slope of $1/DCtA$ and an intercept of $\delta/DCtA$. Hence the DBL thickness can be estimated from the intercept and the concentration of the analyte is calculated from the slope. If the flow of solution varies during the experimental deployment, then δ will be an average value.

$$M = \frac{DCtA}{\Delta g + \delta} \qquad \textbf{(1.7)}$$

$$\frac{1}{M} = \frac{\Delta g}{DCtA} + \frac{\delta}{DCtA} \qquad \textbf{(1.8)}$$

Zhang and Davison[18] examined the effect of the DBL on DGT measurements using Zn^{2+}. They varied the stirring rate from 0 to 1000 rpm and found that above a stirring rate of 400 rpm there was good agreement between Zn^{2+} concentrations measured by DGT and ASV. This indicates that the thickness of the DBL is insignificant relative to the thickness of the diffusive gel at these high stirring rates. The concentration of Zn^{2+} measured by DGT in the absence of stirring was only 50 % of that measured by ASV, indicating a significant DBL thickness. Similar results were obtained by Gimple *et al.*[43] who found that above a flow rate of 0.02 m s^{-1} there was no significant difference in the Cd^{2+} concentration measured by DGT and ASV, and that at a flow rate of 0 m s^{-1} the Cd concentration measured by DGT was ~ 50 % of that measured by ASV.

The thickness of the DBL has been measured in the laboratory and in natural waters using equation 1.8. Scally *et al.*[44] measured a DBL thickness of 0.24 ± 0.02 mm which was in good agreement with the value of 0.23 ± 0.03 mm measured by Warnken *et al.*[34] Warnken *et al.*[34] found that the DBL thickness did not vary at stirring rates above 100 rpm. Zhang *et al.*[25] estimated the DBL thickness in a still pond obtaining a value of 0.39 mm, whereas Alfaro-De la Torre *et al.*[45] also used this method and measured a DBL thickness of 0.31 ± 0.22 mm in a lake when DGT devices were deployed. Warnken *et al.*[34] report a DBL thickness of 0.26 ± 0.02 mm for a river and Zhang and Davison[19] measured a DBL thickness of 0.4 mm in a reasonably fast flowing stream. It is surprising that the DBL for a still pond and a fast flowing stream are similar; other factors may be contributing to the DBL measurement such as biofouling of DGT devices.

Recent laboratory results from Warnken *et al.*[34] suggest that even in well-stirred solutions the assumption that the DBL is negligibly small, and therefore can be ignored when using the DGT equation to calculate the analyte concentration, may not be valid. Warnken *et al.*[34] deployed DGT devices with different diffusive gel layer thicknesses (0.14 to 1.20 mm) in a well-stirred Cd^{2+} solution (stirring rate was 800 rpm). When ignoring the DBL, the ratio of

metal in solution measured by DGT to that measured by inductively coupled mass spectrometry (ICP-MS) (C_{DGT}/C_{Soln}) was 0.91 ± 0.23. This value was an average value for all gel thickness; for the DGT device that contained a 0.8 mm diffusive gel (most commonly used in DGT) the C_{DGT}/C_{Soln} value was ~ 1. However, for these DGT deployments the DBL thickness was 0.18 ± 0.03 mm; when this DBL thickness is taken into account, a C_{DGT}/C_{Soln} ratio of 1.21 ± 0.03 was obtained. Warnken *et al.*[34] showed that this difference could be accounted for if the 'effective' diffusion area of the DGT device is used instead of the geometrical area when calculating the concentration using the DGT equation.

The geometrical area is based on the opening in the cap of the DGT device (typically 3.14 cm^2), whereas the effective area is that available for metal uptake and is larger than the geometrical area due to lateral diffusion within the diffusive gel. When the effective area (typically 3.80 cm^2) is used to calculate the concentration measured by DGT, instead of the geometric area (3.14 cm^2) the C_{DGT}/C_{Soln} ratio was 1.00 ± 0.023. Warnken *et al.*[34] reason that the good agreement between C_{DGT} and C_{Soln} found by other workers, when the DBL thickness is not taken into account, is due to the effects of the significant DBL and effective diffusion area cancelling one another.

1.2.4 Speciation measurements using DGT

The DGT technique measures the free metal ion and metal in labile complexes that can diffuse through the pores of the diffusive gel, and dissociate while travelling through this layer.[16, 18, 19] The analyte must then form a stable complex with the adsorbent in the binding layer.[16] Hence, the measurement of species by the DGT technique is governed by the adsorbent, the diffusive layer thickness, and the pore size of the gel.[12]

The contribution of metal from complex dissociation will depend on the thickness of the diffusive gel as this determines the time-scale in which dissociation of the metal-complex can occur.[18, 19, 44] When the complex dissociates, the concentration gradient towards the adsorbent ensures that the free metal ion diffuses towards the binding layer and hence diminishes reformation of the complex. The residence time of a species in the diffusive layer can be approximated by equation 1.9.[19, 35, 44]

$$t = \frac{\Delta g^2}{2D} \qquad \textbf{(1.9)}$$

For a simple metal ion, the residence time in a 0.8 mm diffusive layer is ~ 6 min; for a metal-fulvate complex this time would be considerably larger (~ 15 min). Metal bound to large colloids and particulate material are excluded from the diffusive layer due to the pore size of the gel.

1.2.4.1 DGT for determining the concentrations of labile inorganic and organically bound metal

For many applications of DGT to natural waters the diffusion coefficient of the free metal ion has been used to calculate the concentration of metal.[20, 22, 41, 46] Whilst this method will yield reliable results when complexation of the metal by humic substances is relatively minor, the use of the free ion diffusion coefficient would lead to an underestimation of metal ion concentration if a significant amount of the metal is complexed. This is because humic substances have diffusion coefficients substantially less than those of the free metal. Therefore when DGT with an open-pore gel is used to measure metal concentrations in natural water, the contribution of metal from humic substances is unknown and only an 'effective' DGT-labile concentration is measured. However, as indicated by Zhang and Davison,[19] this measurement may still be appropriate for accessing bioavailable metal in solution.[19]

The problem of the unknown contribution of humic-bound metal to DGT measurements has been overcome by using a diffusive gel with a reduced pore size (known as a restricted gel) that appreciably slows the diffusion of humic substances compared to the open-pore gel, but has only a relatively minor effect on the diffusion coefficient of the free metal.[12, 17, 19] For example, the diffusion coefficient of Cu^{2+} in the open pore gel (of composition usually used in DGT) and restricted gel at 20 ^{o}C are (6.28 ± 0.13) x 10^{-6} cm^2 s^{-1} and (4.50 ± 0.12) x 10^{-6} cm^2 s^{-1}, respectively, whereas the diffusion coefficients of fulvic acids in the open-pore gel and restricted gel are (1.15 ± 0.04) 10^{-6} cm^2 s^{-1} and (0.37 ± 0.02) 10^{-6} cm^2 s^{-1}, respectively.[17] Zhang and Davison[19] and Zhang[17] have used these findings to separately measure labile organic and labile inorganic species in both synthetic solutions and natural waters using DGT devices containing diffusive gels of three different pore sizes. In this approach, the mass of

metal accumulated by each DGT device (M_{DGT}) is assumed to be a combination of metal from labile inorganic and labile organic complexes. The mass is given by equation 1.10 (if the diffusive gel thickness, diffusion area, and deployment time are the same for all DGT devices) where D_{inorg} and D_{org} are the diffusion coefficients of the inorganic and organic species (through the particular gel), respectively, and C_{inorg} and C_{org} are the concentrations of the labile inorganic and labile organic species, respectively.

$$M_{DGT} = \frac{(D_{inorg}C_{inorg} + D_{org}C_{org})At}{\Delta g} \qquad \textbf{(1.10)}$$

Rearranging equation 1.10 gives equation 1.11, where K is equal to $At/\Delta g$.

$$\frac{M_{DGT}}{KD_{inorg}} = C_{inorg} + \frac{D_{org}C_{org}}{D_{inorg}} \qquad \textbf{(1.11)}$$

Plotting M_{DGT}/KD_{org} versus D_{org}/D_{inorg} gives a straight line with an intercept corresponding to the concentration of labile inorganic species and the slope giving the concentration of labile organic species. This method of calculating the concentration of labile organic and inorganic species assumes that all simple inorganic species have the same diffusion coefficient as the free metal ion in the gel, and that organic complexes can be represented by an average diffusion coefficient in the gel; furthermore, it assumes that labile-metal organic complexes are large molecules (hence the diffusion coefficient of fulvic or humic acid applies) and that small, labile metal-organic complexes have insignificant concentrations compared to the concentration of total inorganic species.[17]

Alternatively in its simplest form, two DGT devices containing diffusive gels of different pore size can be used and equations 1.12 and 1.13 can be solved simultaneously to give C_{org} and C_{inorg}.[12, 19] The values, ${}^{o}M$ and ${}^{r}M$, are the mass of metal accumulated by the DGT devices with open-pore and restricted gels, respectively, and ${}^{o}D$ and ${}^{r}D$ are the diffusion coefficients of species in the open-pore and restricted gels, respectively.

$$ {}^{o}M = \frac{({}^{o}D_{inorg}C_{inorg} + {}^{o}D_{org}C_{org})At}{\Delta g} \qquad \textbf{(1.12)} $$

$$ {}^{r}M = \frac{({}^{r}D_{inorg}C_{inorg} + {}^{r}D_{org}C_{org})At}{\Delta g} \qquad \textbf{(1.13)} $$

The restricted gel DGT device can also be used alone to estimate the concentration of inorganic species by assuming that all of the metal accumulated is derived from inorganic complexes.[17, 19] This gives satisfactory results when complexation of metal by humic substances is moderate at most, but significant errors arise if metal-organic complexes dominate.[19]

1.2.4.2 Effect of adsorbent binding strength

The binding strength of the adsorbent has been shown to influence the fraction of metal measured by the DGT technique.[27, 47] Docekalova and Divis[27] used DGT (some devices contained Chelex-100 and some contained Spheron-Thiol as the adsorbent) to measure Hg concentrations in synthetic solutions and a stream (in-situ). For simple synthetic solutions good agreement was obtained for the calculated Hg concentrations when using the Chelex-100 and Spheron-Thiol adsorbents. However, when DGT was applied to a natural water, the Hg concentration calculated from the mass accumulated in the Spheron-Thiol DGT device was ~ 2.75 times higher than the Hg concentration calculated from the mass accumulated in the Chelex-100 device. Docekalova and Divis[27] explain this difference by the higher affinity of thiol groups than iminodiacetate for Hg. This affinity effect results in the Spheron-Thiol adsorbent 'inducing' dissociation of Hg from its natural complexes. Hence a larger fraction of total Hg is measured with the Spheron-Thiol adsorbent.

Li *et al*.[47] used DGT devices that contained different adsorbents to assess if the binding strength of the adsorbent affects the concentration of Cd and Cu measured by DGT. They used adsorbents that had stability constants ranging from 10^2 to 10^9 for Cd and Cu complexation. Li *et al*.[47] found that for simple synthetic solutions containing metal-EDTA or metal-humate complexes, there was no significant difference in the concentration of metal determined by the DGT devices with various adsorbents. However when applied to natural waters, the small difference in concentrations determined by the various DGT devices were

considered to be statistically significant although they did not always correlate with the stability constants of the metal-adsorbent complexes. Li *et al*.[47] reason that DGT devices with various adsorbents measure different fractions of metal in a natural water, but not in synthetic waters because composition of the natural water is more complex than that of synthetic solutions. Natural waters have a variety of ligands with diverse binding strengths and a range of matrix ions.

1.2.4.3 DGT for Cr^{III} and Cr^{VI} speciation

The DGT technique has been used for oxidation state speciation in which a single DGT assembly has been used to measure both Cr^{III} and Cr^{VI} concentrations in synthetic solutions and soils.[48] It is based on the selective binding of cationic Cr^{III} by the Chelex-100 resin. The Cr^{VI} species exists as a negatively charged species and does not bind to the resin. However, the Cr^{VI} in solution equilibrates with the polyacrylamide diffusive gel. Measuring the mass of Cr in the binding gel allows calculation of the Cr^{III} concentration in solution, whereas measuring the mass of Cr that has equilibrated with the diffusive gel allows the concentration of Cr^{VI} to be calculated. However, two problems need to be addressed when using this method for Cr speciation. Firstly, the DGT assembly is required to be kept closed for > 1 h after retrieval; this step allows Cr^{III} in the diffusive gel to diffuse to the binding layer and be adsorbed. Omitting this step would result in overestimation of the Cr^{VI} concentration due to the presence of Cr^{III} in the diffusive gel. The second consideration is that Cr^{VI} equilibrates with the water in the binding gel and hence the Cr^{III} concentration will be overestimated. The overestimation will be most evident when Cr^{VI} is present in large amounts relative to Cr^{III}. It would seem that this problem may be overcome by allowing the Cr^{VI} to diffuse out of the binding gel before elution.

1.2.5 Advantages of DGT

The in-situ capabilities of the DGT technique is one of the major advantages of the method; it provides a means of measuring labile species in natural systems without most of the problems associated with collection and storage of samples. As mentioned above, DGT measures the kinetically labile fraction of a sample and hence can be used for speciation studies. Additionally, multiple elements can be simultaneously accumulated using DGT, and by using two adsorbents in the one DGT device, it is possible to accumulate both cationic and anionic species at the same time.

The DGT technique preconcentrates the analyte of interest and therefore allows the measurement of species at very low concentrations. When deploying a DGT device for 24 h with a 0.8 mm thick diffusive gel and 3.14 cm^2 diffusion area, and assuming a diffusion coefficient of 6 x 10^{-6} cm^2 and an eluent volume of 1 mL, the concentration of analyte in the eluent will be ~ 20 times greater than the concentration in the bulk solution. The preconcentration factor can be improved by increasing the diffusion area, decreasing the thickness of the diffusive gel, increasing the deployment time, or decreasing the volume of eluent. Furthermore, DGT allows the analyte to be separated from complex matrices such as seawater; this is advantageous as it is well known that matrix species can interfere with many analytical measurements.

The DGT measurement is time-integrated, that is, it measures the average concentration over the deployment period. The DGT technique ensures that the contribution of short-term changes in concentration is included in the measurement. In comparison, grab samples provide a measurement of analyte concentration at discrete times; changes in concentration that occur outside of the sampling period may not contribute to the measurement

The measurement of analyte concentrations by the DGT technique can be carried out over a wide pH and ionic strength range. The actual ranges depend on the adsorbent used. The pH range for use of DGT with the most common adsorbent, Chelex-100, is between ~ 5 and ~ 9.[12] At low pH the uptake of metal by the Chelex-100 resin is reduced, and swelling effects of the diffusive gel at pH > 9 may affect DGT measurements.[12] It has been reported by some authors that at low ionic strengths (0.0001 up to 0.001 mol L^{-1} $NaNO_3$) the concentration measured by DGT does not agree with the concentration in the bulk solution.[41, 45, 49, 50] This has been attributed to the diffusive gel having a slight positive or negative charge which in the case of a negative charge, causes the concentration of cationic species at the diffusive gel-filter membrane interface to increase, and hence the flux is enhanced.[50] It has been shown that if the diffusive gels are conditioned and deployed in 0.001 mol L^{-1} $NaNO_3$, good agreement between the concentration measured by DGT and the concentration in the bulk solution is obtained.[50] Furthermore, DGT can be used at lower ionic strengths (0.0001 mol L^{-1}) as long as the diffusion coefficients are adjusted. Warnken *et al.*[50] have shown that the diffusion coefficients of Cd and Cu are ~ 40 % lower in 0.0001 mol L^{-1} $NaNO_3$ than at higher ionic strengths.

In higher ionic strength solutions (e.g. seawater) the diffusion coefficients of species are ~ 10 % lower than that at low ionic strength; this is due to a difference in viscosity of the solution.[12] In addition, adsorbents such as cation-exchange resins can quickly become exhausted at high ionic strength.[42]

1.3 Arsenic speciation and measurement

1.3.1 Arsenic speciation and concentrations in natural waters

The speciation of As in natural waters is controlled by reactions such as reduction, oxidation, methylation, and adsorption; these affect the solubility, transport, bioavailability, and toxicity of As.[51] Arsenic can exist in a variety of formal oxidation states in the environment (V, III, 0, -III), however the most common oxidation states for As species in natural waters are III and V.[52] In general, the most abundant As species are arsenate and arsenite, which are the inorganic As^{V} and As^{III} species, respectively. Methylated As^{III} and As^{V} species, known as organic As, can be produced by biological activity. In most situations the concentrations of organic As species are appreciably lower than the inorganic As species.[52] Figure 1.3 shows the structure of these various As species (in their uncharged states) and the abbreviations used in this thesis.

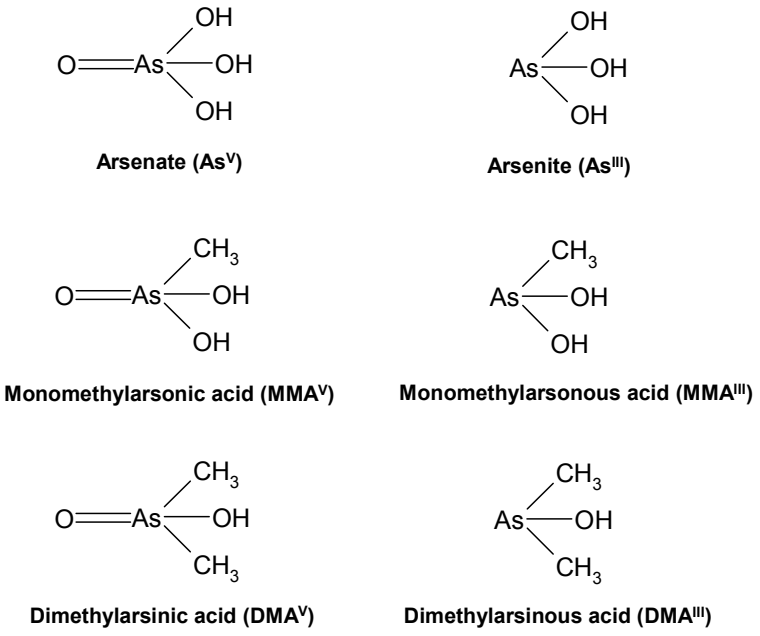

Figure 1.3 Structure of inorganic and organic As species

1.3.1.1 Inorganic As speciation

Redox potential (E_h) and pH are important factors that affect the inorganic speciation of As.[52, 53] Figure 1.4 shows an E_h-pH diagram for aqueous As species. Under oxidizing conditions the As^V species is thermodynamically stable, and under mildly reducing conditions, and/or lower pH, the As^{III} species is favoured. Although not shown in Figure 1.4, dissolved As-sulfide species may be significant in the presence of high concentrations of sulfides (H_2S, S^{2-}), and under reducing conditions at pH < 6, the precipitation of orpiment (As_2S_3) and/or realgar (AsS) can occur.[53, 54]

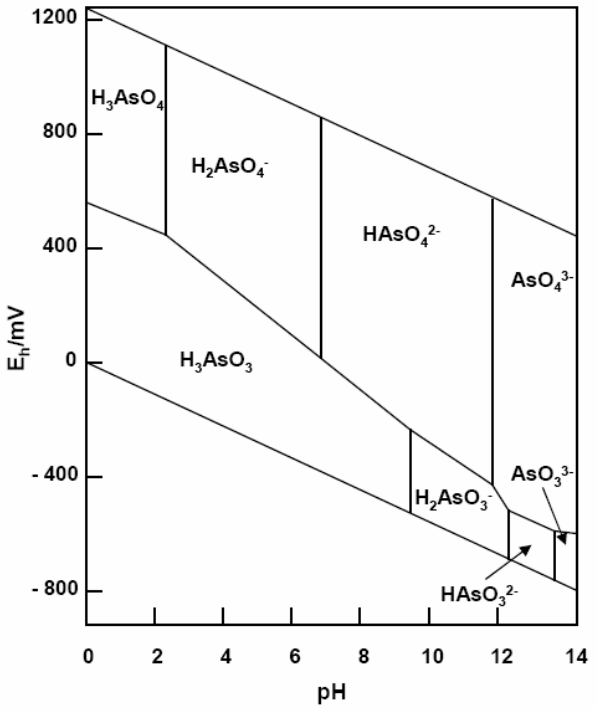

Figure 1.4 E_h-pH diagram for aqueous As species in the system As-O_2-H_2O at 25 ºC. Adapted from Smedley and Kinniburgh.[52]

It is important to note that the species distributions predicted in Figure 1.4 are those that are favoured thermodynamically; however thermodynamically predicted As^V/As^{III} ratios may not be observed in environmental systems. In many oxic and anoxic waters both As species co-exist at appreciable concentration levels.[51, 53, 55] This is because of the slow oxidation of As^{III} by O_2 (half-life ~ 1 year), and the biologically mediated interconversions of As^{III} and As^V.[51, 54, 55] For example, As^V/As^{III} ratios of 10^{15} to 10^{26} are predicted in marine systems, but As^V/As^{III} ratios of 0.1 to 250 are common due to microorganism mediated As conversions.[53]

Microorganisms play an important role in the oxidation and reduction of inorganic As in many environmental systems.[53-55] In lakes and rivers, the inorganic As^{V} species is generally dominant, but, the presence of As^{III} can be maintained in oxic water by biological reduction of As^{V}. Cullen and Reimer[53] note that significant amounts of As^{III} (~ 10 % of total As) have been observed in many uncontaminated surface and seawaters.

Both arsenate and arsenite form oxyanions in aqueous solutions; their degree of protonation depends on their p*K*a values. The p*K*a values for arsenate are 2.20, 6.97, and 11.53; for arsenite the p*K*a values are 9.22, 12.13, and 13.40.[56] The distribution of As^{V} and As^{III} as a function of pH is given in Figure 1.5. Over a wide pH range (4 to 8), the As^{III} species exist mostly as unchanged H_3AsO_3, whereas the As^{V} species exists as negatively charged $H_2AsO_4^-$ and $HAsO_4^{2-}$.

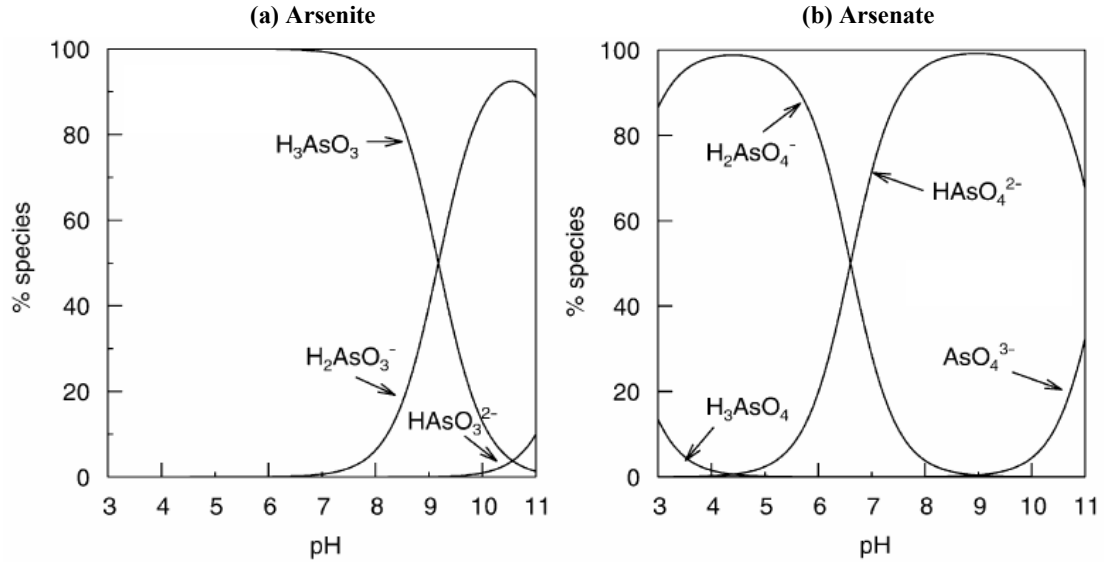

Figure 1.5 Arsenite (a) and arsenate (b) speciation as a function of pH. From Smedley and Kinniburgh.[52]

The As oxidation state plays an important role in toxicity (see section 1.3.2) and mobility. The adsorption of As species to hydroxides of Fe, Al, and Mn, and also clay minerals depends on the oxidation state. In general, the As^{V} species adsorbs strongly to many metal hydroxides and clay minerals, whereas, the As^{III} species is more selective and adsorbs more strongly to iron hydroxides than other adsorbing phases.[54, 57] However, at pH > 8 the adsorption of As^{III} by iron-oxides is greater than that for As^{V} due to electrostatic interactions

between negatively changed As^V species and the negatively charged iron hydroxide surface.[58, 59] Hence, the mobility and solubility of As is a function of its oxidation state, with As^{III} generally considered to be more mobile than As^V.

1.3.1.2 Concentration of As in natural waters

The concentration of As in natural waters varies considerably and depends on the geochemical environment and the extent of anthropogenic inputs.[52, 53, 55] The concentrations of As in unpolluted river and lake water are typically in the range 0.1 to 10.0 μg L^{-1}.[51, 60] However, geothermal influenced waters, or the influx of high-arsenic ground waters, can increase As concentrations considerably, up to 1000 μg L^{-1}.[51-53, 60] Waters affected by mining activity, in which the oxidation of arsenopyrite (FeAsS) can be enhanced thus producing As^V, can also contain similar As levels.[51-53, 60] Concentrations of As in seawater are typically 1.5 μg L^{-1} and are less variable than freshwaters.[53]

Elevated concentrations of As can be found in waters that have been contaminated from the use of As-containing herbicides and insecticides, and the use of chromated copper arsenate as a wood preservative.

The concentrations of methylated As species in natural waters are generally considered to be insignificant. However, elevated concentrations of methylated As species may be found in some surface waters of agricultural areas, in which sodium salts of MMA^V are used as herbicides, and in waters that have high microbial activity.[53, 61]

1.3.2 Toxicity of As^{III} and As^V

The toxicity of As is dependent on its speciation.[60, 62] It is generally accepted that the inorganic As^{III} species shows a higher toxicity than the inorganic As^V species and that these inorganic forms of As are more toxic than the methylated As^V species, DMA^V and MMA^V.[60, 62] It has been shown that H_3AsO_3 is ~ 60 times more toxic than H_3AsO_4 and that these inorganic As species are ~ 100 to 400 times more toxic than DMA^V and MMA^V.[3-5] On the other hand, it has been reported that the methylated As^{III} species, DMA^{III} and MMA^{III}, are at least as toxic as inorganic As species, and that MMA^{III} is up to 26 times more toxic than inorganic As^{III}.[60, 62-64] The methylated As species are metabolites of inorganic As and are proposed to form by a sequential process involving reduction, followed by oxidative

methylation.[62, 63] These reactions are shown in Figure 1.6. There are also essentially non-toxic As species such as arsenobetaine.[4, 63]

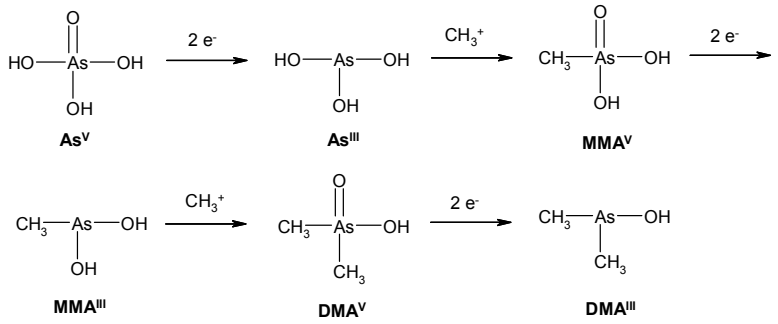

Figure 1.6 Biomethylation of inorganic As involving reduction of As followed by oxidative addition of a methyl group. Adapted from Le *et al*.[63]

1.3.2.1 Mechanism of As^{III} toxicity

The major method of inorganic As^{III} toxicity is by binding to proteins, and inhibiting the action of enzymes and co-factors that are essential for many biochemical proceses.[60, 62] Binding occurs via thiol and hydroxyl groups within these molecules and it is known that As can inhibit more than 200 enzymes in humans.[60] For example, pyruvate dehydrogenase (PDH), an enzyme system which is used in the citric acid cycle, consists of several enzymes and a co-factor containing a dihydrolipoic acid moiety.[60, 62] Inorganic As^{III} inhibits PDH by binding to the dihydrolipoic acid moiety to form an inactivated protein complex, thus preventing the reoxidation of this moiety which is necessary for continual enzymatic activity (Figure 1.7).[60, 62] This transformation can affect production of adenosine-5′-triphosphate (ATP).[62] The MMA^{III} species has been reported to be a more potent inhibitor of PDH and other enzymes, than inorganic As^{III}.[60, 62]

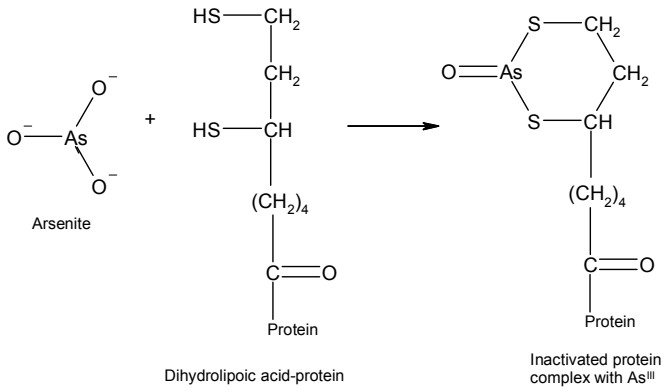

Figure 1.7 Binding of As^{III} to thiol groups of dihydrolipoic acid moiety of a co-factor in the PDH enzyme system. Adapted from Mandal and Suzuki.[60]

1.3.2.2 Mechanism of As^V toxicity

Inorganic As^V does not react directly with enzymes, however it can be reduced in cells to As^{III} and react with enzymes as described above.[60, 62] Due to the similar properties and structure of inorganic As^V and phosphate, inorganic As^V can also have a direct toxicity effect by replacing phosphate in many biochemical processes.[62] For example, As^V can prevent the formation of ATP in the glycolytic pathway.[60, 62] In one step, phosphate is coupled enzymatically with glyceraldehyde-3-phosphate to form 1,3-diphosphoglycerate, however, As^V can replace phosphate in this reaction to form 1-arseno-3-phosphoglycerate which is unstable and becomes hydrolyzed. This reaction prevents the formation of ATP (Figure 1.8).

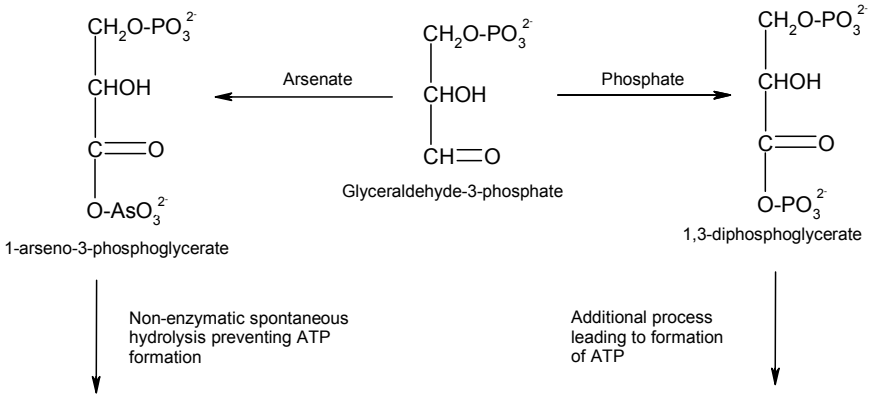

Figure 1.8 Inhibition of glyceraldehyde-3-phosphate by As^V to form 1-arseno-3-phosphoglycerate. Adapted from Mandal and Suzuki.[60]

The As^V species can also react with glucose and gluconate to form glucose-6-arsenate and 6-arsenogluconate, respectively, which resemble glucose-6-phosphate and 6-phosphogluconate, respectively.[62] Arsenate may also replace the phosphate in DNA.[60]

For acute As toxicity, the lethal range of inorganic As has been estimated to be 1 to 3 mg As kg^{-1}.[62] However, chronic As toxicity is more of a concern, especially from exposure to drinking water containing high concentrations of inorganic As. The World Health Organization (WHO) guideline for As in drinking water is 10 µg L^{-1}.[63] Concentrations of As exceeding this level have been reported in many countries.[52, 60, 65] One of the worst instances of As-containing drinking water is in Bangladesh where it is estimated that 35 million people are drinking As-contaminated water with As levels above 50 µg L^{-1}.[65] Some drinking water wells in Bangladesh contain As concentrations close to 5 mg L^{-1}.[65] The source of this As is

proposed to be due to the anoxic reduction of Fe^{III} hydroxides to Fe^{II} in the sediments, leading to the release of adsorbed As into the groundwater.[60]

The human health problems associated with chronic As exposure include effects on the respiratory, cardiovascular, reproductive, renal, and neurological systems;[60, 66, 67] As can also contribute to liver damage, diabetes, and various skin disorders.[66, 67] Chronic exposure to As also increases the risk of various cancers which include those of the skin, bladder, liver, kidney, and lung.[66, 67]

1.3.3 Analytical methods for inorganic As speciation

Numerous methods are available to determine total or a fraction of As species. These include the application of hydride generation, chromatography, capillary electrophoresis, electrochemical techniques such as anodic stripping voltammetry and cathodic stripping voltammetry, use of anion-exchange resins, and photometric methods. These methods are briefly discussed below with an emphasis on inorganic As speciation.

1.3.3.1 Hydride generation

Hydride generation has been extensively used to determine both inorganic and organic As species. This method will only briefly be explained here as chapter 3 is devoted to this technique.

Hydride generation generally involves reaction of an As solution with $NaBH_4$ to produce arsine (AsH_3) which is transported either directly, or after preconcentration, to a detection system. Depending on the reaction conditions, selective hydride generation can be achieved and therefore speciation information obtained. The selective generation of AsH_3 from As^{III}, in the presence of As^{V}, can be achieved by carrying out the hydride generation reaction in citrate buffer ($pH \geq 4.5$),[68, 69] acetate buffer ($pH \geq 5.0$),[70, 71] or low concentrations of acid and/or $NaBH_4$.[72, 73] Total As can be determined either after pre-reduction of As^{V} to As^{III} or using reaction conditions in which both As^{III} and As^{V} are completely reduced to AsH_3, such as the use of high $NaBH_4$ and/or low pH.[72-74] The concentration of As^{V} can be calculated by difference between total As and As^{III}.

Hydride generation is generally a laboratory-based method and therefore samples are required to be collected and returned to the laboratory for analysis, during which time changes in As speciation may occur. Furthermore, this method can suffer from metal ion interferences, and generally the pH of the sample is adjusted before analysis which can affect the distribution of As species.

1.3.3.2 Anodic stripping voltammetry

Anodic stripping voltammetry (ASV) has been used to determine As species in both synthetic and natural waters.[75-81] In ASV, As^{III} and As^{V} are reduced to metallic As and deposited on the electrode surface. Gold-based electrodes have often been used; these can be solid gold electrodes[75, 77, 79] or gold deposited onto another substrate such as carbon or platinum.[76-78, 81] The deposition time can be varied to allow variable amounts of the preconcentration of As; this can be important when determining As at low concentration levels. After the preconcentration step, the deposited As is re-oxidised by applying an anodic potential and the As is stripped from the electrode surface. During this step the current is measured to determine the As concentration.

The use of ASV for As speciation measurement is achieved by depositing As^{III} onto the electrode at a potential at which As^{V} is not considered to be electroactive; the reduction of As^{V} requires a more negative potential (-1.6 to -1.0 V *vs*. Ag/AgCl)[79, 81] than that required for reduction of As^{III} (-0.45 to -0.15 V *vs*. Ag/AgCl).[75-77, 80, 81] This allows the concentration of As^{III} to be measured selectively in the presence of As^{V}. A reducing agent is then often added to the sample to reduce As^{V} to As^{III} and a second measurement is carried out to determine total As.[76, 77] The concentration of As^{V} can be calculated by the difference between total As and As^{III}. Alternatively, an oxidising agent can be added to oxidise As^{III} to As^{V}, and the total As concentration can be determined at the more negative potential required to reduce As^{V}.[81] Also, it can be possible to use conditions in which both As^{V} and As^{III} are reduced simultaneously and the same sensitivity obtained for both species;[79] this allows determination of total As without the need for a prior chemical reduction or oxidation step. The detection limits of ASV for As are generally less than 0.5 ppb;[77-81] however detection limits as low as 0.005 ppb have been reported.[77]

A common problem associated with the use of ASV is interference from metals such as Cu^{II}, Cd^{II} Pb^{II}, Hg^{II}, Fe^{II}, Zn^{II}, and Sb^{III} [75, 77, 79-81] The metal ions may interfere by competing with

As for sites on the electrode surface during the deposition step, and/or formation of a stable intermetallic complex with As.[77, 80, 81] These problems have been minimized by the use of Chelex-100 to remove metal ions prior to measurement, and methods of addition is often used to combat matrix effects on the As measurement.[75-81] A further difficultly in applying ASV to natural waters is the adsorption of organic compounds to the electrode surface which can affect both signal stability and reproducibility.[75, 77, 79, 81] This effect can be minimized by using a Nafion coating on the electrode surface.[80]

Another possible problem with the ASV method is that acid is often added to the sample prior to the As measurement.[75-81] This may change the distribution of As species in the sample and could release As that is adsorbed to colloidal Fe^{III}.

Anodic stripping voltammetry has been used for on-site analysis of As,[80, 81] but not as an in-situ method. Under these conditions, a sample is still required to be collected and associated with this is possible contamination problems. Furthermore, some of the chemical pre-reducing procedures require the sample to be heated; this may not easily be carried out in the field and the robustness of electrochemical methods may be an additional limitation.

1.3.3.3 Cathodic stripping voltammetry

The analysis of As by cathodic stripping voltammetry (CSV) commonly involves the preconcentration of As onto a hanging mercury drop electrode (HMDE) (at ~ -0.4 V *vs*. Ag/AgCl)[82-85] in the presence of Cu^{II} and/or Se^{IV}.[82-85] During the deposition step, As^{III} and Cu^{II}, or Se^{IV}, are reduced to elemental forms and form intermetallic compounds on the electrode surface.[82] The formation of an As-intermetallic species is required as elemental As has low solubility in mercury.[82] After the preconcentration step, the deposited As is stripped from the HMDE by applying a cathodic potential and AsH_3 is formed; during this step the current is measured to determine the As concentration. In a variation of this method a combination of Cu^{II} and Se^{IV} has been used to form a proposed Cu-Se-As compound which increases sensitivity and improves peak shape compared to the use of Cu^{II} alone.[84, 85]

The CSV method for As speciation measurements is similar to the method used in ASV. Firstly the concentration of As^{III} is determined in a sample directly and this is followed by determination of total As after a chemical reduction step to convert As^{V} to As^{III}.[82-85] In many cases the sample is required to be heated to improve reduction efficiency.[83, 84] The detection

limits for As have been reported to be less than 0.5 ppb[83-85] and on-site measurements have been carried out using CSV.[84, 85]

An advantage of CSV over ASV is that the HMDE is a readily renewable electrode and therefore is not affected by "memory effects" that some solid based electrodes can suffer from.[83-85] However, a problem associated with the use of CSV is interference from metals such as Sb^{III}, Bi^{III}, Cd^{II}, Fe^{III}, Sn^{IV} and Zn^{II},[83] and also the adsorption of organic compounds to the HMDE can be an problem.[82, 86] Furthermore, addition of acid to the sample prior to analysis may affect the distribution of As species.

1.3.3.4 Anion exchange resins

Anion exchange resins are commonly employed for determining inorganic As species.[87-97] The methods are based on utilizing the acid dissociation properties of As^{III} and As^{V}. Over a wide pH range (4.0 to 8.0) the As^{III} species exists primarily as unchanged H_3AsO_3; in contrast the As^{V} species exists as negatively charged $H_2AsO_4^-$ and/or $HAsO_4^{2-}$. In general, the As^{III} species passes through the anion-exchange resin, whereas the As^{V} species is retained and preconcentrated. The As^{V} species is then eluted from the resin with acid and the concentration is measured by a suitable technique. The concentration of As^{III} can be determined by the difference between a total As measurement and the concentration of As^{V}. Method detection limits between 0.05 and 4.0 ppb As^{V} have been reported using anion exchange resins.[87, 90, 91, 93-95] The preconcentration factors obtained with the use of anion exchange resins depends on the volume of both the sample and eluent.

Anion exchange resins have been used as both laboratory-based and on-site methods. The resin is generally accommodated within a glass column, but solid-phase cartridges have also been used. In the laboratory, anion exchange resins have been coupled on-line with inductively coupled plasma atomic emission spectrometry (ICP-AES) and ICP-MS.[91, 95] One method used two anion exchange resins in tandem.[91] The sample was passed across the first anion exchange resin removing As^{V} from solution; the effluent solution (containing As^{III}) was then mixed with an oxidising agent to convert As^{III} to As^{V} which was retained on the second anion exchange resin. The anion exchange resins were selectively eluted and a measurement of the As^{V} and As^{III} concentrations was obtained. The advantage of this method is that it allowed As^{III}, after conversion to As^{V}, to be preconcentrated prior to analysis.

The use of anion exchange resins as an on-site speciation method is common;[88, 89, 92-94, 96] this means that problems associated with sample storage are minimized. It has been shown that the results from on-site As measurements can be very different to those measured 24 h later using the same method;[89, 93] this is considered to be due to uncontrolled changes in As speciation. However, even for on-site analysis, a sample needs to be collected, and contamination problems may arise during this step. In many cases the sample is filtered before passing through the anion exchange resin.[87-89] The problems related with filtration have been described earlier.

A further problem associated with the use of anion exchange resins is that anions present in the sample can compete with As^V (which is usually present at relatively low concentrations) for exchange sites on the resin.[87, 88, 90, 97] Anions such as phosphate, sulfate, and chloride have been shown to affect both uptake and the As^V capacity of the anion-exchange resin.[90, 97] This problem may be overcome to a certain extent by increasing the amount of resin or by dilution of the sample; however sample dilution is undesirable as it also decreases the concentration of the analyte. Some anion exchange resins have also been shown to retain up to 25 % of As^{III},[90] and retention of methylated As species (MMA^V and DMA^V) can lead to a further overestimation of the inorganic As^V concentrations.[87, 88, 90, 94]

Another problem sometimes experienced when using anion exchange resins is the precipitation of Fe^{III} within the anion exchange column. The precipitate can adsorb As^V preventing its uptake by the resin.[88, 92] Furthermore it has been proposed that some As bound to Fe^{III} colloids may also be retained or trapped by the resin.[92] These problems have been minimized by adding EDTA, in some cases along with acetic acid, to the sample before passage through the anion exchange resin.[87-89, 92, 96] The EDTA chelates Fe and prevents the formation of Fe^{III} colloids. However, it is possible that the addition of EDTA may affect the distribution of As in a sample by changing the solution pH or having an effect on As that is bound to colloidal Fe. Adjustment of the sample pH before passing it through the anion exchange resin is often carried out to optimize As^V retention;[89, 91] but this step may affect the distribution of As species also.

1.3.3.5 Capillary electrophoresis

Capillary electrophoresis (CE) is a laboratory-based technique that has been used to separate both inorganic and methylated As species.[98-102] The CE technique is based on the migration

of species in solution under the influence of an electric field. It basically consists of two buffer solutions, one of which contains sample, connected via a fused-silica capillary that is 10 to 100 cm long and has an internal diameter of 25 to 100 μm.[103, 104] A voltage is applied across the buffer solutions; cations migrate through the capillary to the cathode and anions migrate to the anode. This migration of ions is known as electrophoretic mobility and depends on the charge of the species and therefore pH.[99, 101, 103, 104] Another important concept in CE is electroosmotic flow. In conventional CE, electroosmotic flow is caused by the formation of an electric double layer of cations at the surface of the inside wall of the silica capillary which is negatively charged above pH ~ 2 due to the silanol groups on the surface.[103, 104] When an electric field is applied, the excess of cations in the double layer ensure net migration of ions to the cathode.[103] A plug-like flow of the entire solution to the cathode occurs; this is known as electroosmotic flow and depends on pH and ionic strength.[103, 104] The electroosmotic flow is sufficiently large to overcome the electrophoretic mobility of anions towards the anode, hence they move slowly towards the cathode.[104] It is the combination of electrophoretic mobility and electroosmotic flow that affect the migration of ions and hence allows species separation. When applied to As speciation, CE utilizes the difference in pK_a values of the As species for separation.

The sensitivity of CE is generally poor when the conventional in-built UV detector is used; this is because the optical pathway is only as wide as the capillary.[101, 103] For As^{III} and As^{V}, detection limits between 100 to 600 ppb and 500 to 2500 ppb have been reported, respectively. These detection limits are too high for the analysis of As in most uncontaminated waters, however coupling CE with a more sensitive detector can lead to appreciably lower detection limits.[100-102] Coupling CE directly with ICP-MS has led to detection limits for various As species in the range 1.0 to 2.0 ppb;[102] coupling CE with hydride generation and then detection by atomic fluorescence spectrometry (AFS) and ICP-MS has led to detection limits in the range 9.0 to 18.0, and 0.03 to 0.04 ppb, respectively.[100, 101] It is important to note that coupling of CE with these instruments is not straight forward.[100-102]

Capillary electrophoresis can suffer interferences from matrix components leading to incomplete separation of some As species.[98-102] Furthermore, the migration time of species in a sample may be different to those in standard solutions, and therefore spiking is often required for peak identification.[101, 102] Interferences by species with the same mobility may

also be problematic.[101] For example, interference from selenite has been observed when determining inorganic As^{III} using UV detection; but the problem can be overcome by using element specific detectors such as ICP-MS and AFS.[101] A further limitation of CE is that buffers and electrolyte may need to be added to the sample, and the pH of the sample may need to be increased or deceased to effect efficient separation of species. These sample changes may affect the As species distribution.

1.3.3.6 Chromatography

In this section, speciation analysis using chromatographic instruments are described. Methods based on simple anion-exchange columns were described in section 1.3.2.4.

The most common form of chromatography used for the separation of As species is ion chromatography which is based on the interaction between charged As species and the functional groups on the stationary phase which is usually an anion or cation exchange column.[64] The As species are separated according to their pK_a values and the retention time is influenced by pH and ionic strength of the mobile phase.[4, 64, 87, 105, 106]

The use of anion exchange columns with various elution strategies have been used to separate As^{III}, As^{V}, DMA^{V}, and MMA^{V},[4, 87, 105, 106] and combining an anion and cation exchange column can allow the separation of As^{V}, As^{III}, DMA^{V}, MMA^{V}, MMA^{III}, DMA^{III}, and arsenobetaine.[4, 64]

A problem associated with ion chromatography is the overlapping of peaks which can occur for some chromatography columns, and the co-elution of other species which may interfere with the detection method.[105] Furthermore, the ionic strength of a sample may affect retention times on the column necessitating dilution of the sample.[64, 105]

Method detection limits for ion chromatography are in the range 0.02 to15 ppb for the various As species when coupled with HG-ICP-MS, ICP-MS and ICP-AES.[64, 87, 105, 106]

1.3.3.7 Spectrophotometric methods

Many of the spectrophotometric methods for As speciation are based on the molybdenum blue strategy in which As^{V} forms a heteropoly acid with molybdate; reduction of the

heteropoly acid leads to a blue coloured complex which can be detected spectrophotometrically. The As^{III} species does not react to form a heteropoly acid, allowing selective determination of the As^{V} species.

Phosphate can interfere with the determination of As^{V} by the molybdenum blue method. Phosphate also forms a heteropoly acid with molybdate which adsorbs over the same wavelength range as the As^{V}-Mo species.[107-109] Interference from phosphate has been minimized by using an anion exchange resin to remove both As^{V} and phosphate.[107] The As^{III} which passes through the resin is then oxidised to As^{V} and determined using the molybdenum blue method. Reducing all of the As in the sample prior to passing through the anion exchange resin allows total As to be determined. An alternative method can be used to determine the As^{V} and As^{III} concentrations in the presence of phosphate.[108, 109] This approach firstly involves selectively reducing As^{V} to As^{III}; this allows the concentration of phosphate to be determined independently of As^{V}. Secondly, As^{III} is oxidised to As^{V} which enables the total concentration of phosphate and inorganic As to be determined. The difference between these two values corresponds to the total concentration of As in solution. Lastly, performing a measurement on the untreated As sample allows the measurement of total phosphate plus As^{V}; the concentration of As^{V} can be calculated by the difference between this value and the phosphate concentration. The concentration of As^{III} is then calculated by difference. A problem with this approach is that if the concentration of phosphate is large relative to As, then the As concentrations are calculated from the difference between two large numbers which can lead to large uncertainties.[107] Furthermore, the addition of reagents for the molybdenum blue methods may change the As species distribution in a sample. Detection limits for these molybdenum blue methods are in the range 1.0 to 8.0 ppb.[107-109]

1.3.4 Preservation strategies and storage of As samples

Many of the techniques described above have been used as laboratory-based methods and require a sample to be collected, stored, and transported before analysis. As stated earlier, a critical requirement for chemical speciation analysis is to maintain the original composition of the sample, however during the time between sampling and analysis, the integrity of the sample may not be maintained as the distribution between As species can be altered. Often there can be large differences in the measured concentration of As species between

immediate determination or fractionation compared to analysis carried out later. The major causes of changes in As speciation during storage have been identified as:

(i) precipitation of Fe^{III}, due to changes in redox potential or pH, to form iron-oxides(hydroxides) which coprecipitate or adsorb As;[88, 96, 110-112]

(ii) microbial activity leading to oxidation or reduction of As;[88, 96, 110, 113, 114]

(iii) photo-oxidation of As^{III} in the presence of Fe^{III}.[88, 96, 110, 113-115]

A variety of strategies have been used to preserve the As speciation in a sample between the time of sampling and the point of analysis. These strategies have varying degrees of success, and conflicting results are often reported by different workers. Preservation methods that have been applied or investigated include: acidification, filtration, refrigeration, freezing, addition of antibiotics, addition of EDTA, and storage in the dark.[88, 110, 112-114] Combinations of these methods are often used.

Addition of acid limits the formation of iron-oxides by increasing Fe^{III} solubility and may also decrease microbial activity.[110-112, 114] The use of EDTA reduces formation of iron-oxides and limits oxidation of As^{III} by complexation with Fe^{III}.[110, 112, 114] Filtration removes colloidal material from solution, including Fe^{III} colloids upon which As can adsorb, and also removes some bacteria and hence decreases microbial activity;[110, 114] the amount of colloidal material and bacteria removed from a sample depends on the pore-size of the filter. Storing samples in the dark can reduce microbial activity and prevents photo-oxidation of As^{III},[110, 114] and refrigeration minimizes microbial activity and slows other chemical reactions.[110] The adsorption of As species to the walls of containers seems to be negligible under normal storage conditions.[13, 116]

1.3.4.1 Photo-oxidation of As^{III}

It has been observed that As^{III} samples containing Fe^{III} can be rapidly oxidised to As^{V} when exposed to light.[88, 96, 114, 115] Based on experimental results, it is proposed that the oxidation of As^{III} is due to the initial presence of $FeOH^{2+}$ and $FeCl^{2+}$ which both absorb UV radiation to produce hydroxyl radicals and dichloro radicals, respectively.[115] These radicals react with As^{III} to produce an intermediate As^{IV} species which then reacts with Fe^{III} to finally produce As^{V}. Oxidation of the As^{IV} intermediate by O_2 can also occur.[115] The overall reaction for As^{III} oxidation in the presence of Fe^{III} is given by equation 1.14.[114]

$$2Fe^{3+} + H_3AsO_3 + H_2O \xrightarrow{h\nu} 2Fe^{2+} + H_3AsO_4 + 2H^+ \qquad \textbf{(1.14)}$$

The As^{III} oxidation mechanism occurs via the hydroxyl radical when the pH is > 2, and by the dichloro radical when the sample is acidified with HCl to pH < 2.[114]

Arsenic samples are generally stored in the dark, and opaque sampling bottles have been used to prevent exposure to light.[88, 96, 110, 112-114] However, it is important to note that oxidation of As^{III} to As^{V} has still been observed in the dark, although at an appreciably lower rate.[114] McClesky *et al.*[114] found that addition of sulfate and/or Fe^{II} to samples containing As^{III} lowered the rate of As^{III} oxidation for samples stored in the light; adding either sulfate or Fe^{II} to As samples stored in the dark, completely prevented the oxidation of As^{III}. Similar behaviour has been observed by Emett and Khoe.[115] It has been proposed that sulfate complexes Fe^{III} to form $FeSO_4^+$ which does not produce a reactive radical species when exposed to light, and that Fe^{II} competes with As^{III} for the hydroxyl or dichloro radical and hence As^{III} oxidation is inhibited.[114, 115] Additionally, Fe^{II} may be capable of reducing the As^{IV} intermediate species back to As^{III}.[115]

1.3.4.2 Preservation of As solutions using acid

A variety of acids have been used alone or in combination with other preservation reagents to investigate the stability of As solutions and samples. These include: HCl,[88, 110, 112-114] HNO_3,[88, 110] H_2SO_4,[88, 96] H_3PO_4,[96] and acetic acid.[96, 111] In general, acids have been successfully used to stabilize simple synthetic As solutions, however their use in more complex solutions and samples has been less successful.

Samanta and Clifford[96] used H_2SO_4 and H_3PO_4 to stabilize a synthetic groundwater sample containing As^{III} and As^{V} for up to 7 days in the absence of Fe; the solutions were stored in the dark at room temperature. In the absence of acid, As^{III} was stable for up to 24 h, but within 72 h, 100 % of As^{III} was oxidised to As^{V}. Similar experiments were carried out in which 3 mg L^{-1} of Fe^{II} was present; they found H_2SO_4 stabilized the inorganic As distribution for up to 28 days, whereas H_3PO_4 was effective for up to 7 days. After this time, oxidation of As^{III} to As^{V} occurred. In the absence of acid, ~ 60 % of As^{III} was oxidised to As^{V} within 24 h, and losses of dissolved As also occurred due to adsorption onto iron-oxides. Samanta and Clifford[96] examined the stabilization of As in synthetic ground water at various pH and E_h values. They

found that under reducing conditions (initially E_h = -100 mV) at pH 6.5 to 8.4, H_2SO_4 and H_3PO_4 could stabilize the As speciation for up to 21 days and 2 days, respectively. However, under oxidising conditions (initially E_h = 200 mV) the use of H_2SO_4 or H_3PO_4 was not able to stabilize the As distribution; significant amounts (~ 25 to 55 %) of As^{III} was oxidised after 24 h.

Bednar *et al.*[88] found that H_2SO_4 could stabilize a simple synthetic solution containing As^{III} and As^{V} for at least 4 days at room temperature when stored in the dark, or exposed to light. They also found that HNO_3 maintained the As speciation when samples were stored in the dark, however if exposed to light, oxidation of As^{III} to As^{V} started to occur after 24 h; they assumed this was due to the redox couple generated by photolytic reduction of nitrate to nitrite. Hydrochloric was an inadequate preservative as As^{III} was oxidised to As^{V} within 24 h. In the absence of acid, As^{V} was reduced to As^{III} which was assumed to be due to microbial activity. For As solutions in the presence of 1 mg L^{-1} Fe^{III}, Bednar *et al.*[88] found that H_2SO_4 preserved the sample for up to 24 h in both dark and light conditions; for storage times > 24 h, oxidation of As^{III} was observed. Nitric acid was an effective preservative when light was excluded, however HCl caused rapid oxidation of As^{V} in both dark and light conditions; the rate of oxidation was faster in the presence of light due to the probable existence of $FeCl^{2+}$ as described earlier. In the absence of acid, the formation of iron-oxide occurred which quickly adsorbed As from solution.

In contrast to the results described above, HCl has been successfully used as a preservative by McClesky *et al.*[114] and Polya *et al.*[110] McClesky *et al.*[114] found that simple synthetic solutions containing both As^{V} and As^{III} could be stabilized with HCl in dark and light conditions for up to 45 days; this result is in direct contrast to that obtained by Bednar *et al.*[88] Furthermore, Polya *et al.*[110] have used HNO_3 and HCl to stabilize a variety of natural water samples for at least 60 days and found no changes in the inorganic distribution of As; these samples were filtered before the addition of acid and stored in the dark at 4 to 6 ºC. However, some samples showed rapid oxidation of As^{III}; this phenomenon was observed for ammonia-rich waters in which microbial populations may have existed. Polya *et al.*[110] have also observed reduction of As^{V} to As^{III} over a 3 month period for natural waters stabilized with HCl; however As-reducing bacteria were known to exist in these waters. They also monitored the As^{III}/As^{V} distribution in 45 diverse ground and surface waters that were filtered, preserved with HCl,

and stored in the dark at 4 ºC. Over a 19 month period the average As^{III} concentration changed by only 0.2 %.

1.3.4.3 Preservation of As solutions using EDTA

Bednar *et al*.[88] investigated the use of EDTA to preserve simple synthetic solutions containing As^{III} and As^{V}. They found that EDTA stabilized the As solution for at least 5 days in both light and dark conditions and that in the presence of 1 mg L^{-1} Fe^{III}, EDTA stabilized the inorganic As distribution for 14 days, again in both dark and light conditions. The use of EDTA was superior to the acid preservatives investigated (H_2SO_4, HNO_3, HCl). Bednar *et al*.[88] used the EDTA preservation method to stabilize groundwater and acid mine drainage samples that had a wide range of matrices. The concentrations of As^{III} and As^{V} measured after fractionation in the field using an anion-exchange resin were compared to the measurement of As^{V} and As^{III} concentrations of EDTA stabilized samples in the laboratory using LC-ICP-MS. Good agreement was obtained between the field fractionation method and the laboratory-based method indicating that the sample had been stabilized by EDTA. This method was able to preserve As samples for up to 3 months.

Samanta and Clifford[96] examined the use of EDTA to preserve As^{V}/As^{III} speciation in synthetic groundwater in the absence of Fe. They found that after 24 h, As^{III} was oxidised to As^{V} when stored in the dark at room temperature; this is in contrast to the results of Bednar *et al*.[88] from above. However, when acetic acid was added along with EDTA the As samples were stabilized for 7 days. In addition, the EDTA/acetic acid preservative method was able to stabilize As samples in the presence of 3 mg L^{-1} Fe^{II} for up to 28 days. Samanta and Clifford[96] used this method to successfully stabilize synthetic groundwater samples that had various pH and E_h values and to preserve natural ground water samples. In the latter work, the authors compared the results from samples analyzed 1 to 2 days after collection with those obtained from an on-site method. They found good agreement and concluded that the EDTA/acetic acid preservation strategy is superior to the use of H_2SO_4 and H_3PO_4.

Gallagher *et al*.[111] successfully used EDTA to preserve a synthetic As^{III} solution at pH 3.8, containing 7 ppm Fe^{III}, for up to 18 h at room temperature. In contrast, when EDTA was not added, As^{III} was not detected in solution after 7 h. However, the use of EDTA to stabilize a synthetic solution was less successful at pH 9.0; the As^{III} concentration decreased by ~ 10 % within 2 h and after 18 h the As^{III} concentration decreased by ~ 60 %. However, the loss of

As^{III} (either due to oxidation or adsorption by iron-oxides) was less than that for an As^{III} solution not preserved with EDTA at the same pH and temperature. The reduced ability of EDTA to preserve As^{III} at high pH was proposed to be due to the presence of significant amounts of colloidal Fe^{III}. Gallagher *et al.*[111] used EDTA, together with acetic acid, to preserve filtered As-containing groundwater samples spiked with Fe^{III}. They found that this method of preservation stabilized all samples (with varying As^{V}/As^{III} concentration ratios) for up to 14 days at room temperature, whereas in the absence of EDTA/acetic acid the speciation of As changed considerably within hours.

However, the use of EDTA has not always been successful.[113] Gault *et al.*[113] compared the use of HCl and EDTA for the preservation of high iron, low E_h ground waters. For samples preserved with HCl, the As^{III}/total-As concentration ratios remained relatively constant over a 14 day period, whereas for samples preserved with EDTA the As^{III}/total-As concentration ratios decreased. This indicates oxidation of As^{III} to As^{V} for the EDTA preserved samples. Oliveira *et al.*[112] also found that EDTA alone, or with the addition of HCl, was not sufficient to stabilize acid mine drainage samples; in some instances the inorganic As speciation changed within 3 h of sampling. Huang and Ilgen[116] found that the As^{V} concentration in a spiked rainwater decreased by ~ 20 % within 7 days in the presence of EDTA.

1.3.4.4 Evaluation of preservation methods

In summary, the discussion above shows that the preservation of As samples is not a straight forward procedure, and that results are often contradictory for seemingly similar preservation strategies. These differences may be due to a variety of factors which include: chemical composition of sample, pH, and microbial activity and populations. Microbes play a large role in determining the As speciation in natural water because they can oxidise and reduce dissolved As over a large range of temperature, pH, and solution composition, in both oxic and anoxic environments.[114] If the preservation method does not reduce microbial activity it is unsurprising that conflicting results are obtained for different samples. Trace impurities in the preservation reagents could also affect stabilization behaviour and therefore be a contributing factor to the inconsistencies in the proposed preservation strategies.

Acid preservatives may have a significant effect on As that is bound to colloidal Fe^{III} as at low pH the Fe^{III} colloids will be more soluble and hence the dissolved As concentration may increase. The use of EDTA may also have an effect on As that is bound to colloidal Fe^{III}.

Oliveira *et al.*[112] observed an increase in As^{V} concentration when using EDTA which may be due to desorption of As^{V} from colloidal Fe. Any such effect could be limited by filtering the sample before preservation (as has been case for many of the preservation strategies above), however there may still be Fe colloids present that are smaller than the pore-size of the filter membrane, and filtering can cause other problems such as dissolved As adsorbing to the filter membrane or the iron-oxide precipitate retained on the membrane. The successful use of EDTA as a preservative requires some knowledge of the concentrations of Fe^{III} and Fe^{II} in a sample, and other competing cations, to ensure complete complexation occurs.

McClesky *et al.*[114] also notes that the choice of preservative may be dictated by the analytical technique used to measure the As concentration in the laboratory. When used as a stabilizer, HCl can interfere with the detection of As by ICP-MS due to the $^{40}Ar^{35}Cl^{+}$ molecular interference on $^{75}As^{+}$; it is possible that EDTA may interfere with some analytical methods. Furthermore, if acid is used as a preservative, some speciation methods involving anion-exchange may not be applicable unless the pH is adjusted.

As mentioned above, the isolation of As samples from light is also important. Samanta and Clifford[96] showed as little as 10 min exposure may cause changes in As speciation in preserved samples and that in some instances the presence of EDTA increased the rate of As^{III} oxidation. This was assumed to be due to a Fe^{III}-EDTA species that undergoes photolysis to generate EDTA radicals which can produce $O_2^{\bullet -}$ upon reaction with O_2. This radical may oxidise As^{III}.

The problems associated with sample preservation and storage can only be fully overcome by using in-situ or on-site methods to immediately fractionate the As species. Some of the problems with the use of on-site As speciation methods have been described above, and truly in-situ As speciation methods are limited. Therefore, the use of DGT for total As and As speciation measurements is an attractive prospect.

1.4 Thesis outline

This thesis examines aspects of environmental speciation using adsorbent-based techniques. The primary objectives of this thesis are to:

i) Investigate the use of DGT to measure total inorganic As.
ii) Develop the DGT method for selective As accumulation and hence inorganic As speciation.
iii) Investigate the use of ETAAS with a coupled microcolumn for kinetic speciation measurements.

Objective (i) is concerned with the measurement of inorganic As^{V} and As^{III} diffusion coefficients through the polyacrylamide diffusive gel using both a diffusion cell and DGT devices that contain an iron-oxide adsorbent (chapter 4). This objective also examines the influence of the membrane filter, and the pre-treatment and pore size of the membrane filter on the diffusion coefficients of either As^{V} or As^{III} (chapter 4). The influence of pH, anions, cations, fulvic acid, and Fe^{III} on the diffusion coefficients, and/or uptake of As^{V} and As^{III} is also addressed (chapter 5). The capacity of the iron-oxide adsorbent, and that effect that the As species have on the uptake of one another is examined (chapter 5).

Objective (ii) is concerned with examining the selective accumulation of As^{III} by DGT. This is carried out by the placement of a negatively charged Nafion membrane at the front of the DGT device to slow the diffusion of the negatively charged As^{V} species. The diffusion coefficients of As^{V} and As^{III} through the Nafion membrane are measured using both a diffusion cell and DGT devices that were modified to accommodate the Nafion membrane (chapter 6). The effects of pH, anions, and cations on the diffusion coefficients of As^{V} and As^{III} through the Nafion membrane is also investigated, and pre-treatment of the Nafion is briefly examined (chapter 6).

The DGT technique is then applied to natural waters in the laboratory to measure total As and to determine the concentrations of As^{III} and As^{V} (chapter 7). Two well waters and a river water spiked with two $[As^{V}]/[As^{III}]$ ratios were used.

Associated with objectives (i) and (ii) was also the investigation and optimization of the hydride generation atomic absorption spectrometry (HG-AAS) method which was used to measure the As concentration in the DGT eluents and other As solutions (chapter 3).

Lastly, objective (iii) is concerned with the preliminary investigation of using a laboratory-based flow system, in which a microcolumn of Chelex-100 adsorbent is coupled with ETAAS, for kinetic speciation of metal complexes (chapter 8). This method would enable the measurement of the inert and labile metal fractions of a water sample. This objective investigates the adsorption of Cu to the material of the microcolumn, and briefly examines issues that may affect the uptake of metal ions by the Chelex-100 resin. Factors such as the type of buffer used to regenerate the Chelex-100 resin, concentration of buffer in solution, and ionic strength, were investigated.

Note that only inorganic As species are of interest in the work for this thesis and hence throughout this thesis 'As^{III}' and 'As^{V}' refer to the inorganic species.

1.5 References

1. Michalke, B., Element speciation definitions, analytical methodology, and some examples. *Ecotoxicology and Environmental Safety* **2003,** 56, (1), 122-139.

2. Florence, T. M.; Morrison, G. M.; Stauber, J. L., Determination of trace-element speciation and the role of speciation in aquatic toxicity. *Science of the Total Environment* **1992,** 125, 1-13.

3. Morrison, G. M. P.; Batley, G. E.; Florence, T. M., Metal speciation and toxicity. *Chemistry in Britain* **1989,** 25, (8), 791-796.

4. B'Hymer, C.; Caruso, J. A., Arsenic and its speciation analysis using high-performance liquid chromatography and inductively coupled plasma mass spectrometry. *Journal of Chromatography A* **2004,** 1045, (1-2), 1-13.

5. Jain, C. K.; Ali, I., Arsenic: Occurrence, toxicity and speciation techniques. *Water Research* **2000,** 34, (17), 4304-4312.

6. Batley, G. E.; Apte, S. C.; Stauber, J. L., Speciation and bioavailability of trace metals in water: Progress since 1982. *Australian Journal of Chemistry* **2004,** 57, (10), 903-919.

7. van Leeuwen, H. P.; Town, R. M.; Buffle, J.; Cleven, R.; Davison, W.; Puy, J.; van Riemsdijk, W. H.; Sigg, L., Dynamic speciation analysis and bioavailability of metals in aquatic systems. *Environmental Science & Technology* **2005,** 39, (22), 8545-8556.

8. Batley, G. E., Collection, preparation, and storage of samples for speciation analysis. In *Trace element speciation: Analytical methods and problems*, Batley, G. E., Ed. CRC Press, Inc.: Florida, 1989; pp 2-24.

9. Reimann, C.; Siewers, U.; Skarphagen, H.; Banks, D., Does bottle type and acid-washing influence trace element analyses by ICP-MS on water samples? A test covering 62 elements and four bottle types: High density polyethene (HDPE), polypropene (PP), fluorinated ethene propene copolymer (FEP) and perfluoroalkoxy polymer(PFA). *Science of the Total Environment* **1999,** 239, (1-3), 111-130.

10. Reimann, C.; Grimstvedt, A.; Frengstad, B.; Finne, T. E., White HDPE bottles as source of serious contamination of water samples with Ba and Zn. *Science of the Total Environment* **2007,** 374, (2-3), 292-296.

11. Benoliel, M. J., Sample storage for inorganic-compounds in surface-water - a review. *International Journal of Environmental Analytical Chemistry* **1994,** 57, (3), 197-206.

12. Buffle, J.; Horvai, G., *In situ monitoring of aquatic systems: Chemical analysis and speciation*. John Wiley & Sons, Inc.: New York, 2000.

13. Quevauviller, P.; Delacalleguntinas, M. B.; Maier, E. A.; Camara, C., A survey on stability of chemical-species in solution during storage - the BCR experience. *Mikrochimica Acta* **1995,** 118, (1-2), 131-141.

14. Sliwka-Kaszynska, M.; Kot-Wasik, A.; Namiesnik, J., Preservation and storage of water samples. *Critical Reviews in Environmental Science and Technology* **2003,** 33, (1), 31-44.

15. Sekaly, A. L. R.; Chakrabarti, C. L.; Back, M. H.; Gregoire, D. C.; Lu, J. Y.; Schroeder, W. H., Stability of dissolved metals in environmental aqueous samples: Rideau river surface water, rain and snow. *Analytica Chimica Acta* **1999,** 402, (1-2), 223-231.

16. Davison, W.; Zhang, H., In-situ speciation measurements of trace components in natural-waters using thin-film gels. *Nature* **1994,** 367, (6463), 546-548.

17. Zhang, H., In-situ speciation of Ni and Zn in freshwaters: Comparison between DGT measurements and speciation models. *Environmental Science & Technology* **2004,** 38, (5), 1421-1427.

18. Zhang, H.; Davison, W., Performance-characteristics of diffusion gradients in thin-films for the in-situ measurement of trace-metals in aqueous-solution. *Analytical Chemistry* **1995,** 67, (19), 3391-3400.

19. Zhang, H.; Davison, W., Direct in situ measurements of labile inorganic and organically bound metal species in synthetic solutions and natural waters using diffusive gradients in thin films. *Analytical Chemistry* **2000,** 72, (18), 4447-4457.

20. Denney, S.; Sherwood, J.; Leyden, J., In situ measurements of labile Cu, Cd and Mn in river waters using DGT. *Science of the Total Environment* **1999,** 239, (1-3), 71-80.

21. Docekalova, H.; Divis, P., Application of diffusive gradient in thin films technique (DGT) to measurement of mercury in aquatic systems. *Talanta* **2005,** 65, (5), 1174-1178.

22. Dunn, R. J. K.; Teasdale, P. R.; Warken, J.; Jordon, M. A.; Arthur, J. M., Evaluation of the in situ, time-integrated DGT technique by monitoring changes in heavy metal concentrations in estuarine waters. *Environmental Pollution* **2007,** 148, (1), 213-220.

23. Teasdale, P. R.; Hayward, S.; Davison, W., In situ, high-resolution measurement of dissolved sulfide using diffusive gradients in thin films with computer-imaging densitometry. *Analytical Chemistry* **1999,** 71, (11), 2186-2191.

24. Twiss, M. R.; Moffett, J. W., Comparison of copper speciation in coastal marine waters measured using analytical voltammetry and diffusion gradient in thin-film techniques. *Environmental Science & Technology* **2002,** 36, (5), 1061-1068.

25. Zhang, H.; Davison, W.; Gadi, R.; Kobayashi, T., In situ measurement of dissolved phosphorus in natural waters using DGT. *Analytica Chimica Acta* **1998,** 370, (1), 29-38.

26. Naylor, C.; Davison, W.; Motelica-Heino, M.; Van den Berg, G. A.; Van der Heijdt, L. M., Potential kinetic availability of metals in sulphidic freshwater sediments. *Science of the Total Environment* **2006,** 357, (1-3), 208-220.

27. Divis, P.; Leermakers, M.; Docekalova, H.; Gao, Y., Mercury depth profiles in river and marine sediments measured by the diffusive gradients in thin films technique with two different specific resins. *Analytical and Bioanalytical Chemistry* **2005,** 382, (7), 1715-1719.

28. Ernstberger, H.; Zhang, H.; Tye, A.; Young, S.; Davison, W., Desorption kinetics of Cd, Zn, and Ni measured in soils by DGT. *Environmental Science & Technology* **2005,** 39, (6), 1591-1597.

29. Naylor, C.; Davison, W.; Motelica-Heino, M.; Van Den Berg, G. A.; Van Der Heijdt, L. M., Simultaneous release of sulfide with Fe, Mn, Ni and Zn in marine harbour sediment measured using a combined metal/sulfide DGT probe. *Science of the Total Environment* **2004,** 328, (1-3), 275-286.

30. Zhang, H.; Lombi, E.; Smolders, E.; McGrath, S., Kinetics of Zn release in soils and prediction of Zn concentration in plants using diffusive gradients in thin films. *Environmental Science & Technology* **2004,** 38, (13), 3608-3613.

31. Motelica-Heino, M.; Naylor, C.; Zhang, H.; Davison, W., Simultaneous release of metals and sulfide in lacustrine sediment. *Environmental Science & Technology* **2003,** 37, (19), 4374-4381.

32. Degryse, F.; Smolders, E.; Oliver, I.; Zhang, H., Relating soil solution Zn concentration to diffusive gradients in thin films measurements in contaminated soils. *Environmental Science & Technology* **2003,** 37, (17), 3958-3965.

33. Zhang, H.; Davison, W.; Knight, B.; McGrath, S., In situ measurements of solution concentrations and fluxes of trace metals in soils using DGT. *Environmental Science & Technology* **1998,** 32, (5), 704-710.

34. Warnken, K. W.; Zhang, H.; Davison, W., Accuracy of the diffusive gradients in thin-films technique: Diffusive boundary layer and effective sampling area considerations. *Analytical Chemistry* **2006,** 78, (11), 3780-3787.

35. Scally, S.; Davison, W.; Zhang, H., Diffusion coefficients of metals and metal complexes in hydrogels used in diffusive gradients in thin films. *Analytica Chimica Acta* **2006,** 558, (1-2), 222-229.

36. Zhang, H.; Davison, W., Diffusional characteristics of hydrogels used in DGT and DET techniques. *Analytica Chimica Acta* **1999,** 398, (2-3), 329-340.

37. Garmo, O. A.; Royset, O.; Steinnes, E.; Flaten, T. P., Performance study of diffusive gradients in thin films for 55 elements. *Analytical Chemistry* **2003,** 75, (14), 3573-3580.

38. Downard, A. J.; Panther, J.; Kim, Y. C.; Powell, K. J., Lability of metal ion-fulvic acid complexes as probed by FIA and DGT: A comparative study. *Analytica Chimica Acta* **2003,** 499, (1-2), 17-28.

39. Scally, S.; Zhang, H.; Davison, W., Measurements of lead complexation with organic ligands using DGT. *Australian Journal of Chemistry* **2004,** 57, (10), 925-930.

40. Murdock, C.; Kelly, M.; Chang, L. Y.; Davison, W.; Zhang, H., DGT as an in situ tool for measuring radiocesium in natural waters. *Environmental Science & Technology* **2001,** 35, (22), 4530-4535.

41. Sangi, M. R.; Halstead, M. J.; Hunter, K. A., Use of the diffusion gradient thin film method to measure trace metals in fresh waters at low ionic strength. *Analytica Chimica Acta* **2002,** 456, (2), 241-251.

42. Chang, L. Y.; Davison, W.; Zhang, H.; Kelly, M., Performance characteristics for the measurement of Cs and Sr by diffusive gradients in thin films (DGT). *Analytica Chimica Acta* **1998,** 368, (3), 243-253.

43. Gimpel, J.; Zhang, H.; Hutchinson, W.; Davison, W., Effect of solution composition, flow and deployment time on the measurement of trace metals by the diffusive gradient in thin films technique. *Analytica Chimica Acta* **2001,** 448, (1-2), 93-103.

44. Scally, S.; Davison, W.; Zhang, H., In situ measurements of dissociation kinetics and labilities of metal complexes in solution using DGT. *Environmental Science & Technology* **2003,** 37, (7), 1379-1384.

45. Alfaro-De la Torre, M. C.; Beaulieu, P. Y.; Tessier, A., In situ measurement of trace metals in lakewater using the dialysis and DGT techniques. *Analytica Chimica Acta* **2000,** 418, (1), 53-68.

46. Gimpel, J.; Zhang, H.; Davison, W.; Edwards, A. C., In situ trace metal speciation in lake surface waters using DGT, dialysis, and filtration. *Environmental Science & Technology* **2003,** 37, (1), 138-146.

47. Li, W. J.; Zhao, H. J.; Teasdale, P. R.; John, R.; Wang, F. Y., Metal speciation measurement by diffusive gradients in thin films technique with different binding phases. *Analytica Chimica Acta* **2005,** 533, (2), 193-202.

48. Ernstberger, H.; Zhang, H.; Davison, W., Determination of chromium speciation in natural systems using DGT. *Analytical and Bioanalytical Chemistry* **2002,** 373, (8), 873-879.

49. Peters, A. J.; Zhang, H.; Davison, W., Performance of the diffusive gradients in thin films technique for measurement of trace metals in low ionic strength freshwaters. *Analytica Chimica Acta* **2003,** 478, (2), 237-244.

50. Warnken, K. W.; Zhang, H.; Davison, W., Trace metal measurements in low ionic strength synthetic solutions by diffusive gradients in thin films. *Analytical Chemistry* **2005,** 77, (17), 5440-5446.

51. Plant, J. A.; Kinniburgh, D. G.; Smedley, P. L.; Fordyce, F. M.; Klinck, B. A., Arsenic and selenium. In *Treatise on geochemistry*, Holland, H. D.; Turekian, K. K., Eds. Elsevier: New York, 2003; Vol. 9, pp 17-66.

52. Smedley, P. L.; Kinniburgh, D. G., A review of the source, behaviour and distribution of arsenic in natural waters. *Applied Geochemistry* **2002,** 17, (5), 517-568.

53. Cullen, W. R.; Reimer, K. J., Arsenic speciation in the environment. *Chemical Reviews* **1989,** 89, (4), 713-764.

54. Inskeep, W. P.; McDermott, T. R.; Fendorf, S., Arsenic (V)/(III) cycling in soils and natural waters: Chemical and microbiological processes. In *Environmental chemistry of arsenic*, Frankenberger, W. T., Ed. Marcel Dekker, Inc.: New York, 2002; pp 183-215.

55. Hering, J. G.; Kneebone, P. E., Biogeochemical controls on arsenic ocurence and mobility in water supplies. In *Environmental chemistry of arsenic*, Frankenberger, W. T., Ed. Marcel Dekker, Inc.: New York, 2002; pp 155-181.

56. Jain, A.; Raven, K. P.; Loeppert, R. H., Arsenite and arsenate adsorption on ferrihydrite: Surface charge reduction and net OH^- release stoichiometry. *Environmental Science & Technology* **1999,** 33, (8), 1179-1184.

57. Goldberg, S., Competitive adsorption of arsenate and arsenite on oxides and clay minerals. *Soil Science Society of America Journal* **2002,** 66, (2), 413-421.

58. Dixit, S.; Hering, J. G., Comparison of arsenic(V) and arsenic(III) sorption onto iron oxide minerals: Implications for arsenic mobility. *Environmental Science & Technology* **2003,** 37, (18), 4182-4189.

59. Jain, A.; Loeppert, R. H., Effect of competing anions on the adsorption of arsenate and arsenite by ferrihydrite. *Journal of Environmental Quality* **2000,** 29, (5), 1422-1430.

60. Mandal, B. K.; Suzuki, K. T., Arsenic round the world: A review. *Talanta* **2002,** 58, (1), 201-235.

61. Bednar, A. J.; Garbarino, J. R.; Ranville, J. F.; Wildeman, T. R., Presence of organoarsenicals used in cotton production in agricultural water and soil of the southern United States. *Journal of Agricultural and Food Chemistry* **2002,** 50, (25), 7340-7344.

62. Hughes, M. F., Arsenic toxicity and potential mechanisms of action. *Toxicology Letters* **2002,** 133, (1), 1-16.

63. Le, X. C.; Lu, X. F.; Li, X. F., Arsenic speciation. *Analytical Chemistry* **2004,** 76, (1), 26A-33A.

64. Xie, R. M.; Johnson, W.; Spayd, S.; Hall, G. S.; Buckley, B., Arsenic speciation analysis of human urine using ion exchange chromatography coupled to inductively coupled plasma mass spectrometry. *Analytica Chimica Acta* **2006,** 578, (2), 186-194.

65. Rahman, M. M.; Sengupta, M. K.; Chowdhury, U. K.; Lodh, D.; Das, B.; Ahamed, S.; Mandal, D.; Hossain, M. A.; Mukherjee, S. C.; Pati, S.; Saha, K. C.; Chakaborti, D., Arsenic around the world - an overview. In *Managing arsenic in the environment: From soil to human health*, Naidu, R.; Smith, E.; Owens, G.; Bhattacharya, P.; Nadebaum, P., Eds. CSIRO Publishing: Collingwood, 2006; pp 3-30.

66. National Research Council, *Arsenic in drinking water - 2001 update*. National Academy Press: Washington, D.C., 2001.

67. Centeno, J. A.; Tchounwou, P. B.; Patolla, A. K.; Mullick, F. G.; Murakata, L.; Meza, E.; Todorov, T.; Longfellow, D.; Yedjou, C. G., Environmental pathology and health effects of arsenic poisoning. In *Managing arsenic in the environment: From soil to human health*,

Naidu, R.; Smith, E.; Owens, G.; Bhattacharya, P.; Nadebaum, P., Eds. CSIRO Publishing: Collingwood, 2006; pp 311-327.

68. Bermejo-Barrera, P.; Moreda-Pineiro, J.; Moreda-Pineiro, A.; Bermejo-Barrera, A., Selective medium reactions for the 'arsenic(III)', 'arsenic(V)', dimethylarsonic acid and monomethylarsonic acid determination in waters by hydride generation on-line electrothermal atomic absorption spectrometry with in situ preconcentration on Zr-coated graphite tubes. *Analytica Chimica Acta* **1998,** 374, (2-3), 231-240.

69. Gonzalez, J. C.; Lavilla, I.; Bendicho, C., Evaluation of non-chromatographic approaches for speciation of extractable As(III) and As(V) in environmental solid samples by FI-HGAAS. *Talanta* **2003,** 59, (3), 525-534.

70. Anderson, R. K.; Thompson, M.; Culbard, E., Selective reduction of arsenic species by continuous hydride generation .1. Reaction media. *Analyst* **1986,** 111, (10), 1143-1152.

71. Cabon, J. Y.; Cabon, N., Determination of arsenic species in seawater by flow injection hydride generation in situ collection followed by graphite furnace atomic absorption spectrometry - stability of As(III). *Analytica Chimica Acta* **2000,** 418, (1), 19-31.

72. Anthemidis, A. N.; Zachariadis, G. A.; Stratis, J. A., Determination of arsenic(III) and total inorganic arsenic in water samples using an on-line sequential insertion system and hydride generation atomic absorption spectrometry. *Analytica Chimica Acta* **2005,** 547, (2), 237-242.

73. Coelho, N. M. M.; da Silva, A. C.; da Silva, C. M., Determination of As(III) and total inorganic arsenic by flow injection hydride generation atomic absorption spectrometry. *Analytica Chimica Acta* **2002,** 460, (2), 227-233.

74. Liang, L. A.; Lazoff, S.; Chan, C.; Horvat, M.; Woods, J. S., Determination of arsenic in ambient water at sub-part-per-trillion levels by hydride generation Pd coated platform collection and GFAAS detection. *Talanta* **1998,** 47, (3), 569-583.

75. Kopanica, M.; Novotny, L., Determination of traces of arsenic(III) by anodic stripping voltammetry in solutions, natural waters and biological material. *Analytica Chimica Acta* **1998,** 368, (3), 211-218.

76. Rasul, S. B.; Munir, A. K. M.; Hossain, Z. A.; Khan, A. H.; Alauddin, M.; Hussam, A., Electrochemical measurement and speciation of inorganic arsenic in groundwater of Bangladesh. *Talanta* **2002,** 58, (1), 33-43.

77. Song, Y.; Swain, G. M., Total inorganic arsenic detection in real water samples using anodic stripping voltammetry and a gold-coated diamond thin-film electrode. *Analytica Chimica Acta* **2007,** 593, (1), 7-12.

78. Dai, X.; Nekrassova, O.; Hyde, M. E.; Compton, R. G., Anodic stripping voltammetry of arsenic(III) using gold nanoparticle-modified electrodes. *Analytical Chemistry* **2004,** 76, (19), 5924-5929.

79. Salaun, P.; Planer-Friedrich, B.; van den Berg, C. M. G., Inorganic arsenic speciation in water and seawater by anodic stripping voltammetry with a gold microelectrode. *Analytica Chimica Acta* **2007,** 585, (2), 312-322.

80. Feeney, R.; Kounaves, S. P., On-site analysis of arsenic in groundwater using a microfabricated gold ultramicroelectrode array. *Analytical Chemistry* **2000,** 72, (10), 2222-2228.

81. Huang, H. L.; Dasgupta, P. K., A field-deployable instrument for the measurement and speciation of arsenic in potable water. *Analytica Chimica Acta* **1999,** 380, (1), 27-37.

82. Barra, C. M.; dos Santos, M. M. C., Speciation of inorganic arsenic in natural waters by square-wave cathodic stripping voltammetry. *Electroanalysis* **2001,** 13, (13), 1098-1104.

83. Ferreira, M. A.; Barros, A. A., Determination of As(III) and As(V) in natural waters by cathodic stripping voltammetry at a hanging mercury drop electrode. *Analytica Chimica Acta* **2002,** 459, (1), 151-159.

84. He, Y.; Zheng, Y.; Locke, D. C., Cathodic stripping voltammetric analysis of arsenic species in environmental water samples. *Microchemical Journal* **2007,** 85, (2), 265-269.

85. He, Y.; Zheng, Y.; Ramnaraine, M.; Locke, D. C., Differential pulse cathodic stripping voltammetric speciation of trace level inorganic arsenic compounds in natural water samples. *Analytica Chimica Acta* **2004,** 511, (1), 55-61.

86. Li, H.; Smart, R. B., Determination of sub-nanomolar concentration of arsenic(III) in natural waters by square wave cathodic stripping voltammetry. *Analytica Chimica Acta* **1996,** 325, (1-2), 25-32.

87. Bednar, A. J.; Garbarino, J. R.; Burkhardt, M. R.; Ranville, J. F.; Wildeman, T. R., Field and laboratory arsenic speciation methods and their application to natural-water analysis. *Water Research* **2004,** 38, (2), 355-364.

88. Bednar, A. J.; Garbarino, J. R.; Ranville, J. F.; Wildeman, T. R., Preserving the distribution of inorganic arsenic species in groundwater and acid mine drainage samples. *Environmental Science & Technology* **2002,** 36, (10), 2213-2218.

89. Bombach, G.; Klemm, W.; Greif, A., An analytical method for the separation and determination of As(III) and As(V) in seepage and acid mine drainage water. *Microchimica Acta* **2005,** 151, (3-4), 203-208.

90. Impellitteri, C. A., Effects of pH and competing anions on the speciation of arsenic in fixed ionic strength solutions by solid phase extraction cartridges. *Water Research* **2004,** 38, (5), 1207-1214.

91. Jitmanee, K.; Oshima, M.; Motomizu, S., Speciation of arsenic(III) and arsenic(V) by inductively coupled plasma-atomic emission spectrometry coupled with preconcentration system. *Talanta* **2005,** 66, (3), 529-533.

92. Karori, S.; Clifford, D.; Ghurye, G.; Samanta, G., Development of a field speciation method for inorganic arsenic species in groundwater. *Journal American Water Works Association* **2006,** 98, (5), 128-141.

93. Kim, M. J., Separation of inorganic arsenic species in groundwater using ion exchange method. *Bulletin of Environmental Contamination and Toxicology* **2001,** 67, (1), 46-51.

94. Le, X. C.; Yalcin, S.; Ma, M. S., Speciation of submicrogram per liter levels of arsenic in water: On-site species separation integrated with sample collection. *Environmental Science & Technology* **2000,** 34, (11), 2342-2347.

95. Packer, A. P.; Ciminelli, V. S. T., A simplified flow system for inorganic arsenic speciation by preconcentration of As(V) and separation of As(III) in natural waters by ICP-MS. *Atomic Spectroscopy* **2005,** 26, (4), 131-136.

96. Samanta, G.; Clifford, D. A., Preservation of inorganic arsenic species in groundwater. *Environmental Science & Technology* **2005,** 39, (22), 8877-8882.

97. Smichowski, P.; Valiente, L.; Ledesma, A., Simple method for the selective determination of As(III) and As(V) by ETAAS after separation with anion exchange mini-column. *Atomic Spectroscopy* **2002,** 23, (3), 92-97.

98. Akter, K. F.; Chen, Z.; Smith, L.; Davey, D.; Naidu, R., Speciation of arsenic in ground water samples: A comparative study of CE-UV HG-AAS and LC-ICP-MS. *Talanta* **2005,** 68, (2), 406-415.

99. Forte, G.; D'Amato, M.; Caroli, S., Capillary electrophoresis speciation analysis of various arsenical compounds. *Microchemical Journal* **2005,** 79, (1-2), 15-19.

100. Richardson, D. D.; Kannamkumarath, S. S.; Wuilloud, R. G.; Caruso, J. A., Hydride generation interface for speciation analysis coupling capillary electrophoresis to inductively coupled plasma mass spectrometry. *Analytical Chemistry* **2004,** 76, (23), 7137-7142.

101. Yin, X. B.; Yan, X. P.; Jiang, Y.; He, X. W., On-line coupling of capillary electrophoresis to hydride generation atomic fluorescence spectrometry for arsenic speciation analysis. *Analytical Chemistry* **2002,** 74, (15), 3720-3725.

102. Van Holderbeke, M.; Zhao, Y. N.; Vanhaecke, F.; Moens, L.; Dams, R.; Sandra, P., Speciation of six arsenic compounds using capillary electrophoresis inductively coupled plasma mass spectrometry. *Journal of Analytical Atomic Spectrometry* **1999,** 14, (2), 229-234.

103. Harris, D. C., *Quantitative chemical analysis*. 7th ed.; W.H. Freeman and Company: New York, 2007.

104. Kellner, S.; Mermet, J. M.; Otto, M.; Widmer, H. M., *Analytical chemistry: The approved text to the FECS cirriculum analytical chemistry*. Wiley-VCH: New York, 1998.

105. Gettar, R. T.; Garavaglia, R. N.; Gautier, E. A.; Batistoni, D. A., Determination of inorganic and organic anionic arsenic species in water by ion chromatography coupled to hydride generation-inductively coupled plasma atomic emission spectrometry. *Journal of Chromatography A* **2000,** 884, (1-2), 211-221.

106. Ronkart, S. N.; Laurent, V.; Carbonnelle, P.; Mabon, N.; Copin, A.; Barthelemy, J. P., Speciation of five arsenic species (arsenite, arsenate, MMAA(V), DMAA(V) and AsBet) in different kind of water by HPLC-ICP-MS. *Chemosphere* **2007,** 66, (4), 738-745.

107. Dasgupta, P. K.; Huang, H. L.; Zhang, G. F.; Cobb, G. P., Photometric measurement of trace As(III) and As(V) in drinking water. *Talanta* **2002,** 58, (1), 153-164.

108. Tsang, S.; Phu, F.; Baum, M. M.; Poskrebyshev, G. A., Determination of phosphate/arsenate by a modified molybdenum blue method and reduction of arsenate by $S_2O_4^{2-}$. *Talanta* **2007,** 71, (4), 1560-1568.

109. Dhar, R. K.; Zheng, Y.; Rubenstone, J.; van Geen, A., A rapid colorimetric method for measuring arsenic concentrations in groundwater. *Analytica Chimica Acta* **2004,** 526, (2), 203-209.

110. Polya, D. A.; Lythgoe, P. R.; Abou-Shakra, F.; Gault, A. G.; Brydie, J. R.; Webster, J. G.; Brown, K. L.; Nimfopoulos, M. K.; Michailidis, K. M., IC-ICP-MS and IC-ICP-HEX-MS determination of arsenic speciation in surface and groundwaters: Preservation and analytical issues. *Mineralogical Magazine* **2003,** 67, (2), 247-261.

111. Gallagher, P. A.; Schwegel, C. A.; Wei, X. Y.; Creed, J. T., Speciation and preservation of inorganic arsenic in drinking water sources using EDTA with IC separation and ICP-MS detection. *Journal of Environmental Monitoring* **2001,** 3, (4), 371-376.

112. Oliveira, V.; Sarmiento, A. M.; Gomez-Ariza, J. L.; Nieto, J. M.; Sanchez-Rodas, D., New preservation method for inorganic arsenic speciation in acid mine drainage samples. *Talanta* **2006,** 69, (5), 1182-1189.

113. Gault, A. G.; Jana, J.; Chakraborty, S.; Mukherjee, P.; Sarkar, M.; Nath, B.; Polya, D. A.; Chatterjee, D., Preservation strategies for inorganic arsenic species in high iron, low-Eh groundwater from West Bengal, India. *Analytical and Bioanalytical Chemistry* **2005,** 381, (2), 347-353.

114. McCleskey, R. B.; Nordstrom, D. K.; Maest, A. S., Preservation of water samples for arsenic(III/V) determinations: An evaluation of the literature and new analytical results. *Applied Geochemistry* **2004,** 19, (7), 995-1009.

115. Emett, M. T.; Khoe, G. H., Photochemical oxidation of arsenic by oxygen and iron in acidic solutions. *Water Research* **2001,** 35, (3), 649-656.

116. Huang, J. H.; Ilgen, G., Blank values, adsorption, pre-concentration, and sample preservation for arsenic speciation of environmental water samples. *Analytica Chimica Acta* **2004,** 512, (1), 1-10.

Chapter 2

Experimental

This chapter outlines the equipment, reagents and general procedures used for the experimental work described in this thesis. Specific procedures are described in the relevant chapters.

2.1 Clean room protocols

All experimental work, unless otherwise stated, was carried out in a Class-350 clean room. Air enters the room through high efficiency particle (HEPA) filters and removes particulates from the air in the clean room by maintaining a constant laminar flow through the room. Air exits the room through vents that are positioned such that the filtered air passes through the entire room before being removed. The clean room also contained a Class-3.5 laminar flow hood in which preparation of solutions and DGT gels was carried out in.

Before entering the changing room, shoes were removed. Once inside, a lint-free polyester overcoat, overshoes, and a hair-net were worn to reduce contamination. Disposable polyethylene or powder-free rubber gloves were used in the clean room when manipulating reagents and samples. Disposable sticky mats were placed on the floor inside the clean room and the change room to remove particles from overshoes. Plastic sheets were placed on top of the clean room benches and used as work surfaces to minimize contamination. The plastic was replaced at least daily.

To minimize contaminants and dust entering the clean room, all items taken into the clean room were wiped with a damp Durx™ clean room wipe in the change room. The use of paper in the clean room was kept to a minimum as this can cause dust. The clean room was cleaned weekly to remove any dust build-up. This involved sweeping and mopping of floors, wiping all surfaces using a damp Durx™ clean room wipe, renewing the sticky mats, and replacing dirty or worn overshoes.

To reduce the possibility of contamination from metal items, the metal fittings in the room were made of stainless steel, or were sealed by painting. No other metal items were allowed in the clean room.

2.2 Reagents

2.2.1 Water

High purity Milli-Q water (≥ 18 MΩ cm^{-1}) was used to prepare all solutions and to clean glassware and containers. This was obtained from a four-bowl Milli-Q® water purification system (Millipore Corp) in which distilled water is passed sequentially through a Super-C carbon cartridge, Ion-Ex anion and cation exchange cartridges, an Organex-Q cartridge, and lastly a Millipak® 0.22 μm pore size filter.

2.2.2 Chemicals

A list of chemicals used in the work for this thesis as well as their grades and manufacturers is given in Table 2.1 All chemicals were used as supplied unless otherwise stated.

2.2.3 Analytical standards

2.2.3.1 As^V stock solutions

A stock solution of 1000 ppm As^V was prepared by dissolving 0.416 g of sodium arsenate (ACS, Sigma-Aldrich) in 10 mL of concentrated hydrochloric acid (Aristar, BDH) and diluting to 100 mL with Milli-Q water. The 1000 ppm As^V stock solution was prepared daily.

Further stock solutions of As^V in 1 % v/v HCl (Aristar, BDH) were prepared by initial dilution of the 1000 ppm As^V stock solution.

Two As^V standards (500 ppb and 5 ppb) which were prepared by dilution of the 1000 ppm As^V stock solution were analyzed by an independent laboratory (Environmental Laboratory Services (ESL) Ltd., Lower Hutt, New Zealand). Good agreement was obtained between the calculated concentration of As and that determined by ESL; this indicates the integrity of the stock solution prepared above using sodium arsenate.

Chemical	Grade	Manufacturer
2-(N-morpholino)ethanesulfonic acid (MES)	≥ 99.5 %	Sigma
Acetic acid	Analar	BDH Chemicals
Acrylamide solution (40 %)	Electran	BDH Chemicals
Ammonium acetate	Analar	BDH Chemicals
Ammonium chloride	ACS	Scharlau
Ammonium nitrate	Analar	BDH Chemicals
Ammonium persulfate	Analar	BDH Chemicals
Arsenious oxide (As_2O_3)	Analar	Hopkin & Williams
Cadmium nitrate atomic absorption standard	-	BDH Chemicals
Calcium acetate	Analar	BDH Chemicals
Calcium nitrate ($Ca(NO_3)_2.4H_2O$)	> 98 %	May and Baker
Copper nitrate atomic absorption standard	-	BDH Chemicals
DGT gel cross-linker (2 %)	-	DGT Research
Disodium hydrogen phosphate	Analar	BDH Chemicals
Hydrochloric acid	Aristar	BDH Chemicals
Iron nitrate ($Fe(NO)_3.9H_2O$)	Analar	BDH Chemicals
Iron nitrate atomic absorption standard	-	Merck
L-Cysteine	> 99 %	Applichem
Magnesium Sulfate	Analar	BDH Chemicals
N,N,N'N'-tetramethylethylenediamne (TEMED)	99 %	Aldrich
Nitric acid	Aristar	BDH Chemicals
Palladium chloride	-	Merck
Potassium chloride	Analar	BDH Chemicals
Potassium dihydrogen phosphate	Analar	BDH Chemicals
Potassium hydrogen phthalate	Analar	Scharlau
Potassium hydroxide	Anlalar	Scharlau
Potassium nitrate	Suprapur	Merck
Sodium acetate	Analar	Scharlau
Sodium acetate	Suprapur	Merck
Sodium arsenate ($Na_2HAsO_4.7H_2O$)	ACS	Sigma-Aldrich
Sodium borohydride	GPR	BDH Chemicals
Sodium chloride	Aristar	BDH Chemicals
Sodium hydroxide*	Analar	BDH Chemicals
Sodium hydroxide	Aristar	BDH Chemicals
Sodium nitrate	Analar	BDH Chemicals
Sodium silicate ($Na_2SiO_3.5H_2O$)	Analar	BDH Chemicals

Table 2.1 List of chemicals used in the experimental work for this thesis

*Analar sodium hydroxide was used only to stabilize the $NaBH_4$ solution

2.2.3.2 As^{III} stock solutions

A stock solution of 1000 ppm As^{III} was prepared by dissolving 0.132 g of arsenious oxide (Analar, Hopkin and Williams) in 2.5 mL of 1 mol L^{-1} NaOH. This solution was sonicated to dissolve the arsenious oxide; 50 mL of Milli-Q water was added and this was followed by 10 mL of concentrated HCl (Aristar, BDH). The solution was diluted to 100 mL with Milli-Q water. The 1000 ppm As^{III} stock solution was prepared daily.

Further stock solutions of As^{III} in 1 % v/v HCl (Aristar, BDH) were prepared by initial dilution of the 1000 ppm As^{III} stock solution.

The As^{V} content of a 50 ppm As^{III} stock solution was examined using the ammonium molybdate/antimony potassium tartrate method to determine if any oxidation of As^{III} had occurred during preparation of the stock solution, or was present as an impurity in the arsenious oxide. It was found that this As^{III} stock solution contained ~ 0.05 ppm As^{V}; this corresponds to 0.1 % of the total As.

Two As^{III} standards (500 ppb and 5 ppb) which were prepared by dilution of the 1000 ppm As^{III} stock solution were analyzed by an independent laboratory (Environmental Laboratory Services (ESL) Ltd., Lower Hutt, New Zealand). Good agreement was obtained between the calculated concentration of As and that determined by ESL; this indicates the integrity of the stock solution prepared above using arsenious oxide.

2.2.3.3 Metal standard solutions

Copper, cadmium, and iron standards were prepared by dilution of 1000 ppm Spectrosol® atomic absorption standards (BDH and Merck). All metal standards contained 1 % v/v HNO_3.

2.2.4 Preparation of buffer stock solutions

2.2.4.1 Sodium acetate buffers

Three different sodium acetate buffers were used in the work for this thesis.

Sodium acetate buffer (0.25 mol L^{-1}, pH 5.0) that was used for the HG-AAS experiments was prepared by dissolving 41.0 g of sodium acetate (Analar, Scharlau) in ~ 1 L of Milli-Q water;

16.5 mL of concentrated acetic acid (Analar, BDH) was added and then the solution was diluted to 2 L.

Sodium acetate buffer (1 mol L^{-1}) that was used for all DGT experiments was prepared by dissolving 41.0 g of sodium acetate (Analar, Scharlau) in ~ 450 mL of Milli-Q water. Concentrated HNO_3 (Aristar, BDH) was added until pH 5.0 was obtained and then the solution was diluted to 500 mL.

Sodium acetate buffer (1 mol L^{-1}) that was used for all Chelex-100 microcolumn experiments was prepared by dissolving 41.0 g of sodium acetate (Aristar, Merck) in ~ 450 mL of Milli-Q water. Concentrated HNO_3 (Aristar, BDH) was added until pH 5.0 was obtained and then the solution was diluted to 500 mL.

2.2.4.2 Ammonium acetate buffer

Ammonium acetate buffer (1 mol L^{-1}) was prepared by dissolving 7.7 g of ammonium acetate (Analar, BDH) in ~ 80 mL of Milli-Q water. Concentrated HNO_3 (Aristar, BDH) was added until pH 5.0 was obtained and then the solution was diluted to 100 mL.

Ammonium acetate buffer (0.05 mol L^{-1}) was prepared by dissolving 0.385 g of ammonium acetate (Analar, BDH) in ~ 80 mL of Milli-Q water. Concentrated HNO_3 (Aristar, BDH) was added until pH 5.0 was obtained and then the solution was diluted to 100 mL.

2.2.4.3 Calcium acetate buffer

Calcium acetate buffer (0.05 mol L^{-1}) was prepared by dissolving 0.495 g of calcium acetate (Analar, BDH) in ~ 80 mL of Milli-Q water. Concentrated HNO_3 (Aristar, BDH) was added until pH 5.0 was obtained and then the solution was diluted to 100 mL.

2.2.4.4 MES buffer

A 0.05 mol L^{-1} 2-(N-morpholino)ethanesulfonic acid (MES) buffer was prepared by dissolving 0.976 g of MES (≥ 99.5 %, Sigma) in ~ 80 mL of Milli-Q water; 1 mol L^{-1} NaOH (Aristar, BDH) was added until pH 5.5 was obtained and then the solution was diluted to 100 mL.

2.2.4.5 Phthalate buffer (pH 4.01)

Potassium hydrogen phthalate ($KHC_6H_4(COO)_2$) (Analar, Scharlau) was oven-dried at 110 ^oC for 2 h and then stored in a desiccator over anhydrous $CaCl_2$. To prepare the buffer, 5.10 g of the dried solid was dissolved in 500 mL of Milli-Q water.

2.2.4.6 Phosphate buffer (pH 7.00)

Disodium hydrogen phosphate (Na_2HPO_4) (Analar, BDH) and potassium dihydrogen phosphate (KH_2PO_4) (Analar, BDH) were oven-dried at 40 ^oC for 2 h and then stored in a desiccator over anhydrous $CaCl_2$. To prepare the buffer, 1.95 g of Na_2HPO_4 and 1.36 g of KH_2PO_4 was dissolved in 500 mL of Milli-Q water.

2.2.5 Fulvic acid samples

The fulvic acid employed for the DGT work was the FAG1 sample. It was isolated from the B_h horizon of a gley podsol soil by Gregor *et al.*[1] using an acid pyrophosphate-XAD-7 method.

The fulvic acid employed for the Chelex-100 microcolumn work was the B1F sample. It was previously isolated by Powell and Fenton[2] from International Humic Substance Society reference peat by an acid pyrophosphate-XAD-7 method.

2.2.6 Gases

For ETAAS measurements, the graphite furnace was bathed in zero grade nitrogen (> 99.999 %) whereas zero grade argon (> 99.999 %) was used as the carrier gas in the hydride generator. Both gasses were supplied by BOC.

2.3 DGT procedures and protocols

2.3.1 Preparation of iron-oxide

The iron-oxide was prepared using a similar method to that described by Zhang *et al*;[3] 8 g of $Fe(NO_3)_3.9H_2O$ (Analar, BDH) was dissolved in 200 mL of Milli-Q water, then 1 mol L^{-1} NaOH (Analar, BDH) was added very slowly, while vigorously stirring, until pH 7.5 was obtained. A dark brown-red coloured precipitate formed which is characteristic of ferrihydrite. The NaOH was added slowly to ensure that the pH did not rise above 8.0. After a pH of 7.5

was obtained, the iron-oxide solution was left for at least 30 min to ensure the pH had stabilized and to consolidate the precipitate. The iron-oxide precipitate was washed five times with Milli-Q water by decanting the surface water from the precipitate. The iron-oxide was stored under Milli-Q water in a plastic bottle and refrigerated (4 ^{o}C) until use.

The pH was carefully monitored as uncontrolled preparation of the iron-oxide may lead to a mixture of ferrihydrite, goethite and hematite[3] which may have different binding properties for As species.

2.3.2 Preparation of iron-oxide gel and diffusive gels

2.3.2.1 Preparation of gel solution

Gel solution was prepared by mixing 7.5 g of DGT agarose-derived cross-linker (2 %) (DGT Research Ltd, Lancaster, UK) and 23.75 mL of Milli-Q water together in a clean plastic container; 18.75 mL of acrylamide solution (40 %) (Electran, BDH) was added and the gel solution was mixed thoroughly by stirring. The gel solution was stored in a refrigerator (4 ^{o}C) until use.

2.3.2.2 Preparation of diffusive gel

The diffusive gel was prepared by mixing 10 mL of gel solution and 70 µL of a 10 % ammonium persulfate (Analar, BDH) solution (prepared daily by dissolving 0.1 g of ammonium persulfate in 1 mL of Milli-Q water) together in a clean plastic container; 25 µL of N,N,N'N'-tetramethylethylenediamne (TEMED) (99 % Aldrich) was then added. The resulting solution was carefully mixed by stirring, and then cast between two glass plates as detailed in section 2.3.2.4. If the solution is mixed too vigorously, bubbles and/or foam can form which makes casting of gels and obtaining a uniform diffusive gel, difficult.

The glass plate assemblies were placed in an oven at 45 ^{o}C for at least 1 h to set the gels. The gels were removed from the glass plates and soaked in 500 mL of Milli-Q water for at least 24 h to hydrate the gel and to allow unreacted reagents to diffuse out of the gel. The water was changed four times with a 2 to 3 h soaking period between each change. The gel was conditioned in 0.01 mol L^{-1} $NaNO_3$ (Analar, BDH) solution for at least 24 h prior to use and was stored in the same solution at room temperature in the dark. Disks were cut from the gel sheet with a 2.5 cm diameter plastic cutter.

The thickness of the diffusive gels was measured using an in-house built micrometer which was connected to a multimeter. The difference in height when the micrometer tip touches a metal platform to that when it touches a diffusive gel disk on top of the metal platform was used to determine the diffusive gel thickness. A change in resistance was used to determine that the tip of the micrometer was touching the diffusive gel or the metal platform. One complete revolution of the micrometer head was equivalent to 0.5 mm. Using this method, the average thickness of the diffusive gels was determined as 0.80 ± 0.04 mm (n = 9). The uncertainty associated with the diffusive gel thickness is the standard deviation of the mean from replicate diffusion gel thickness measurements.

2.3.2.3 Preparation of iron-oxide gel

The iron-oxide was prepared for use by filtering a small portion of the iron-oxide solution with Whatman 541 hardened ashless filter paper to remove most of the Milli-Q water that it was stored in. It was then pressed between two pieces of filter paper to remove excess water. The iron-oxide gel was prepared by thoroughly mixing 2.5 g of the damp iron-oxide and 10 mL of gel solution together in a clean plastic container; care was taken to ensure that no large fragments of iron-oxide existed. Then 60 µL of a 10 % ammonium persulfate (Analar, BDH) solution was added to the iron-oxide gel solution and carefully mixed, this was followed by 15 µL of TEMED (99 % Aldrich). The resulting solution was carefully mixed by stirring, and then cast between five glass plates as detailed in section 2.3.2.4. The glass plate assemblies were placed in an oven at 45 ^{o}C for at least 1 h to set the gels. The gels were removed from the glass plates and soaked in 500 mL of Milli-Q water for at least 24 h to hydrate the gel and to allow unreacted reagents to diffuse out of the gel. The water was changed four times with a 2 to 3 h soaking period between each change. The gel was stored in Milli-Q water and refrigerated (4 ^{o}C) until use. Disks were cut from the gel sheet with a 2.5 cm or 2 cm diameter plastic cutter, depending on their use. Figure 2.1 shows an iron-oxide gel disk.

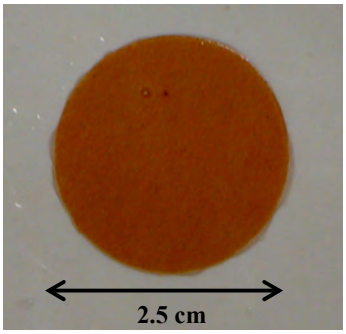

Figure 2.1 Iron-oxide gel disk

Each iron-oxide gel disk contained 0.45 ± 0.05 mg of Fe; this was determined by eluting gel disks with concentrated HCl and measuring the Fe concentration in the eluent. The mass of As within each iron-oxide gel disk (the analytical blank) was determined by measuring the concentration of As in the eluent solution from eluting four iron-oxide gels; it was found that on average the iron-oxide gel disk contained 7.1 ± 0.7 ng of As.

2.3.2.4 Gel casting procedures

The gel plates used were of two different sizes: 10 cm x 10 cm for diffusive gel preparation, and 7.5 x 7.5 cm for iron-oxide gel preparation. In addition, plastic spacers of different thicknesses were used; 0.25 mm and 0.5 mm thick plastic spacers were used to prepare iron-oxide gels of 0.4 mm thickness and diffusive gels of 0.8 mm thickness when hydrated, respectively. The glass plates and plastic spacers were cleaned and stored in 10 % v/v HNO_3 (Aristar, BDH). For use, the glass plates and plastic spacers were rinsed with Milli-Q water and dried with Durx™ clean room wipes. The spacer was placed around three edges of the glass plate, and another glass plate was placed on top of the assembly. The second glass plate was offset by ~ 5 mm to allow easier pipetting of the iron-oxide gel and diffusive gel solutions. The glass plates were clamped together using plastic clips which were made in-house. The iron-oxide gel or diffusive gel solutions were pipetted between the glass plates in a smooth, controlled manner to ensure a uniform distribution of the mixture within the assembly. The glass plates were laid flat in an oven to allow the gel to set, after which time the clips were removed and the glass plates were separated with a razor blade to remove the gel.

2.3.3 Diffusion cell

2.3.3.1 Diffusion cell for measurement of As diffusion coefficients through diffusive gel and membrane filter

The diffusion coefficients of As^{V} and As^{III} through the diffusive gel and membrane filter were measured using a diffusion cell constructed in-house; it was based on a pseudo-steady-state diffusion cell design similar to that described by Zhang and Davison.[4] The diffusion cell consists of two Perspex compartments (10 cm x 3 cm x 3 cm) which are separated by a 0.25 mm thick Teflon spacer. The compartments and the Teflon spacer have a 1.5 cm diameter opening where the gel and membrane filter are placed. The exposed area of the diffusive gel and membrane filter is 1.77 cm^2. The two compartments are held together using six nuts and

bolts. Both compartments are stirred continuously with magnetic-followers activated by magnetic stirrers (Rank Brothers, Cambridge, UK). The diffusion cell experiments were carried out in the Class-350 clean room. Figure 2.2 shows the diffusion cell that was used to measure the As diffusion coefficients through diffusive gels and membrane filters. The combined thickness of the diffusive gel and membrane filter was used for all diffusion coefficient calculations unless stated otherwise.

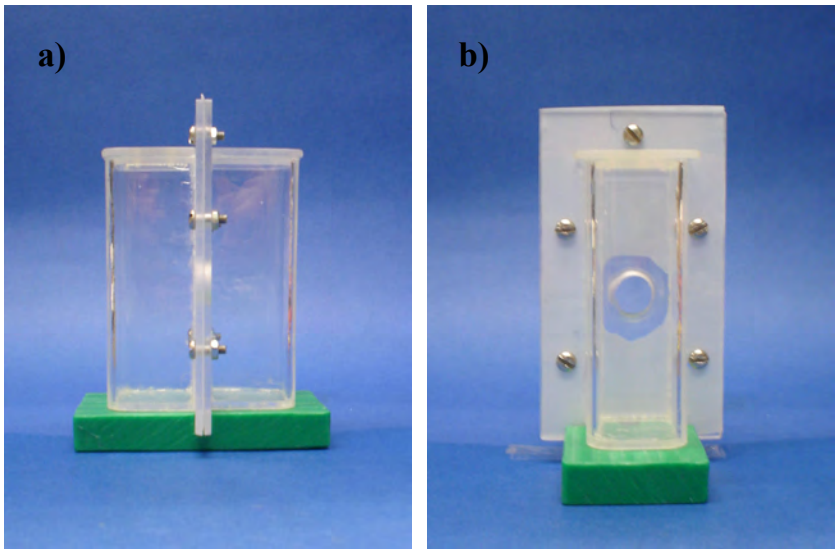

Figure 2.2 Photo of diffusion cell used to measure diffusion coefficients of As through diffusive gels and membrane filters; a) shows the front on view and b) shows the side on view.

2.3.3.2 Diffusion cell for measurement of As diffusion coefficients through Nafion membrane

The diffusion coefficients of As^{V} and As^{III} through the Nafion membrane were measured using a diffusion cell that was specifically designed to accommodate the thin Nafion membrane and prevent leakage of solution from one compartment of the diffusion cell to the other. The diffusion cell consists of two Perspex compartments (8 cm x 4.5 cm x 3.5 cm); at the contact face, one of the Perspex compartments has a 2.5 cm diameter recess (2 mm deep) in which the Nafion membrane is placed, the other compartment has a 2.5 cm diameter raised region. This allows the two compartments to fit tightly together and provide a good seal with the Nafion membrane. A 0.5 mm thick plastic spacer is also placed between the Nafion membrane and the raised region to produce a tight seal. Both compartments of the diffusion cell, and the plastic spacer, have a 2.5 cm diameter opening which allows species to diffuse

from one compartment to the other. The exposed area of the Nafion membrane is 3.14 cm^2. The two compartments of the diffusion cell are held together securely with a clamp which was made in-house. A pin located on the clamp is screwed tightly against the center of the diffusion cell to firmly hold the two compartments together. Both compartments are stirred continuously with magnetic-followers activated by magnetic stirrers (IKA-MINI-MR). The diffusion cell experiments were carried out in the Class-350 clean room. Figure 2.3 shows the diffusion cell that was used to measure the As diffusion coefficients through the Nafion membrane.

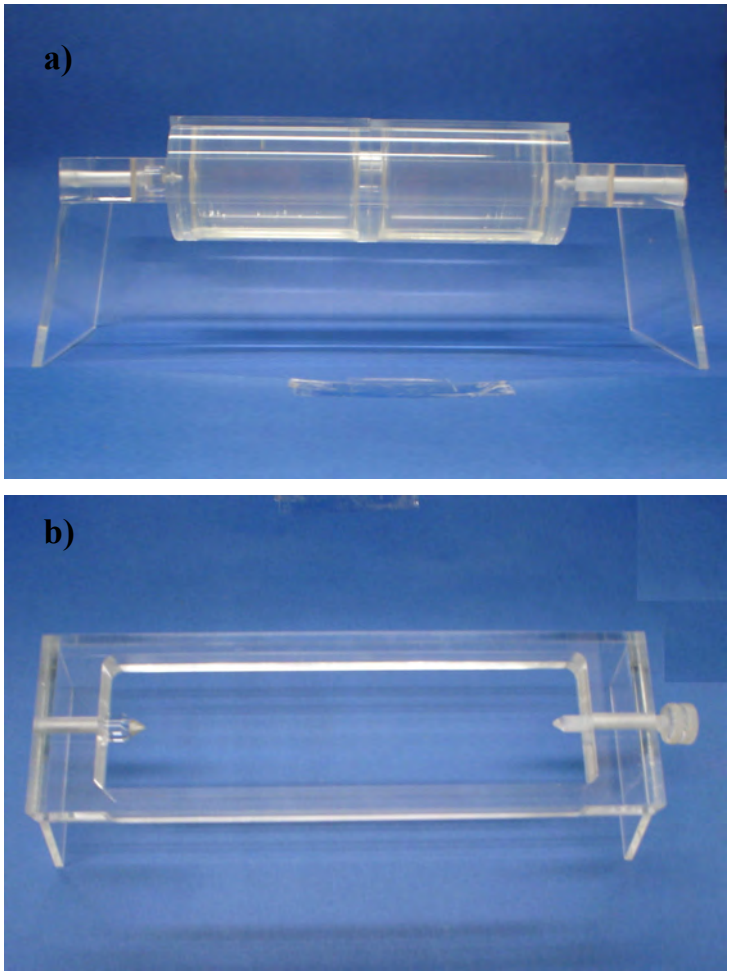

Figure 2.3 Photo of a) diffusion cell used to measure diffusion coefficients of As through the Nafion membrane and b) the clamp that was used to hold the two compartments of the diffusion cell together.

2.3.4 DGT devices

2.3.4.1 DGT devices for measurement of As diffusion coefficients through diffusive gel and membrane filter

The DGT devices that were used to measure the diffusion coefficients of As^{III} and As^{V} through the diffusive gel and membrane filter were supplied by DGT Research Ltd (Lancaster, UK). They consisted of a backing cylinder and a front cap with a 2 cm diameter window. Three holes were added to the base of the backing cylinder in-house to allow the DGT device to be opened without damaging it and hence they could be reused. This was done by aligning the three holes in the base of the backing cylinder with three complementary pins that were located on a plastic base; the DGT assembly was pressed down gently to separate the backing cylinder from the front cap. The DGT devices were reused until the backing cylinder and front cap became too loose to provide a tight seal. Figure 2.4 shows the DGT devices that were used.

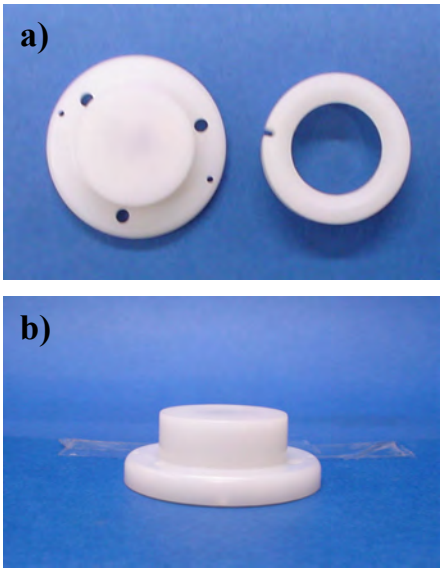

Figure 2.4 Photos of the DGT device that was used to measure the As diffusion coefficients through diffusive gels and membrane filters; a) shows a plan view of the backing cylinder and front cap, b) shows a side-on view of the backing cylinder.

2.3.4.2 DGT devices for measurement of As diffusion coefficients through Nafion membrane

The DGT devices that were used to measure the diffusion coefficients of As^{III} and As^{V} through the Nafion membrane were the same as described above, except that they were

slightly modified to prevent leakage of solution around the membrane. A 0.4 mm deep recess (2 cm in diameter) was drilled into the top of the backing cylinder to accommodate the iron-oxide gel and ~ 3 mm was removed from the bottom of the front cap to ensure a tight fit between the cap and the backing cylinder.

2.3.5 DGT experiments and procedures

2.3.5.1 Assembly of DGT devices and DGT blanks

The non-Nafion DGT devices were assembled by placing a disk of iron-oxide gel on top of the backing cylinder and this was overlain by a disk of diffusive gel and finally a membrane filter. The front cap was placed on top of the backing cylinder assembly and pushed down gently and evenly using a glass plate to ensure uniform pressure. The combined thickness of the diffusive gel and membrane filter was used for all diffusion coefficient calculations unless stated otherwise.

The Nafion DGT devices were assembled by placing a disk of iron-oxide gel (2 cm diameter) within the recess of the backing cylinder; this was overlain by a disk of Nafion (2.5 cm diameter). Figure 2.5 shows a plan view of the backing cylinder which has an iron-oxide gel placed in the recess. The Nafion membrane is extended to the outer edges of the backing cylinder. The front cap was placed on top of the backing cylinder assembly and pushed down gently and evenly using a glass plate to ensure uniform pressure.

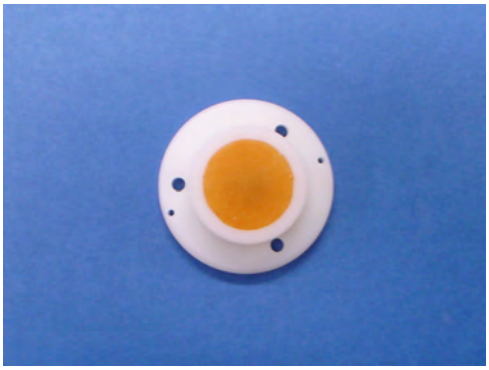

Figure 2.5 Plan view of Nafion DGT device with iron-oxide gel located in the 0.4 mm deep recess (2 cm in diameter).

Blank DGT devices were prepared and subjected to all procedures except deployment. Blank DGT devices were stored in a plastic bag during the deployment period. Plastic tweezers

were used for all manipulations of diffusive gels, iron-oxide gels, membrane filters and Nafion membranes.

2.3.5.2 Deployment of DGT devices

For deployment, DGT devices were held in a Perspex cube-shaped holder (shown in Figure 2.6). The Perspex holder could accommodate up to 30 DGT devices. The holder was placed in a 5 L plastic container which contained the solution of interest. Stirring of the DGT deployment solution was accomplished using a Bibby hotplate/stirrer. Each setting on the stirrer corresponds to an increment in stirring rate of 155 rpm. All DGT experiments were carried out in a temperature-controlled room.

Figure 2.6 Perspex cube holder used to retain DGT devices in place during experiments.

2.3.5.3 Retrieval of DGT devices and elution of iron-oxide gel

After deployment, the DGT devices were removed from the Perspex holder and immediately immersed in Milli-Q water. The DGT devices were washed thoroughly with Milli-Q water before disassembling and removal of the iron-oxide gel. The iron-oxide gels were rinsed with Milli-Q water; excess water was removed from the gel by carefully dabbing on a Durx™ clean room wipe. The iron-oxide gels were placed in acid-cleaned plastic centrifuge tubes and eluted with 2 mL of concentrated HCl (Aristar, BDH) for 24 h on an orbital shaker. After 24 h, 8 mL of Milli-Q water was added to the eluent and left for a further 16 to 24 h before analysis. The addition of water allowed the eluent solution to be handled easier as concentrated HCl caused the iron-oxide gel to deform. Without the addition of water, sampling of the eluent was difficult and often samples became contaminated because of

extensive handling. Immediately prior to sampling the eluent, the plastic centrifuge tubes were given a brief but vigorous shake by hand.

The mass of As in the eluent was measured by HG-AAS. The volume of the iron-oxide gel was taken into account when calculating the mass of As in the eluent. For the non-Nafion DGT device, the volume of the iron-oxide gel was estimated to be 0.16 mL;[5] for the Nafion DGT device, the volume of the iron-oxide gel was estimated to be 0.10 mL.

2.3.6 Membrane filters and pre-treatment

Cellulose nitrate membrane filters were obtained from Schleicher and Schuell. The membrane filters were 0.1 mm thick, 2.5 cm in diameter, and had a pore size of 0.025 μm. Before use, the filters were soaked in Milli-Q water for 24 h and cleaned by soaking in 5 % v/v HNO_3 (Aristar, BDH) for 24 h; they were then rinsed in Milli-Q water and stored in a 0.01 mol L^{-1} $NaNO_3$ (Aristar, BDH) solution at room temperature until use. The membrane filters were reused; after use the membranes were soaked in Milli-Q water for 24 h and cleaned in 5 % v/v HNO_3 (Aristar, BDH) for 24 h, and were stored in the same solution as above.

2.3.7 Nafion membrane and pre-treatment

The 0.05 mm thick Nafion 112 membrane (15 cm x 15 cm) was purchased from Alfa Aesar. The Nafion membrane was hydrated for 1 week and then cut into 2.5 cm diameter disks using a stainless steel cutter that was fabricated in-house. The membranes were cleaned by soaking in 5 % v/v HNO_3 (Aristar, BDH) for 24 h; they were then rinsed in Milli-Q water and stored in a 0.01 mol L^{-1} $NaNO_3$/0.025 mol L^{-1} sodium acetate (pH 5.0) solution at room temperature until use. The Nafion membranes were reused; after use the membranes were soaked in Milli-Q water for 24 h and cleaned in 5 % v/v HNO_3 for 24 h, and were stored in the same solution as above.

2.4 ETAAS instrumentation and protocols

The analysis of As, Fe, Cd, and Cu was carried out using a GBC 908 atomic absorption spectrometer. This was fitted with a GF3000 graphite furnace workhead/power supply, and a PAL 3000 autosampler. Background correction was carried out using a Photron deuterium

arc lamp. For As determinations, this instrument was coupled with a GBC HG3000 hydride generator system.

2.4.1 ETAAS and graphite furnace parameters

2.4.1.1 Instrumental parameters

The instrumental parameters for the determination of Cd, Cu, and Fe by ETAAS are shown in Table 2.2.

Element	HCL* manufacturer	Lamp current /mA	Wavelength /nm	Slit width /nm	Slit height
Cadmium	Pye Unicam Ltd.	6.0	228.8	0.5	Reduced
Copper	Pye Unicam Ltd.	8.0-14.0	324.8	0.5	Reduced
Iron	Pye Unicam Ltd.	6.0-18.0	248.3	0.2-2.0	Reduced

Table 2.2 Instrumental parameters used for the determination of Cd, Cu, and Fe by ETAAS.

*HCL = Hollow cathode lamp

2.4.1.2 Graphite furnace heating programs

The graphite furnace heating programs for the determination of Cd, Cu, and Fe by ETAAS are shown in Tables 2.3, 2.4, and 2.5, respectively.

Step	Final Temperature/^{o}C	Ramp time/s	Hold time/s	Inert gas	Read
1	90	1.0	0.0	Yes	No
2	120	20.0	20.0	Yes	No
3	150	5.0	5.0	Yes	No
4	400	10.0	5.0	Yes	No
5	200	3.6	5.0	No	No
6	2300	1.1	2.0	No	Yes
7	2300	1.6	2.0	Yes	No

Table 2.3 Graphite furnace heating program for Cd measurements by ETAAS

Step	Final Temperature/°C	Ramp time/s	Hold time/s	Inert gas	Read
1	90	10.0	0.0	Yes	No
2	120	10.0	10.0	Yes	No
3	150	10.0	10.0	Yes	No
4	800	15.0	10.0	Yes	No
5	400	3.1	5.0	No	No
6	2200	0.9	3.0	No	Yes
7	2400	0.1	2.0	Yes	No

Table 2.4 Graphite furnace heating program for Cu measurements by ETAAS

Step	Final Temperature/°C	Ramp time/s	Hold time/s	Inert gas	Read
1	95	1.0	1.0	Yes	No
2	110	10.0	15.0	Yes	No
3	150	5.0	10.0	Yes	No
4	1400	15.0	5.0	Yes	No
5	100	6.6	2.0	No	No
6	2200	1.1	2.0	No	Yes
7	2600	1.0	2.0	Yes	No

Table 2.5 Graphite furnace heating program for Fe measurements by ETAAS

2.4.1.3 Graphite furnaces

GBC and Photron graphite furnaces were used for all ETAAS measurements.

2.4.2 Arsenic analysis by hydride generation atomic absorption spectrometry (HG-AAS)

2.4.2.1 HG 3000 hydride generator

The flow manifold and set up for the HG 3000 hydride generator is shown in Figure 2.7. Arsine gas (AsH_3) that was produced during the reaction of $NaBH_4$ with the As sample was separated from the liquid phase by the gas-liquid separator and transported to the graphite furnace by a stream of argon. The AsH_3 was accumulated on a pre-deposited Pd modifier, located within the graphite furnace, by inserting a glass capillary (which is connected to the gas-liquid separator via Tygon tubing) manually into the dosing hole of the furnace.

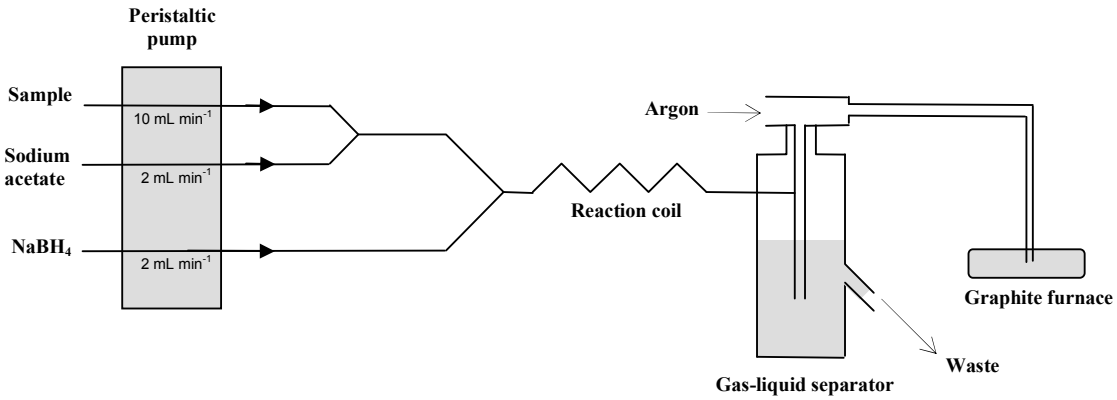

Figure 2.7 Schematic diagram of HG3000 hydride generation set-up used in the work for this thesis. All tubing used was supplied with the HG3000 except that used to deliver AsH_3 into the graphite furnace. The delivery tube was constructed using Ismatec tygon tubing (2.06 mm internal diameter) which was connected to a glass capillary so that the sample could be introduced into the graphite furnace.

The gas-liquid separator that was supplied with the HG 3000 hydride generator was modified in-house to prevent solution from entering the Tygon delivery tubing and causing a blockage. Figure 2.8 shows the gas-liquid separator that was supplied with the HG 3000 hydride generator, and the supplied gas-liquid separator that had been modified by including an extra connector between the separator cap and the neck of the gas-liquid separator.

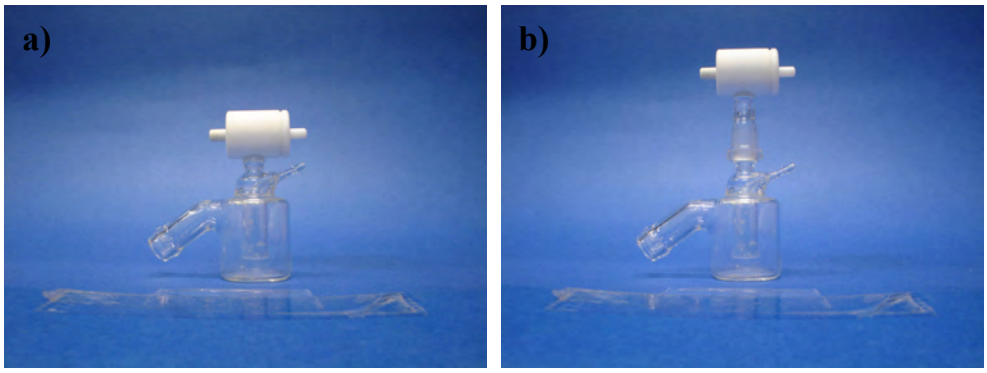

Figure 2.8 Photos of a) gas-liquid separator supplied with the HG3000 hydride generator, and b) modified gas-liquid separator used in the work for this thesis.

2.4.2.2 ETAAS and graphite furnace parameters

The instrumental parameters and the graphite furnace heating program for As measurements by HG-AAS are shown in Tables 2.6 and 2.7, respectively.

Parameter	Value
Lamp manufacturer	Photron
Lamp current/mA	10-16
Wavelength/nm	193.7
Slit width/nm	1.0
Slit height	Reduced

Table 2.6 Instrumental parameters for As measurements by HG-AAS.

Step	Final Temperature/^{o}C	Ramp time/s	Hold time/s	Inert gas	Read
1	45	0.1	0	Yes	No
2	110	10	10	Yes	No
3	150	10	15	Yes	No
4	800	10	15	Yes	No
5	300	5	5	Yes	No
6	300	5	30	No	No
7	300	0	5	No	No
8	300	5	15	Yes	No
9	150	3.3	10	No	No
10	2400	1.2	2	No	Yes
11	2600	0.2	2	Yes	No

Table 2.7 Graphite furnace heating program for As measurements by HG-AAS.

The Pd^{II} modifier (20 μL) was deposited in the graphite furnace in step 1 and thermally pre-treated at 800 ^{o}C in step 4. The AsH_3 was accumulated at 300 ^{o}C in the graphite furnace in step 6.

2.4.2.3 HG-AAS chemical and physical parameters

The chemical and physical parameters used for determination of As by HG-AAS are summarized in Table 2.8.

Parameter	Value
[$NaBH_4$]	0.12 mol L^{-1}
[NaOH] in $NaBH_4$ solution	0.05 mol L^{-1}
[Pd^{II}]	100 ppm
Volume of Pd^{II} solution	20 µL
[HCl] in sample	0.25 % v/v
[Sodium acetate]	0.25 mol L^{-1}
[L-cysteine]*	0.25 % w/v
$NaBH_4$ flow rate	2 mL min^{-1}
Sodium acetate flow rate	2 mL min^{-1}
Sample flow rate	10 mL min^{-1}
Argon flow rate	28 mL min^{-1}
Pd pre-treatment temperature	800 ^oC
Accumulation temperature	300 ^oC
Accumulation time	30 s
Atomization temperature	2600 ^oC

Table 2.8 Chemical and physical parameters used for the analysis of As by HG-AAS.

*Note that L-cysteine was only added to samples for total As analyses.

When using the parameters described in Table 2.8, and the ETAAS and graphite furnace parameters in Tables 2.6 and 2.7, respectively, the As^{III} and total As detection limits were 0.01 and 0.005 ppb, respectively. Note that peak height was used to quantify all As measurements unless stated otherwise.

2.4.2.4 Preparation of reagents for HG-AAS

The preparation of reagents that were used for the generation and accumulation of AsH_3 are detailed below.

A 0.12 mol L^{-1} $NaBH_4$ solution in 0.05 mol L^{-1} NaOH was prepared by dissolving 1 g of NaOH (Analar, BDH) in ~ 350 mL of Milli-Q water, then 2.27 g of $NaBH_4$ (GPR, BDH) was added and made up to 500 mL. This solution was prepared daily to counter decomposition of $NaBH_4$.

Sodium acetate buffer (0.25 mol L^{-1}, pH 5.0) was prepared by dissolving 41.0 g of sodium acetate (Analar, Scharlau) in ~ 1 L of Milli-Q water; 16.5 mL of concentrated acetic acid (Analar, BDH) was added and then the solution was diluted to 2 L.

A 100 ppm Pd^{II} solution was prepared by adding 0.0166 g of $PdCl_2$ (Merck) and 2.5 mL of concentrated HNO_3 (Aristar, BDH) to ~ 80 mL of Milli-Q water; this solution was heated to assist the dissolution of $PdCl_2$. The solution was made up to 100 mL.

A 0.1 mol L^{-1} L-cysteine solution was prepared by dissolving 6.25 g of L-cysteine in 500 mL of Milli-Q water. This solution was prepared daily.

2.4.2.5 Preparation of standards and samples for HG-AAS

For As^{III} analyses, As^{III} standards in the concentration range 0 to 0.8 ppb were prepared by dilution of a 100 ppb As^{III} working stock solution (which was prepared by sequential dilution of the 1000 ppm As^{III} stock solution). The required As^{III} aliquot was added to ~ 20 mL of Milli-Q water, which contained 0.25 mL of concentrated HCl (Aristar, BDH), and made up to 100 mL.

For total As analyses, As^{V} standards in the concentration range 0 to 0.4 ppb were prepared by dilution of a 100 ppb As^{V} working stock solution (which was prepared by sequential dilution of the 1000 ppm As^{V} stock solution). L-cysteine (> 99 %, Applichem) was added to the As^{V} standards to reduce As^{V} to As^{III}. The required As^{V} aliquot was added to 20 mL of 0.1 mol L^{-1} L-cysteine and left for 45 to 60 min; 0.25 mL of concentrated HCl (Aristar, BDH) was then added and the solution made up to 100 mL. The concentration of L-cysteine in the As^{V} standards was 0.02 mol L^{-1}, which is equal to 0.25 % w/v.

Arsenic samples were prepared in the same way as above (depending on the particular As analysis) except that if the sample had already been acidified then the volume of HCl added was such that both standards and samples contained 0.25 % v/v HCl. In some circumstances the volume of the As sample added resulted in a HCl concentration greater than 0.25 % v/v; for these analyses the amount of HCl in the standards was increased so that both standards and samples contained the same concentration of HCl.

At pH 5.0, As^{V} does not form significant amounts of AsH_3 from its reaction with $NaBH_4$ whereas As^{III} does. This allowed the concentrations of As^{III} and As^{V} to be determined in samples containing both As species. Samples containing both As^{III} and As^{V} were first analyzed selectively for As^{III}, then for total As by adding L-cysteine. Addition of 0.25 % w/v L-cysteine to an As^{V} solution gives the same analytical response as addition of 0.25 % w/v L-

cysteine to an As^{III} solution of the same As concentration. The concentration of As^{V} is determined by the difference between the total As and As^{III} measurements.

2.4.3 Coupling of microcolumn with ETAAS

2.4.3.1 Microcolumns

Teflon and polycarbonate microcolumns were fabricated in-house for this experimental work. The microcolumns consisted of three parts (a, b, and c) as shown in Figure 2.9.

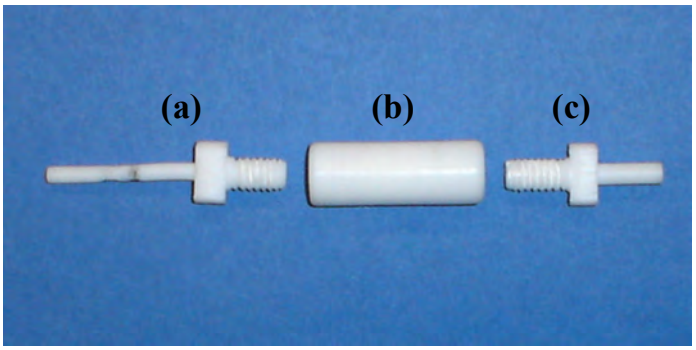

Figure 2.9 Teflon microcolumn used to couple with ETAAS instrument shown in three parts. Part (b) is the central part of the microcolumn which contains a cavity that is packed with the adsorbent. Parts (a) and (c) are connectors which allow the microcolumn to be coupled with the autosampler system of the ETAAS.

Parts (a) and (c) had a 1 mm wide bore drilled through them which allowed Teflon tubing to be inserted to form the injection tip, and to allow the microcolumn to be coupled with the autosampler system. Parts (a) and (c) are screwed into the central part (b) of the microcolumn. The volume of the Teflon microcolumn was 14.7 µL (internal diameter = 1.2 mm, length = 13 mm); the volume of the polycarbonate microcolumn was 23.1 µL (internal diameter = 1.4 mm, length = 15 mm). The microcolumn was inserted into the PAL 3000 autosampler arm as shown in Figure 2.10.

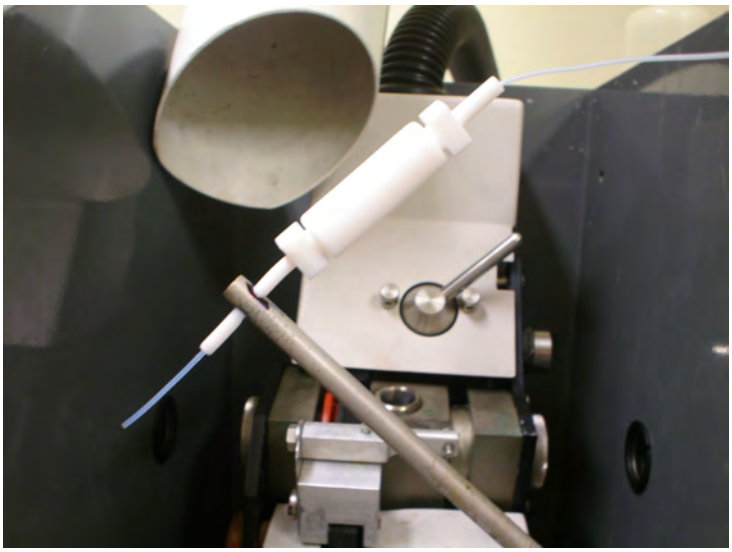

Figure 2.10 Photo showing Teflon microcolumn inserted into the autosampler arm of the ETAAS instrument.

2.4.3.2 Adsorbents

The majority of the microcolumn-ETAAS work utilized Chelex-100 resin as the adsorbent; some work was also briefly carried out using controlled pore glass that was derivatised with 8-hydroxyquinoline (CPG-8HQ). The Chelex-100 resin was purchased from BioRad (200-400 mesh, Na form); CPG-8HQ was purchased from Pierce Chemical (particle size 125-177 μm, pore diameter 500 Å).

Each adsorbent was pre-cleaned by soaking sequentially in 1 mol L^{-1} HNO_3 and 1 mol L^{-1} NaOH for 30 min (while on an orbital shaker). The adsorbent was then rinsed with Milli-Q water and soaked in 0.5 mol L^{-1} ammonium acetate buffer (pH 5.0) before being packed into the micocolumn as a slurry. One end of the microcolumn was attached to a syringe which enabled the adsorbent to be drawn into the microcolumn and packed. The adsorbent was retained within the microcolumn by using a circular piece of fine nylon mesh (50 μm mesh size) which was placed between the resin and the connectors at both ends of the microcolumn. The microcolumn was packed daily with new adsorbent to prevent problems that can occur when the adsorbent is continuously converted from the acidic to the basic form.

2.4.3.3 Microcolumn-ETAAS setup

The microcolumn-ETAAS set-up is illustrated schematically in Figure 2.11. The set-up contained a 3-way valve which was built in-house; this allowed the autosampler to be

operated in its conventional form (with the microcolumn in place), or alternatively the autosampler syringe system could be isolated and thus buffer could be pumped across the column using a peristaltic pump.

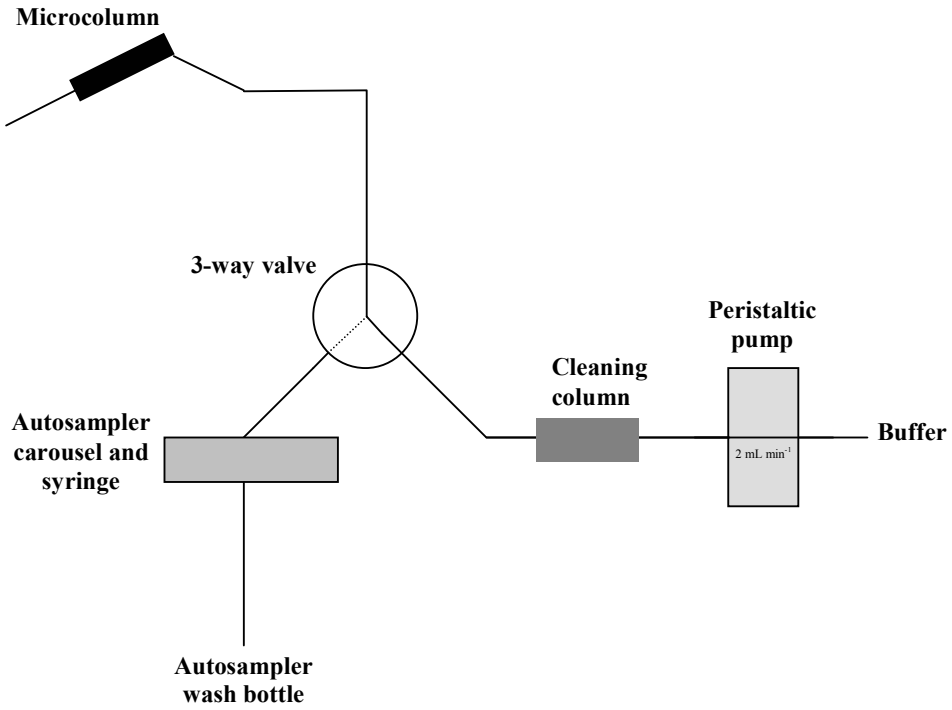

Figure 2.11 Schematic representation of the microcolumn-ETAAS set-up used in the work for this thesis. Manifold tubing was PTFE microbore (0.55 mm internal diameter); Isamatec tygon tubing (0.95 mm internal diameter) was used to connect PTFE tubing together. The flow across the microcolumn was controlled by the autosampler in its conventional form (i.e. autosampler syringe) or by an Alitea peristaltic pump using Ismatec tygon pump tubing. The pump speed was 2 mL min^{-1}. The buffer line contained a column of Chelex-100 to purify the buffer on-line. The injection speed of sample into the furnace was 4 μL s^{-1}.

2.4.3.4 Microcolumn-ETAAS procedure and experimental conditions

The procedure for use of the microcolumn-ETAAS system is shown below:

i) Ammonium acetate (0.05 mol L^{-1}) is pumped across the microcolumn for 3 min at a flow rate of 2 mL min^{-1}.
ii) Milli-Q water is pumped across the microcolumn for 3 min at a flow rate of 2 mL min^{-1}.

iii) The 3-way valve is switched to the position that allows the autosampler to operate in its conventional form.

iv) The ETAAS instrument is started and the microcolumn-autosampler system withdraws sequentially 10 µL of Milli-Q water, 10 µL of sample, and 25-35 µL of Milli-Q water. These solutions are contained in Teflon cups which are located in the autosampler tray.

v) The sample and Milli-Q water aliquots are injected into the graphite furnace and analyzed using the heating program and parameters described in section 2.4.1. This signal represents the 'inert' fraction of metal in a sample.

vi) The microcolumn-autosampler system withdraws sequentially 10 µL of Milli-Q water, 10 µL of 1 mol L^{-1} HNO_3 and 25-35 µL of Milli-Q water. These solutions are contained in Teflon cups which are located in the autosampler tray. The Teflon cup that contained the sample in step (iv) is replaced manually with a Teflon cup that contained 1 mol L^{-1} HNO_3.

vii) The HNO_3 and Milli-Q water aliquots are injected into the graphite furnace and analyzed using the heating program and parameters described in section 2.4.1. This signal represents the 'labile' (column-exchanged) fraction of metal in a sample.

viii) The 3-way valve is switched to the other position and steps (i)-(vii) are repeated with another sample or to carry out repeat measurements.

Steps (i) and (ii) are to buffer the microcolumn and to remove residual buffer from within the microcolumn, respectively. The Milli-Q water aliquot (10 µL) that is taken up before the sample or HNO_3 aliquot, in steps (iv) and (vi), ensures that all of the sample or HNO_3 is displaced from within the pore volume of the Chelex-100 resin during injection into the graphite furnace. The Milli-Q water aliquot (25-35 µL) that is taken up after the sample or HNO_3 aliquot, in steps (iv) and (vi), ensures that the sample or HNO_3 aliquot is passed completely across the microcolumn.

The samples were prepared in a solution containing 0.005 mol L^{-1} ammonium acetate (pH 5.0).

2.5 Miscellaneous equipment

2.5.1 Glassware and cleaning protocol

All glassware was of a minimum 'B' grade standard. Glass bulb pipettes were calibrated regularly by weighing the mass of Milli-Q water dispensed at a known temperature. All glassware and plastic containers and bottles were thoroughly washed before use by applying the following cleaning protocol:

1. In the standard laboratory:
   i) Wash thoroughly using tap water and detergent.
   ii) Rinse in Milli-Q water.
   iii) Immerse in 10 % v/v Analar HNO_3 for at least 24 h. This solution was contained in a 10 L glass bath which had been acid washed.
   iv) Rinse thoroughly in Milli-Q water and leave to soak for at least 24 h. This solution was contained in a 10 L glass bath which had been acid washed.

2. In the clean room
   i) Immerse in 1 % v/v Aristar HNO_3 for at least 24 h. This solution was contained in either a 5 L plastic beaker or a 10 L glass bath which had been acid washed.
   ii) Wash thoroughly with Milli-Q water and soak for at least 24 h. This solution was contained in either a 5 L plastic beaker or a 10 L glass bath which had been acid washed.
   iii) Wash thoroughly with Milli-Q water and air dry. All cleaned volumetric flasks were filled with Milli-Q water and stored; all other glassware and plastic components were stored in either plastic containers or plastic bags.

Glassware and plastic components that were already in the clean room were only exposed to the second part of the cleaning process whereas glassware and plastic components that were brought into the clean room were exposed to both parts of the cleaning process. Glassware that had come into contact with highly concentrated As or metal solutions (> 1 ppm) were re-exposed to the entire cleaning process. In addition, a set of volumetric flasks were kept aside that were only used for highly concentrated As or metal solutions; this was done to minimize contamination between samples.

The Milli-Q water in the water baths was replaced daily; the HNO_3 in the acid baths was changed at least every three months.

2.5.2 Micropipettes

Gilson Pipetteman™ micropipettes were used to measure small solution volumes. The four micropipettes used were: P20 (2-20 μL), P100 (20-100 μL), P200 (50-200 μL), and the P1000 (200-1000 μL). For larger volumes (0.5 to 5 mL), an Eppendorf Research 5000 pipette was used. These micropipettes were calibrated daily by weighing the mass of Milli-Q water dispensed at a known temperature. Appropriate micropipette tips were used as supplied, without further cleaning.

2.5.3 pH measurement

The measurement of pH was made using a pH meter (Hanna Instruments, HI88424) which was calibrated with standard phthalate (pH 4.01) and phosphate buffers (pH 7.00). The preparation of these buffers is described in sections 2.2.4.5 and 2.2.4.6.

2.5.4 Filtration

Schleicher and Schuell cellulose nitrate membrane filters (0.025 μm) were used to filter all samples. Membrane filters were used in an acid-washed glass vacuum-filtration apparatus that had been pre-rinsed with the solution to be filtered.

2.5.5 Balance

A Mettler AE163 balance was used for all weighing. This balance was calibrated regularly using the internal calibration system.

2.5.6 Orbital shaker

A Bioline orbital shaker (Edwards Instrument Co.) was used to mix the DGT eluents.

2.6 Speciation calculations

Solution speciation was modeled using the computer program SPECIES which is part of the IUPAC Stability Constants Database.[6] The appropriate stability and protonation constants were obtained from the IUPAC Stability Constants Database unless otherwise stated. Tables 2.9 and 2.10 show the stability and protonation constants that were used for the speciation calculations associated with the DGT and the microcolumn work, respectively. The stability constants ($\beta_{p,q,r}$) are given according to the reaction:

$$pH^{+} + qM^{n+} + rL^{n'-} \rightleftharpoons H_pM_qL_r^{(p + qn - rn')+}$$

Species	(*p,q,r*)	log $\beta_{(p,q,r)}$
Arsenate (AsO_4^{3-})		
$HAsO_4^{2-}$	(*1,0,1*)	11.50
$H_2AsO_4^{-}$	(*2,0,1*)	18.44
H_3AsO_4	(*3,0,1*)	20.63
$CaAsO_4^{-}$	(*0,1,1*)	4.30
$CaHAsO_4$	(*1,1,1*)	14.25
$CaH_2AsO_4^{+}$	(*2,1,1*)	19.83
Arsenite (AsO_3^{3-})		
$HAsO_3^{2-}$	(*1,0,1*)	13.41*
$H_2AsO_3^{-}$	(*2,0,1*)	25.52*
H_3AsO_3	(*3,0,1*)	34.74*

Table 2.9 Stability constants ($\beta_{p,q,r}$) used for solution speciation calculations for the DGT work.

*These stability constants were obtained from Wilkie and Hering.[7]

Species	(*p,q,r*)	log $\beta_{(p,q,r)}$
*MIDA**		
HMIDA	(*1,0,1*)	9.65
H_2MIDA	(*2,0,1*)	11.77
Cd(MIDA)	(*0,1,1*)	6.77
Acetate (CH_3COO^{-})		
CH_3COOH	(*1,0,1*)	4.76
$Cd(CH_3COO)^{+}$	(*0,1,1*)	1.93
$Cd(CH_3COO)_2$	(*0,1,2*)	3.15
Ammonia (NH_3)		
$Cd(NH_3)^{2+}$	(*0,1,1*)	2.66
$Cd(NH_3)_2^{2+}$	(*0,1,2*)	4.75
$Cd(NH_3)_3^{2+}$	(*0,1,3*)	6.18
$Cd(NH_3)_4^{2+}$	(*0,1,4*)	7.11
$Cd(NH_3)_5^{2+}$	(*0,1,5*)	6.82
$Cd(NH_3)_6^{2+}$	(*0,1,6*)	4.40
NH_4^{+}	(*1,0,1*)	9.11

Table 2.10 Stability constants ($\beta_{p,q,r}$) used for solution speciation calculations for the Chelex-100 microcolumn work.

*MIDA = methyliminodiacete; this ligand was used to model the Chelex-100 resin

2.7 References

1. Gregor, J. E.; Powell, H. K. J.; Town, R. M., Evidence for aliphatic mixed-mode coordination in copper(II)-fulvic acid complexes. *Journal of Soil Science* **1989,** 40, (3), 661-673.

2. Powell, H. K. J.; Fenton, E., Size fractionation of humic substances: Effect on protonation and metal binding properties. *Analytica Chimica Acta* **1996,** 334, (1-2), 27-38.

3. Zhang, H.; Davison, W.; Gadi, R.; Kobayashi, T., In situ measurement of dissolved phosphorus in natural waters using DGT. *Analytica Chimica Acta* **1998,** 370, (1), 29-38.

4. Zhang, H.; Davison, W., Diffusional characteristics of hydrogels used in DGT and DET techniques. *Analytica Chimica Acta* **1999,** 398, (2-3), 329-340.

5. Zhang, H.; Davison, W., Direct in situ measurements of labile inorganic and organically bound metal species in synthetic solutions and natural waters using diffusive gradients in thin films. *Analytical Chemistry* **2000,** 72, (18), 4447-4457.

6. Pettit, L.; Powell, H. K. J. *'SC-Database: Stability Constants Database'*, IUPAC, Academic Software, Oxford: 2005.

7. Wilkie, J. A.; Hering, J. G., Adsorption of arsenic onto hydrous ferric oxide: Effects of adsorbate/adsorbent ratios and co-occurring solutes. *Colloids and Surfaces a-Physicochemical and Engineering Aspects* **1996,** 107, 97-110.

Chapter 3

Investigation and optimization of hydride generation atomic absorption spectrometry (HG-AAS) for As determination

3.1 Introduction

Hydride generation is an analytical method employed to determine those elements that can form volatile stable hydrides. These elements include As, Sb, Bi, Ge, Pb, Sn, Se and Te.[1] The hydrides of the first 6 elements above are generally known as arsine (AsH_3), stibine (SbH_3), bismuthine (BiH_3), germane (GeH_4), plumbane (PbH_4), and stannane (SnH_3), respectively.[2] Briefly, the method employed for this work involves reaction of an acidified As^{III} or As^{V} solution with $NaBH_4$ (stabilized with NaOH) to produce AsH_3 gas. Arsine is transported to the graphite furnace (using a flow of argon) where it is accumulated by adsorption on a metallic Pd coating within the graphite furnace. The Pd is deposited in an earlier step as a Pd^{II} salt and converted to metallic Pd by pre-treatment at high temperatures. The adsorbed As species and Pd are volatilized from the surface of the graphite furnace at high temperatures and during the atomization step atomic As is produced. The As adsorbs radiation from an appropriate light source within an atomic absorption spectrometer.

A variety of detection methods have been used to determine the hydride that is generated. These include: atomic absorption[3-5] (which encompasses flame, electrothermal, and quartz tube atomization), atomic emission,[6, 7] and atomic fluorescence[8-11]spectrometry. In addition, mass spectrometry detection has also been used.[12-14] Furthermore, hydride generation has been coupled with various chromatographic methods that enable separation of various hydride forming species.[5, 7, 8, 10, 14] This can lead to chemical speciation information.[5, 7, 8, 10, 14] The hydride generation method has been applied to a variety of matrices; these include animal and plant tissues,[4, 8, 13-15] blood,[9] urine,[5, 9, 14] and a range of natural waters.[7, 10-12] The

hydride generation method is diverse with regards to the samples that can be analyzed and the detection methods that can be used.

The advantages of hydride generation include: (i) separation of the analyte from the matrix, which leads to a reduction in spectral interferences;[16] (ii) in some instances, preconcentration or accumulation of the hydride, thus resulting in an increase in sensitivity; and (iii) selective hydride generation.

The hydride generation process can be considered as consisting of four steps.[2] First, generation and separation of the hydride from the liquid phase; second, accumulation/trapping of the hydride (if necessary); third, transport of the hydride; and fourth, atomization of the hydride. Steps two and three can be inter-changeable. The following sections explain some of these steps and processes in more detail.

3.1.1 Generation of hydrides

The generation of hydrides can be accomplished by the use of wet chemical methods such as metal/acid or tetrahydroborate reduction.[1] Tetrahydroborate reduction is the most common wet chemical method used and is discussed further in section 3.1.1.1. Alternatively, electrochemical methods can be used for generation of the hydride.[17-19] In electrochemical hydride generation (EcHG) the analyte is converted to the corresponding hydride at the cathode surface. EcHG is not as common as wet chemical methods, even though, according to Denkhaus *et al*.,[19] it offers distinct advantages. These advantages include: (i) the absence of $NaBH_4$, which is an expensive reagent and is susceptible to introducing contamination; (ii) EcHG does not depend on analyte oxidation state when using some cathode materials, so the need to pre-reduce the analyte is not required (pre-reduction is explained in section 3.1.1.2); and (iii) under appropriate conditions, interferences in the solution and gas phase can be reduced. However the reasons why EcHG is not commonly used may be due to some of the problems of this technique suggested by Denkhaus *et al*.[19] These include the difficulty in forming a reproducible solid electrode surface, and if the correct electrode material is not used, the formation of hydrides can be negatively or positively affected by contaminant ions.

3.1.1.1 Hydride generation using $NaBH_4$

Sodium borohydride is the most common tetrahydroborate reductant used to generate hydrides. The exact mechanism which leads to the formation of hydrides is not well understood and there are generally two types of mechanism described in the literature. These are classified as either a "nascent hydrogen" or "non-nascent hydrogen" mechanism.[1]

In the nascent hydrogen mechanism the effective species in the reduction process is assumed to be atomic hydrogen or "nascent hydrogen". Atomic hydrogen is formed during the acid decomposition of $NaBH_4$ (reaction 3.1) and the analyte is reduced to the hydride by atomic hydrogen according to reaction (3.2),[1] where *m* represents the oxidation state of the analyte and *n* is the coordination number of the hydride.

$$BH_4^- + 3H_2O + H^+ \longrightarrow H_3BO_3 + 8H \qquad \textbf{(3.1)}$$

$$A^{m+} + (m+n)H \longrightarrow AH_n + mH^+ \qquad \textbf{(3.2)}$$

The excess un-reacted atomic hydrogen forms molecular hydrogen, which is one of the final products of acid hydrolysis of tetrahydroborate species, through reactions of the type shown by equations 3.3 and 3.4.[20] The validity of the hypothesis of hydride generation by the nascent hydrogen mechanism has never been demonstrated.[21]

$$H + H \longrightarrow H_2 \qquad \textbf{(3.3)}$$

$$H + H_2O \longrightarrow H_2 + OH \qquad \textbf{(3.4)}$$

A variety of acids have been used to assist decomposition of $NaBH_4$; these include hydrochloric,[22-33] nitric,[32-34] perchloric,[33, 35] sulfuric,[32] acetic,[22, 32, 33, 36] citric,[32] and thioglycolic[22, 36] acids. In addition, citrate,[22, 32, 36] acetate,[30, 32] and Tris(hydroxymethyl)-aminomethane[30] buffers have also been used as reaction media. Due to the decomposition of $NaBH_4$ in acidic media, NaOH is nearly always added to the $NaBH_4$ solution to stabilize it during its use. In some instances the $NaBH_4$ solution is also refrigerated to avoid decompostion,[29, 37] however, frequently it is prepared daily to prevent decomposition from occurring.[22, 23, 25, 26, 31-33, 38-42] On some occasions, no effort is made to stabilize the $NaBH_4$ solution.[33, 43, 44]

The second hydride generation mechanism proposes that the hydride is formed by the action of hydrogen bonded directly to boron through the formation of a hydroboron intermediate. This mechanism has gained support through studies carried out using deuterium labelled reagents. [20, 45-47]

3.1.1.2 Pre-reduction of analyte and selective hydride generation

For analytes such as As, Sb, Se, and Te, pre-reduction is often required to convert the analyte to its lower oxidation state. In their higher oxidation states these analytes are either not converted to their corresponding hydride or the conversion is less efficient.[1] Pre-reduction is important when determining total As concentration as it ensures that the rate of hydride formation is the same for all As species, therefore a single standard can be used for calibration.[27] Measurement of total inorganic As can be achieved without pre-reduction by choosing appropriate hydride generation conditions. This usually involves the use of high $NaBH_4$ and/or acid concentrations.[23, 31, 41] Under these conditions the rate of formation of the hydride is similar for all species. However, the high acid conditions employed can increase the As blank signal and the increase in H_2 produced can lead to an increase in the level of background noise,[39] therefore pre-reduction does offer some advantages.

For As, many of the pre-reduction methods use KI[36, 38] or L-cysteine.[24, 25, 27-29, 34, 35, 37, 39, 48, 49] Reduction by L-cysteine has the advantage of requiring milder conditions than for KI. Potassium iodide requires strong acidic conditions for both the sample and reduction medium;[23] this may result in large amounts of by-products (H_2O, CO_2 and H_2) which may be detrimental to certain detection methods.[29] In addition, high acid concentrations can lead to corrosion of instrument parts.[49] Other advantages of using L-cysteine include: faster and more efficient reduction than KI;[28, 37] increase in sensitivity;[28, 29, 39, 50] and decrease of interferences by transition metals (section 3.1.3.2). Importantly, using L-cystine results in the same sensitivity for both organic and inorganic As species under certain conditions,[24, 25, 27, 37] and therefore total As can be determined.

In some circumstances, the species dependency of hydride generation can be advantageous. Selective hydride generation can be carried out, depending on the reaction conditions, and therefore speciation information can be obtained. For example in the case of inorganic As speciation, the procedure is based on omitting the pre-reduction step and determining As^{III} under reaction conditions in which reduction of As^{III} to the hydride is favourable, but

reduction of As^V is not. This has been achieved by using citrate buffer (pH ≥ 4.5),[22, 36] acetate buffer (pH ≥ 5),[30, 32] or low concentrations of acid and/or $NaBH_4$.[23, 31] Total As can then be determined via pre-reduction of As^V to As^{III}, or selecting conditions in which complete reduction of both forms of As can be achieved (as discussed above). The concentration of As^V can then be calculated by difference. It has been suggested by many researchers that the As species must be fully protonated in order to generate AsH_3.[25, 27, 32, 36]

3.1.2 Use of modifiers to trap and stabilize hydrides

In HG-AAS, the graphite furnace is utilized as both the hydride trapping site and the atomization cell. Early studies employed bare graphite furnaces as the trapping medium. A small amount of the pyrolytic-graphite coating was removed from the surface of the furnace to activate the surface for the trapping of As and Sb hydrides.[51, 52] In general, poor trapping efficiencies for Se, As and Ge hydrides were obtained when pyrolytic-graphite coated furnaces were used rather than electrographite furnaces.[40, 42, 53] Electrographite is a porous material that allows diffusion of analyte species into the material and is relatively reactive towards metals.[54] The porosity and reactivity of electrographite may induce peak tailing, memory effects, or incomplete atomization of the sample. Pyrolytic-graphite coated furnaces are produced by heating an electrographite furnace in 5 % methane/argon.[54] The pyrolytic-graphite forms a dense and essentially pore-less layer on the electrographite base material with a high oxidation resistance and an extremely low permeability.[55] The pyrolytic-graphite reduces both diffusion of analyte into the graphite and the chemical reactivity of the graphite.[54]

There are a number of disadvantages for the trapping of hydrides on bare graphite furnaces; these include the need for a well-developed porous graphite structure for optimum trapping efficiency, high accumulation temperature for some elements (As and Sb), and little chance of multi-element determinations due to differences in thermal trapping parameters between elements.[44] These problems can be overcome with the use of modifiers such as Pd, which act as a substrate onto which the analyte hydride can be adsorbed.[44] Where used in this thesis, Pd implies Pd(s) formed by thermal decomposition of a Pd^{II} salt. The use of Pd leads to an improvement in the thermal stability of the hydride species.[56] Significant improvements in sensitivity and precision for Pd treated graphite furnaces compared to bare graphite furnaces have been reported.[57] Liang *et al*.[41] observed greater than a 6-fold increase in sensitivity when

a Pd coated furnace was used rather than a bare pyrolytic-graphite coated furnace to trap AsH_3. Walcerz *et al*.[40] reported that the use of Pd resulted in greater than a 4-fold increase in sensitivity for electrographite furnaces, and greater than a 40-fold increase in sensitivity for pyrolytic-graphite coated graphite furnaces when determining As. Walcerz *et al*.[40] also found better sensitivity on pyrolytic-graphite coated furnaces for Sb determinations compared to electrographite furnaces.

This significant improvement in sensitivity for the Pd-based system (and other modifiers) is due to the stabilizing effect of the metal on the analyte at high temperatures. This reduces loss of volatile precursor species which leads to an increase in sensitivity,[44] and higher ashing temperatures may be used which can be advantageous in reducing interferences. Furthermore, because volatilization of the analyte species is occurring at a higher temperature, there is more efficient dissociation of any molecular species. In addition, due to the increase in sensitivity observed in the presence of modifier, sample dilution can be used to decrease interferent concentrations.[43] Lastly, trapping of the hydride within the graphite furnace prior to atomization eliminates problems associated with variable rates of hydride formation and evolution.[43]

Many different modifiers have been used for the trapping of hydrides. These include, but are not limited to, Pd,[33, 38, 40-44, 53, 56, 58-61] Zr,[22, 42] Ir,[22, 30, 38, 48, 56, 62, 63] Pt,[44, 53, 59] Rh[38, 44, 56, 58, 62] Ru,[38, 44, 58, 59, 62] W,[22] Ni,[53] Ag,[59] and Ce.[59].

3.1.2.1 Permanent and non-permanent modifiers

Modifiers can be generally classified into two groups: permanent and non-permanent. Non-permanent modifiers must be deposited into the graphite furnace after each atomization step. Permanent modifiers generally can be used for numerous furnace firings without deterioration of analytical performance. The elements most commonly used as permanent modifiers are Pt-group metals with high melting points (Rh, Ru, Ir).

Palladium is an example of a non-permanent modifier; its melting and boiling points are 1555 ^{o}C and 2964 ^{o}C, respectively.[64] At temperatures normally used for atomization (> 2200 ^{o}C), some Pd would be volatilized from the furnace. However, for permanent modifiers such as Ir (melting and boiling points are 2447 ^{o}C and 4428 ^{o}C, respectively[64]), the modifier is retained within the furnace, at temperatures normally required for atomization, because of its low

volatility. Therefore Ir is not required to be deposited after each atomization step. In addition, very stable carbide forming elements (W, Ta, Zr) can also be used as permanent modifiers.[55] Zr, Ir and W permanent coatings have been used for up to 500 accumulation/atomization cycles without the need to re-deposit modifier.[22] However, Garbos *et al*.[42] reported that for a Zr modifier, only 80 cycles could be carried out before deterioration of the analytical signal was observed, presumably due to loss of Zr modifier. The lifetime of permanent modifiers depends on the type of matrix and acids used, the pyrolysis, atomization and cleaning temperatures, and the corresponding times of the individual steps.[65] The quality of the graphite furnace surface may also have an effect on the lifetime of permanent modifiers.

The use of permanent modifiers offers advantages over non-permanent modifiers. These can include; longer tube lifetime, improved detection limits for some modifiers, better long-term signal stability, simpler and quicker heating programmes, higher sample throughput, and lower analytical costs. [62]

Mixed modifiers have also been used.[33, 48, 62] Lima *et al*.[62] compared the use of single permanent modifiers (Rh, Ir, Ru) with mixed permanent modifiers (W-Rh, W-Ir, W-Ru), in which W was deposited first. There was no advantage in using mixed permanent modifiers for the determination of As in a water reference material. The maximum pyrolysis temperature was 1400 ^{o}C in each case. However, for the analysis of more complex solid reference materials, the maximum pyrolysis temperatures obtained for mixed-modifiers were 50 to 150 ^{o}C greater than their single modifier analogues. Furthermore, improved reproducibility and better analyte recoveries, of certified values in reference materials, were obtained when using W-Rh, W-Ir and W-Ru mixed modifiers, when compared with single Rh, Ru and Ir modifiers. Yang and Zhang[33] reported a 40 % increase in sensitivity when a mixed Pd-Zr modifier was used in comparison to just Pd. In addition, the use of the mixed Pd-Zr modifier increased the pyrolysis temperature from 1300 to 1500 ^{o}C.

3.1.2.2 Pd modifiers

Palladium is a very effective modifier that can be used to stabilize many elements to several hundred degrees higher than the temperature possible when no modifier is used.[60] An increase in pyrolysis temperature between 400 and 800 ^{o}C can be achieved depending on the analyte of interest.[61] Palladium is still extensively used even though it is required to be

deposited after each atomization step; in some instances Pd has been reported to give better sensitivities than permanent modifiers.[42, 44, 58, 59]

Palladium can be used to stabilize hydride species such as AsH_3 (as in the work in this thesis) or to stabilize analytes that are injected directly into the graphite furnace from a solution. In the absence of a modifier, Volynsky and Wennrich[58] found that the maximum pyrolysis temperature for As, Se and In was 500, 200, and 600 ^oC, respectively. However, in the presence of Pd, the pyrolysis temperature for As, Se, and In could be increased to 1300, 1200 and 1400 ^oC, respectively, without the lost of analyte from the furnace. Pyrolysis temperatures for As in the presence of Pd have been reported to be as high as 1500 ^oC.[56] The temperature at which the hydride is accumulated (i.e. accumulation temperature) on the Pd surface can also be important. A variety of optimum accumulation temperatures have been reported; these range from 160[41] to 600 ^oC.[43]

The change in appearance temperature (the temperature at which the analyte signal appears) when Pd is used, is believed to be due to the formation of some sort of Pd-As species.[60] It is generally accepted that Pd metal acts as the modifier.[61] Pre-treatment of the Pd modifier by heating to 1000 ^oC[33] or using reducing agents such as ascorbic acid, hydroxylamine hydrochloride, and hydrogen[33, 61] can reduce the metal salt to its metallic form. Voth-Beath and Shrader[61] found considerable differences in the performance of the Pd modifier depending on the reduction method used. Scanning electron micrographs of the various surfaces illustrated that the size and distribution of the Pd particles on the graphite surface varied with the reduction method used.

Even though the addition of reducing agents offers some advantages, thermal reduction (or pre-treatment at high temperatures) of Pd seems to be the most common way of forming metallic Pd on the graphite furnace. Reported pre-treatment temperatures for the Pd modifier vary from as low as 100 ^oC[60] up to 1200 ^oC,[38, 40] with many reported different temperatures within this range.[33, 43, 44, 53, 56, 58, 59, 61]

Often a surfactant is added along with the modifier solution.[40, 42, 53] In some instances this can improve reproducibility and sensitivity;[53] presumably by promoting a more even distribution of Pd over the graphite surface.

3.1.2.3 Pd modifier mechanism

The exact mechanism of action of the Pd modifier is not very well understood. In a recent review by Ortner *et al*.,[55] they comment that the literature is full of very different and often contradictory proposals for the mechanism of action of Pd modifiers. The main reason for these contradictory explanations is the differences in experimental conditions, and the methods used to investigate transformations of solid analyte compounds. [55, 66] Volynsky and de Loos-Vollebregt[66] comment that differences in the amounts of analyte used in ETAAS and in model studies may reach 6 orders of magnitude. This may result in various reaction paths for the same analyte-modifier-graphite systems.[66] Even experiments with realistic analyte to modifier mass ratios, but with an unrealistic relation to the mass of the graphite furnace system, may lead to misleading conclusions.[55]

It is suggested by some workers that the hydride forms an inter-metallic species or alloy with metallic Pd on the graphite surface.[53, 60] However, Ortner *et al*.[55] disagree that analyte stabilization occurs by formation of intermetallic compounds or thermally stabilized alloys. They make the comment that the modifier to analyte ratio is 1000:1 to 100000:1 in all practical cases. However, all inter-metallic compounds or thermally stable alloys are only formed at mass ratios from 1:1 to 100:1. Therefore, they conclude that such compounds cannot be formed and those that found such compounds used unrealistic analyte to modifier mass ratios. Instead, they proposed that Pd forms intercalation compounds with the graphite. The intercalated Pd metal forms strong covalent bonds with easily volatile elements, leading to their stabilization at high temperatures. The action of the modifier is not an effect of the modifier present in particles on the surface, but of activated modifier atoms in the near surface region (to a depth of approximately 10 μm).

Rettberg and Beach[67] examined the effect of Pd on the absorbance signals for As, Cd, Cr, Pb, Sn and Tl. They found that when the mass of modifier was increased, the analyte appearance temperature increased to higher values. The authors conclude that given the large excess of Pd relative to analyte, this observation cannot be explained by more complete conversion of the analyte to the inter-metallic form, and therefore bulk effects may be contributing to the stabilizing action of Pd.

Sturgeon *et al*.[44] showed that the release of the bulk of Pd from the graphite surface was approximately 500 ^{o}C earlier than release of As from the Pd surface. In addition, comparisons

of absorbance profiles for Pd in the presence and absence of a large amount of As showed that the release of Pd is delayed by 160 ^{o}C in the presence of As; this presumably reflects the formation of a less volatile Pd-As species.

3.1.3 Interferences

Interferences in hydride generation can be classified as either liquid-phase or gas-phase interferences.[1] Liquid-phase interferences can occur either during formation of the hydride or its transfer from solution, whereas gas-phase interferences affect the analyte during transport of the hydride to the atomizer/detector. Spectral interferences in hydride generation are less of a problem than in liquid sampling methods due to the separation of the analyte from the matrix.[57] All interferences can have either a direct effect (only observed during interferent generation) or a memory effect (if interference persists after the interferent is removed from the system).[1]

3.1.3.1 Liquid-phase Interferences

Yan and Ni[2] have classified liquid-phase interferences into two groups; compound interferences and matrix interferences. Compound interferences (errors) most commonly arise if the oxidation state of the analyte in the sample is not the same as in the standard solution. For example, the kinetics of hydride generation is different for the formation of the hydride from As^{III}, than from As^{V}. These interferences can be overcome easily by controlling hydride generation conditions or using a pre-reducing strategy (both discussed earlier). Matrix interferences occur when components in the matrix affect the formation or release of the hydride from solution.

3.1.3.2 Matrix interferences

Inorganic species such as Ni^{II},[26, 28, 32, 39, 43, 49, 50, 68-70] Cu^{II},[26, 28, 32, 39, 49, 50, 68-71] Co^{II},[26, 28, 32, 39, 43, 50, 68-71] Zn^{II},[28, 32, 68-70] Cd^{II},[43, 68-71] Pb^{II},[68] Fe^{II},[28, 39, 69] Fe^{III},[28, 29, 32, 68-71] Ag^{I},[28, 68-70] Au^{III}, Pd^{II},[28, 43, 69, 70] Pt^{IV},[28, 43, 69, 70] and Rh^{III} [43] have been shown to interfere with the determination of hydride species.

It is suggested that the interference by transition metals is related to reduction of the metal by $NaBH_4$; producing a finely dispersed metal precipitate. This precipitate can then adsorb and decompose the analyte hydride.[26, 68] Alternatively, the interfering metal ions may react with

$NaBH_4$ to produce metal borides, not elemental metals. The metal borides then cause capture and decomposition of hydrides due to the high reactivity of metal boride species.[50] In addition, the catalytic effect of transition metal ions on the acid decomposition of $NaBH_4$ may play a role.[2]

A variety of methods have been used to eliminate or minimize the interference by transition metals on the generation of hydrides. These include: increasing the concentration of HCl;[26, 43, 69] decreasing the $NaBH_4$ concentration;[26, 43] use of masking agents such as L-cysteine,[28, 39, 43, 50, 69, 70] L-cystine,[69, 70] thiourea,[32, 50, 68, 71] EDTA,[32, 71] Chelex-100,[29, 72] KCN,[71] KI,[50, 71] 1,10-phenanthroline,[32, 50] and thiosemicarbazide.[32, 50] Decreasing the length of the reaction coil has also been suggested to minimize interferences by reducing the reaction time between $NaBH_4$ and the interfering ion.[43, 73]

In addition to interference from transition metals, interference from other hydride-forming elements has also been observed. The elements Bi^{III},[28, 34, 43] Pb^{II},[28] Se^{IV} [28, 34, 43] and Sb^{III} [43] have all been shown to interfere with the hydride generation of As at various concentrations. An *et al.*[43] suggest that this type of interference is due to competition for the active sites of the Pd modifier. The authors showed that Sb^{III} interference on As^{III} could be overcome by increasing the mass of Pd deposited within the furnace. This illustrates the importance of an adequate deposit of Pd when generating hydrides in the presence of other hydride-generating species.

3.1.4 Efficiency of As hydride generation and analyte accumulation

Sturgeon *et al.*,[44] Docekal *et al.*,[74] and Burguera and Burguera[59] reported that the overall efficiency for the generation, transfer, and accumulation of AsH_3 on a Pd modifier, is ~ 100 %. In contrast, Walcerz *et al.*[40] reported an overall 45 % efficiency for the AsH_3 hydride generation/capture process when using a Pd modifier. Yang and Zhang [33] reported an overall 60 % efficiency for As hydride generation/capture for a Pd modifier system, and 96 % for a Pd-Zr based modifier system. These values are derived from a comparison of characteristic masses obtained from the hydride generation method, with those resulting from direct injection of the same mass of analyte and modifier in the form of an aqueous solution.

The efficiency of adsorption for some hydrides can depend on both the type and age of the graphite furnace.[40, 53, 56, 61] Even in the presence of Pd, Walcerz *et al*.[40] observed a difference between pyrolytic-graphite coated and electrographite furnaces for As determinations. The sensitivity for As measurements was ~ 25 % higher for the pyrolytic-graphite coated furnaces than electrographite furnaces. Similar results were obtained for Ge hydrides.[53] Furthermore, in the presence of Pd, Voth-Beach and Shrader[61] reported poorer recoveries for Tl when new pyrolytic-graphite coated furnaces were used in comparison to aged graphite furnaces. The authors comment that it is likely that Pd particle size and distribution is influenced by the chemistry of the graphite furnace. In addition, their results could not always be exactly reproduced; this variation was explained by differences in graphite furnaces.

3.1.5 Chapter outline

As this introduction shows, there are many physical and chemical parameters that contribute to the hydride generation technique. Optimized conditions reported in the literature are sometimes conflicting. These variances are a result of the type of hydride generation used: batch, flow, or continuous hydride generation, and the experimental set up used which includes both the chemical and physical conditions. Therefore, in this work a range of parameters were investigated and optimized for As determination. These included the Pd pre-treatment temperature, mass of Pd, surface area of furnace covered by Pd and the temperature at which AsH_3 is accumulated on the Pd surface. The concentrations and effects of $NaBH_4$, NaOH, HCl, and L-cysteine were also investigated and optimized. Furthermore an investigation of argon flow rate, effect of Fe^{III}, and the influence of furnace age and type were carried out.

The effect of Fe^{III} and any interference it causes is an important parameter to investigate because an iron-oxide based DGT adsorbent is employed in the work for this thesis. In addition, because HCl is used as the eluent for this adsorbent, the effect of HCl was examined.

3.2 Experimental

All general parameters and procedures such as pump flow rates, temperature programs, and preparation of reagents and samples, are the same as described in section 2.4.2 unless otherwise stated.

3.2.1 Pd modifier parameters

A number of parameters associated with the Pd modifier were investigated to establish their effect on measurement sensitivity. These parameters were pre-treatment temperature, accumulation temperature, and mass and surface area of Pd.

3.2.1.1 Pd pre-treatment temperature

The Pd pre-treatment temperature was varied from 150 to 1600 ^{o}C. Palladium (2 μg) was added to the graphite furnace as 20 μL of a 100 ppm Pd^{II} solution ($PdCl_2$, 5 % v/v HNO_3), "dried" at 150 ^{o}C and subjected to the appropriate pre-treatment temperature before accumulation of AsH_3 at 300 ^{o}C. Different treatments were compared on the basis of the As sensitivity after atomization at 2400 ^{o}C. For this work, 0.22 ppb As^{V} (0.25 % v/v HCl, 0.25 % w/v L-cysteine), 0.12 mol L^{-1} $NaBH_4$ (0.05 mol L^{-1} NaOH), and 0.25 mol L^{-1} sodium acetate buffer (pH 5.0) were used. For pre-treatment temperatures < 300 ^{o}C, the accumulation temperature was the same as the pre-treatment temperature. This was carried out to make sure that the observed effect was due to the pre-treatment temperature of Pd and not the higher temperature used for accumulation.

3.2.1.2 Mass of Pd

The mass of Pd was varied from 0.2 to 2 μg by depositing from 20 μL of 10 to 100 ppm $PdCl_2$ (5 % v/v HNO_3) solution. The $PdCl_2$ solution was "dried" and pre-treated at 150 ^{o}C and 800 ^{o}C, respectively. Arsine was accumulated at 300 ^{o}C and atomization was carried out at 2400 ^{o}C. Palladium chloride solutions were prepared by appropriate dilution of a 100 ppm standard and acidified with HNO_3 (5 % v/v). For this work, 0.5 ppb As^{III} (0.25 % v/v HCl), 0.12 mol L^{-1} $NaBH_4$ (0.05 mol L^{-1} NaOH), and 0.25 mol L^{-1} sodium acetate buffer (pH 5.0) were used.

3.2.1.3 Pd surface area

The effect of furnace surface area covered with Pd was examined by varying the volume of solution from which Pd^{II} was deposited into the graphite furnace. The mass of Pd was kept constant at 2 μg. The volume of 50 to 200 ppm $PdCl_2$ solution (5 % HNO_3) was varied from 10 to 40 μL, "dried" at 150 ^oC and pre-treated at 800 ^oC. Arsine was accumulated at 300 ^oC and atomization was carried out at 2400 ^oC. For this work, 0.5 ppb As^{III} (0.25 % v/v HCl), 0.12 mol L^{-1} $NaBH_4$ (0.05 mol L^{-1} NaOH), and 0.25 mol L^{-1} sodium acetate buffer (pH 5.0) were used.

3.2.1.4 Accumulation temperature

The accumulation temperature was varied from 25 to 600 ^oC. Palladium (2 μg) was deposited from 20 μL of a 100 ppm Pd^{II} solution ($PdCl_2$, 5 % v/v HNO_3), "dried" at 150 ^oC and pre-treated at 800 ^oC. Atomization was carried out at 2400 ^oC. For this work, 0.2 ppb As^V (0.25 % v/v HCl and 0.25 % w/v L-cysteine), 0.12 mol L^{-1} $NaBH_4$ (0.05 mol L^{-1} NaOH), and 0.25 mol L^{-1} sodium acetate buffer (pH 5.0) were used.

3.2.2 Effect of $NaBH_4$ and NaOH concentrations

The effects that the concentrations of $NaBH_4$ and NaOH have on the generation of AsH_3 from As^{III} and As^V solutions were examined. These measurements were made in the absence and presence of L-cysteine.

3.2.2.1 Effect of $NaBH_4$ concentration at constant NaOH concentration

The concentration of $NaBH_4$ was varied from 0.04 to 0.28 mol L^{-1}. The study was carried out under conditions in which the concentration of NaOH (0.05 mol L^{-1}) was constant for each $NaBH_4$ concentration. Palladium (2 μg) was deposited from 20 μL of a 100 ppm Pd^{II} solution ($PdCl_2$, 5 % v/v HNO_3), "dried" at 150 ^oC and pre-treated at 800 ^oC. Arsine was accumulated at 300 ^oC and atomization was carried out at 2400 ^oC. For this work, 0.25 ppb As^V (0.25 % v/v HCl and 0.25 % w/v L-cysteine), 0.5 ppb As^{III} (0.25 % v/v HCl), and 0.25 mol L^{-1} sodium acetate buffer (pH 5.0) were used.

3.2.2.2 Effect of $NaBH_4$ concentration at varying NaOH concentrations

The concentration of $NaBH_4$ was varied from 0.04 to 0.24 mol L^{-1}. The concentration of NaOH was also varied, however the [$NaBH_4$]/[NaOH] ratio was held constant at 0.8. Table

3.1 shows the various concentrations of $NaBH_4$ and NaOH used for these experiments. Palladium (2 μg) was deposited from 20 μL of a 100 ppm Pd^{II} solution ($PdCl_2$, 5 % v/v HNO_3), "dried" at 150 ^oC and pre-treated at 800 ^oC. Arsine was accumulated at 300 ^oC and atomization was carried out at 2400 ^oC. For this work, 0.2 ppb As^V (0.25 % v/v HCl, 0.25 % w/v L-cysteine), 0.4 ppb As^{III} (0.25 % v/v HCl), and 0.25 mol L^{-1} sodium acetate buffer (pH 5.0) were used.

$[NaBH_4]$/mol L^{-1}	[NaOH]/mol L^{-1}	$[NaBH_4]$/[NaOH]
0.04	0.05	0.8
0.08	0.1	0.8
0.12	0.15	0.8
0.16	0.2	0.8
0.20	0.25	0.8
0.24	0.3	0.8

Table 3.1 Table showing various $NaBH_4$ and NaOH concentrations used to examine the effect of $NaBH_4$ concentration at constant $[NaBH_4]$/[NaOH] ratio.

3.2.2.3 Effect of NaOH concentration at optimum $NaBH_4$ concentration

The concentration of NaOH was varied from 0.05 to 0.5 mol L^{-1} at 0.12 mol L^{-1} $NaBH_4$. Palladium (2 μg) was deposited from 20 μL of a 100 ppm Pd^{II} solution ($PdCl_2$, 5 % v/v HNO_3), "dried" at 150 ^oC and pre-treated at 800 ^oC. Arsine was accumulated at 300 ^oC and atomization was carried out at 2400 ^oC. For this work, 0.5 ppb As^{III} (0.25 % v/v HCl), 0.25 ppb As^V (0.25 % v/v HCl, 0.25 % w/v L-cysteine), 0.12 mol L^{-1} $NaBH_4$, and 0.25 mol L^{-1} sodium acetate buffer (pH 5.0) were used.

3.2.3 Hydrochloric acid concentration

The concentration of HCl in the As sample solutions was varied from 0 to 2.4 mol L^{-1} for As^V (L-cysteine present) and from 0 to 4.2 mol L^{-1} for As^{III} (L-cysteine absent), to establish its effect on sensitivity. Palladium (2 μg) was deposited from 20 μL of a 100 ppm Pd^{II} solution ($PdCl_2$, 5 % v/v HNO_3), "dried" at 150 ^oC and pre-treated at 800 ^oC. Arsine was accumulated at 300 ^oC and atomization was carried out at 2400 ^oC. For this work,0.5 ppb As^{III}, 0.25 ppb As^V (0.25 % w/v L-cysteine), 0.12 mol L^{-1} $NaBH_4$ (in 0.05 mol L^{-1} NaOH), and 0.25 mol L^{-1} sodium acetate buffer (pH 5.0) were used.

3.2.4 Effect of graphite furnace age and type

The effect of the graphite furnace surface quality was examined by performing measurements on new and aged graphite furnaces. In addition, graphite furnaces from the same batch and from different batches were compared. Palladium (2 μg) was deposited from 20 μL of a 100 ppm Pd^{II} solution ($PdCl_2$, 5 % v/v HNO_3), "dried" at 150 ^oC, and pre-treated at 800 ^oC or 1400 ^oC. Arsine was accumulated at 300 ^oC and atomization was carried out at 2400 ^oC. For this work, 0.5 ppb As^V (0.25 % v/v HCl, 0.25 % w/v L-cysteine), 0.12 mol L^{-1} $NaBH_4$ (0.05 mol L^{-1} NaOH), and 0.25 mol L^{-1} sodium acetate buffer (pH 5.0) were used.

3.2.5 Effect of Fe^{III}

To establish the effect of Fe^{III} on sensitivity the concentration of Fe^{III} present in standard As solutions was varied from 0 to 2 ppm for As^{III} (L-cysteine absent) and 0 to 200 ppm for As^V (L-cysteine present). Palladium (2 μg) was deposited from 20 μL of a 100 ppm Pd^{II} solution ($PdCl_2$, 5 % v/v HNO_3), "dried" at 150 ^oC and pre-treated at 800 ^oC. Arsine was accumulated at 300 ^oC and atomization was carried out at 2400 ^oC. For this work, 0.4 ppb As^{III} (0.25 % v/v HCl), 0.2 ppb As^V (0.25 % v/v HCl, 0.25 % w/v L-cysteine), 0.12 mol L^{-1} $NaBH_4$ (0.05 mol L^{-1} NaOH), and 0.25 mol L^{-1} sodium acetate buffer (pH 5.0) were used. A 1000 ppm $Fe(NO_3)_3$ atomic absorption standard was used as the Fe^{III} stock solution. In the absence of L-cysteine, Fe^{III} was added to acidified Milli-Q water before the addition of As^{III}. In the As^V experiments, Fe^{III} was added to the L-cysteine solution followed by As; HCl was added 45 to 60 min later.

3.2.6 Effect of argon flow rate

The flow rate of argon was varied from 0 to 100 mL min^{-1} using the flow regulator within the hydride generator unit. The flow rate was measured by using an inverted measuring cylinder and measuring the volume of water displaced from the measuring cylinder by the argon flow exiting the hydride generator unit, before connecting to the gas-liquid separator. Palladium (2 μg) was deposited from 20 μL of a 100 ppm Pd^{II} solution ($PdCl_2$, 5 % v/v HNO_3), "dried" at 150 ^oC and pre-treated at 800 ^oC. Arsine was accumulated at 300 ^oC and atomization was carried out at 2400 ^oC. For this work, 2 ppb As^{III} (0.25 % v/v HCl), 0.16 mol L^{-1} $NaBH_4$ (0.05 mol L^{-1} NaOH), and 0.25 mol L^{-1} sodium acetate buffer (pH 5.0) were used.

3.3 Results

For this section, sensitivity has been accessed in terms of the height of the absorbance peak unless otherwise stated.

3.3.1 Pd modifier parameters

3.3.1.1 Pd pre-treatment temperature

The Pd pre-treatment temperature affected As sensitivity. The two sets of data illustrated in Figure 3.1 represent measurements undertaken on different days with graphite furnaces from different batches, however all other chemical and physical parameters were similar. For data set 1 (●) there was no significant difference in sensitivity (absorbance) as the temperature was increased from 150 to 800 ^{o}C. However, at temperatures between 800 and 1400 ^{o}C there was a small increase in sensitivity from 0.200 to 0.245, before a marked decrease at temperatures greater than 1400 ^{o}C. Data set 2 (□) showed similar behavior to data set 1, except it showed a small increase in sensitivity for pre-treatment temperatures in the range 200 to 600 ^{o}C. In addition, the decrease in sensitivity for data set 1 was observed at a lower temperature (> 1200 ^{o}C) compared to data set 1 (> 1400 ^{o}C).

Experiments were also carried in which 20 µL of 100 ppb Pd^{II} solution ($PdCl_2$, 1 % v/v HNO_3) was injected directly into the graphite furnace (a different furnace was used from those discussed above) and Pd absorbance monitored at 340.5 nm. This showed that Pd is volatilized from the furnace at temperatures greater than 1350 ^{o}C, which coincides with the decrease observed in the As sensitivity.

The pre-treatment temperature also affected the absorbance-time profiles of the transient As signals observed for both data sets 1 (Figure 3.2) and 2 (not shown). At low temperatures (≤ 800 ^{o}C) the profiles are non-symmetrical with a shoulder evident on the low-temperature side of the signal, resulting in a double peak. As the temperature was increased from 150 to 800 ^{o}C this shoulder diminished and the absorbance signal became more symmetrical. Between 800 ^{o}C and 1400 ^{o}C the half-width of the absorbance signal decreased; this coincides with the increase in sensitivity in this temperature range as discussed previously for data set 1. Furthermore, for data set 1 and 2, there is very little change in peak area in the pre-treatment temperature range 150-1400 ^{o}C (data not shown). The appearance times of the signals varied slightly with pre-treatment temperature as shown in Table 3.2.

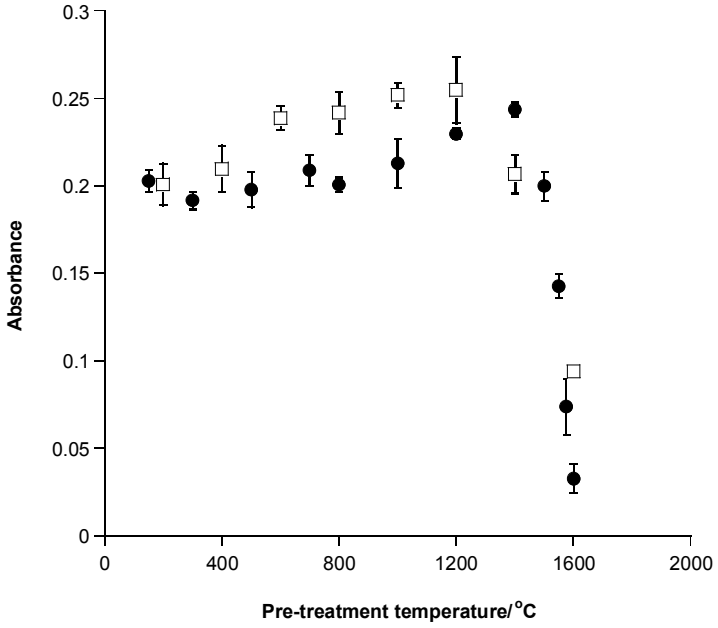

Figure 3.1 Effect of Pd pre-treatment temperature on As^V sensitivity for data set 1 (●) and data set 2 (□). The concentration of As^V was 0.22 ppb (0.25 % v/v HCl, 0.25 % w/v L-cysteine), the $NaBH_4$, NaOH, and sodium acetate buffer (pH 5.0) concentrations were 0.12, 0.05 and 0.25 mol L^{-1}, respectively. Palladium (2 μg) was deposited from 20 μL of 100 ppm $PdCl_2$ solution (5 % v/v HNO_3) and "dried" at 150 ^oC. Arsine was accumulated at 300 ^oC (for pre-treatment temperatures less than 300 ^oC the accumulation temperature was the same as the pre-treatment temperature). Atomization was carried out at 2400 ^oC. The uncertainty associated with each datum point is the standard deviation of the mean for at least 3 measurements.

Pretreatment temperature/^{o}C	Appearance time/s
150	0.95 ± 0.10
300	0.90 ± 0.06
500	0.95 ± 0.05
700	0.97 ± 0.06
800	0.99 ± 0.03
1000	1.02 ± 0.04
1200	0.95 ± 0.03
1400	1.09 ± 0.02

Table 3.2 Effect of Pd pre-treatment temperature on appearance time of As signals. The uncertainty associated with the appearance time the standard deviation of the mean for triplicate measurements.

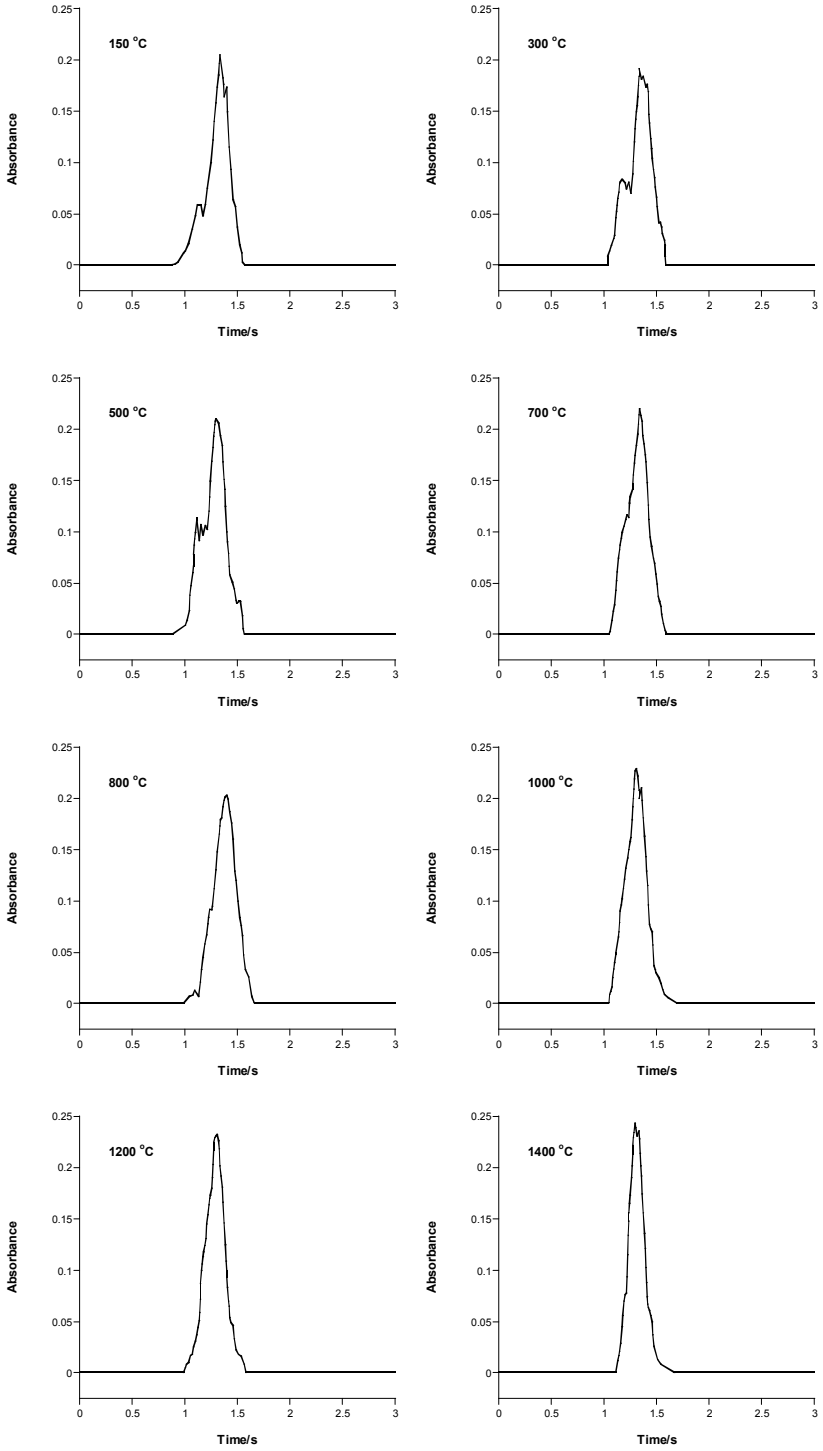

Figure 3.2 Effect of Pd pre-treatment temperature on absorbance-time profiles of As^{V} signals.

3.3.1.2 Mass of Pd

A small increase in sensitivity was observed as the mass of Pd was increased from 0.2 to 2 μg; this is illustrated in Figure 3.3. In contrast, the peak area values showed little change between 0.2 and 2 μg (data not shown). It is important to note that a signal was not observed in any experiments when accumulation occurred on a bare graphite furnace (i.e. no Pd deposited), indicating the inactivity of the graphite surface or its inability to retain As under the thermal conditions used.

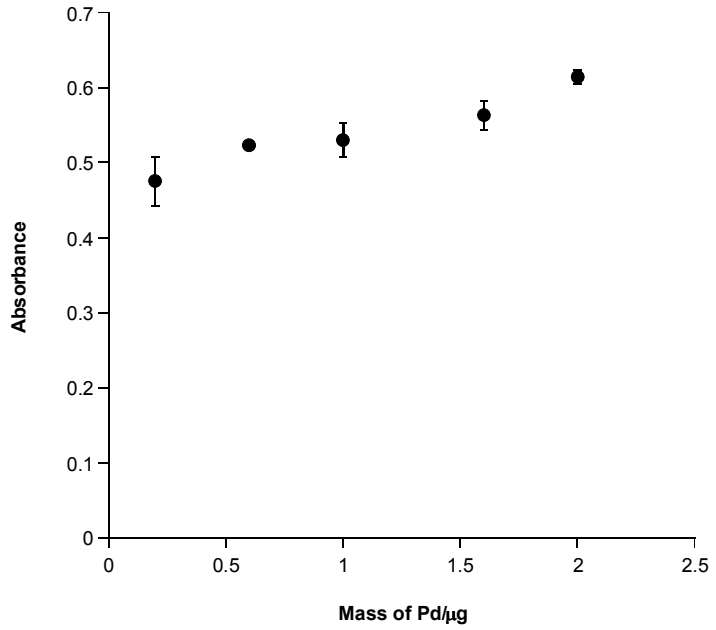

Figure 3.3 Effect of Pd mass on As^{III} sensitivity. The concentration of As^{III} was 0.5 ppb (0.25 % v/v HCl). Palladium (2 μg) was deposited from 20 μL of 10 to 100 ppm $PdCl_2$ solutions (5 % v/v HNO_3) and "dried" at 150 ^oC. Palladium was pre-treated at 800 ^oC. All other parameters and conditions were the same as in Figure 3.1. The uncertainty associated with each datum point is the standard deviation of the mean for at least 3 measurements.

Peak profile was also dependent on the mass of Pd used (Figure 3.4). At 0.2 μg of Pd the signals were broad and double peaks were evident. As the mass of Pd was increased the appearance of double peaks progressively disappeared and the signal became narrower.

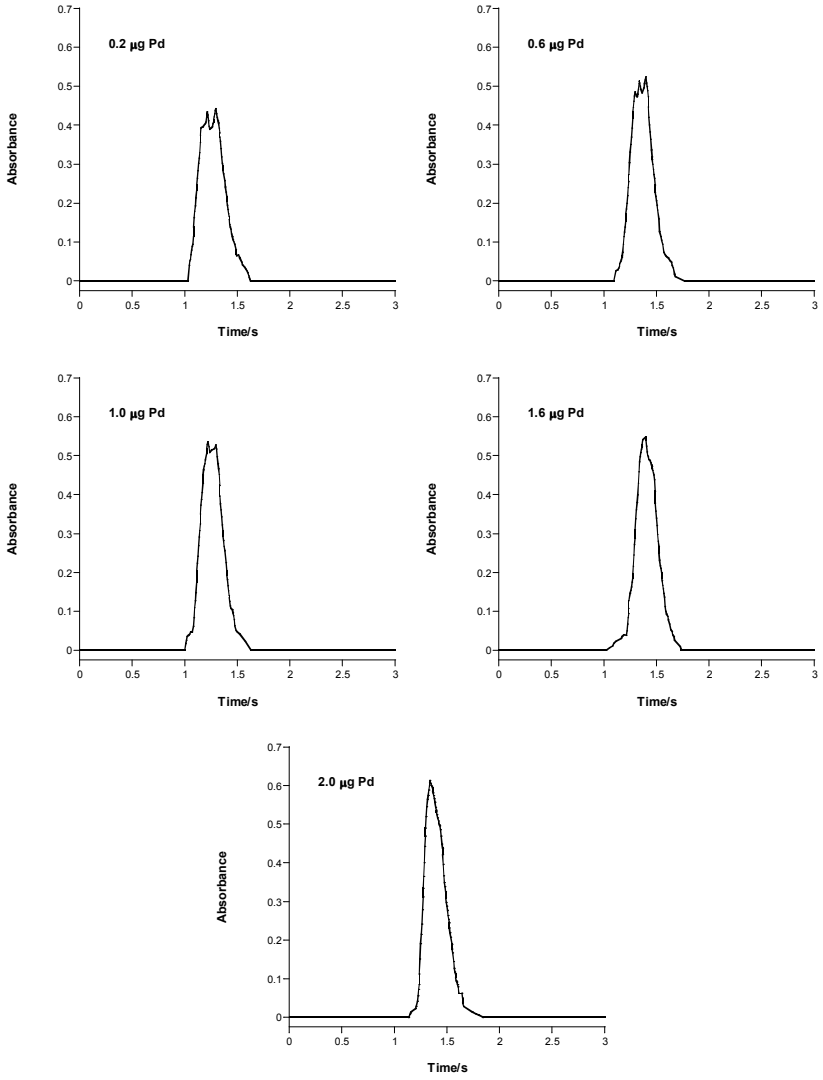

Figure 3.4 Effect of Pd mass on absorbance-time profiles of As^{III} signals.

There was no significant difference in the appearance time of the As signals at various Pd masses, as illustrated in Table 3.3.

Mass of Pd/µg	Appearance time/s
2	1.07 ± 0.01
1.6	1.02 ± 0.04
1	0.99 ± 0.05
0.6	1.01 ± 0.03
0.2	1.06 ± 0.06

Table 3.3 Effect of Pd mass on appearance time of As signal. The uncertainty associated with the appearance time is the standard deviation of the mean for triplicate measurements.

3.3.1.3 Pd surface area

Varying the $PdCl_2$ volume from 10 to 40 µL and therefore varying the surface area of the furnace covered by Pd, had no influence on the As signal in terms of either sensitivity or peak profile. Table 3.4 shows the As absorbance for various $PdCl_2$ volumes.

Volume of $PdCl_2$/µL	Absorbance
10	0.479 ± 0.011 (n = 3)
20	0.476 ± 0.017 (n = 6)
30	0.470 ± 0.021 (n = 3)
40	0.485 ± 0.009 (n = 5)

Table 3.4 Effect of Pd volume on As absorbance. The concentration of As^{III} was 0.5 ppb (0.25 % v/v HCl), the $NaBH_4$, NaOH, and sodium acetate (pH 5.0) concentrations were 0.12, 0.05 and 0.25 mol L^{-1}, respectively. Palladium (2 µg) was deposited from 10 to 40 µL of 50 to 200 ppm $PdCl_2$ solutions (5 % v/v HNO_3) and "dried" and pre-treated at 150 ^oC and 800 ^oC, respectively. Arsine was accumulated at 300 ^oC and atomization was carried out at 2400 ^oC. The uncertainty associated with the absorbance values is the standard deviation of the mean for replicate measurements. The number of replicate measurements is denoted by the 'n' value in brackets.

3.3.1.4 Accumulation Temperature

Varying the accumulation temperature from 25 to 600 ^oC had a minor affect on the amount of AsH_3 accumulated, as indicated in Figure 3.5. Peak profile was not affected. Temperatures above 600 ^oC could not be examined with the current system as damage to the glass capillary delivery tube occurred at high temperatures. The high standard deviation of the datum point at 600 ^oC may be due to degradation or damage of the glass capillary.

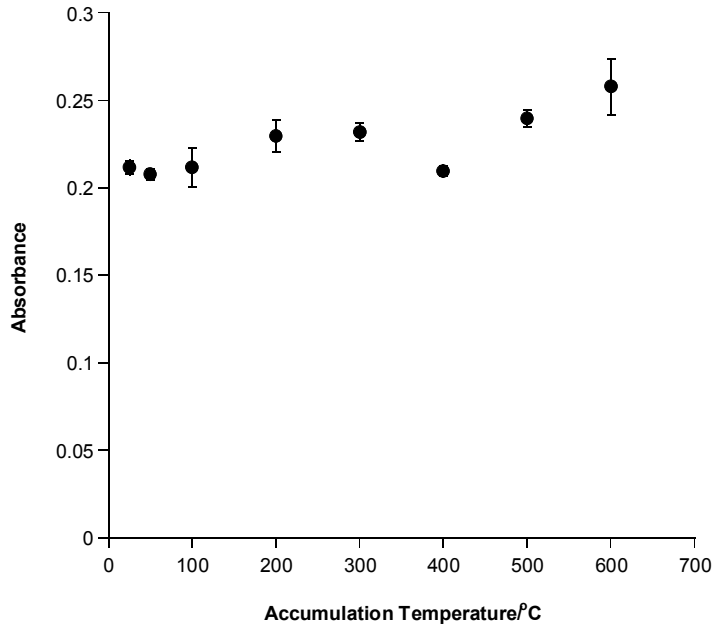

Figure 3.5 Effect of accumulation temperature on As^V sensitivity. The concentration of As^V was 0.2 ppb (0.25 % v/v HCl, 0.25 % w/v L-cysteine). Palladium was pre-treated at 800 °C. Arsine was accumulated from 25 to 600 °C. All other parameters and conditions were the same as in Figure 3.1. The uncertainty associated with each datum point is the standard deviation of the mean for at least 3 measurements.

3.3.2 Effect of $NaBH_4$ and NaOH concentrations

3.3.2.1 Effect of $NaBH_4$ concentration at constant NaOH concentration

The effect of $NaBH_4$ concentration on As sensitivity, at constant NaOH concentration (0.05 mol L^{-1}), is different for As^{III} and As^V (0.25 % w/v L-cysteine), as illustrated in Figure 3.6. At $NaBH_4$ concentrations $\geq$ 0.2 mol L^{-1}, the absorbance of As^V and As^{III} was the same, but at lower $NaBH_4$ concentrations the production of AsH_3 is measurably more efficient for As^V (with L-cysteine) (□) than for As^{III} (●).

For As^{III} (●), as the concentration of $NaBH_4$ was varied from 0.04 to 0.2 mol L^{-1}, the sensitivity increased nearly linearly; thereafter there was no change in sensitivity as the concentration of $NaBH_4$ was increased up to 0.28 mol L^{-1}. In contrast, for As^V in the presence of 0.25 % w/v L-cysteine, the sensitivity increased as the $NaBH_4$ concentration was varied in the range 0.04 to 0.12 mol L^{-1}; no further significant increase in sensitivity was observed for higher $NaBH_4$ concentrations. Note that in Figure 3.6, the maximum absorbance signal arising from the As^{III} and As^V (with L-cysteine) solutions was the same, but the concentration

of As^{V} is half that of As^{III}. In the system used in the work for this thesis, the sensitivity for As^{V} was always approximately twice that for As^{III}; this is a result of the presence of L-cysteine and is described in section 3.4.2.1.

For As^{III} the ratio between maximum sensitivity and sensitivity at 0.04 mol L^{-1} is ~ 3.4; for As^{V} this ratio is ~ 1.8, indicating the larger effect that [$NaBH_4$] has on As^{III} sensitivity.

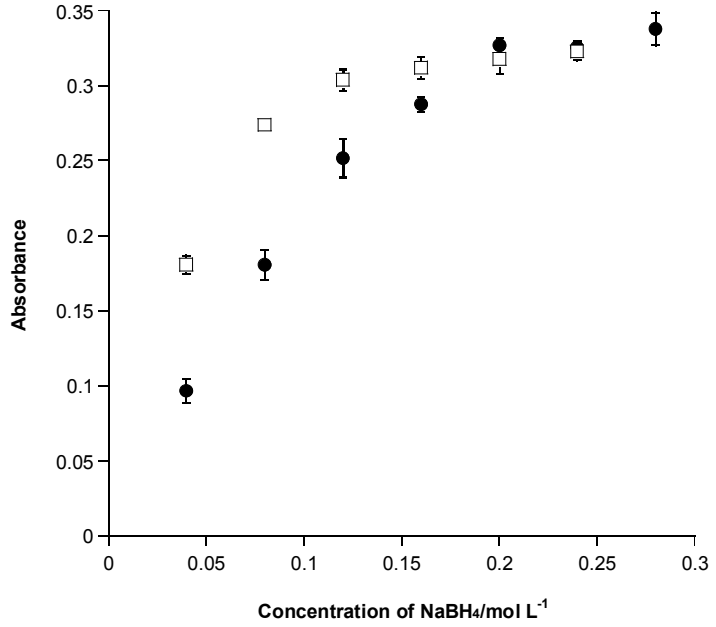

Figure 3.6 Effect of $NaBH_4$ concentration on As^{III} (●) and As^{V} (□) sensitivity. The concentration of As^{III} was 0.5 ppb (0.25 % v/v HCl), the concentration of As^{V} was 0.25 ppb (0.25 % v/v HCl, 0.25 % w/v L-cysteine). The concentration of $NaBH_4$ was varied from 0.04 to 0.28 mol L^{-1} at [NaOH] = 0.05 mol L^{-1}. Palladium was pre-treated at 800 ^{o}C. All other parameters and conditions were the same as in Figure 3.1. The uncertainty associated with each datum point is the standard deviation of the mean for at least 3 measurements.

Table 3.5 shows the pH of the reaction mixture exiting the reaction coil at various $NaBH_4$ concentrations for As^{III} and As^{V} (L-cysteine). These results indicate that the difference in sensitivity at low $NaBH_4$ concentration is unlikely to be a result of pH differences in the reaction mixtures for the As^{III} and As^{V} (L-cysteine) samples.

$[NaBH_4]$/mol L^{-1}	pH – As^{III}	pH – As^{V}
0.04	4.65	4.60
0.08	4.91	4.89
0.12	5.21	5.17
0.16	5.79	5.66
0.20	8.08	7.45
0.24	8.39	8.07
0.28	8.53	-

Table 3.5 Table showing the pH of the reaction mixture exiting the reaction coil at various $NaBH_4$ concentrations for 0.5 ppb As^{III} (0.25 % v/v HCl) and 0.25 ppb As^{V} (0.25 % v/v HCl, 0.25 % w/v L-cysteine).

3.3.2.2 Effect of $NaBH_4$ concentration at varying NaOH concentration

The effect of varying $NaBH_4$ concentration, at constant $[NaBH_4]$/[NaOH] ratio on sensitivity is illustrated in Figure 3.7. For both As^{III} (●) and As^{V} (in the presence of 0.25 % w/v L-cysteine) (□) the maximum absorbance is at 0.12 mol L^{-1} $NaBH_4$. It was observed that $NaBH_4$ concentration has less of an influence on As^{V} sensitivity than As^{III}. The pH of the reaction mixture exiting the reaction coil is shown in Table 3.6 for both As^{III} and As^{V} (L-cysteine). Again, this indicates that the difference in sensitivity at low $NaBH_4$ concentration is unlikely to be a result of pH differences in the reaction mixture for the As^{III} and As^{V} (L-cysteine) samples. At high $NaBH_4$ concentration the pH of the reaction mixture of the As^{V} (L-cysteine) samples was lower than for the As^{III} samples.

$[NaBH_4]$/mol L^{-1}	NaOH/mol L^{-1}	pH – As^{III}	pH – As^{V}
0.04	0.05	4.61	4.60
0.08	0.1	5.15	5.14
0.12	0.15	8.32	7.76
0.16	0.2	8.75	8.32
0.20	0.25	9.71	8.64
0.24	0.3	11.58	9.19

Table 3.6 Table showing the pH of the reaction mixture exiting the reaction coil at various $NaBH_4$ and NaOH concentrations for 0.4 ppb As^{III} (0.25 % v/v HCl) and 0.2 ppb As^{V} (0.25 % v/v HCl, 0.25 % w/v L-cysteine).

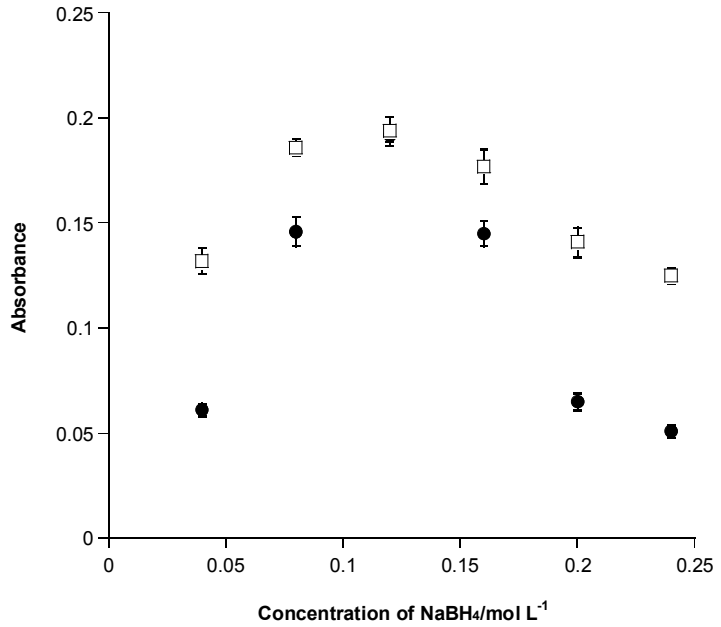

Figure 3.7 Effect of $NaBH_4$ concentration at constant $[NaBH_4]/[NaOH]$ ratio on As^{III} (●) and As^{V} (□) sensitivity. The $[NaBH_4]$ was varied from 0.04 to 0.24 mol L^{-1}. The $[NaBH_4]/[NaOH]$ was 0.8. The concentration of As^{III} was 0.4 ppb (0.25 % v/v HCl), the concentration of As^{V} was 0.2 ppb (0.25 % v/v HCl, 0.25 % w/v L-cysteine). Palladium was pre-treated at 800 ^{o}C. All other parameters and conditions were the same as in Figure 3.1. The uncertainty associated with each datum point is the standard deviation of the mean for at least 3 measurements.

3.3.2.3 Effect of NaOH concentration at optimum $NaBH_4$ concentration

The effect of NaOH concentration on sensitivity for As^{III} and As^{V} (0.25 % w/v L-cysteine) at optimum $NaBH_4$ concentration (0.12 mol L^{-1}) is illustrated in Figure 3.8. For both As^{III} (●) and As^{V} (□) the sensitivity was constant at low NaOH concentration then decreased significantly above 0.1 mol L^{-1} NaOH for As^{III}, and above 0.15 mol L^{-1} NaOH for As^{V}. The effect was more significant for As^{III} than As^{V}. The pH of the reaction mixture exiting the reaction coil is shown in Table 3.7 for both As^{III} and As^{V} (L-cysteine). The reaction mixture for the As^{V} (L-cysteine) samples showed lower pH at high NaOH concentration than for As^{III} samples.

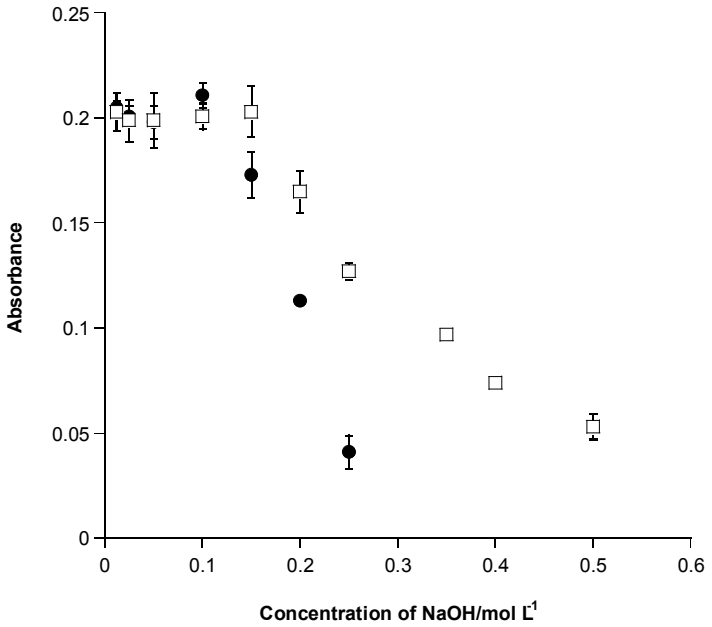

Figure 3.8 Effect of NaOH concentration on As^{III} (●) and As^{V} (□) sensitivity. The concentration of As^{III} was 0.5 ppb (0.25 % v/v HCl), the concentration of As^{V} was 0.25 ppb (0.25 % v/v HCl, 0.25 % w/v L-cysteine). The NaOH concentration was varied from 0.0125 to 0.2 mol L^{-1} for As^{III} and from 0.0125 to 0.5 mol L^{-1} for As^{V}. Palladium was pre-treated at 800 ^{o}C. All other parameters and conditions were the same as in Figure 3.1. The uncertainty associated with each datum point is the standard deviation of the mean for at least 3 measurements.

[NaOH]/mol L^{-1}	pH – As^{III}	pH – As^{V}
0.0125	4.83	4.83
0.025	4.84	4.91
0.05	5.07	5.10
0.1	5.61	5.65
0.125	6.21	6.26
0.15	8.41	7.77
0.2	8.86	8.18
0.25	11.30	8.67
0.35	-	9.91
0.4	-	11.15
0.5	-	11.85

Table 3.7 Effect of NaOH concentration on pH of the reaction mixture exiting the reaction coil for 0.4 ppb As^{III} (0.25 % v/v HCl) and 0.2 ppb As^{V} (0.25 % v/v HCl, 0.25 % w/v L-cysteine).

3.3.3 Hydrochloric acid concentration

Increasing the concentration of HCl resulted in the hydride generation becoming more vigorous for both As^{III} and As^{V} (with L-cysteine) measurements.

3.3.3.1 Effect of HCl concentration on As^{III} sensitivity in the absence of L-cysteine

Varying the concentration of HCl from 0.012 to 0.048 mol L^{-1} had little effect on the sensitivity for As^{III} samples in the absence of L-cysteine. Increasing the HCl concentration further to 0.242 mol L^{-1} resulted in a slight decrease in sensitivity, however, further increasing the HCl concentration up to 3.6 mol L^{-1}, resulted in doubling the sensitivity. These results are illustrated in Figure 3.9. The pH of the mixture exiting the reaction coil is shown in Table 3.8 for As^{III}.

[HCl]/mol L^{-1}	pH
0	8.32
0.0121	5.80
0.0242	5.14
0.0363	4.81
0.0484	4.55
0.0605	4.21
0.0726	3.90
0.0968	2.22
0.121	1.80
0.242	1.36
0.363	1.20
0.484	1.10
0.605	1.01

Table 3.8 Effect of HCl concentration on pH of the reaction mixture exiting the reaction coil for 0.5 ppb As^{III}.

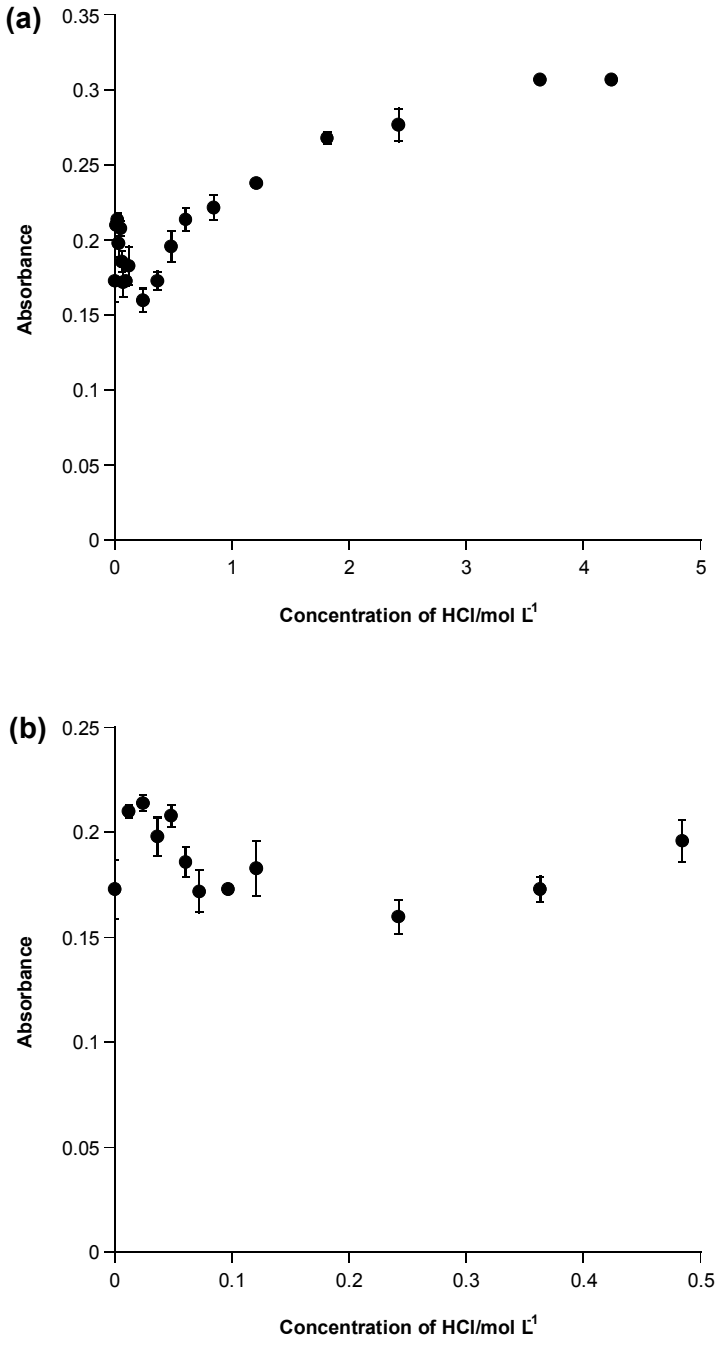

Figure 3.9 Effect of HCl concentration on As^{III} sensitivity; (b) is an enlargement of (a) in the HCl concentration range 0 to 0.5 mol L^{-1}. The concentration of HCl was varied from 0 to 4.2 mol L^{-1}. The concentration of As^{III} was 0.5 ppb (0.25 % v/v HCl). Palladium was pre-treated at 800 ^{o}C. All other parameters and conditions were the same as in Figure 3.1. The uncertainty associated with each datum point is the standard deviation of the mean for at least 3 measurements.

3.3.3.2 Effect of HCl concentration on As^V sensitivity in the presence of L-cysteine

Varying the concentration of HCl from 0 to 0.06 mol L^{-1} had little effect on the sensitivity for As^V samples in the presence of L-cysteine. However, as the concentration of HCl increased from 0.06 to 0.12 mol L^{-1}, a rapid decrease in sensitivity was observed. At concentrations greater than 0.12 mol L^{-1} the sensitivity was approximately constant. These results are illustrated in Figure 3.10. The pH of the mixture exiting the reaction coil is shown in Table 3.9 for As^V (L-cysteine).

[HCl]/mol L^{-1}	pH
0	7.89
0.0121	6.09
0.0242	5.36
0.0363	4.96
0.0484	4.76
0.0605	4.48
0.0726	4.15
0.0968	2.97
0.121	2.01
0.1815	1.56
0.242	1.38

Table 3.9 Effect of HCl concentration on pH of the reaction mixture exiting the reaction coil for 0.25 ppb As^V (0.25 % w/v L-cysteine).

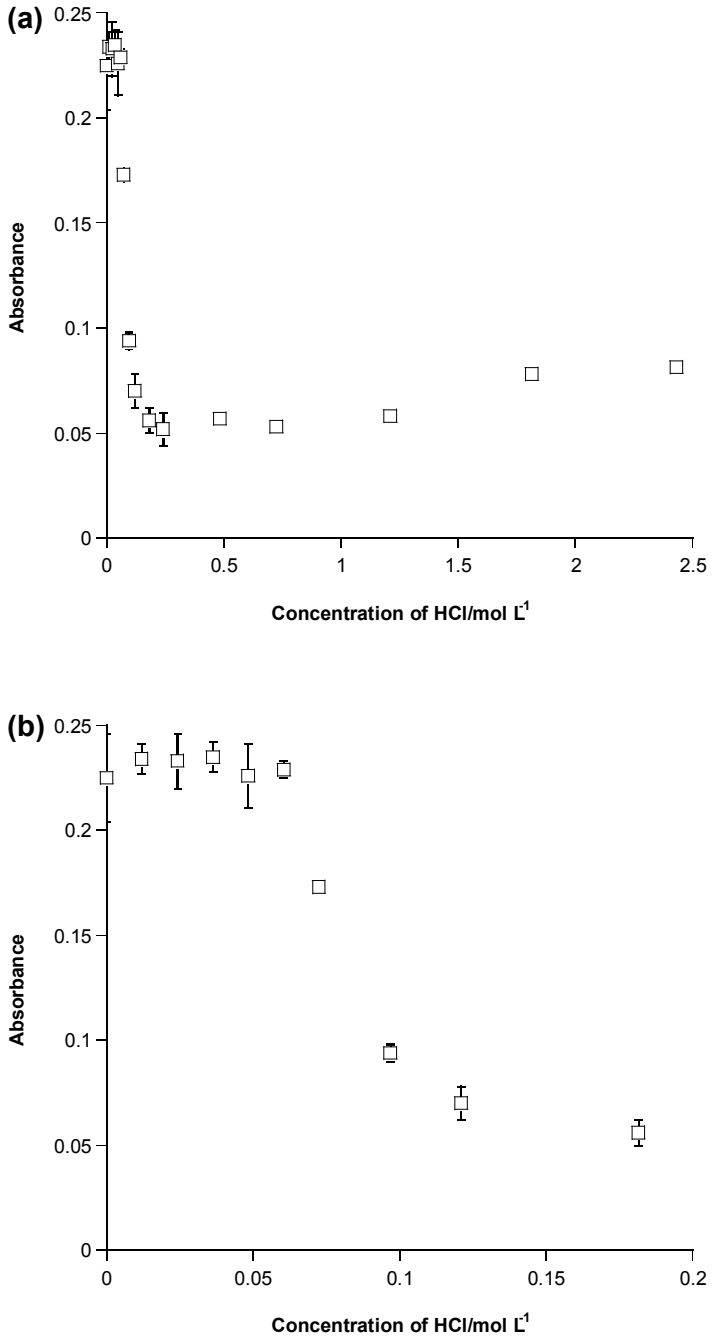

Figure 3.10 Effect of HCl concentration on As^V sensitivity; (b) is an enlargement of (a) in the HCl concentration range 0 to 0.2 mol L^{-1}.The concentration of As^V was 0.25 ppb (0.25 % w/v L-cysteine). The concentration of HCl was varied from 0 to 2.4 mol L^{-1} . Palladium was pre-treated at 800 ^oC. All other parameters and conditions were the same as in Figure 3.1. The uncertainty associated with each datum point is the standard deviation of the mean for at least 3 measurements.

3.3.4 Effect of graphite furnace age and type

The effect that furnace age has on both peak profile and sensitivity is shown in Figure 3.11. When an aged graphite furnace is used very structured peaks are evident and peak width is broader than that for a new graphite furnace. In contrast, the area values show little difference, indicating that the mass of AsH_3 accumulated is the same for both furnaces. For an aged furnace, the As signal appears at a lower temperature; the appearance time is (0.91 ± 0.01) s compared to (1.12 ± 0.03) s for a new graphite furnace.

For the aged graphite furnace, peak-profile could not be improved when the volume of Pd solution and mass of Pd added to the furnace was increased. Furthermore, a signal was not observed in the absence of Pd which indicates the inactivity of a bare graphite furnace under the conditions used.

Experiments were carried out in which Cd^{II} and Cu^{II} standard solutions were injected directly into the new and aged graphite furnaces and their absorbances monitored at 228.8 and 324.8 nm, respectively. The results showed no observable difference between the old and new graphite furnaces used in this work, with regards to appearance time and peak-profile, indicating that the poor peak-profile obtained was specific to the Pd-As system.

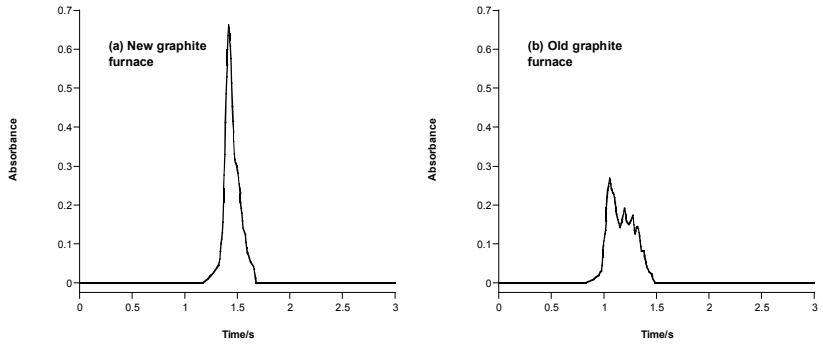

Figure 3.11 Effect of both (a) new graphite furnace and (b) old graphite furnace, on peak profile and sensitivity. The concentration of As^{V} was 0.5 ppb (0.25 % v/v HCl, 0.25 % w/v L-cysteine). The Pd was pre-treated at 800 ^{o}C. All other parameters and conditions were the same as in Figure 3.1.

Measurements were made with new and used graphite furnaces at two different Pd pre-treatment temperatures (800 or 1400 ^{o}C). These results are shown in Table 3.10 below. The

furnaces were different from those used to obtain the spectra in Figure 3.11, however they were from the same batch of graphite furnaces. It was unknown how many firings the old furnace had been used for, but it was estimated to be > 200.

	Absorbance at 800 ^{o}C	**Absorbance at 1400 ^{o}C**	**Absorbance ratio***
New graphite furnace	0.231 ± 0.005	0.207 ± 0.012	1.12 ± 0.09
Old graphite furnace	0.194 ± 0.008	0.112 ± 0.005	1.73 ± 0.15

Table 3.10 Effect of Pd pre-treatment temperature on As^{V} sensitivity for new and old graphite furnaces. The concentration of As^{V} was 0.22 ppb (0.25 % v/v HCl, 0.25 % w/v L-cysteine). The concentrations of $NaBH_4$, NaOH, and sodium acetate buffer (pH 5.0) were 0.12, 0.05, and 0.25 mol L^{-1}, respectively. The Pd solution was "dried" at 150 ^{o}C and pre-treated at 800 ^{o}C or 1400 ^{o}C. Arsine was accumulated at 300 ^{o}C and atomization was carried out at 2400 ^{o}C. The uncertainty associated with the absorbance values is the standard deviation of the mean from triplicate measurements.

*Ratio of absorbance obtained at 800 ^{o}C to that obtained at 1400 ^{o}C

At a Pd pre-treatment temperature of 800 ^{o}C, the new graphite furnace displayed a higher sensitivity than the old graphite furnace; this was observed on many occasions as represented in Figure 3.11. However, a greater difference was observed when the Pd pre-treatment temperature was increased to 1400 ^{o}C; the decrease in sensitivity is more extreme for the old graphite furnace than for the new graphite furnace.

In addition to differences between new and old graphite furnaces with regards to sensitivity and peak profile, variability in furnace performance between the same brand of furnaces, but different batches, and between furnaces in the same batch, were also observed. Additionally, differences in both sensitivity and absorbance-time profile were found between different brands of furnaces. Poor peak profiles were obtained intermittently even when using optimized conditions and using graphite furnaces that had previously and subsequently given good results.

3.3.5 Effect of Fe^{III}

Figure 3.12 shows the effects of Fe^{III}, present in As^{III} and As^{V} (L-cysteine) solutions, on sensitivity for As measurements. For As^{III} (●) (L-cysteine absent), the sensitivity decreased dramatically as the concentration of Fe^{III} was increased from 0 to 2 ppm Fe^{III}, whereas for

As^V (□) in the presence of L-cysteine there was no significant change in sensitivity between 0 and 2 ppm Fe^{III}. For As^{III} and As^V, varying the concentration of Fe^{III} from 0 to 2 ppm had no affect on the pH of the reaction mixture exiting the reaction coil; it remained constant at pH ~ 5.

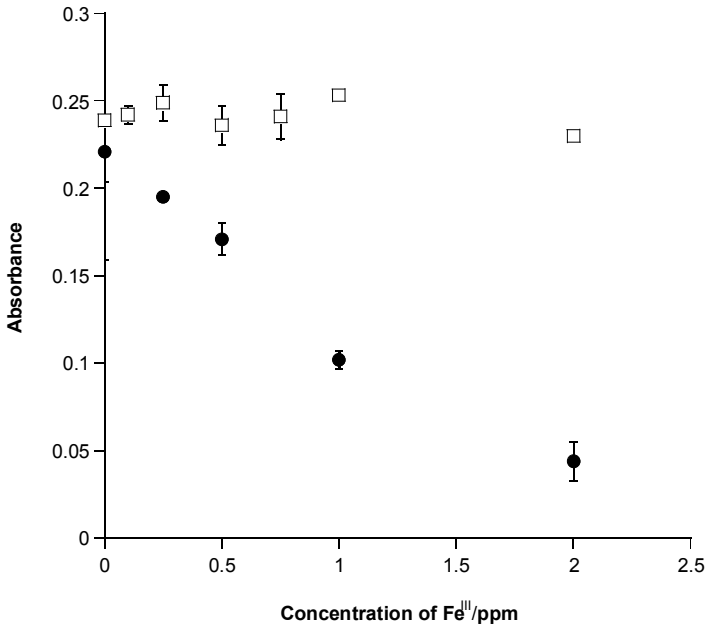

Figure 3.12 Effect of Fe^{III} concentration on As^{III} (●) and As^V (□) sensitivity. The concentration of As^{III} was 0.4 ppb (0.25 % v/v HCl), the concentration of As^V was 0.2 ppb (0.25 % v/v HCl, 0.25 % w/v L-cysteine). Palladium was pre-treated at 800 ^oC. All other parameters and conditions were the same as in Figure 3.1. The uncertainty associated with each datum point is the standard deviation of the mean for at least 3 measurements.

Higher concentrations of Fe^{III} were examined for the As^V-L-cysteine system. It was observed that Fe^{III} (0 to 50 ppm) had little effect on As sensitivity. At Fe^{III} concentrations above 50 ppm, a rapid decrease in sensitivity was observed. These results are illustrated in Figure 3.13. Increasing the Fe^{III} concentration from 0 to 50 ppm had little effect on pH, but at higher Fe^{III} concentrations, pH decreased significantly due to the acidity associated with the Fe^{III} standard solution. This is illustrated in Table 3.11. In addition, adding Fe^{III} to the As solutions containing L-cysteine resulted in a blue colour which faded with time.

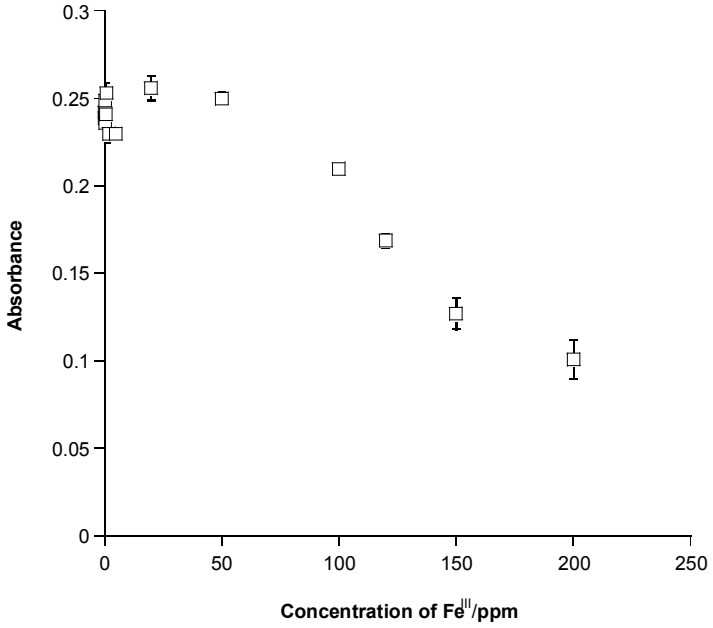

Figure 3.13 Effect of Fe^{III} concentration on As^{V} sensitivity. The concentration of As^{V} was 0.2 ppb (0.25 % v/v HCl, 0.25 % w/v L-cysteine). Palladium was pre-treated at 800 ^{o}C. All other parameters and conditions were the same as in Figure 3.1. The uncertainty associated with each datum point is the standard deviation of the mean for at least 3 measurements.

$[Fe^{III}]$/ppm	pH
0	5.48
0.25	5.45
0.5	5.48
1	5.45
2	5.39
20	5.07
50	4.64
100	4.08
120	3.65
150	2.62
200	1.88

Table 3.11 Effect of Fe^{III} concentration on pH of the reaction mixture exiting the reaction coil for 0.2 ppb As^{III} (0.25 % v/v HCl, 0.25 % w/v L-cysteine).

3.3.6 Effect of argon flow rate

Figure 3.14 shows that argon flow rate has a large effect on sensitivity. The maximum response was observed in the absence of an argon flow. The sensitivity was constant between 4 and 28 mL min^{-1}within experimental uncertainty. However, the reproducibility was poor at flow rates below 14 mL min^{-1}. At flow rates greater than 28 mL min^{-1} there was a rapid decrease in sensitivity, with no signal observed at 100 mL min^{-1}.

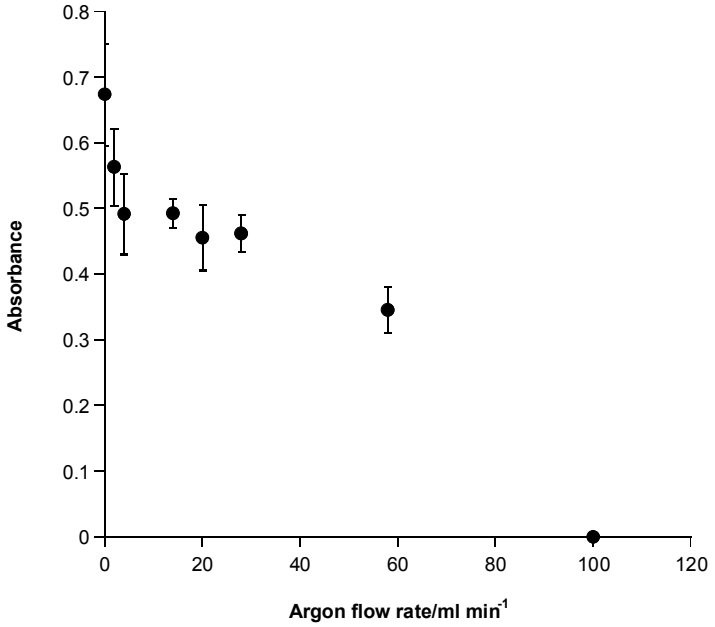

Figure 3.14 Effect of argon flow rate on As^{III} sensitivity. The concentration of As^{III} (0.25 % v/v HCl) was 2 ppb. The concentration of $NaBH_4$ and NaOH was 0.16 and 0.05 mol L^{-1}, respectively. Palladium was pre-treated at 800 ^oC. All other parameters and conditions were the same as in Figure 3.1. The uncertainty associated with each datum point is the standard deviation of the mean for at least 3 measurements.

3.4 Discussion

3.4.1 Pd modifier parameters

3.4.1.1 Pd pre-treatment temperature

The reported temperatures used to pre-treat (reduce) the Pd deposit vary widely; temperatures from as low as 110 ^oC [60] up to as high 1200 ^oC [38, 40] have been reported. There have not been many studies carried out to optimize this parameter. An *et al.*[43] report that final drying temperatures of the Pd solution between 200 and 1000 ^oC did not affect the As response; other than that, no further details are provided by this author.

It is generally accepted that Pd deposited into the furnace as a salt solution will be converted to metallic Pd at high temperatures.[33] In the work carried out for this thesis, hydride accumulation was observed for pre-treatment temperatures as low as 150 ^{o}C (section 3.3.1.1). Many other workers have also observed good accumulation efficiencies at pre-treatment temperatures ≤ 160 ^{o}C.[33, 41, 59, 60] Burguera and Burguera[59] and Li *et al*.[75] have suggested that hydrogen introduced into the furnace during the accumulation of the hydride may assist in reduction of the Pd^{II} salt to metallic Pd; therefore allowing sufficient trapping of hydrides at low Pd pre-treatment temperatures. Voth-Beach and Shrader[61] examined a variety of Pd reduction methods including hydrogen, which was introduced as 5 % hydrogen in 95 % argon. Even though this procedure did result in Pd reduction, atomization signals were typically broad and irreproducible. Absorbance profiles with shoulders and more than one peak maxima were seen for a variety of elements. Similar behaviour was observed in this thesis at low Pd pre-treatment temperatures.

In the work for this thesis, slightly different results with regards to As sensitivity and overall effect of Pd pre-treatment temperature were obtained for experiments carried out on different days; even though similar chemical and physical parameters were used. These differences may be due to the age, and therefore the quality of the graphite furnace used, for each experiment (see section 3.3.4). However, the general trends were clear. The decrease in sensitivity observed at high pre-treatment temperatures is likely due to volatilization of Pd from the graphite furnace and therefore removal of the adsorption surface for AsH_3. Volatilization of Pd was shown to occur at > 1350 ^{o}C, which coincides with the decrease in As sensitivity observed.

Increasing the pre-treatment temperature resulted in an improvement of peak shape. The peak shoulders diminished, resulting in more symmetrical peak profiles. This kind of behaviour (i.e. improvement in peak shape with increasing pre-treatment temperature) has not, to our knowledge, been reported in the literature. This behaviour may indicate that at high pre-treatment temperatures the Pd distribution on the graphite surface is more uniform, with regards to surface area and/or Pd phases. Hydride release from two different surfaces may give rise to the double peak formation observed at lower pre-treatment temperatures. This explanation is supported by the observation of a general increase in appearance temperature of the As signal as the Pd pre-treatment temperature is increased. An increase in the stability of the As species on the Pd surface is consistent with a different Pd or Pd-As phase. The

increase in sensitivity for data set 1 (Figure 3.1), for the temperature range 800 to 1400 ^{o}C, may be due to better uniformity of the Pd distribution and/or a different Pd phase. This may lead to better adsorption and/or atomization of As from the Pd modifier, giving rise to higher and narrower peaks.

Imperfect coatings have been experimentally observed for Pd, Rh and Ir on graphite, particularly when coatings are formed by injection rather than electroplating.[63]

A Pd pre-treatment temperature of 800 ^{o}C was chosen for future work. Even though higher sensitivity was obtained for data set 1 for pre-treatment temperatures of 1400 ^{o}C, this temperature was not considered optimum because of the inconsistencies between the two data sets.

3.4.1.2 Mass of Pd

Increasing the mass of Pd from 0.2 μg to 2 μg resulted in an increase in As sensitivity of ~ 25 % (see section 3.3.1.2). In contrast, the constant peak area values observed in this range indicate the amount of AsH_3 accumulated is independent of Pd mass. Reasonable agreement was obtained between the results presented in this thesis and those from the literature for the same mass range. Burguera and Burguera[59] varied the mass of Pd from 0.25 to 5 μg and observed an increase in sensitivity of less than 10 % from minium to maximum sensitivity. At masses > 4 μg the absorbance-time profiles were delayed and distorted, leading to a decrease in sensitivity. They attributed this to a change in rate of desorption of AsH_3 from the Pd surface. This behaviour has also been observed by other workers. [43, 44] Sturgeon *et al*.[44] and An *et al*.[43]observed this delayed/distorted phenomenon at Pd masses between 10 to 15 μg, however, peak area was not affected. Sturgeon *et al*.[44] found that increasing the mass of Pd from 0.02 to 1 μg resulted in a 3-fold increase in sensitivity. However, over a similar mass range to the experiments conducted in this thesis (0.1 to 2 μg), a 35 % increase in sensitivity was reported. Niedzielski and Siepak[76] varied the mass of Pd from 0.5 to 5 μg and observed a general increase in sensitivity; however this increase was most significant between 0.5 and 2 μg (35 % increase) with only a small increase at higher Pd masses. Lastly, Zhang *et al*.[44] observed ~ 15 % increase in sensitivity as the mass of Pd was increased from 0.25 to 1 μg. There was no change in sensitivity observed thereafter up to 10 μg. For many of the literature reports, it is unclear whether peak height or peak area was used for interpretation of results.

Therefore, direct comparisons can be difficult as we found there was an increase in peak height with increasing Pd mass but no significant change in peak area.

An increase in mass of Pd, should lead to an increase in surface area available for analyte trapping.[44] Therefore one could assume that the increase in sensitivity is a result of more AsH_3 adsorbing. However, this is contradicted by the area values which indicate that there is no significant difference in the amount of AsH_3 captured. Therefore it is likely that the increase in mass is either affecting the distribution of Pd (or AsH_3) on the graphite surface, or is affecting the AsH_3 desorption process during the release and atomization stage; resulting in an increase in sensitivity. This is supported by the changes observed in the absorbance-time profiles. An increase in Pd mass leads to more symmetrical, narrower peaks and removal of 'double peak' formation; there are no reports in the literature regarding this behaviour (i.e. an increase in mass of Pd.

A Pd mass of 2 μg was considered optimum; therefore this mass of Pd was used for future work.

3.4.1.3 Pd surface area

There was no significant change in As sensitivity as the volume of Pd^{II} solution was varied from 10 to 40 μL at a constant mass of 2 μg (section 3.3.1.3). This indicates that under the conditions used in the work for this thesis, the area of the furnace surface covered with Pd does not play a significant role in AsH_3 accumulation. These results are similar to those of Burguera and Burguera,[59] who varied the volume of Pd^{II} solution from 5 to 50 μL at a constant Pd mass of 2 μg. They observed a 12 and 5 % increase in sensitivity as the Pd volume was increased from 5 to 30 μL and 10 to 30 μL, respectively. Increasing the volume to greater than 30 μL had no effect. In contrast, Sturgeon *et al*.[44] observed a significant effect of Pd volume at a constant Pd mass of 4 μg. Increasing the Pd^{II} solution volume from 2.5 to 50 μL resulted in a 100 % increase in sensitivity, and increasing the volume from 10 to 50 μL resulted in a 60 % increase in sensitivity.

The differences between the results obtained from Sturgeon *et al*.,[44] and the results of Burguera and Burguera[59] and those obtained in this thesis, cannot be explained by a difference in the mass of As deposited. Burguera and Burguera[59] deposited 2 ng of As, whereas Sturgeon *et al*.,[44] and the work in this thesis used 1 ng of As. The difference may be

due to the higher mass of Pd used by Sturgeon *et al*.[44] At higher masses of Pd, the volume of Pd^{II} solution may have a more significant effect than at lower Pd masses. It is possible that in the work for this thesis, and that of Burguera and Burguera,[59] the mass of Pd is limiting and that is why the effect of Pd volume is not as significant as that observed by Sturgeon *et al*.[44] Assuming that for the experiments carried out in this thesis, at low Pd mass the Pd forms domains rather than a continuous layer; the morphology of the Pd deposit may remain the same as the volume is increased, although the deposit will be more spread out. Alternatively, with higher masses of Pd, the deposit may be continuous on the graphite surface at low modifier volumes, whereas at higher volumes a change of morphology to more separated Pd deposits (domains) may occur. This may result in an increase in surface area of the modifier, which may lead to better trapping of AsH_3.

The flow rate of argon may also be a factor. The flow rate used in the work for this thesis was 28 mL min^{-1}; Burguera and Burguera[59] used a flow rate of 40 mL min^{-1} and Sturgeon *et al*.[44] used a flow rate of 50 mL min^{-1}. For the higher flow rate used by Sturgeon *et al*.[44] it may be necessary to use a larger area of Pd.

A Pd^{II} solution volume of 20 μL was used for future work.

3.4.1.4 Accumulation temperature

Varying the AsH_3 accumulation temperature from 25 to 600 ^oC had only a minor effect on the amount of AsH_3 accumulated on the Pd surface (section 3.3.1.4) These results are in reasonable agreement with those of Burguera and Burguera,[59] Walcerz *et al*.,[40] Zhang *et al*.,[60] and Liang *et al*.;[41] within the temperature range studied. Burguera and Burguera[59] varied the accumulation temperature from 50 to 1200 ^oC. They found no significant effect on sensitivity between 50 and 800 ^oC. Temperatures above 800 ^oC resulted in a decrease in As sensitivity. Similar results were reported by Walcerz *et al*.[40] who varied the accumulation temperature from 100 to 1100 ^oC; a decrease in As signal was observed above 700 ^oC. Zhang *et al*.[60] found no change in As response over the temperature range 100 to 1200 ^oC. Liang *et al*.[41] reported sufficient hydride accumulation at 30 ^oC and only a 10 % increase in sensitivity as the accumulation temperature was increased from 30 to 300 ^oC. Liang *et al*.[41] also found better reproducibility at higher temperatures, and a decrease in sensitivity was observed above 600 ^oC. These similar results by various authors were obtained for a wide range of Pd pre-treatment temperatures (120 to 1200 ^oC) and Pd masses (2 to 50 μg) . This indicates that

the effect of accumulation temperature is independent of the mass of Pd or the temperature at which it is pre-treated.

Sturgeon *et al.*[44] found very little effect of accumulation temperature in the range 200 to 600 ^{o}C. However, later results from the same research group[43] are in conflict with their earlier results.[43] Their later results showed a 15 % increase in trapping efficiency as the accumulation temperature was increased from 200 to 600 ^{o}C. They attribute this discrepancy to probable differences in the furnace and the gas flow designs of the atomizer. Niedzielski and Siepak[38] examined the effect of varying the accumulation temperature from 50 to 400 ^{o}C. They found that increasing the accumulation temperature from 50 to 200 ^{o}C resulted in a 25 % increase in sensitivity; above 200 ^{o}C a small decrease in sensitivity was observed.

Sturgeon *et al.*[44] found very low trapping efficiencies at 25 ^{o}C; this is in direct contrast to results from this thesis which showed very good sensitivity at 25 ^{o}C. Sturgeon *et al.*[44] observed a 140 % increase in sensitivity between 25 and 200 ^{o}C, and a 30 % increase between 100 to 200 ^{o}C; thereafter there was no change in response up to 600 ^{o}C. They used a pre-treatment temperature of 400 ^{o}C and 4 μg of Pd.

The results in this thesis and those of Liang *et al.*[41] and Burguera and Burguera[59] demonstrate that efficient trapping of AsH_3 can occur in the range 25 to 50 ^{o}C. This low trapping temperature suggests that the hydride undergoes a catalytic dissociation on the Pd surface rather than a thermal decomposition, as mentioned by Sturgeon *et al.*[44] Burguera and Burguera[59] and Zhang *et al.*[60] also came to the same conclusion as they observed efficient trapping of AsH_3 at temperatures less than that required for thermal decomposition of the hydride.

The variation in the effect of accumulation temperature on sensitivity reported in the literature may be a result of several effects, such as differences in pre-treatment temperature, mass of Pd, carrier gas flow-rate, and differences in graphite surfaces.

For future work an accumulation temperature of 300 ^{o}C was used due to the slightly better sensitivity obtained than at lower accumulation temperatures.

3.4.2 Effect of $NaBH_4$ and NaOH concentrations

3.4.2.1 Effect of $NaBH_4$ concentration at constant NaOH concentration

The effect of $NaBH_4$ concentration on sensitivity depended on whether L-cysteine was absent or present (section 3.3.2.1). At $NaBH_4$ concentrations $\geq$ 0.2 mol L^{-1}, the response for As^V (L-cysteine) and As^{III} is the same, but at lower $NaBH_4$ concentrations the production of AsH_3 is more efficient for As^V (L-cysteine) than for As^{III}. The optimum $NaBH_4$ concentration for As^{III} occurs at $\geq$ 0.2 mol L^{-1}; for As^V the optimum sensitivity occurred at $\geq$ 0.12 mol L^{-1} $NaBH_4$.

It is difficult to make direct comparisons to other results in the literature as the effect of $NaBH_4$ is likely to depend on the concentrations of NaOH, HCl, and L-cysteine, and such physical parameters as reagent and sample flow rates.

For As^{III} in the absence of L-cysteine, results from Coelho *et al.*[23] and Anthemidis *et al.*[31] are in reasonable agreement with the results from this thesis. Coelho *et al.*[23] observed a rapid increase in sensitivity as the $NaBH_4$ concentration was increased from 0.024 to 0.12 mol L^{-1}; the maximum As^{III} sensitivity was obtained between 0.12 and 0.24 mol L^{-1} $NaBH_4$; thereafter no significant difference was observed. Anthemidis *et al.*[31] observed a nearly linearly increase in As^{III} sensitivity as the $NaBH_4$ concentration was increased from 0.024 to 0.36 mol L^{-1}; thereafter no significant change in sensitivity was observed up to 0.72 mol L^{-1}. This was carried out at 1.5 mol L^{-1} HCl; similar results were also obtained at 9.0 mol L^{-1} HCl. The reason for the higher concentration of $NaBH_4$ required to reach maximum sensitivity, relative to the $NaBH_4$ concentration used in the work for this thesis, may be due to the higher concentration of HCl used. Acid decomposes $NaBH_4$,[1] therefore more $NaBH_4$ may be required to efficiently convert all As^{III} to AsH_3 at high acid concentrations.

Shraim *et al.*[24] examined the effect of $NaBH_4$ concentration in the absence and presence of L-cysteine at various HCl concentrations. The effect of $NaBH_4$ concentration on sensitivity depended on the concentration of HCl used. For As^{III} (absence of L-cysteine), similar results to those reported in this thesis were observed at 0.1 mol L^{-1} HCl. A rapid increase was observed between 0.024 and 0.24 mol L^{-1} $NaBH_4$; thereafter no significant change in sensitivity was observed. For As^V in the presence of L-cysteine, a rapid increase in sensitivity was observed between 0.024 and 0.144 mol L^{-1} $NaBH_4$; thereafter no significant change in sensitivity was observed up to 0.5 mol L^{-1}. This is similar to the results from this thesis with

the maximum sensitivity being obtained at a lower $NaBH_4$ concentration when L-cysteine is used.

The results from the work in this thesis and that obtained by Shraim *et al*.[24] indicate that L-cysteine increases the efficiency of the hydride generation reaction. Results from other workers have shown that the presence of L-cysteine increases sensitivity.[28, 29, 39, 50] Feng *et al*.,[29] and Chen *et al*.,[28] both found that increasing the L-cysteine concentration in an As^{III} sample resulted in an increase in sensitivity. For the determination of Ge, Brindle and Le[50] found that the Ge signal was enhanced by approximately 100 % in the presence of L-cysteine. They used UV-Vis spectroscopy to examine the interaction between $NaBH_4$ and L-cysteine. They found a shift in the UV-Vis absorption peak to longer wavelength when L-cysteine and $NaBH_4$ were mixed compared with solutions of L-cystine and $NaBH_4$ alone. This implies that an interaction has occurred between $NaBH_4$ and L-cysteine. Brindle and Le[50] further examined the relationship between $NaBH_4$ and L-cysteine on the signal by varying the L-cysteine concentration at various $NaBH_4$ concentrations, and then varying the $NaBH_4$ concentration at various L-cysteine concentrations. At low L-cysteine concentrations a higher $NaBH_4$ concentration is required for efficient hydride generation, whereas a very low concentration of $NaBH_4$ is needed if the L-cysteine concentration is high. These results show the interdependence of L-cysteine and $NaBH_4$ concentrations on the generation of the hydride.

Brindle and Le[50] also found that the Ge signal was enhanced in the presence of penicillamine and thioglycerol (both thiol-containing species), however, the signal was not enhanced in the presence of S-methyl-L-cysteine, histidine, or glycine, which do not contain thiol groups. Therefore, they proposed that the interaction between $NaBH_4$ and L-cysteine is through the thiol group of L-cysteine (equation 3.5).

$$BH_4^- + R\text{-}SH \longrightarrow BH_3\text{-}S\text{-}R^- + H_2 \qquad \textbf{(3.5)}$$

This type of reaction for L-cysteine and $NaBH_4$ was supported by ^{13}B NMR which showed evidence of the BH_3-SR^- species. They proposed that this BH_3-SR^- species is a more efficient reductant in the hydride generation process than BH_4^-, leading to signal enhancement.

Howard and Salou[39] believe that the enhancement of analyte sensitivity in the presence of L-cysteine has more to do with the formation of reduced As-cysteine complexes than the formation of a better reductant. Tsalev *et al.*[48] also allude to the possibility that analyte complexation by L-cysteine may result in improved reduction processes, leading to higher chemical yields and/or better kinetics. It is generally accepted that reaction of As^{III} and As^{V} with compounds containing thiol groups yield the thiolate complex of As^{III} [24, 25, 27, 39, 45] (after reduction of As^{V} to As^{III}). This is shown below for As^{V} (equation 3.6) and As^{III} (equation 3.7).[45]

$$2R\text{-}SH + AsO(OH)_3 \longrightarrow RS\text{-}SR + As(OH)_3 + H_2O \qquad \textbf{(3.6)}$$

$$As(OH)_3 + 3R\text{-}SH \longrightarrow As(SR)_3 + 3H_2O \qquad \textbf{(3.7)}$$

The As-cysteine complexes react with $NaBH_4$ and generate the hydride as is shown in reaction 3.8.[45]

$$AsSR_3 + 3BH_4^- \longrightarrow AsH_3 + 3BH_3 + 3RS^- \qquad \textbf{(3.8)}$$

Therefore it is possible that the thiolate complex of the analyte is more easily reduced by $NaBH_4$, than the oxyanion, and this is why signal enhancement in the presence of L-cysteine occurs.

The concentration of $NaBH_4$ used in future work was 0.12 mol L^{-1} for both As^{III} and As^{V} (L-cysteine) measurements. Even though this was not optimum for As^{III} measurements, high $NaBH_4$ concentrations resulted in liquid entering the hydride delivery tube at various times. This problem may result in interference due to hydride losses.[1]

3.4.2.2 Effect of $NaBH_4$ concentration at varying NaOH concentration

The effect of $NaBH_4$ concentration at a constant $[NaBH_4]/[NaOH]$ ratio (i.e. at varying NaOH concentrations) is very different from that at constant NaOH concentration (section 3.3.2.2). The major difference is that at high $NaBH_4$ concentrations (> 0.12 mol L^{-1}) a decrease in sensitivity for both As^{III} and As^{V} (in the presence of L-cysteine) is observed. This decrease in sensitivity is more marked for As^{III} than for As^{V} (L-cysteine) and the maximum sensitivity for As^{V} (L-cysteine present) is shown for a wider range of $NaBH_4$ concentration

than that for the As^{III} samples. These observations imply that the L-cysteine system is more tolerant of higher NaOH concentrations. This may be due to the effect discussed above, which is that the L-cystiene-$NaBH_4$ is a better reducing agent than $NaBH_4$ alone. Alternatively, the buffering effect of the L-cysteine may be advantageous.

Maintaining a constant [$NaBH_4$]/[NaOH] ratio also leads to an increase in NaOH concentration as the concentration of $NaBH_4$ is increased. Therefore it is likely that the sensitivity decrease observed at high $NaBH_4$ concentrations is actually due to high NaOH concentration. However, this decrease may not be solely due to a pH effect; results from section 3.3.2.1 showed maximum hydride generation was obtained at similar pH to those here. There are no reported studies in the literature that examine the effect of $NaBH_4$ concentration while maintaining a constant [$NaBH_4$]/[NaOH] ratio.

3.4.2.3 Effect of NaOH concentration at optimum $NaBH_4$ concentration

The effect of NaOH concentration was dependent on the presence of L-cysteine (section 3.3.2.3). For As^{V} samples in the presence of L-cysteine, sensitivity was less affected by NaOH concentration than for As^{III} samples in the absence of L-cysteine, again indicating the more efficient production of AsH_3 in the presence of L-cysteine. This may be due to the buffering effect of the L-cysteine; this is supported by the fact that the mixture exiting the reaction coil for the As^{V} samples containing L-cysteine showed a lower pH than the As^{III} solutions that did not contain L-cysteine. For As^{III} samples the decrease in sensitivity occurred at NaOH concentrations above 0.1 mol L^{-1}; for As^{V} in the presence of L-cysteine the decrease was observed at NaOH concentrations above 0.15 mol L^{-1}.

Yin *et al.*[34] examined the effect of NaOH on As^{V} sensitivity in the presence of L-cysteine. This was carried out at 4 different HNO_3 concentrations. The effect of NaOH was highly dependent on the concentration of HNO_3. At low HNO_3 concentrations (0.029 and 0.072 mol L^{-1}) similar results were obtained to those in this thesis. Yin *et al.*[34] observed maximum sensitivity at approximately 0.18 mol L^{-1} NaOH; thereafter a rapid decrease in sensitivity was observed up to 0.5 mol L^{-1} NaOH. However, at high acid concentrations (0.29 mol L^{-1}), they observed a near linear increase in sensitivity as the concentration of NaOH was increased up to 0.5 mol L^{-1}.

Feng *et al*.[29] examined the effect of HCl concentration on As^{III} in the presence of L-cysteine at different NaOH concentrations. They found that the effect of HCl was highly dependent on the concentration of NaOH used. Feng *et al*.[29] and Yin *et al*.[34] did not undertake studies of As samples in the absence of L-cysteine.

A NaOH concentration of 0.05 mol L^{-1} was used for future work in this thesis.

3.4.3 Hydrochloric acid concentration

The effect of HCl concentration in the analyte sample depended on whether L-cysteine was present or absent. Many of the studies that have examined the effect of HCl have carried out the hydride generation reaction in an HCl medium. The experiments for this thesis were carried out in a sodium acetate buffer medium, with the HCl being added only to the As standard samples. These differences in the medium used make comparisons difficult.

3.4.3.1 Effect of HCl concentration on As^{III} sensitivity in the absence of L-cysteine

In the absence of L-cysteine, addition of a small amount of acid to give a final HCl concentration of 0.012 mol L^{-1}, showed a 20 % increase in As^{III} sensitivity compared to the sensitivity obtained in the absence of acid (section 3.3.3.1). The sensitivity was constant between 0.012 and 0.048 mol L^{-1} HCl. Between 0.048 and 0.242 mol L^{-1} HCl, the sensitivity decreased; further increase in HCl concentration resulted in a gradual increase in sensitivity, reaching maximum and constant values at $\geq$ 3.6 mol L^{-1} HCl.

There have been many studies carried out examining the effect of HCl concentration on the sensitivity of As^{III} in the absence of L-cysteine.[23-25, 27-33] The results from most of these studies are very similar.

Anderson *et al*.,[32] Le *et al*.,[27] Shraim *et al*.,[24] and Carrero *et al*.[25] all observed a sharp increase in As^{III} sensitivity within the HCl concentration range 0 to 1 mol L^{-1}. Both Cabon and Cabon[30] and Yang and Zhang[33] observed a rapid increase in sensitivity in the concentration range 0 to 0.2 mol L^{-1}. Chen *et al*.[28] observed a rapid increase in sensitivity as the HCl concentration was increased up to 0.1 mol L^{-1}, whereas Anthemidis *et al*.[31] observed an increase in As^{III} sensitivity up to 2 mol L^{-1}. After this rapid increase in sensitivity, there is generally no significant difference in sensitivity upon increasing the HCl concentration

further. The large increase in sensitivity upon addition of HCl was not observed in this thesis work. Table 3.12 below summarises the increase in sensitivity observed over various HCl concentration ranges from the literature.

HCl concentration range/mol L^{-1} [a]	Ratio[b]	Reference
0.05-0.2	5	[33]
0.1-1	2.2	[32]
0.1-2	2.3	[31]
0.05-3	4	[25]
0.1-2	4	[24]
0.01-0.1	10	[28]
0.05-0.2	4	[30]
0.005-0.01	4	[29]
0.1-2.5	10	[27]
0-0.02	1.2	this work
0-3.6	1.7	this work

Table 3.12 Summary and comparison of literature results regarding the increase in sensitivity with increasing HCl concentration.

[a]Concentration range in which the increase in sensitivity was observed.

[b]Ratio of sensitivities at high and low end of HCl concentration range as indicated in the table.

Note that some of the HCl concentrations and absorbance readings were estimated by reading directly from figures

Table 3.12 shows that the increase in sensitivity upon addition of HCl reported by other workers is significantly greater than that from the results in this thesis. In addition, none of the reported results showed a decrease in sensitivity before increasing again as the results in this thesis showed. This difference may be due to the medium that the hydride generation reaction is carried out in. The results from the literature were all carried out in an HCl medium.

A second possibility to account for the difference between the results from this thesis and those by other workers, is that there may be a change in the mechanism of hydride generation at higher HCl concentrations. In many of the experiments carried out in the presence of L-cysteine a decrease in sensitivity is observed before a final increase at high HCl concentrations. Carrero *et al*.[25] proposed that under the conditions used in their study, AsH_3 generation may be occurring by two different mechanisms: (i) a first mechanism which takes place at very low acid concentrations; and (ii) a second mechanism which takes place at

higher acid concentrations. It is possible that two mechanisms may be occurring in the hydride generation system used in this work.

For As^{III} measurements, an HCl concentration of 0.03 mol L^{-1} was used for future work. Even though maximum sensitivity was obtained at ≥ 3.6 mol L^{-1} HCl, this was not chosen as it would require large amounts of Aristar grade HCl.

3.4.3.2 Effect of HCl concentration on As^V sensitivity in the presence of L-cysteine

The results from this thesis showed that As^V samples, in the presence of L-cysteine, gave constant and maximum sensitivity within the HCl concentration range 0 to 0.06 mol L^{-1}, before a marked decrease in sensitivity as the HCl concentration was increased up to 0.12 mol L^{-1}. At concentrations > 0.75 mol L^{-1} there is evidence to suggest a gradual increase in As^V sensitivity (section 3.3.3.2).

Carrero *et al.*[25] and Shraim *et al.*[24] examined the effect of HCl concentration on the sensitivity of a number of As species in the presence of L-cysteine. Both groups observed a rapid increase in sensitivity for As^V on the addition of small amounts of HCl. However, both Carrero *et al.*[25] and Shraim *et al.*[24] found that increasing the HCl concentration beyond 0.1 mol L^{-1} resulted in a sharp decrease in sensitivity; furthermore, at concentrations > 2 mol L^{-1} the sensitivity increased again to reach a maximum and constant value between 9 to 10 mol L^{-1}. Le *et al.*[27] observed similar behaviour to that of Carrero *et al.*[25] and Shraim *et al.*,[24] except that the HCl concentration range that gave maximum values, and the HCl concentration where decrease and increase in sensitivity occurred, were different.

The results of Chen *et al.*[28] are the most similar to ours. In the presence of L-cysteine Chen *et al.*[28] varied the HCl concentration from 0.005 to 0.1 mol L^{-1}. They observed maximum sensitivity over the HCl concentration range 0.01 to 0.03; the increase in sensitivity from that measured at 0.005 mol L^{-1} to the maximum sensitivity was only 10 %. At HCl concentrations > 0.03 mol L^{-1}, a decrease in sensitivity was observed.

Overall, except for the initial increase in sensitivity, the results in this thesis are in reasonable agreement with those from the literature. For further As^V measurements in the presence of L-cysteine, an HCl concentration of 0.03 mol L^{-1} was used.

3.4.4 Effect of graphite furnace

The difference in sensitivity observed for new and old graphite furnaces (section 3.3.4) is likely due to the corrosion of the graphite furnace and removal of some of the pyrolytic-graphite coating. For old graphite furnaces this may mean that there is the possibility of more than one type of Pd-carbon surface upon which adsorption can occur, resulting in a non-uniform rate of release of As from the Pd modifier. The differences in appearance temperature of the As signal between new (1.12 s) and old (0.91 s) graphite furnaces support this explanation. For new furnaces the As is retained to higher temperatures than for old furnaces, which indicates an increase in stability of the AsH_3-Pd product for the newer graphite furnace. In addition, the difference between the effects of Pd pre-treatment temperatures for aged and new furnaces indicates that the age of the furnace can affect other parameters and this may be why different results are reported in the literature for seemingly similar conditions.

Walcerz *et al*.[40] found differences in both As and Sb sensitivity between Pd coated electrographite furnaces and Pd coated pyrolytic-graphite furnaces. The sensitivity was lower when the electrographite furnace was used. Doidge *et al*.[53] carried out Ge measurements using Pd coated electrographite and Pd coated pyrolytic-graphite furnaces. Like Walcerz *et al*.,[40] they found that sensitivity was higher for the pyrolytic-graphite furnaces than the electrographite furnaces. Walcerz *et al*.[40] found a 25 % difference in sensitivity between the electrographite and pyrolytic-graphite furnaces for As, and a 45 % difference for Sb. The difference in integrated absorbance was less, which agrees with the results from this thesis for a new and aged graphite furnace. Doidge *et al*.[53] observed a 55 % increase in sensitivity for Ge at the pyrolytic-graphite furnace compared with the electrographite furnace. These results suggest that pyrolytic-graphite furnaces and electrographite furnaces behave differently with respect to both the graphite-Pd-As or graphite-Pd-Ge system. This is not surprising due to the different porosities of the two graphite surfaces. It is possible that when a pyrolytic-graphite furnace is aged, there are actually two types of adsorption sites for the analyte: Pd-electrographite sites exposed by ablation of the pyrolytic-graphite, and Pd-pyrolytic-graphite sites. If these sites show different behaviour (as indicated by the literature results above) then this may be a possible reason for the complex peak structure that is observed with old graphite furnaces. Furthermore, although in the absence of Pd, electrographite graphite furnaces are reported to be better at adsorbing hydride species than pyrolytic-graphite

furnaces,[40, 42, 53] this is unlikely to be the reason for the complex peak structure observed in the work for this thesis, as in the absence of Pd an As signal was not obtained.

Volynsky and Wennrich[58] also observed differences between 'new' and 'old' pyrolytic-graphite furnaces when using modifiers with direct liquid sample injection, rather than hydride generation accumulation. Lower characteristic masses (correlating to higher sensitivity) for As, Se, and In were obtained for graphite furnaces that had been used for less than 40 analyses compared to furnaces that had been used for more than 40 when using Ru and Rh as modifiers. Furthermore, characteristic masses obtained on different days, but using the same experimental conditions and modifier, varied significantly. Furthermore, Volynsky and Wennrich[58] observed double peaks and poor peak shape for As, Se, and In standard solutions in the presence of a Pd modifier. They comment that pronounced differences in peak shapes indicate that the process in the graphite atomizer may vary even for the same chemical modifier and also that the complex shape of the signals indicate that at least two In-Pd and As-Pd compounds are present in the graphite furnace after the pyrolysis stage. This could be due to differences in the surface of the graphite furnace.

Kopysc *et al*.[56] also observed pronounced differences in peak shape with different graphite furnaces. They examined the direct injection of Se, As and Sb solutions in the presence of a Pd modifier. Kopysc *et al*.[56] found that using graphite tubes from one box ("tube 1") for repetitive determinations resulted in good peak signals. However it was not always possible to reproduce these good results with other graphite tubes. They refer to these tubes as "tube 2". When Pd was pre-reduced on "tube 2", asymmetrical and non-reproducible signals were obtained. This behaviour was specifically observed for both As and Sb and to a lesser extent for Se. A further examination of more graphite tubes found that some behave as "tube 1" and others behaved as "tube 2". It was thought that fast ablation of the surface of the "tube 2" series was the reason for this phenomenon. However, observations of the graphite surface with a scanning electron microscope gave no evidence for such a correlation. Kopysc *et al*.[56] also comment that the shape of the signals does not change within the lifetime of the tube; this is contradictory to the observations in this thesis, as in some instances when a tube that had shown to have double peak behaviour was used the next day, it was found that this behaviour had disappeared.

Voth-Beach and Shrader[61] also comment that the surface of the graphite furnace is another parameter affecting performance of the Pd modifier. However, they report that new pyrolytic-graphite coated graphite tubes gave poorer recoveries for direct Se injections, than old pyrolytic-graphite coated tubes (50-100 previous injections). This contradicts the results from the work in this thesis and those of Volynsky and Wennrich.[58] Voth-Beach and Shrader[61] comment that it is likely that Pd particle size and distribution are influenced by the chemistry of the graphite surface. In addition, their results could not always be exactly reproduced.

The general improvement in sensitivity for mixed modifiers over their single modifier analogues;[33, 62] indicates that the graphite surface plays an important role and it is not just the Pd-As interaction that is important. Graphite furnaces treated with W before application of modifier showed more extensive and uniform modifier distribution.[65] Some of the results from this thesis and those discussed in the literature, indicate that the use of Pd as a chemical modifier is very sensitive to the quality of the graphite furnace. The results from this section of work and that from the literature illustrate the highly dependent nature of the analyte modifier interaction on the quality of the graphite surface. This is likely to be a major contribution to some of the inconsistent results reported in the literature.

3.4.5 Effect of Fe^{III} on sensitivity

The experiments for this thesis were carried out in a sodium acetate/acetic acid reaction medium. There have been no reports examining the effect of transition metals on analyses carried out in this medium. This makes it difficult to compare results to those of other workers.

3.4.5.1 Effect of Fe^{III} on As^{III} sensitivity in the absence of L-Cysteine

For As^{III} in the absence of L-cysteine, an Fe^{III} concentration as low as 0.25 ppm decreased the sensitivity by ~ 12 %, at 2 ppm Fe^{III} the reduction in sensitivity was ~ 80 % (section 3.3.5).

For the hydride generation system used in the work for this thesis, the interference by Fe^{III} occurs at a much lower concentration than that reported by other workers. Uggerud and Lund,[68] Chen *et al*.,[28] Feng *et al*.[29] and Anderson *et al*.,[32] all report higher concentrations of Fe^{III} before interference is observed. Uggerud and Lund[68] report a 45 % decrease in sensitivity for As^{III} at an Fe^{III} concentration of 100 ppm, whereas the results from this thesis

showed a 50 % decrease in sensitivity at 1 ppm Fe^{III}. Chen *et al.*[28] observed only a 7 % decrease in sensitivity at 20 ppm Fe^{III}, while Feng *et al.*[29] observed a 7 % decrease in sensitivity for Fe^{III} concentrations as high as 5 ppm. Anderson *et al.*[32] observed no significant effect on hydride generation at a Fe^{III} concentration of 100 ppm.

The large differences between the results present in this thesis and those from the literature may be due to the differences in the concentration of HCl used. Hydrochloric acid concentration has been shown to play a critical role in preventing and reducing interferences arising from transition metals.[26, 43, 69] It is thought that the high HCl concentration increases the solubility of the reduced metal (see section 3.1.3.2), and/or the compound formed between the analyte element and the interferent.[26] Alternatively, another possible explanation could be competition for the $NaBH_4$ between the acid and interfering metal ion. More $NaBH_4$ is consumed by the higher acid concentrations and therefore less is available for reduction of the interfering element to the metal.[26] Welz and Schubert-Jacobs[26] suggest that competition for the $NaBH_4$ between the analyte and interferent is excluded because of the very small amount of reductant required for hydride formation. Welz and Schubert-Jacobs[26] also comment that formation of chloro complexes of the interfering metal may be important in preventing interference.

Welz and Schubert-Jacobs[26] report that for the determination of As^{III}, an increase in the HCl concentration from 0.5 to 5 mol L^{-1} resulted in an increase of the tolerance limit for Cu^{2+} from 100 to 500 mg L^{-1}, and for Ni^{2+} from 3 to 100 mg L^{-1}. Boampong *et al.*[69] compared the use of 1.4 and 5 mol L^{-1} HCl to reduce interferences. Increasing the concentration from 1.4 to 5 mol L^{-1} HCl leads to 100 % efficiency in AsH_3 production in the presence of Fe^{II}, Fe^{III}, and Cd^{II} at 1000 mg L^{-1}, and Cu^{II} at 10 000 mg L^{-1}. Similar results were found by An *et al.*;[43] increasing the HCl concentration from 1 to 5 mol L^{-1} led to 100 % efficiency in AsH_3 production in the presence of Co^{II} and Ni^{II} and an improvement in signal response in the presence of Rh^{III}, Pt^{IV}, Pd^{II}, Au^{III} and Sn^{IV}.

The experiments in this thesis were carried out at pH 5.0 using 0.25 mol L^{-1} sodium acetate buffer. The pH did not change significantly over the Fe^{III} concentration range studied. In the studies from the literature mentioned above, the pH was < 2. Uggerud and Lund[68] used an HCl concentration of 0.05 mol L^{-1} as their reaction medium, Chen *et al.*[28] used 0.01 mol L^{-1}, Feng *et al.*[29] used 0.12 mol L^{-1} and Anderson *et al.*[32] used 5 mol L^{-1}. At the pH used in

experiments for this thesis (pH 5.0), the Fe^{III} species present would be $Fe(OH)_{3\,(s)}$ (which can adsorb As) whereas for the work reported in the literature the Fe^{III} species would be in the dissolved phase (e.g. $Fe(H_2O)_6^{3+}$ and $Fe(OH)(H_2O)_5^{2+}$). Therefore it is possible that pH is the reason for the differences observed. However, Anderson *et al*.[32] also carried out experiments using a citric acid/sodium citrate medium (0.4 mol L^{-1} in sodium citrate, pH 6.0) and found no significant interference up to 100 ppm Fe^{III}. There is no indication whether the pH of the solution changed during their experiments. It is possible that a citrate based medium may be more tolerant to Fe^{III} interference than an acetate based medium due to differences in complexation. Sodium citrate has been shown to increase the tolerance level for Ni^{II} and Cu^{II} interferences in Ge determinations.[50]

3.4.5.2 Effect of Fe^{III} on As^{V} sensitivity in the presence of L-cysteine

For As^{V} in the presence of L-cysteine, a concentration of 50 ppm Fe^{III} could be tolerated before a decrease in sensitivity was observed. The decrease in sensitivity for As^{V} observed in the presence of L-cysteine coincides with a decrease in pH of the reaction mixture exiting the reaction coil, however this is unlikely to be the cause of the decrease as previous results (section 3.3.3) show that sufficient hydride generation occurs at these low pH values.

For As^{V} in the presence of L-cysteine, Yin *et al*.[34] observed a 7 and 20 % decrease in sensitivity at 1 and 10 ppm Fe^{III}, respectively. This was carried out for 2 ppb As^{V} in the presence of 0.08 mol L^{-1} L-cysteine. These concentrations of Fe^{III} that cause interference are lower than those reported in this thesis. However, Chen *et al*.[28] found no interference at 200 ppm Fe^{III} using 125 ppb As and 0.5 % w/v L-cysteine; this Fe^{III} concentration is approximately 4 times higher than the upper limit of interference-free determinations reported in this thesis. Chen *et al*.[28]used a higher concentration of L-cysteine and in addition, their experiments were carried out in 0.02 mol L^{-1} HCl. Both of these factors may be reasons why they were able to observe higher Fe^{III} concentrations without interference.

The large differences in the concentration of Fe^{III} that can be tolerated in the absence and presence of L-cysteine indicates that L-cysteine plays a critical role in preventing interference of Fe^{III} on the generation of AsH_3. The results from this thesis show that in the presence of L-cysteine, a 200 fold increase in Fe^{III} concentration can be tolerated, compared to the absence of L-cysteine. This improvement in metal interference tolerance level using L-cysteine has also been reported in the literature for Fe^{III} and other transition metal ions.[28, 39, 43, 49, 69]

In the absence of L-cysteine, Howard and Salou[39] observed interferences on the As signal by Co^{II}, Cu^{II}, Fe^{II} and Ni^{II} at < 1 ppm. However, addition of L-cysteine resulted in full recovery of the As signal at these low metal concentrations. Furthermore, for Co^{II}, Cu^{II}, and Fe^{III} no significant interference was observed at concentrations as high as 50 ppm in the presence of L-cysteine. This behaviour was found for As^{V}, As^{III}, MMAA and DMAA. Chen *et al*.[28]showed that without L-cysteine, Au^{III}, Pt^{IV}, Pd^{II}, Ag^{I}, Ni^{II}, Co^{II}, Cu^{II}, Fe^{III}, Fe^{II} and Zn^{II} interfered with the hydride generation process. Addition of L-cysteine (0.5 % w/v) resulted in an increase in the tolerance to interference by 1 to 3 orders of magnitude, depending on the interferent.

Howard and Salou[39] suggest that L-cysteine can protect against metal ion interference due to its metal complexing ability, therefore, presumably preventing reduction of the interfering metal ion. Brindle and Le[50] used UV-Vis spectroscopy to determine whether there is any evidence for the formation of a complex between L-cysteine and Ni^{II} and Co^{II}. The absorption spectra of Ni^{II} and Co^{II} in distilled water and in 0.01 mol L^{-1} L-cysteine solution showed no difference, suggesting that formation of a complex was unlikely between L-cysteine and these transition metals, under the conditions used. However, the results from this thesis show that when Fe^{III} was added to L-cysteine, a blue colour was produced which disappeared with time. The intensity of the colour and the time required for decolourisation depended on the amount of Fe^{III} present; Fe^{III} is known to form a blue complex with L-cysteine.[77, 78] Complexation by L-cysteine may be an important factor for preventing Fe^{III} interference. Brindle and Le[50] did observe a shift in the UV-Vis absorption peak when L-cysteine and $NaBH_4$ were mixed, compared with the UV-Vis spectra of L-cysteine and $NaBH_4$ individually (as already discussed in section 3.4.2.1). This suggests that a reaction has occurred between $NaBH_4$ and L-cysteine and the authors suggest that interference from transition metals may be decreased owing to selective reduction by this intermediate species compared to $NaBH_4$ alone.

3.4.6 Effect of argon flow rate

The argon flow rate significantly affects As sensitivity (section 3.3.6). The highest sensitivity was obtained when the argon flow was turned off. This suggests that sufficient H_2 is being produced from the reaction of $NaBH_4$ and acid/buffer, to transport the generated AsH_3 to the graphite furnace. However the reproducibility was poorest at low argon flow rates. The rapid

decrease in sensitivity above 28 mL min^{-1} is presumably due to a decrease in residence time of AsH_3 in the vicinity of the Pd modifier, resulting in lower adsorption efficiency.

Toa and Fang[79], for Ge determinations, reported that the effects from the carrier gas flow rate were negligible and the amount of hydrogen generated during the reaction was sufficient to transport the hydride to the graphite furnace; therefore, no carrier gas was used in their work. These results are similar to those present in this thesis in that the maximum sensitivity was observed in the absence of the carrier gas.

The results of Walcerz *et al.*[40] agree well with the findings in this thesis. The argon carrier gas flow rate was varied from 33 to 166 mL min^{-1} and a steady decrease in the sensitivity was noted. The general trend was similar to that present in this thesis, except that sufficient hydride adsorption was still achieved at flow rates > 100 mL min^{-1}. The authors suggest that the decrease in sensitivity may be due to shorter residence times inside the graphite furnace and/or local cooling of the graphite furnace by the gas flow. Cooling of the graphite furnace during the accumulation step is unlikely to affect the results from this thesis as it was found that sufficient deposition of AsH_3 occurred on the Pd surface for temperatures as low as 25 ^oC.

Other workers' results do not agree with those from this thesis. Zhang *et al.*[60] varied the argon flow rate from 100 to 1000 mL min^{-1}. They observed a rapid increase in sensitivity between 100 and 400 mL min^{-1}; thereafter no significant change in sensitivity was observed. In addition, Yang and Zhang[33] found that AsH_3 could be adsorbed in the graphite furnace at relatively high flow rates (350 to 750 mL min^{-1}). Liang *et al.*[41] comment that the purging gas flow rate may be as high as 200 mL min^{-1} without breakthrough because of the high affinity of the Pd coated platform for AsH_3.

It is unclear as to why different workers observed different findings with regards to the influence of carrier flow rate. It is possible that the mass of Pd has an effect. An increase in Pd mass results in an increase in surface area.[44] Hence a larger mass of Pd may be able to capture the AsH_3 more efficiently at higher carrier flow rates. The experiments for this thesis were carried out using 2 µg of Pd; Zhang *et al.*[60] used 5 µg, Liang *et al.*[41] used 18 µg, Yang and Zhang[33] used 15 µg, and Walcerz *et al.*[40] used 10 µg. Furthermore, the type of gas-liquid separator may also contribute to the differences observed. Depending on the gas-liquid

separator used, higher carrier flow rates may result in more acid fumes or water vapour entering the delivery tubing, causing gas phase interferences. This is also probably related to the acid and $NaBH_4$ concentrations and the reagent and sample flow rates.

3.5 Conclusion

This section of work shows that there are a number of parameters that affect the performance and therefore sensitivity of the hydride generation method. Many of the chemical parameters investigated were dependent on the presence or absence of L-cysteine. In addition, the effect of $NaBH_4$ was dependent on the concentration of NaOH. The interdependent nature of many of these parameters has been illustrated in this thesis and reported in the literature. This is one of the reasons why the optimized conditions found in the literature are rather variable.

Another factor that is likely to contribute to the variability in reported optimized conditions is the graphite furnace. The results from this thesis used showed differences in peak-profile and pre-treatment temperatures when new and old graphite furnaces were compared. Therefore, it is recommended that individual optimization of the hydride generating system should be carried out rather than relying on optimized conditions reported in the literature.

3.6 References

1. Dedina, J., Flow methods in gas-liquid separations. In *Flow analysis with atomic spectrometric detectors*, Sanz-Medel, A., Ed. Elesvier: New York, 1999.

2. Yan, X. P.; Ni, Z. M., Vapor generation atomic-absorption spectrometry. *Analytica Chimica Acta* **1994,** 291, (1-2), 89-105.

3. Karadjova, I. B.; Lampugnani, L.; Dedina, J.; D'Ulivo, A.; Onor, M.; Tsalev, D. L., Organic solvents as interferents in arsenic determination by hydride generation atomic absorption spectrometry with flame atomization. *Spectrochimica Acta Part B-Atomic Spectroscopy* **2006,** 61, (5), 525-531.

4. Matusiewicz, H.; Krawczyk, M., On-line hyphenation of hydride generation with in situ trapping flame atomic absorption spectrometry for arsenic and selenium determination. *Analytical Sciences* **2006,** 22, (2), 249-253.

5. Sur, R.; Dunemann, L., Method for the determination of five toxicologically relevant arsenic species in human urine by liquid chromatography-hydride generation atomic absorption spectrometry. *Journal of Chromatography B-Analytical Technologies in the Biomedical and Life Sciences* **2004,** 807, (2), 169-176.

6. Boutakhrit, K.; Claus, R.; Bolle, F.; Degroodt, J. M.; Goeyens, L., Open digestion under reflux for the determination of total arsenic in seafood by inductively coupled plasma atomic emission spectrometry with hydride generation. *Talanta* **2005,** 66, (4), 1042-1047.

7. Gettar, R. T.; Garavaglia, R. N.; Gautier, E. A.; Batistoni, D. A., Determination of inorganic and organic anionic arsenic species in water by ion chromatography coupled to hydride generation-inductively coupled plasma atomic emission spectrometry. *Journal of Chromatography A* **2000,** 884, (1-2), 211-221.

8. Simon, S.; Tran, H.; Pannier, F.; Potin-Gautier, M., Simultaneous determination of twelve inorganic and organic arsenic compounds by liquid chromatography-ultraviolet irradiation-hydride generation atomic fluorescence spectrometry. *Journal of Chromatography A* **2004,** 1024, (1-2), 105-113.

9. Adair, B. M.; Hudgens, E. E.; Schmitt, M. T.; Calderon, R. L.; Thomas, D. J., Total arsenic concentrations in toenails quantified by two techniques provide a useful biomarker of chronic arsenic exposure in drinking water. *Environmental Research* **2006,** 101, (2), 213-220.

10. Bohari, Y.; Astruc, A.; Astruc, M.; Cloud, J., Improvements of hydride generation for the speciation of arsenic in natural freshwater samples by HPLC-HG-AFS. *Journal of Analytical Atomic Spectrometry* **2001,** 16, (7), 774-778.

11. Leal, L. O.; Forteza, R.; Cerda, V., Speciation analysis of inorganic arsenic by a multisyringe flow injection system with hydride generation-atomic fluorescence spectrometric detection. *Talanta* **2006,** 69, (2), 500-508.

12. Sanchez-Rodas, D.; Gomez-Ariza, J. L.; Giraldez, I.; Velasco, A.; Morales, E., Arsenic speciation in river and estuarine waters from southwest Spain. *Science of the Total Environment* **2005,** 345, (1-3), 207-217.

13. Menegario, A. A.; Gine, M. F., Rapid sequential determination of arsenic and selenium in waters and plant digests by hydride generation inductively coupled plasma-mass spectrometry. *Spectrochimica Acta Part B-Atomic Spectroscopy* **2000,** 55, (4), 355-362.

14. Nakazato, T.; Taniguchi, T.; Tao, H.; Tominaga, M.; Miyazaki, A., Ion-exclusion chromatography combined with ICP-MS and hydride generation-ICP-MS for the determination of arsenic species in biological matrices. *Journal of Analytical Atomic Spectrometry* **2000,** 15, (12), 1546-1552.

15. Matusiewicz, H.; Slachcinski, M., Simultaneous determination of hydride forming and Hg in sonicate slurries of biological and elements (As, Sb, Se, Sn) environmental reference materials by hydride generation microwave induced plasma optical emission spectrometry (SS-HG-MIP-OES). *Microchemical Journal* **2006,** 82, (1), 78-85.

16. Nakahara, T., Hydride generation techniques in atomic spectroscopy. In *Advances in atomic spectroscopy*, Sneddon, J., Ed. JAI Press: Greenwich, 1995; Vol. 2, pp 139-178.

17. Li, X.; Jia, J.; Wang, Z. H., Speciation of inorganic arsenic by electrochemical hydride generation atomic absorption spectrometry. *Analytica Chimica Acta* **2006,** 560, (1-2), 153-158.

18. Ding, W. W.; Sturgeon, R. E., Evaluation of electrochemical hydride generation for the determination of arsenic and selenium in sea water by graphite furnace atomic absorption with in situ concentration. *Spectrochimica Acta Part B-Atomic Spectroscopy* **1996,** 51, (11), 1325-1334.

19. Denkhaus, E.; Golloch, A.; Guo, X. M.; Huang, B., Electrolytic hydride generation (Ec-HG) - a sample introduction system with some special features. *Journal of Analytical Atomic Spectrometry* **2001,** 16, (8), 870-878.

20. D'Ulivo, A., Chemical vapor generation by tetrahydroborate(III) and other borane complexes in aqueous media - a critical discussion of fundamental processes and mechanisms involved in reagent decomposition and hydride formation. *Spectrochimica Acta Part B-Atomic Spectroscopy* **2004,** 59, (6), 793-825.

21. D'Ulivo, A.; Onor, M.; Pitzalis, E., Role of hydroboron intermediates in the mechanism of chemical vapor generation in strongly acidic media. *Analytical Chemistry* **2004,** 76, (21), 6342-6352.

22. Bermejo-Barrera, P.; Moreda-Pineiro, J.; Moreda-Pineiro, A.; Bermejo-Barrera, A., Selective medium reactions for the 'arsenic(III)', 'arsenic(V)', dimethylarsonic acid and monomethylarsonic acid determination in waters by hydride generation on-line electrothermal atomic absorption spectrometry with in situ preconcentration on Zr-coated graphite tubes. *Analytica Chimica Acta* **1998,** 374, (2-3), 231-240.

23. Coelho, N. M. M.; da Silva, A. C.; da Silva, C. M., Determination of As(III) and total inorganic arsenic by flow injection hydride generation atomic absorption spectrometry. *Analytica Chimica Acta* **2002,** 460, (2), 227-233.

24. Shraim, A.; Chiswell, B.; Olszowy, H., Speciation of arsenic by hydride generation-atomic absorption spectrometry (HG-AAS) in hydrochloric acid reaction medium. *Talanta* **1999,** 50, (5), 1109-1127.

25. Carrero, P.; Malave, A.; Burguera, J. L.; Burguera, M.; Rondon, C., Determination of various arsenic species by flow injection hydride generation atomic absorption spectrometry: Investigation of the effects of the acid concentration of different reaction media on the generation of arsines. *Analytica Chimica Acta* **2001,** 438, (1-2), 195-204.

26. Welz, B.; Schubertjacobs, M., Mechanisms of transition-metal interferences in hydride generation atomic-absorption spectrometry .4. Influence of acid and tetrahydroborate concentrations on interferences in arsenic and selenium determinations. *Journal of Analytical Atomic Spectrometry* **1986,** 1, (1), 23-27.

27. Le, X. C.; Cullen, W. R.; Reimer, K. J., Effect of cysteine on the speciation of arsenic by using hydride generation atomic-absorption spectrometry. *Analytica Chimica Acta* **1994,** 285, (3), 277-285.

28. Chen, H. W.; Brindle, I. D.; Le, X. C., Prereduction of arsenic(V) to arsenic(III), enhancement of the signal, and reduction of interferences by L-cysteine in the determination of arsenic by hydride generation. *Analytical Chemistry* **1992,** 64, (6), 667-672.

29. Feng, Y. L.; Chen, H. Y.; Tian, L. C.; Narasaki, H., Off-line separation and determination of inorganic arsenic species in natural water by high resolution inductively coupled plasma mass spectrometry with hydride generation combined with reaction of arsenic(V) and L-cysteine. *Analytica Chimica Acta* **1998,** 375, (1-2), 167-175.

30. Cabon, J. Y.; Cabon, N., Determination of arsenic species in seawater by flow injection hydride generation in situ collection followed by graphite furnace atomic absorption spectrometry - stability of As(III). *Analytica Chimica Acta* **2000,** 418, (1), 19-31.

31. Anthemidis, A. N.; Zachariadis, G. A.; Stratis, J. A., Determination of arsenic(III) and total inorganic arsenic in water samples using an on-line sequential insertion system and hydride generation atomic absorption spectrometry. *Analytica Chimica Acta* **2005,** 547, (2), 237-242.

32. Anderson, R. K.; Thompson, M.; Culbard, E., Selective reduction of arsenic species by continuous hydride generation .1. Reaction media. *Analyst* **1986,** 111, (10), 1143-1152.

33. Yang, L. L.; Zhang, D. Q., In situ preconcentration and determination of trace arsenic in botanical samples by hydride generation-graphite furnace atomic absorption spectrometry with Pd-Zr as chemical modifier. *Analytica Chimica Acta* **2003,** 491, (1), 91-97.

34. Yin, X.; Hoffmann, E.; Ludke, C., Differential determination of arsenic(III) and total arsenic with L-cysteine as prereductant using a flow injection non-dispersive atomic absorption device. *Fresenius Journal of Analytical Chemistry* **1996,** 355, (3-4), 324-326.

35. Shraim, A.; Chiswell, B.; Olszowy, H., Use of perchloric acid as a reaction medium for speciation of arsenic by hydride generation-atomic absorption spectrometry. *Analyst* **2000,** 125, (5), 949-953.

36. Gonzalez, J. C.; Lavilla, I.; Bendicho, C., Evaluation of non-chromatographic approaches for speciation of extractable As(III) and As(V) in environmental solid samples by FI-HGAAS. *Talanta* **2003,** 59, (3), 525-534.

37. Tsalev, D. L.; Sperling, M.; Welz, B., Flow-injection hydride generation atomic absorption spectrometric study of the automated on-line pre-reduction of arsenate, methylarsonate and dimethylarsinate and high-performance liquid chromatographic separation of their L-cysteine complexes. *Talanta* **2000,** 51, (6), 1059-1068.

38. Niedzielski, P.; Siepak, M., Speciation analysis of inorganic form of arsenic in ground water samples by hydride generation atomic absorption spectrometry with insitu trapping in graphite tube. *Central European Journal of Chemistry* **2005,** 3, (1), 82-94.

39. Howard, A. G.; Salou, C., Cysteine enhancement of the cryogenic trap hydride AAS determination of dissolved arsenic species. *Analytica Chimica Acta* **1996,** 333, (1-2), 89-96.

40. Walcerz, M.; Garbos, S.; Bulska, E.; Hulanicki, A., Continuous-flow hydride generation for the preconcentration and determination of arsenic and antimony by GFAAS. *Fresenius Journal of Analytical Chemistry* **1994,** 350, (12), 662-666.

41. Liang, L. A.; Lazoff, S.; Chan, C.; Horvat, M.; Woods, J. S., Determination of arsenic in ambient water at sub-part-per-trillion levels by hydride generation Pd coated platform collection and GFAAS detection. *Talanta* **1998,** 47, (3), 569-583.

42. Garbos, S.; Walcerz, M.; Bulska, E.; Hulanicki, A., Simultaneous determination of Se and As by hydride generation atomic absorption spectrometry with analyte concentration in a graphite furnace coated with zirconium. *Spectrochimica Acta Part B-Atomic Spectroscopy* **1995,** 50, (13), 1669-1677.

43. An, Y.; Willie, S. N.; Sturgeon, R. E., Flow-injection hydride generation determination of arsenic with insitu concentration in a graphite-furnace. *Spectrochimica Acta Part B-Atomic Spectroscopy* **1992,** 47, (12), 1403-1410.

44. Sturgeon, R. E.; Willie, S. N.; Sproule, G. I.; Robinson, P. T.; Berman, S. S., Sequestration of volatile element hydrides by platinum group elements for graphite-furnace atomic-absorption. *Spectrochimica Acta Part B-Atomic Spectroscopy* **1989,** 44, (7), 667-682.

45. Kumar, A. R.; Riyazuddin, P., Mechanism of volatile hydride formation and their atomization in hydride generation atomic absorption spectrometry. *Analytical Sciences* **2005,** 21, (12), 1401-1410.

46. D'Ulivo, A.; Mester, Z.; Sturgeon, R. E., The mechanism of formation of volatile hydrides by tetrahydroborate(III) derivatization: A mass spectrometric study performed with deuterium labeled reagents. *Spectrochimica Acta Part B-Atomic Spectroscopy* **2005,** 60, (4), 423-438.

47. D'Ulivo, A.; Mester, Z.; Meija, J.; Sturgeon, R. E., Mechanism of generation of volatile hydrides of trace elements by aqueous tetrahydroborate(III). Mass spectrometric studies on reaction products and intermediates. *Analytical Chemistry* **2007,** 79, (7), 3008-3015.

48. Tsalev, D. L.; Dulivo, A.; Lampugnani, L.; DiMarco, M.; Zamboni, R., Thermally stabilized iridium on an integrated, carbide-coated platform as a permanent modifier for hydride-forming elements in electrothermal atomic absorption spectrometry .3. Effect of L-cysteine. *Journal of Analytical Atomic Spectrometry* **1996,** 11, (10), 989-995.

49. Welz, B.; Sucmanova, M., L-cysteine as a reducing and releasing agent for the determination of antimony and arsenic using flow-injection hydride generation atomic-absorption spectrometry .2. Interference studies and the analysis of copper and steel. *Analyst* **1993,** 118, (11), 1425-1432.

50. Brindle, I. D.; Le, X. C., Reduction of interferences in the determination of germanium by hydride generation and atomic emission-spectrometry. *Analytica Chimica Acta* **1990,** 229, (2), 239-247.

51. Sturgeon, R. E.; Willie, S. N.; Berman, S. S., Hydride generation atomic-absorption determination of arsenic in marine-sediments, tissues and sea-water with insitu concentration in a graphite-furnace. *Journal of Analytical Atomic Spectrometry* **1986,** 1, (2), 115-118.

52. Sturgeon, R. E.; Willie, S. N.; Berman, S. S., Hydride generation atomic-absorption determination of antimony in seawater with insitu concentration in a graphite-furnace. *Analytical Chemistry* **1985,** 57, (12), 2311-2314.

53. Doidge, P. S.; Sturman, B. T.; Rettberg, T. M., Hydride generation atomic-absorption spectrometry with insitu pre-concentration in a graphite-furnace in the presence of palladium. *Journal of Analytical Atomic Spectrometry* **1989,** 4, (3), 251-255.

54. Butcher, D. J.; Sneddon, J., *A practical guide to graphite furnace atomic absorption spectrometry*. John Wiley & Sons, INC.: New York, 1998.

55. Ortner, H. M.; Bulska, E.; Rohr, U.; Schlemmer, G.; Weinbruch, S.; Welz, B., Modifiers and coatings in graphite furnace atomic absorption spectrometry - mechanisms of action (a tutorial review). *Spectrochimica Acta Part B-Atomic Spectroscopy* **2002,** 57, (12), 1835-1853.

56. Kopysc, E.; Bulska, E.; Wennrich, R., On the use of noble metals modifiers for simultaneous determination of As, Sb and Se by electrothermal atomic absorption spectrometry. *Spectrochimica Acta Part B-Atomic Spectroscopy* **2003,** 58, (8), 1515-1523.

57. Dedina, J.; Tsalev, D. L., *Hydride generation atomic absorption spectrometry*. John Wiley & Sons INC.: New York, 1995.

58. Volynsky, A. B.; Wennrich, R., Comparative efficiency of Pd, Rh and Ru modifiers in electrothermal atomic absorption spectrometry for the simultaneous determination of As, Se and In in a sodium sulfate matrix. *Journal of Analytical Atomic Spectrometry* **2001,** 16, (2), 179-187.

59. Burguera, M.; Burguera, J. L., Flow-injection electrothermal atomic-absorption spectrometry for arsenic speciation using the fleitmann reaction. *Journal of Analytical Atomic Spectrometry* **1993,** 8, (2), 229-233.

60. Zhang, L.; Ni, Z. M.; Shan, X. Q., Insitu concentration of metallic hydrides in a graphite-furnace coated with palladium. *Spectrochimica Acta Part B-Atomic Spectroscopy* **1989,** 44, (3), 339-346.

61. Vothbeach, L. M.; Shrader, D. E., Investigations of a reduced palladium chemical modifier for graphite-furnace atomic-absorption spectrometry. *Journal of Analytical Atomic Spectrometry* **1987,** 2, (1), 45-50.

62. Lima, E. C.; Brasil, J. L.; Vaghetti, J. C. P., Evaluation of different permanent modifiers for the determination of arsenic in environmental samples by electrothermal atomic absorption spectrometry. *Talanta* **2003,** 60, (1), 103-113.

63. Tsalev, D. L.; Dulivo, A.; Lampugnani, L.; DiMarco, M.; Zamboni, R., Thermally stabilized iridium on an integrated, carbide-coated platform as a permanent modifier for hydride-forming elements in electrothermal atomic absorption spectrometry .2. Hydride generation and collection, and behaviour of some organoelement species. *Journal of Analytical Atomic Spectrometry* **1996,** 11, (10), 979-988.

64. Volynsky, A. B., Mechanisms of action of platinum group modifiers in electrothermal atomic absorption spectrometry. *Spectrochimica Acta Part B-Atomic Spectroscopy* **2000,** 55, (2), 103-150.

65. Tsalev, D. L.; Slaveykova, V. I.; Lampugnani, L.; D'Ulivo, A.; Georgieva, R., Permanent modification in electrothermal atomic absorption spectrometry - advances, anticipations and reality. *Spectrochimica Acta Part B-Atomic Spectroscopy* **2000,** 55, (5), 473-490.

66. Volynsky, A. B.; de Loos-Vollebregt, M. T. C., Vaporization of Pb, as and Ga alone and in the presence of Pd modifier studied by electrothermal vaporization-inductively coupled mass spectrometry. *Spectrochimica Acta Part B-Atomic Spectroscopy* **2005,** 60, (11), 1432-1441.

67. Rettberg, T. M.; Beach, L. M., Peak profile characteristics in the presence of palladium for graphite-furnace atomic-absorption spectrometry. *Journal of Analytical Atomic Spectrometry* **1989,** 4, (5), 427-432.

68. Uggerud, H.; Lund, W., Use of thiourea in the determination of arsenic, antimony, bismuth, selenium and tellurium by hydride generation inductively-coupled plasma-atomic emission-spectrometry. *Journal of Analytical Atomic Spectrometry* **1995,** 10, (5), 405-408.

69. Boampong, C.; Brindle, I. D.; Le, X. C.; Pidwerbesky, L.; Ponzoni, C. M. C., Interference reduction by L-cystine in the determination of arsenic by hydride generation. *Analytical Chemistry* **1988,** 60, (11), 1185-1188.

70. Brindle, I. D.; Le, X. C.; Li, X. F., Convenient method for the determination of trace amounts of germanium by hydride generation direct-current plasma atomic emission-

spectrometry - interference reduction by L-cystine and L-cysteine. *Journal of Analytical Atomic Spectrometry* **1989,** 4, (2), 227-232.

71. Pohl, P.; Zyrnicki, W., Study of chemical and spectral interferences in the simultaneous determination of As, Bi, Sb, Se and Sn by hydride generation inductively coupled plasma atomic emission spectrometry. *Analytica Chimica Acta* **2002,** 468, (1), 71-79.

72. Feng, Y. L.; Narasaki, H.; Chen, H. Y.; Tian, L. C., Speciation of antimony(III) and antimony(V) using hydride generation inductively coupled plasma atomic emission spectrometry combined with the rate of pre-reduction of antimony. *Analytica Chimica Acta* **1999,** 386, (3), 297-304.

73. Yamamoto, M.; Yasuda, M.; Yamamoto, Y., Hydride-generation atomic-absorption spectrometry coupled with flow-injection analysis. *Analytical Chemistry* **1985,** 57, (7), 1382-1385.

74. Docekal, B.; Dedina, J.; Krivan, V., Radiotracer investigation of hydride trapping efficiency within a graphite furnace. *Spectrochimica Acta Part B-Atomic Spectroscopy* **1997,** 52, (6), 787-794.

75. Zhang, L.; McIntosh, S.; Carnrick, G. R.; Slavin, W., Hydride generation flow-injection using graphite-furnace detection - emphasis on determination of tin. *Spectrochimica Acta Part B-Atomic Spectroscopy* **1992,** 47, (5), 701-709.

76. Niedzielski, P.; Siepak, M.; Novotny, K., Determination of inorganic arsenic species As(III) and As(V) by high performance liquid chromatography with hydride generation atomic absorption spectrometry detection. *Central European Journal of Chemistry* **2004,** 2, (1), 82-90.

77. Jameson, R. F.; Linert, W.; Tschinkowitz, A.; Gutmann, V., Anaerobic oxidation of cysteine to cystine by iron(III) .1. The reaction in acidic solution. *Journal of the Chemical Society-Dalton Transactions* **1988**, (4), 943-946.

78. Page, F. M., The ferric thiol reaction - the iron cysteine complexes - their constitution and optical properties. *Transactions of the Faraday Society* **1955,** 51, (7), 919-925.

79. Tao, G. H.; Fang, Z. L., Determination of trace and ultra-trace amounts of germanium in environmental-samples by preconcentration in a graphite-furnace using a flow-injection hydride generation technique. *Journal of Analytical Atomic Spectrometry* **1993,** 8, (4), 577-584.

Chapter 4

Measurement of As^{V} and As^{III} diffusion coefficients through diffusive gels and membrane filters

4.1 Introduction

To calculate the concentration of an analyte in the bulk solution (C) from the DGT technique (using equation 4.1), the diffusion coefficient (D) of the analyte in the polyacrylamide diffusive gel needs to be measured.

$$C = \frac{M\Delta g}{DtA} \qquad \textbf{(4.1)}$$

C = concentration of analyte in bulk solution
M = mass of analyte accumulated on adsorbent
D = diffusion coefficient of analyte in diffusive gel
t = deployment time
Δg = thickness of diffusive layer (diffusive gel + membrane filter)
A = sampling window area

The diffusion coefficients of many analytes through polyacrylamide diffusive gels are reported in the literature. For metal ions, the diffusion coefficients are generally 85 to 100 % of the analyte diffusion coefficient in water[1-5] and depend on the composition of the diffusive gel used.[1] Information regarding the diffusion coefficients of As^{V} or As^{III} species through polyacrylamide diffusive gel, or in water, is limited. Therefore, the As^{V} and As^{III} diffusion coefficients through polyacrylamide diffusive gel needed to be measured for this thesis work. In this chapter, 'As^{V}' refers to the $H_2AsO_4^-$ species and 'As^{III}' refers to the H_3AsO_3 species, unless stated otherwise. The experiments described in this chapter were carried out at pH 5.0; at this pH the As^{V} species, $H_2AsO_4^-$, and As^{III} species, H_3AsO_3, predominate.

4.1.1 DGT adsorbents

For DGT to be successfully used, an appropriate adsorbent is required that adsorbs analyte that diffuses through the diffusive gel. A variety of adsorbents have been applied for the DGT technique. Chelex-100 (iminodiacetate chelating resin) has been used most extensively to accumulate a variety of metal ions; these include Ni,[6-8] Cu,[6-12] Cd,[6, 7, 9-11, 13] Zn,[5, 6, 9, 13] Pb,[6, 14] Co,[6, 9] Mn,[9, 11, 13, 15] Ca,[7, 16] Mg,[7, 16] Fe,[13] and Al [15, 17, 18]. However, many other adsorbents have also been reported. Silver iodide has been used for sulfide determinations,[19] a cation exchange resin for Cs and Sr,[3] ammonium molybdophosphate (more selective than a general cation exchange resin) for Cs,[20] Spheron-Thiol resin for Hg,[21] TEVA resin for Tc,[22] and iron-oxides for $H_2PO_4^-$,[23, 24] MoO_4^- [23] and $HAsO_4^{2-}$ [25] determinations. Adsorbents have also been mixed together (i.e. Chelex-100 and iron-oxide) to enable the use of a single DGT device to accumulate both anions and cations.[23] Furthermore, a DGT probe combining both Chelex-100 and silver iodide binding gels have been used to measure metals and sulphide simultaneously.[26, 27]

All of the adsorbents described above consist of a binding agent immobilized in a polyacrylamide gel. Adsorbents have also been prepared in which the gel has been chemically modified, or formed as a co-polymer, to contain functional groups capable of binding Cu and Cd selectively;[28-30] therefore no additional binding agent is required. In other approaches, a solid-state phosphate ion exchange membrane has been used for Cu and Cd determinations[31] and a solid-state membrane containing amino groups was used for determining U species.[32] In addition to solid-based adsorbents, a liquid-based adsorbent (a solution of poly-4-styrenesulfonate) has also been accommodated in specially designed DGT devices for Cd and Cu measurements.[30, 33]

For the work in this thesis, an iron-oxide based adsorbent was used. Iron-oxides strongly adsorb both As^V and As^{III} and have previously been incorporated in DGT devices for As DGT work.[25] For a discussion on As^V and As^{III} adsorption by iron-oxides see chapter 5.

4.1.2 Measuring diffusion coefficients

Westrin *et al.*[34] reviewed a variety of methods that have been used to measure diffusion coefficients of species through gels. They concluded that the use of a diaphragm cell (also known as a diffusion cell) was the most accurate and precise method for measuring diffusion

coefficients in gels. For DGT applications, diffusion cells have been extensively utilized to measure diffusion coefficients of species through the polyacrylamide diffusive gel.

4.1.2.1 Measuring diffusion coefficients using a diffusion cell

The diffusion cell used in the work for this thesis has been described in chapter 2 and only a brief description will be given here. The diffusion cell consists of two compartments (A and B). These compartments are connected by a 1.5 cm diameter opening. A disk of diffusive gel is placed between the openings and the whole assembly is clamped together. Carrier solution is introduced into both compartments; however, compartment A is also spiked with the diffusing species of interest. Both compartments are continually stirred to ensure formation of a thin diffusive boundary layer (DBL) adjacent to the diffusive gel. Due to the analyte concentration gradient between the two compartments, the analyte diffuses from compartment A through the diffusive gel into compartment B. The cumulative mass of analyte diffused from compartment A to compartment B increases linearly with time and is calculated from measuring the concentration in compartment B. Measurements are commenced 5 to 10 min after adding analyte to compartment A; this is to allow establishment of a linear concentration gradient through the gel. The diffusion coefficient (D) is calculated from the slope of a linear plot of the measured mass of analyte that has passed through the diffusive gel *vs*. time, and using equation 4.2. During the few hours that it takes to carry out a diffusion cell experiment, the change in concentration (C) in compartment A is negligible.

$$D = \frac{slope\Delta g}{CA} \qquad \textbf{(4.2)}$$

4.1.2.2 Measuring diffusion coefficients using DGT devices

DGT devices can also be used to measure the diffusion coefficient of the analyte through the diffusive gel. When deployed in analyte solution, the mass of analyte diffused through the diffusive gel and accumulated on the adsorbent increases linearly with time. As above, and using a series of devices, plotting the mass of analyte accumulated on the adsorbent as a function of time, and using the slope of this plot and equation 4.2, the diffusion coefficient can be calculated. However, a further parameter needs to be considered when determining the diffusion coefficient using DGT devices; the mass accumulated on the adsorbent is measured after elution and hence elution efficiency is important. For metal ions, elution from the

Chelex-100 adsorbent is usually carried out by using 1 to 2 mol L^{-1} HNO_3; however the elution is not always quantitative.[7, 13, 35, 36]

4.1.2.3 Measuring elution efficiency

The elution efficiency is a measure of how completely the accumulated analyte is removed from the adsorbent. It is measured by loading the adsorbent with a known mass of analyte and determining the mass of analyte that is removed from the adsorbent after elution. The elution efficiency is often determined over a range of mass loadings;[7, 13, 16] other workers have used only one mass loading to determine the elution efficiency.[36]

To establish the mass of analyte loaded on the adsorbent, the adsorbent is immersed in a solution of known analyte concentration and volume. After a period of time, the adsorbent is removed and the mass of analyte not taken up by the adsorbent is determined by measuring the concentration of analyte in solution. Therefore, the mass (M) of analyte on the adsorbent can be determined (equation 4.3).

$$M_{\text{Adsorbent}} = M_{\text{Initially in solution}} - M_{\text{Left in solution}} \qquad \textbf{(4.3)}$$

In some cases, adsorption of analyte to solution containers may need to be considered to obtain an accurate value for the mass of analyte not removed by the adsorbent. The slope of a plot of the mass of analyte loaded onto the adsorbent, when using more than one mass loading, against the mass of analyte eluted from the adsorbent, provides the elution efficiency.[7, 13]

It is important to note that the diffusion cell experiment directly measures the diffusion coefficient of the analyte through the diffusive gel, whereas the experiment using DGT devices measures an 'effective' diffusion coefficient. This is because, when using DGT devices, the diffusion coefficient that is measured is a combination of diffusion of the analyte thorough the diffusive gel and the binding ability of the adsorbent.[2] If the adsorbent binds the analyte rapidly and reduces the concentration of the analyte at the diffusive gel-adsorbent interface to zero, then both methods should give similar diffusion coefficients. However, if the adsorbent does not bind the analyte rapidly, the effective diffusion coefficient measured by DGT may be less than that measured by the use of a diffusion cell.[2] The use of DGT

devices to measure diffusion coefficients also reflects the uncertainty in elution efficiency and the effective cross-sectional area for diffusion.

4.1.3 Use of membrane filters in DGT

In DGT a membrane filter is usually placed in front of the DGT device to prevent particles from adhering to the gel surface.[5] Particle adhesion may affect diffusion of species through the gel.[5] The rate of diffusion of metal ions through the membrane filter and diffusion gel has been reported to be indistinguishable from the rate of diffusion through a diffusive gel alone;[1, 3, 5, 24] therefore the membrane filter is generally treated as an extension of the diffusive gel layer. For most DGT work, 0.45 μm membrane filters are used; however, the work in this thesis used a 0.025 μm membrane filter to achieve exclusion of colloidal-size particles. Examining diffusion of As species through this membrane filter and investigating the effect of membrane pore size and membrane preparation on diffusion, has not presently been carried out.

4.1.4 Chapter Outline

This chapter is mainly concerned with the measurement of As^{V} and As^{III} diffusion coefficients through the diffusive gel and membrane filter. This was carried out by using both a diffusion cell, and DGT devices utilizing an iron-oxide adsorbent. The elution efficiency of As^{V} from the iron-oxide gel was also determined. In addition, the effect of the membrane filter, including pore size and preparation, was examined to observe what affect this would have on diffusion of As species. Unless stated otherwise, all gels used for the work described in this and following chapters were prepared in our laboratory.

4.2 Experimental

4.2.1 Elution efficiency from iron-oxide gel

The elution efficiency from the iron-oxide gel was determined by immersing iron-oxide gel disks in 10 mL of 20, 40, 60, 80, and 100 ppb As^{V} solutions for 24 h. This was carried out in triplicate for each As^{V} concentration. The five As^{V} solutions were prepared by diluting 2.5 mL of 1 mol L^{-1} sodium acetate buffer, 1 mL of 1 mol L^{-1} $NaNO_3$, and an aliquot of 1250 ppb As^{V}, to 100 mL. The following volumes: 8, 6.4, 4.8, 3.2, and 1.6 mL of 1250 ppb As^{V} were added to give 100, 80, 60, 40, and 20 ppb As^{V}, respectively. The concentrations of $NaNO_3$

and sodium acetate in the As^V solutions were 0.01 and 0.025 mol L^{-1}, respectively. The pH of the As^V solutions was adjusted to 5.0 using 1 mol L^{-1} NaOH.

Ten mL of the above solutions were added to acid-washed plastic containers; one iron-oxide gel disk was added to each container and left for 24 h on an orbital shaker to adsorb As^V from solution. After 24 h, the iron-oxide gel disks were removed from the As^V solutions and rinsed with Milli-Q water; excess water was removed from the adsorbent by carefully dabbing on Durx™ clean room wipes. The iron-oxide gel disks were placed in acid-cleaned plastic centrifuge tubes and eluted with 2 mL of concentrated HCl for 24 h on an orbital shaker. After 24 h, 8 mL of Milli-Q water was added to the eluent and left for 16 to 24 h on an orbital shaker before the As concentration in the eluent solution was measured using HG-AAS.

The concentrations of As^V initially present in solution (before adsorbent immersed) and present at the end of the experiment (after adsorbent immersed) were measured. In addition, at the end of the experiment (after the iron-oxide gels were retrieved) 1mL of concentrated HCl was added to each As^V solution. After 24 h on an orbital shaker the As^V concentration in the solution was determined. This procedure was carried out to remove any As^V species that may have adsorbed to the sides of the containers during the experiment. By including this step, the exact mass of As^V adsorbed by the iron-oxide adsorbent can be determined and hence a precise elution efficiency can be calculated.

4.2.2 Measurement of As^V and As^{III} diffusion coefficients through polyacrylamide diffusive gel and membrane filter at pH 5 using a diffusion cell

Measurement of diffusion coefficients of As^V and As^{III} through the diffusive gel and membrane filter were carried out by placing a piece of diffusive gel and a 0.025 μm cellulose nitrate membrane filter (Schleicher & Schuell) in the opening that separates the two sides of the diffusion cell. The membrane filter was placed on the side of the gel facing the solution containing As. This was done to emulate the set-up used when deploying DGT devices. The membrane filters were firstly soaked in Milli-Q water for 24 h and cleaned in 5 % v/v HNO_3 for 24 h. The membrane was then rinsed in Milli-Q water and stored in 0.01 mol L^{-1} $NaNO_3$.

Both sides of the diffusion cell contained 0.7 mL of 1 mol L^{-1} $NaNO_3$, 1.75 mL of 1 mol L^{-1} sodium acetate (pH 5.0), and 66.85 mL of Milli-Q water; 0.7 mL of 1000 ppm As^{V} or 1000 ppm As^{III} was added to compartment A of the diffusion cell to give an approximate As^{V} or As^{III} concentration of 10 ppm. Concentrated HCl (70 μL) was added to compartment B of the diffusion cell to equal the concentration of HCl in compartment A due to As standards being prepared in 10 % v/v HCl. In addition, 0.63 mL of Milli-Q water was added to compartment B so that both sides of the diffusion cell contained the same volume. The final concentrations of $NaNO_3$ and sodium acetate in both sides of the diffusion cell were 0.01 and 0.025 mol L^{-1}, respectively. The pH of the solution in both sides of the diffusion cell was adjusted to 5.0 using 1 mol L^{-1} NaOH. The pH was measured at the end of the experiment to make sure that it had not changed significantly. Both sides of the diffusion cell were stirred using small magnetic followers.

Samples of solution were removed from compartment B of the diffusion cell (1.1 to 0.1 mL for As^{V} experiments and 2.6 to 0.2 mL for As^{III} experiments) every 15 mins so that the As concentration could be determined after appropriate dilution. An equivalent volume was removed from compartment A to maintain the same volume in each side of the diffusion cell. Replicate samples were removed and analysed from compartment B of the diffusion cell for at least 2 sampling times to determine reproducibility. The temperature in compartment A of the diffusion cell at the start and end of the experiment was measured. In addition, whenever replicate samples were removed for analysis, the temperature was also measured. It is the average of these temperature measurements that is reported in the results section.

Samples were removed from compartment A of the diffusion cell at the start and end of the experiment to determine the actual (rather than calculated) concentration of As initially present (it is this initial As concentration that is used to determine the diffusion coefficients) and to make sure that the As concentration did not change significantly during the experiment. For the As^{V} diffusion coefficient experiments, samples were removed for As^{III} analysis to make sure that reduction of As^{V} had not occurred during the experiment. All samples removed during the experiments were analysed within 2 h.

For the determination of the As^{III} diffusion coefficient, the diffusion cell experiment was carried out in duplicate, whereas for the determination of the As^{V} diffusion coefficient, only one experiment was carried out.

4.2.3 Measurement of As^{V} and As^{III} diffusion coefficients through polyacrylamide diffusive gel and membrane filter at pH 5 using DGT devices

The diffusion coefficients of As^{V} and As^{III} through the diffusive gel and membrane filter were determined using DGT devices. This was carried out by deploying DGT devices in As^{V} and As^{III} solutions for set times. The DGT devices were assembled and deployed as described in chapter 2. The membrane filters used for this work were 0.025 μm cellulose nitrate membrane filters (Schleicher & Schuell). The membrane filters were initially soaked in Milli-Q water for 24 h and cleaned in 5 % v/v HNO_3 for 24 h. The membrane was then rinsed in Milli-Q water and stored in 0.01 mol L^{-1} $NaNO_3$.

The As deployment solutions were prepared by diluting 40 mL of 1 mol L^{-1} $NaNO_3$, 100 mL of 1 mol L^{-1} sodium acetate (pH 5.0), and 24 mL of either 10 ppm As^{V} or 10 ppm As^{III}, to 4 L. The volume of solution was sufficiently large to avoid significant depletion of As by the DGT devices. Using this volume, the amount of As removed from solution was < 5 %. The final concentrations of $NaNO_3$, sodium acetate, and As in the deployment solutions were 0.01 mol L^{-1}, 0.025 mol L^{-1}, and ~ 60 ppb, respectively. A small volume of 1 mol L^{-1} NaOH was added to adjust the pH to ~ 5.0. The pH of the As deployment solutions were measured at the start, end, and approximately half way through the experiments. The deployment solutions were left to stand for ~ 1 h before DGT devices were deployed. Fifteen DGT devices were deployed in the well-stirred solution (stirring rate was 620 rpm) and removed at various times to give deployment times from ~ 4 to 32 h. The exact deployment times were recorded. At each retrieval time, 3 DGT devices were removed so triplicate samples could be obtained. The temperature was recorded at the start and end of the experiment as well as each time DGT devices were retrieved. It is the average of these temperature measurements that is reported in the results section. After retrieval, DGT devices were placed in Milli-Q water and then washed thoroughly before disassembling and removal of the iron-oxide gel adsorbent. The same elution and analysis procedure was used as described in section 4.2.1.

Samples were removed from the As deployment solutions at the start and end of the experiment to confirm that the As concentration did not change significantly over this time. These samples were stabilized by adding concentrated HCl to give a final concentration of 1.1 mol L^{-1} HCl and analysed at the same time as the DGT eluents. The As concentrations

determined from these samples were used to calculate the diffusion coefficients. In addition, an As^{III} analysis was carried out on the deployment solution at end of the experiment to make sure that reduction of As^{V} had not occurred (for As^{V} experiments) or oxidation of As^{III} had not occurred (for As^{III} experiments).

For As^{V}, this experiment was carried out in duplicate. The first experiment utilized diffusive gels that were supplied by DGT Research Ltd. (Lancaster, U.K.); the second experiment used diffusive gels that had been prepared in our laboratory. For As^{III}, this experiment was carried out 4 times in total; all experiments used diffusive gels prepared in our laboratory.

When calculating As^{V} and As^{III} diffusion coefficients using DGT devices, a 100 % elution efficiency was assumed.

4.2.4 Effect of membrane filter and pre-treatment of membrane on mass of As accumulated by DGT

The effect of the membrane filter on the diffusion of As^{III} was investigated. In addition, different types of membrane filters with different pore sizes, and the effect of membrane conditioning were examined with respect to the diffusion of As^{V}.

4.2.4.1 Effect of membrane filter on mass of As^{III} accumulated by DGT devices

DGT devices were deployed in an As^{III} solution with and without membrane filters. The masses of As^{III} accumulated on the iron-oxide adsorbent were compared to determine if the presence of a membrane filter in front of the diffusive gel affected the measured As^{III} diffusion coefficient. The membrane filters were initially soaked in Milli-Q water for 24 h and cleaned in 5 % v/v HNO_3 for 24 h. The membrane was then rinsed in Milli-Q water and stored in 0.01 mol L^{-1} $NaNO_3$.The DGT devices were assembled and deployed as described in chapter 2.

The As^{III} deployment solution was prepared by diluting 40 mL of 1 mol L^{-1} $NaNO_3$, 100 mL of 1 mol L^{-1} sodium acetate (pH 5.0), and 24 mL of 10 ppm As^{III}, to 4 L. The volume of solution was sufficiently large to avoid significant depletion of As by the DGT devices. Using this volume, the amount of As removed from solution was < 3 %. The final concentrations of $NaNO_3$, sodium acetate, and As^{III} in the deployment solution were 0.01 mol

L^{-1}, 0.025 mol L^{-1}, and ~ 60 ppb, respectively. A small volume of 1 mol L^{-1} NaOH was added to adjust the pH to 5.0. The pH and temperature of the As^{III} solution was measured at the start and end of the experiment. It is the average of these two temperatures that is reported in the results section. The As^{III} deployment solution was left to stand for ~ 1 h before DGT devices were deployed. Three DGT devices with membrane filters (Schleicher & Schuell 0.025 μm pore size cellulose nitrate membrane) and three DGT devices without membrane filters were deployed in the well-stirred solution (stirring rate 620 rpm) for ~ 21 h. The exact deployment time was recorded. For the DGT devices without membrane filters, a circular gasket was cut from the membrane material and included in the DGT assembly. This ensured that the position of the gel and filter were the same for both types of DGT devices. After retrieval, DGT devices were placed in Milli-Q water and then washed thoroughly before disassembling and removal of the iron-oxide gel adsorbent. The same elution and analysis procedure was used as described in section 4.2.1.

Samples were removed from the As^{III} solution at the start and end of the experiment to make sure the As concentration did not change significantly during the experiment. These samples were stabilized by adding concentrated HCl to give a final concentration of 1.1 mol L^{-1} HCl and analysed at the same time as the DGT eluents. In addition, an As^{III} analysis was carried out on the deployment solution at the end of the experiment to make sure that oxidation of As^{III} had not occurred during the experiment.

4.2.4.2 Effect of membrane type, pore size and acid washing of membrane on mass of As^{V} accumulated by DGT devices

The effects of membrane type, pore size, and pre-treatment of the membrane were investigated to determine whether any of these factors affected the diffusion coefficient of As^{V}. DGT devices with various membrane filters were deployed in an As^{V} solution and the mass of As^{V} accumulated on the iron-oxide adsorbent was measured. The DGT devices were assembled and deployed as described in chapter 2.

The As^{V} deployment solution was prepared by diluting 40 mL of 1 mol L^{-1} $NaNO_3$, 100 mL of 1 mol L^{-1} sodium acetate (pH 5.0) and 0.25 mL of 1000 ppm As^{V}, to 4 L. Using this volume, the amount of As removed from solution was < 5 %. The final concentrations of $NaNO_3$, sodium acetate, and As^{V} in the deployment solution were 0.01 mol L^{-1}, 0.025 mol L^{-1}, and ~ 63 ppb, respectively. A small volume of 1 mol L^{-1} NaOH was added to adjust the

solution pH to 5.0. The pH and temperature of the As^V solution was measured at the start and end of the experiment. In addition, the temperature was measured at two other times during the experiment. It is the average of these temperature measurements that is reported in the results section. The As^V deployment solution was left to stand for ~ 1 h before DGT devices were deployed in the well stirred solution (stirring rate 620 rpm).

The following membrane types and pre-treatments were used: 0.025 μm pore size nitrocellulose membrane filters that had been soaked in 5 % v/v HNO_3 for 24 h and stored in 0.01 M $NaNO_3$; 0.025 μm pore size nitrocellulose membrane filters that had been stored in 0.01 M $NaNO_3$; 0.45 μm pore size nitrocellulose membrane filters that had been soaked in 5 % v/v HNO_3 for 24 h and stored in 0.01 M $NaNO_3$; and 0.45 μm pore size nitrocellulose membrane filters that had been stored in 0.01 M $NaNO_3$. These membranes were all from Schleicher & Schuell. In addition, Millipore mixed ester membrane filters (0.45 μm pore size) that had been soaked in 5 % v/v HNO_3 for 24 h and stored in 0.01 M $NaNO_3$ were also used. All membranes were soaked in Milli-Q water for 24 h before these treatments. The thickness of the 0.025 μm and 0.45 μm Schleicher & Schuell membrane filters were 100 and 140 μm, respectively. The thickness of the 0.45 μm Millipore membrane filters was 150 μm.

Ten DGT devices were deployed for ~ 6 h and another ten DGT devices were deployed for ~ 24 h to examine the effect of membrane type and membrane preparation on the diffusion of As^V. The exact deployment times were recorded. After retrieval, DGT devices were placed in Milli-Q water and then washed thoroughly before disassembling and removal of the iron-oxide gel adsorbent. The same elution and analysis procedure was used as described in section 4.2.1.

Samples were removed from the As^V solution at the start and end of the experiment to make sure the As concentration had not changed significantly during the experiment. These samples were stabilized by adding concentrated HCl to give a final concentration of 1.1 mol L^{-1} HCl and analysed at the same time as the DGT eluents. In addition, an As^{III} analysis was carried out on the deployment solution at the end of the experiment to make sure that reduction of As^V had not occurred during the experiment.

4.3 Results

4.3.1 Elution efficiency from iron-oxide gel

The elution efficiency from the iron-oxide gel was determined by immersing iron-oxide gel disks in 10 mL of 20, 40, 60, 80, and 100 ppb As^V solutions for 24 h. Analysis of the As^V solutions at the end of the uptake time indicated no As^V remaining in solution. Furthermore, no As^V was detected in these solutions after addition of HCl. This indicates that As^V did not adsorb to the containers during the experiment and that uptake of As^V by the iron-oxide adsorbent was quantitative at every As^V concentration. Hence, for each experiment, the mass of As^V loaded onto the iron-oxide gel was the same as that initially in the uptake solution.

The elution efficiency was determined from the slope of the plot of mass of As^V eluted *vs.* mass As^V adsorbed on the gel (Figure 4.1). Using this slope an elution efficiency of 96 ± 5 % was determined when using concentrated HCl as the eluent.

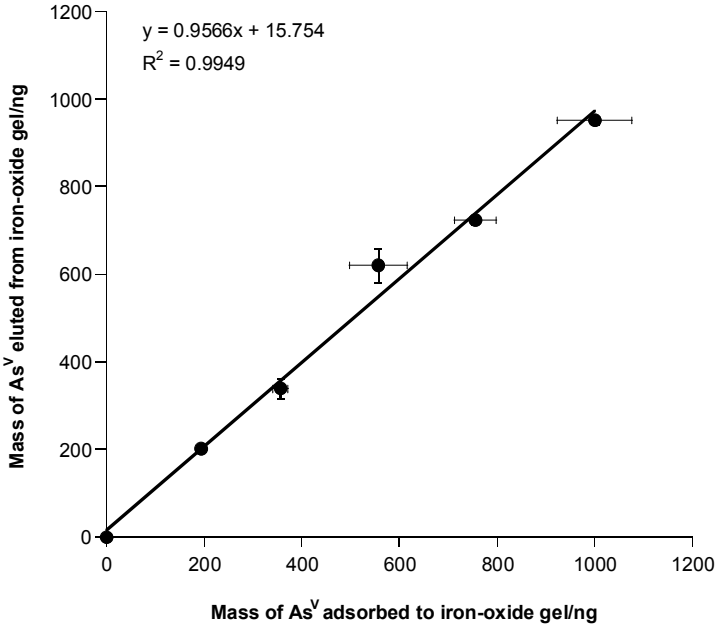

Figure 4.1 Measured mass of As^V eluted from the iron-oxide adsorbent at various As^V masses adsorbed by the adsorbent. The uncertainty associated with the mass of As^V eluted from the iron-oxide gel corresponds to the standard deviation of the mean for triplicate iron-oxide deployments. The uncertainty associated with mass of As^V adsorbed to the iron-oxide gel corresponds to the standard deviation of the mean for triplicate measurements of As^V initially present in solution.

The experiment was repeated and an elution efficiency of 108 ± 5 % was obtained; this is in reasonable agreement with the first experiment. The uncertainty associated with both values is the standard deviation of the slope used to determine the elution efficiency. For further work, a 100 % elution efficiency was assumed for DGT calculations.

As a quality control procedure later in this work, a small number of samples were analyzed off-site by ICP-MS. Hydrochloric acid could not be used; hence HNO_3 was briefly examined as an eluent. A ~ 100 % elution efficiency was obtained when concentrated HNO_3 was used. This was determined by comparing the mass of As eluted from the iron-oxide adsorbent when concentrated HCl was used, to that when concentrated HNO_3 was used. However, unless stated otherwise, concentrated HCl was used as the eluent for remaining work.

4.3.2 Measurement of As^V and As^{III} diffusion coefficients through polyacrylamide diffusive gel and membrane filter at pH 5 using a diffusion cell

4.3.2.1 As^V diffusion coefficients

Figure 4.2 shows a plot of amount of As in compartment B of the diffusion cell *vs*. time after addition of As^V to compartment A. Good linearity is observed between the mass of As^V diffused through the diffusive gel and membrane filter, and time. The As^V diffusion coefficient through the diffusive gel and membrane filter was calculated from the slope of the plot in Figure 4.2 and using equation 4.2. The As^V diffusion coefficient through the diffusive gel and membrane filter was calculated to be (4.85 ± 0.35) x 10^{-6} cm^2 s^{-1} (pH 5.1, 24.0 ± 0.5 ^oC) when using the following parameters: slope = 55.908 ng min^{-1}; Δg = 0.09 cm; C = 9800 ppb; and A = 1.77 cm^2. The uncertainty associated with the diffusion coefficient is a combination of the uncertainties in the slope of the diffusion cell plot (i.e. standard deviation of slope), the thickness of the diffusive gel, and the initial concentration of As present in compartment A of the diffusion cell.

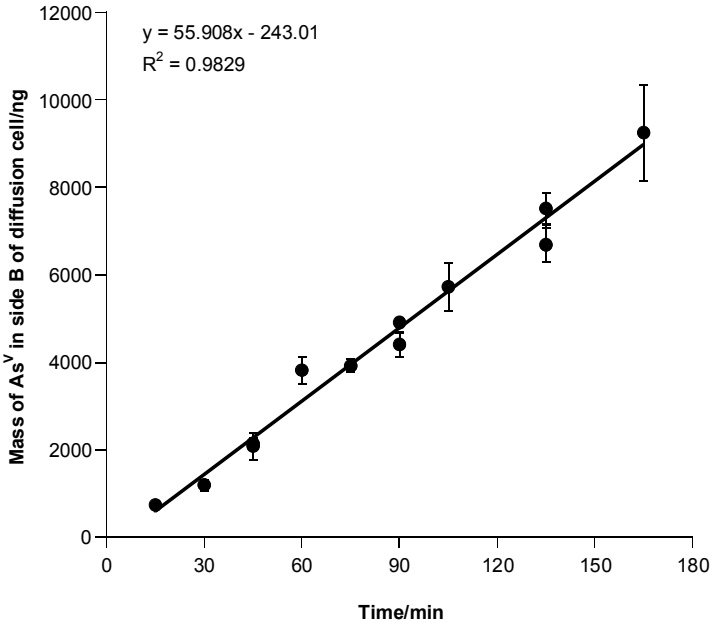

Figure 4.2 Mass of As^V diffused through the diffusive gel and membrane filter with time during an As^V diffusion cell experiment. The uncertainty associated with each datum point is the standard deviation of the mean for at least two HG-AAS measurements. The concentrations of As^V, $NaNO_3$, and sodium acetate were 9800 ppb, 0.01 mol L^{-1}, and 0.025 mol L^{-1}, respectively. The average temperature during the experiment was 24.0 ± 0.5 ^oC. The pH was 5.1.

4.3.2.2 As^{III} diffusion coefficients

The result from one As^{III} diffusion cell experiment is shown in Figure 4.3. Good linearity was obtained between the mass of As^{III} diffused through the diffusive gel and filter membrane, and time. Using the slope from Figure 4.3 and equation 4.2, the As^{III} diffusion coefficient through the diffusive gel and membrane filter was calculated to be (6.15 ± 0.30) x 10^{-6} cm^2 s^{-1} (pH 5.0, 25.5 ± 0.5 ^oC) when using the following parameters: slope = 64.907 ng min^{-1}; Δg = 0.09 cm; C = 8950 ppb; and A = 1.77 cm^2.

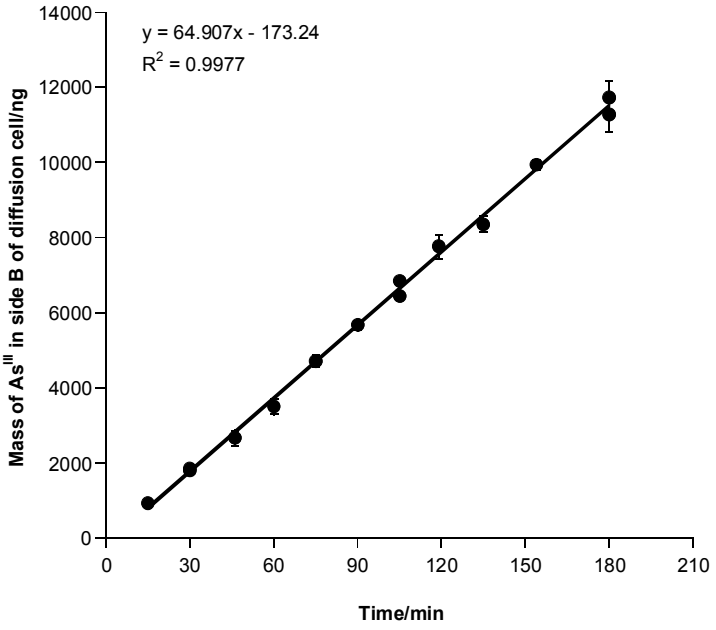

Figure 4.3 Mass of As^{III} diffused through the diffusive gel and membrane filter with time during an As^{III} diffusion cell experiment. The uncertainty associated with each datum point is the standard deviation of the mean for at least two HG-AAS measurements. The concentrations of As^{III}, $NaNO_3$, and sodium acetate were 8950 ppb, 0.01 mol L^{-1}, and 0.025 mol L^{-1}, respectively. The average temperature during the experiment was 25.5 ± 0.5 ^oC. The pH was 5.0.

A duplicate experiment gave a diffusion coefficient of (6.60 ± 0.35) x 10^{-6} cm^2 s^{-1} (pH 5.1, 24.5 ± 0.5 ^oC); this agrees within experimental uncertainty with the first value. The uncertainties associated with the diffusion coefficients were derived from the same factors as described in the previous section (4.3.2.1). Averaging the two calculated values and reporting an uncertainty of 1 standard deviation gives an As^{III} diffusion coefficient of (6.40 ± 0.30) x 10^{-6} cm^2 s^{-1}.

4.3.3 Measurement of As^V and As^{III} diffusion coefficients through polyacrylamide diffusive gel and membrane filter at pH 5 using DGT devices

4.3.3.1 As^V diffusion coefficients

The results from one DGT deployment experiment are illustrated in Figure 4.4 below. When DGT devices were deployed for different times, the measured mass of As accumulated on the adsorbent increased linearly with time; this is expected from the DGT theory. Assuming a

100 % elution efficiency and using equation 4.2 and the slope of the plot in Figure 4.4, the As^V diffusion coefficient through the diffusive gel and membrane filter using DGT devices was calculated to be (4.85 ± 0.35) x 10^{-6} cm^2 s^{-1} (pH 4.9, 24.5 ± 0.5 ^oC) when using the following parameters: slope = 36.480 ng h^{-1}; Δg = 0.09 cm; C = 59.8 ppb; and A = 3.14 cm^2. This diffusion coefficient was measured using diffusive gels prepared by DGT Research Ltd.

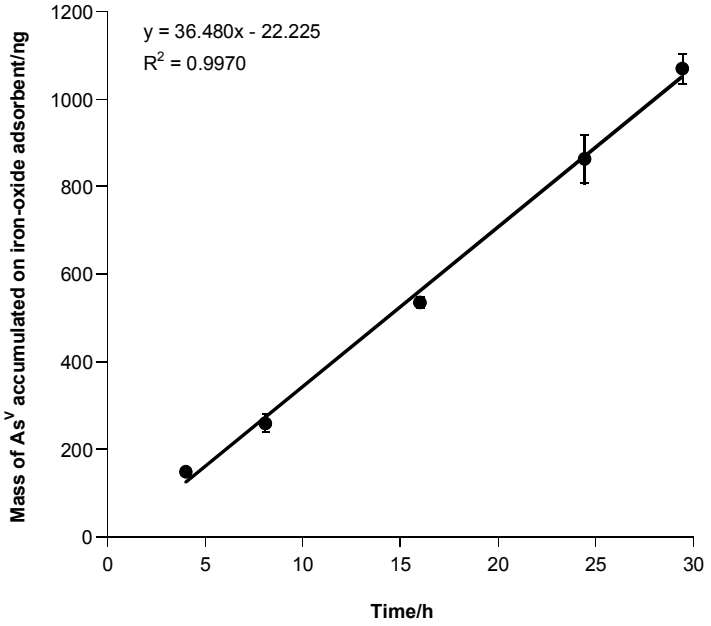

Figure 4.4 Mass of As^V accumulated on the iron-oxide adsorbent within DGT devices at various times. The uncertainty associated with each datum point is the standard deviation of the mean for triplicate DGT deployments. The concentrations of As^V, $NaNO_3$, and sodium acetate were 59.8 ppb, 0.01 mol L^{-1}, and 0.025 mol L^{-1}, respectively. The average temperature during the experiment was 24.5 ± 0.5 ^oC. The pH was 4.9.

When this experiment was repeated using diffusive gels prepared in our laboratory, an As^V diffusion coefficient of (4.95 ± 0.35) x 10^{-6} cm^2 s^{-1} (pH 4.9, 24.5 ± 0.5 ^oC) was obtained. This value agrees within experimental uncertainty with the first value. The uncertainties associated with the diffusion coefficients are a combination of the uncertainty of the slope of the DGT plot (i.e. standard deviation of slope), the thickness of the diffusive gel, and the initial concentration of As^V present in the deployment solution. For both DGT experiments the expected negative y-intercept was observed for the DGT plots. The relative standard deviations of triplicate DGT deployments were generally < 10 %.

Averaging the two calculated diffusion coefficient values and reporting an uncertainty of 1 standard deviation gives an As^V diffusion coefficient of (4.90 ± 0.05) x 10^{-6} cm^2 s^{-1}.

4.3.3.2 As^{III} diffusion coefficients

The results from one DGT deployment experiment are illustrated in Figure 4.5 below. When DGT devices were deployed for different times, the measured mass of As on the adsorbent increased linearly with time. Assuming an elution efficiency of 100 % and using equation 4.2 and the slope of the plot shown in Figure 4.5, the As^{III} diffusion coefficient through the diffusive gel and membrane filter using DGT devices was calculated to be (6.00 ± 0.40) x 10^{-6} cm^2 s^{-1} (pH 5.0, 23.0 ± 0.5 ^oC) when using the following parameters: slope = 43.768 ng h^{-1}; Δg = 0.09 cm; C = 58.0 ppb; and A = 3.14 cm^2.

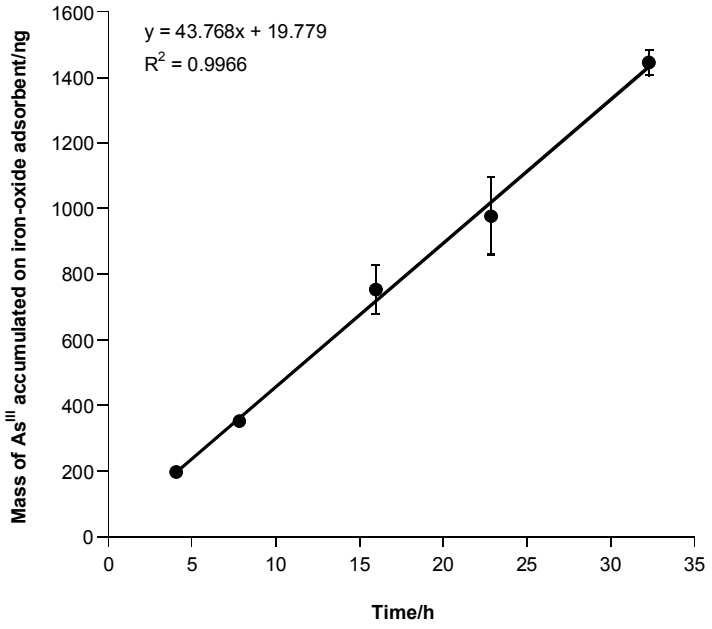

Figure 4.5 Mass of As^{III} accumulated on the iron-oxide adsorbent within DGT devices at various times. The uncertainty associated with each datum point is the standard deviation of the mean for triplicate DGT deployments. The concentrations of As^{III}, $NaNO_3$, and sodium acetate were 58.0 ppb, 0.01 mol L^{-1}, and 0.025 mol L^{-1}, respectively. The average temperature during the experiment was 23.0 ± 0.5 ^oC. The pH was 5.0.

This experiment was repeated a further 3 times. These results are shown in Table 4.1 below. All experiments agree within experimental uncertainty. The reported uncertainties were

derived from the same factors as described in the previous section (4.3.3.1). The standard deviation of triplicate DGT deployments was generally < 10 %.

Experiment	As^{III} diffusion coefficient	Temperature
1	(6.00 ± 0.40) x 10^{-6} cm^2 s^{-1}	23.0 ± 0.5 °C
2	(5.80 ± 0.50) x 10^{-6} cm^2 s^{-1}	23.0 ± 1.5 °C
3	(6.35 ± 0.60) x 10^{-6} cm^2 s^{-1}	22.5 ± 0.5 °C
4	(5.70 ± 0.35) x 10^{-6} cm^2 s^{-1}	24.0 ± 1.0 °C

Table 4.1 As^{III} diffusion coefficients measured through a diffusive gel and filter membrane. All experiments were carried out at pH 5.

Averaging the four calculated diffusion coefficient values from Table 4.1 and reporting an uncertainty of 1 standard deviation gives an As^{III} diffusion coefficient of (5.95 ± 0.30) x 10^{-6} cm^2 s^{-1}.

For all As^{III} DGT experiments a positive y-intercept was observed for the DGT plots. However, a negative intercept is expected due to the time required to establish a linear concentration gradient through the gel. The y-intercepts ranged from ~ 20 to ~ 65 ng. Table 4.2 shows the values of the positive y-intercepts obtained during this work when determining As^{III} diffusion coefficients, along with the standard deviation of the intercepts and the effect on the slope of forcing the lines of best fit through (0,0) (modified slope).

Experiment	y-intercept	sd[a]	Slope/ng h^{-1} [b]	Modified slope[c]	Ratio of slopes[d]
1	20 ng	29	44	45	0.98
2	59 ng	35	46	49	0.94
3	31 ng	57	49	51	0.96
4	66 ng	37	46	49	0.94

Table 4.2 Table showing plot parameters from the As^{III} DGT experiments.

[a]standard deviation of y-intercept

[b]slope of plot as in Figure 4.5

[c]slope when line of best fit is forced through (0,0)

[d]ratio of "slope" to "modified slope"

4.3.4 Effect of membrane filter and pre-treatment of membrane on mass of As accumulated by DGT

4.3.4.1 Effect of membrane filter on mass of As^{III} accumulated by DGT devices

Comparison of the mass of As^{III} accumulated in the presence and absence of the 0.025 μm membrane filter is presented in Table 4.3. The mass accumulated by DGT devices in the absence of a membrane filter is greater than the mass accumulated by the DGT devices in the presence of a membrane filter. This is expected due to the reduction in the thickness of the diffusion layer for the DGT devices without a membrane filter.

Experiment	Accumulated Mass	Predicted Mass	A-Mass/P-Mass[a]
Membrane present	1025 ± 30 ng	945 ± 80 ng	1.08 ± 0.15
Membrane absent	1120 ± 55 ng	1065 ± 90 ng	1.05 ± 0.15

Table 4.3 Mass of As^{III} accumulated within DGT devices at 25 ± 1 °C and pH 4.95. The predicted mass is calculated using equation 4.1 and using the As^{III} diffusion coefficients reported in section 4.3.3.2. Note that for calculation of the predicted mass a Δg value of 0.9 and 0.8 mm was used for the membrane present and membrane absent experiments, respectively. The uncertainty associated with the accumulated mass is 1 standard deviation of the mean for triplicate DGT deployments. The uncertainty associated with the predicted mass is a combination of the uncertainty associated with the As^{III} diffusion coefficient, the concentration of As^{III} initially in solution, and the thickness of the diffusive gel.

[a]accumulated mass/predicted mass

In calculation of the predicted mass in the presence of a membrane filter, the thickness of the gel and membrane, and the diffusion coefficient of As^{III} in the diffusive gel were used. To calculate the predicted mass in the absence of the membrane filter the thickness of the gel, and the diffusion coefficient of As^{III} through the gel was used. The uncertainty of replicate DGT deployments was < 5 % for both experiments.

4.3.4.2 Effect of membrane type, pore size, and acid washing of membrane on mass of As^{V} accumulated by DGT devices

The results of experiments designed to test the effect of membrane type and pre-treatment, on mass of As^{V} accumulated by DGT devices, are shown in Figure 4.6. Due to the differences in the thickness of some of the membranes used, and therefore the length of the diffusion path, the results have been normalized to allow appropriate comparisons.

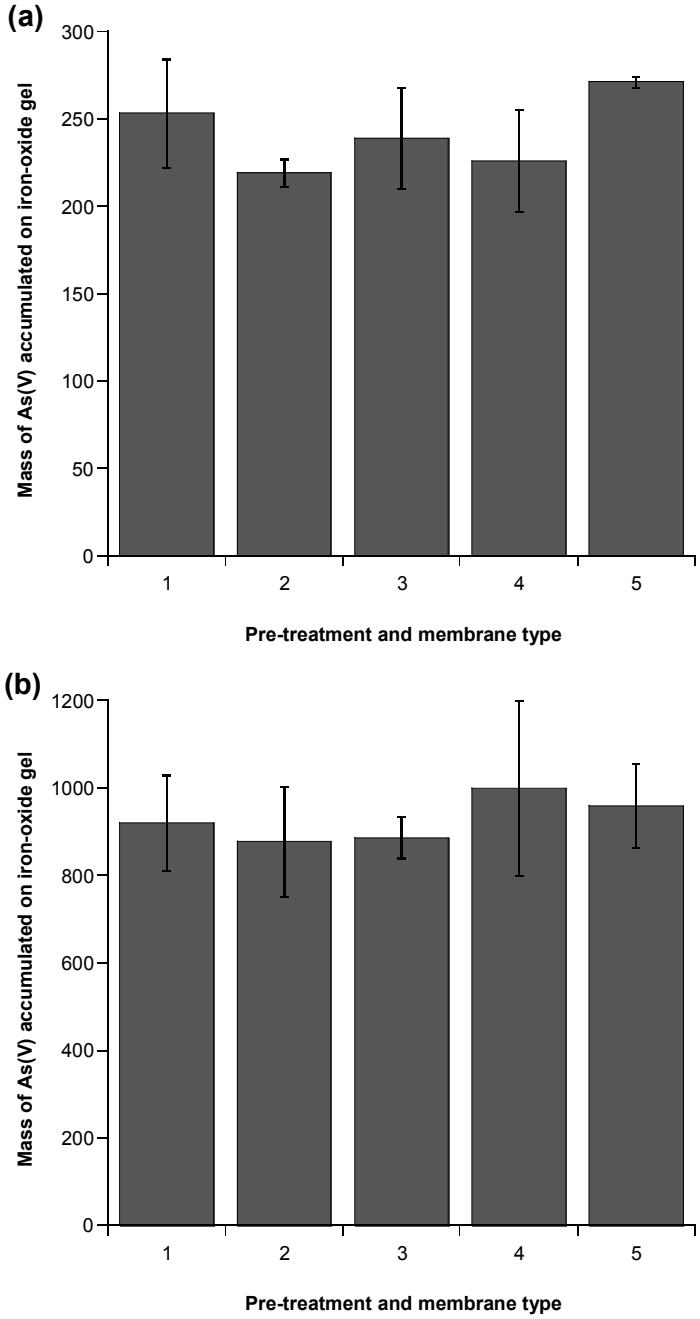

Figure 4.6 Normalized mass of As^V accumulated on iron-oxide adsorbent within DGT devices using various membranes and pre-treatments at a) 6h and b) 24 h. The pH of the As^V solution was 4.95. The temperature was 24 ± 1 ^oC. The uncertainty in the mass accumulated with each pre-treatment is 1 standard deviation of the mean from duplicate DGT deployments. The pre-treatments and membranes used were: 1) 0.025 µm S & S membrane filter, 5 % v/v HNO_3 for 24 h, stored in 0.01 mol L^{-1} $NaNO_3$; 2) 0.025 µm S & S membrane filter, stored in 0.01 mol L^{-1} $NaNO_3$; 3) 0.45 µm S & S membrane filter, 5 % v/v HNO_3 for 24 h, stored in 0.01 mol L^{-1} $NaNO_3$; 4) 0.45 µm S & S membrane filter, stored in 0.01 mol L^{-1} $NaNO_3$; 5) 0.45 µm Millipore membrane filter, 5 % v/v HNO_3 for 24 h, stored in 0.01 mol L^{-1} $NaNO_3$.

4.4 Discussion

4.4.1 Elution efficiency from iron-oxide gel

The elution efficiency of As from the iron-oxide gel adsorbent was determined to be 100 %, within experimental uncertainty, using both concentrated HCl and concentrated HNO_3 as the eluent. The finding that concentrated HNO_3 is an efficient eluent is important because it offers the possibility of analysing eluents using ICP-MS. Hydrochloric can cause problems with ICP-MS analyses such as interference by $ArCl^+$ (m/z 75) which has the same mass as As. The elution efficiency experiments were carried out using iron-oxide gels loaded with As^V. From the work carried out for this thesis, it was suggested that As^{III} had been at least partially oxidised to As^V either on the iron-oxide adsorbent or during the elution process. Partial oxidation of As^{III} on the surface of iron-oxides has been reported.[37, 38] Therefore it was assumed that the elution efficiency is also 100 % after loading the gel adsorbent with As^{III}; good agreement between the As^{III} diffusion coefficient measured using a diffusion cell and DGT devices confirms this assumption.

For metal ions such as Zn, Cd, Cu, Ni, Co, Pb, and Mn, elution from a Chelex-100 adsorbent has found to be non-quantitative when using 1 mL of 1 to 2 mol L^{-1} HNO_3.[7, 13, 35, 36] For these metal ions, elution efficiencies between 75 and 85 % have been reported.[7, 13, 35, 36] Zhang and Davison[13] report that the elution efficiency was independent of elution time (1 h to 1 week) and did not vary when HNO_3 concentration was increased up to 3 mol L^{-1}. For Ca and Mg, Dahlqvist *et al*.[16] obtained elution efficiencies > 95 % for Chelex-100 when using 5 mL of 1 mol L^{-1} HNO_3. Sangi *et al*.[6] reported elution efficiencies of > 95 % for Cd^{II}, Co^{II}, Ni^{II} and Pb^{II} when using Chelex-100 and 10 mL of 2 mol L^{-1} HNO_3. These elution efficiencies are considerably higher than those reported by Alfaro-De la Torre *et al*.,[7] Zhang and Davison,[13] Warken *et al*.[35] and Warken *et al*.[36] Sangi *et al*.[6] found that the elution efficiency was independent of elution time (10 to 480 min), volume (1 to 50 mL) and acid concentration (1 to 2.5 mol L^{-1}). Sangi *et al*.[6] determined the elution efficiency by completely digesting some adsorbent gels with 16 mol L^{-1} HNO_3 to measure their residual metal content, whereas those reported previously[7, 13, 35, 36] have used a similar method to that described in our work.

Garmo *et al*.[2] used concentrated nitric acid as an eluent and found elution efficiencies close to 100 % for most metals. It is unclear how the elution efficiency was determined. In comparison to previous reported elution efficiencies they conclude that elution with

concentrated HNO_3 is both more quantitative and more reproducible than with 1 mol L^{-1} HNO_3. Mason *et al.*[23] used 1 mol L^{-1} HCl to elute Mn, Zn, Cu, and Cd from an adsorbent containing Chelex-100 and iron-oxide; this resulted in an average elution efficiency of 92 %. When 1 mol L^{-1} HNO_3 was used as the eluent, the elution efficiency was close to 80 %; this agrees with those elution efficiencies discussed above.[7, 13, 35, 36] These results suggest that elution of metal ions from a Chelex-100 adsorbent is more efficient when using HCl. During the work for this thesis, it was found that using concentrated HCl changed the form of the adsorbent gel; it became weaker and was easier to "pull" apart. There was less change in the gel when concentrated HNO_3 was used, which implies that a reaction had occurred in the presence of HCl. This change in the gel properties may be a factor explaining the higher elution efficiencies obtained by Mason *et al.*[23] when using 1 mol L^{-1} HCl as the eluent in comparison to 1 mol L^{-1} HNO_3.

Using a similar iron-oxide adsorbent to that employed in the work for this thesis, but the analyte $H_2PO_4^-$, Zhang *et al.*[24] obtained a 100 % elution efficiency when using 0.25 mol L^{-1} H_2SO_4 as an eluent and Mason *et al.*[23] obtained a 90 % elution efficiency when using 1 mol L^{-1} HCl. Sulfuric acid was not used for the work in this thesis because optimization of the HG-AAS technique utilised HCl. Elution efficiencies from 88 to 100 % have been reported for metals using a variety of non-Chelex 100 based adsorbents using various conditions.[3, 28, 31, 32, 39]

The good linearity in Figure 4.1 (section 4.3.1) indicates that the As elution efficiency is independent of the amount of As adsorbed to the iron-oxide adsorbent, over the As^V mass range investigated. This is important as it has been suggested that the metal loading of a Chelex-100 adsorbent may affect the elution efficicncy.[35] Warnken *et al.*[35]obtained an elution efficiency of ~ 85 % for a range of metal ions using low metal loadings on the adsorbent. Zhang *et al.*[13] obtained lower elution efficiencies (~ 80 %) for moderate to high adsorbent loadings. The difference was attributed to the amount of metal on the Chelex-100 adsorbent.[35] Dahlqvist *et al.*[16] found that the elution efficiency of Ca (98 %) from Chelex-100 was independent of the mass of Ca^{2+} bound to the adsorbent (13 to 130 ng) when 5 mL of 1 mol L^{-1} HNO_3 was used as the eluent. Chang *et al.*[3] found that the elution efficiency of Sr from a cation exchange resin was independent of the mass of Sr bound to the adsorbent (40 to 465 ng) when 2 mL of 2 mol L^{-1} HNO_3 was used. However, when using 1 mL of 3, 2 or 1

mol L^{-1} HNO_3, the elution efficiency was dependent on the mass of Sr loaded onto the cation exchange resin.

4.4.2 Measurement of As^V and As^{III} diffusion coefficients through polyacrylamide diffusive gel and membrane filter at pH 5 using a diffusion cell and DGT devices

This section discusses the results from section 4.3.2 (measurement of As^V and As^{III} diffusion coefficients through polyacrylamide diffusive gel and membrane filter at pH 5 using a diffusion cell) and section 4.3.3 (measurement of As^V and As^{III} diffusion coefficients through polyacrylamide diffusive gel and membrane filter at pH 5 using DGT devices).

The As^V diffusion coefficient measured through a diffusive gel and membrane filter, by the use of a diffusion cell, was (4.85 ± 0.35) x 10^{-6} cm^2 s^{-1}. The average As^V diffusion coefficient determined by the use of DGT devices was (4.90 ± 0.05) x 10^{-6} cm^2 s^{-1} (n = 2). These values are in good agreement with each other.

For As^{III}, the average diffusion coefficient measured through a diffusive gel and membrane filter, by the use of a diffusion cell, was (6.40 ± 0.30) x 10^{-6} cm^2 s^{-1} (n = 2). The average As^{III} diffusion coefficient determined by the use of DGT devices was (5.95 ± 0.30) x 10^{-6} cm^2 s^{-1} (n = 4). These values agree within experimental uncertainty. Good linearity for all DGT experiments indicates the validity of using DGT for As determinations. Garmo *et al.*[2] found good agreement between diffusion coefficients measured using DGT devices and reported diffusion coefficients in which diffusion cells were used to measure diffusion coefficients, for most analytes investigated. For some analytes the diffusion coefficient measured by DGT was lower than that from diffusion cell experiments due to poor uptake by the adsorbent within the DGT devices.

The diffusion cell measures the diffusion coefficient of species through the diffusive gel and membrane filter. In contrast, the use of DGT devices to measure diffusion coefficients gives an effective diffusion coefficient; this is a combination of diffusion through the diffusive gel and membrane filter, as well as a measure of the binding ability of the adsorbent. The good agreement between the As^V diffusion coefficients determined by the use of a diffusion cell and by DGT devices, indicates that uptake of As^V by the iron-oxide adsorbent is rapid and

quantitative. For As^{III}, even though the diffusion coefficients determined using a diffusion cell and DGT devices agree within experimental uncertainty, the average diffusion coefficient determined using a diffusion cell was greater than that for DGT devices. A slightly lower diffusion coefficient measurement by the DGT devices method may not be unreasonable. As^{III} is generally considered to be taken up less effectively by iron-oxides than As^{V},[40] therefore, the effective diffusion coefficient measured by DGT may be less than the diffusion coefficient measured using a diffusion cell. In addition, the assumption that As^{III} elution from the adsorbent is quantitative may not be valid.

For the As^{III} diffusion coefficients measured using DGT devices, a positive y-intercept was obtained for the DGT plots (Table 4.2 from section 4.3.3.2). For experiments 1 and 3, even though the y-intercepts are positive, when the uncertainty is taken into account (i.e. standard deviation of y-intercept), the y-intercepts may be negative. However, for experiments 2 and 4 this is not the case. A positive intercept could be due to As already adsorbed to the iron-oxide adsorbent before the start of the experiment. However, blank measurements showed that this is unlikely to be the case, and at present the positive intercept cannot be accounted for. The positive intercept is unlikely to have a significant influence on the calculated diffusion coefficients, as it is the slope of the plot that is used to determine the diffusion coefficients. In addition, forcing the line of best fit through (0,0) had little affect on the calculated slope of the graph (illustrated in Table 4.2 from section 4.3.3.2) or the R^2 value for the line of best fit.

The diffusion coefficient of As^{V} through the diffusive gel and membrane filter is less than the diffusion coefficient for the As^{III} species. The As^{V} species ($H_2AsO_4^-$) is expected to diffuse through the diffusive gel more slowly than As^{III} (H_3AsO_3). The charged As^{V} species can be expected to have a larger hydration sphere than the uncharged As^{III} species. Furthermore, at pH 5, the As^{V} species is negatively charged; hence the As^{V} species will have a Na^+ counter ion associated with it which is expected to decrease the diffusion coefficient.

The reports of As^{III} and As^{V} diffusion coefficients in the literature are limited. The diffusion coefficients of As^{III} and As^{V} have been measured previously in this laboratory.[41] In one set of experiments, Stillwell[41] used a diffusion cell with a diffusive gel and membrane filter to measure the As diffusion coefficients. The experiments were carried out at pH 5 and 22 ^{o}C, in a 0.01 mol L^{-1} $NaNO_3$ and 0.05 mol L^{-1} sodium acetate medium. For As^{V}, Stillwell[41] reported an average diffusion coefficient value of (3.15 ± 0.20) x 10^{-6} cm^2 s^{-1} (n = 3). The uncertainty

is 1 standard deviation of the mean from triplicate measurements. For As^{III}, two experiments were carried out, however, the values did not agree within experimental uncertainty. The values were (6.50 ± 0.20) x 10^{-6} cm^2 s^{-1} and (4.50 ± 0.20) x 10^{-6} cm^2 s^{-1}. The uncertainty associated with these values is the standard deviation of the slope from diffusion cell plots.

Stillwell[41] also used DGT devices to measure As^V and As^{III} diffusion coefficients, however a different adsorbent was used to that employed in this thesis. Stillwell[41] used Chelex-100 resin that had been derivatised with Fe^{3+} and then hydrolyzed to form an iron-oxide bound to the resin. Using this adsorbent, As^V and As^{III} diffusion coefficients of (3.40 ± 0.40) x 10^{-6} cm^2 s^{-1} and (4.10 ± 0.35) x 10^{-6} cm^2 s^{-1} were calculated, respectively. The DGT measurements were carried out in a 0.0125 mol L^{-1} sodium acetate medium at pH 5; it is unclear whether the solution contained $NaNO_3$. The As^V diffusion coefficients measured by Stillwell[41] using a diffusion cell and DGT devices agree within experimental uncertainty. For As^{III}, good agreement is also obtained if the higher value using the diffusion cell (i.e. (6.50 ± 0.20) x 10^{-6} cm^2 s^{-1}) is ignored. However, none of the values agree within experimental uncertainty with those obtained in the work for this thesis, even though diffusive gels that had the same ratio of cross-linker to acrylamide were used. However, Stillwell[41] did obtain a higher diffusion coefficient for As^{III} than As^V as was observed in this work.

Fitz *et al*.[25] used DGT as part of a study to measure As removal in soils by an As hyper-accumulator plant. Fitz *et al*.[25] measured the diffusion coefficient of As^V ($HAsO_4^{2-}$) through the diffusive gel using a diffusion cell. No further details of the measurement are given (i.e. whether a membrane was present or the composition of the diffusion cell solutions). They obtained a value of (5.69 ± 0.14) x 10^{-6} cm^2 s^{-1}. This does not agree with the As^V value measured in the work for this thesis, however, the As^V species are different; other differences in solution composition may also be a factor. Because the $HAsO_4^{2-}$ species has a double negative charge, it would be expected that the diffusion coefficient would be lower than the $H_2AsO_4^-$ diffusion coefficient that was measured in the work for this thesis, however this is not the case. This assumptions seems to be valid as the diffusion coefficient of $H_2PO_4^-$ is greater than the diffusion coefficient of HPO_4^{2-} in water;[42] this is likely due to the increase in hydration of the more highly charged HPO_4^{2-}.

Early DGT work showed that the diffusion coefficients of metal ions through the diffusive gel were indistinguishable from those in water.[5] However, since this early work, the

composition of the commonly used diffusive gel has changed due to a difference in the manufacturing process of the cross-linker from 1997 onwards.[1] This change has resulted in a gel with a slightly smaller pore size;[1] it is this gel that is currently used in the majority of DGT work.[1] The measured diffusion coefficients for metal ions through this diffusive gel are ~ 85 % of the ion diffusion coefficient in water.[1] However, this proportion can be considerably lower when comparing the diffusion coefficients of oxyanions through the diffusive gel to those in water. Zhang *et al.*[24] measured the salt diffusion coefficient of KH_2PO_4 through a polyacrylamide diffusive gel. After converting to a self diffusion coefficient and correcting for temperature, the calculated diffusion coefficient of $H_2PO_4^-$ through the gel was 6.05 x 10^{-6} cm^2 s^{-1} at 25 ^oC. This value is ~ 72 % of the measured value in water at 25 ^oC (8.46 x 10^{-6} cm^2 s^{-1}).[42] Mason *et al.*[23] measured the MoO_4^- diffusion coefficient through a polyacrylamide diffusive gel; after correcting for temperature a value of 6.48 x 10^{-6} cm^2 s^{-1} at 25 ^oC was obtained. This value is ~ 65 % of the diffusion coefficient in water at 25 ^oC (9.91 x 10^{-6} cm^2 s^{-1}).[42] The As^V diffusion coefficient that was measured in the work for this thesis using a diffusion cell is between 50 and 57 % of the value in water at 25 ^oC (9.05 x 10^{-6} cm^2 s^{-1});[42] this takes account of the uncertainty associated with the As^V diffusion coefficient through the diffusive gel. There are no reported diffusion coefficients for As^{III} in water.

Zhang *et al.*[24] reasoned that the difference between the diffusion coefficient of $H_2PO_4^-$ in the diffusive gel and that in water may be due to $H_2PO_4^-$ reacting weakly with the diffusive gel which has sites of positive charge and hence slows diffusion through the gel. This could be occurring in the work carried out in this thesis, leading to a smaller diffusion coefficient for As^V through the gel than in water. Polyacrylamide diffusive gels used in DGT work are suspected of having sites that may interact with metal ions.[1, 4, 6, 10, 43] It is these sites that are assumed to cause the erratic behaviour of DGT at low ionic strength.[1, 4, 6, 7, 10, 43] Peters *et al.*[10] reported erratic DGT results at low ionic strength for Cd and Cu measurements. Values for $[C]_{DGT}/[C]_{Soln}$ (i.e. ratio of concentration measured by DGT to concentration in solution) varied from 0.5 to 3. Sangi *et al.*[6] observed enhanced diffusion of Cd^{II} at low ionic strength. At ionic strengths > 0.001 mol L^{-1} there was little change in the measured diffusion coefficients. Sangi *et al.*[6] also found that Cd^{II} was bound to the diffusive gel at low ionic strength. Scally *et al*[1] and Warnken *et al.*[43] found that at low ionic strength $[C]_{DGT}/[C]_{Soln}$ was ~ 0.5.

Warnken *et al*.[43] describes two factors affecting gel-metal ion interactions: (1) a gel charge, which affects DGT measurements by modifying the flux of metal ions at low ionic strength (< 0.001 mol L^{-1}), and (2) binding of cations to the gel, which is most important at low metal concentrations. The gel charge can either be positive or negative. It is suggested that the negative charge is caused by an excess of reaction products, whereas the positive charge is due to the protonation of gels by the slightly acidic water that is used to wash them.[43] If the gel is negatively charged then this causes the concentration of cations at the diffusive gel-solution interface to be elevated and the concentration gradient becomes steeper than it would be without the charge effect. A positively charged gel has the opposite affect, it depresses the metal concentration at the gel surface. The diffusion coefficient through the gel is unaffected, but the flux from the solution to the adsorbent, and therefore the effective diffusion coefficient in the diffusive gel, is enhanced (for a negatively charged gel) . These problems can be overcome by deploying DGT in solutions of higher ionic strength > 0.001 mol L^{-1}. This type of effect is unlikely to be the reason why the As^{V} diffusion coefficients measured in the work for this thesis, through the diffusive gel, are lower than that in water. This is because the gels that were used in the work for this thesis were conditioned in 0.01 mol L^{-1} $NaNO_3$, and all experiments were carried out in 0.01 mol L^{-1} $NaNO_3$. However, Warnken *et al*.[43] observed that the binding of cations to the diffusive gel is independent of ionic strength; this indicates a specific interaction with the diffusive gel. Therefore this may be a factor as to why the diffusion coefficients of As measured through the diffusive gels are less than that in water. Binding of anions to the polyacrylamide diffusive gel has not been reported. This behaviour could be examined by equilibrating diffusive gels with an As solution and measuring the concentration of As in the diffusive gel. If the concentration of As in the diffusive gel is greater than the concentration of As in solution then this would suggest that As is interacting with the diffusive gel. This method has been used to examine the reactivity of diffusive gels with cations.[3, 4, 6, 21, 43]

Zhang and co-workers[44] have measured As^{V} and As^{III} diffusion coefficients through diffusive gels without membrane filters; however these results are unpublished. Using a similar solution composition as for the work in this thesis (i.e. 0.01 mol L^{-1} $NaNO_3$, 0.025 mol L^{-1} sodium acetate, pH 4.8), Zhang and co-workers[44] obtained diffusion coefficients for As^{V} and As^{III} of 6.17 x 10^{-6} cm^2 s^{-1} and 9.41 x 10^{-6} cm^2 s^{-1} respectively at 25 ^{o}C. The As^{V} diffusion coefficient measured by Zhang and co-workers[44] is ~ 1.3 times larger than that measured for the work in this thesis using a diffusion cell; the As^{III} diffusion coefficient measured by

Zhang and co-workers[44] is ~ 1.5 times larger. The As^V diffusion coefficient measured by Zhang and co-workers[44] is 68 % of the As^V diffusion coefficient in water. These diffusion coefficients do not agree with those measured in the work for this thesis even when a 10 % uncertainty is assumed for their results.

It is unclear why there is a difference between the diffusion coefficients measured in the work for this thesis and that carried out by Zhang and co-workers.[44] In the work carried out for this thesis, DGT deployments were carried out with diffusive gels purchased from DGT Research Ltd. and with diffusive gels prepared in our laboratory; there was no significant difference in the diffusion coefficients for these two gels. In addition, it is unlikely to be a result of a significant diffusive boundary layer adjacent to the diffusive gel, as there was good agreement between diffusion cell experiments and DGT experiments, which utilized different stirring apparatus. Furthermore, the stirring speeds that were used were above 600 rpm; this is above the 400 rpm threshold reported by Zhang and Davison[13] and the 100 rpm threshold reported by Warnken *et al*.[35] at which DGT is independent of stirring rate.

4.4.3 Effect of membrane filter and pre-treatment of membrane on mass of As accumulated by DGT

The effect of the membrane filter was examined to see if this was a reason why the diffusion coefficients measured through the diffusive gel were different from those in water and to explain the differences between our results and the unpublished results of Zhang and co-workers.[44]

4.4.3.1 Effect of membrane filter on mass of As^{III} accumulated by DGT devices

Good agreement between the predicted mass and accumulated mass for the experiments in which membrane filters were absent indicates that the membrane filter has no significant effect on the diffusion coefficient of As^{III}. If diffusion through the membrane filter was significantly different (i.e. slower) from diffusion through the diffusive gel, then the accumulated mass in the absence of the filter membrane would be significantly greater than the predicted mass, because the predicted mass calculation uses the As^{III} diffusion coefficient through a diffusive gel and membrane filter. Therefore it seems that the diffusion coefficient of As^{III} through the membrane filter is indistinguishable from that through the diffusive gel. This agrees with the work of Zhang *et al*.,[24] Zhang and Davison,[5] Chang *et al*.[3] and Scally *et*

al.,[1] who all found that there was no significant difference in diffusion coefficients of metal ions measured through a diffusive gel and membrane filter, to the diffusive gel alone.

4.4.3.2 Effect of membrane type, pore size and acid washing of membrane on mass of As^V accumulated by DGT devices

According to the Schleicher and Schuell catalogue, nitric acid may cause shrinking or swelling of the membrane filter pore structure, and hence the effect of acid washing the filter membranes was examined. Results showed that the membrane preparation procedure, the pore size of the membrane, and the type of membrane had no significant effect on the normalized mass of As^V accumulated within DGT devices. The mass accumulated by all DGT devices agreed within experimental uncertainty once normalized for the difference in the thickness of the membrane filters. Therefore the preparation of the membrane and the membrane type and pore size does not significantly influence the diffusion of As^V.

4.5 Conclusion

The As^V and As^{III} diffusion coefficients measured through a diffusive gel and membrane filter using a diffusion cell were (4.85 ± 0.35) x 10^{-6} cm^2 s^{-1} and (6.40 ± 0.30) x 10^{-6} cm^2 s^{-1} (n = 2), respectively. Using DGT devices, the As^V and As^{III} diffusion coefficients were (4.90 ± 0.05) x 10^{-6} cm^2 s^{-1} (n = 2) and (5.95 ± 0.30) x 10^{-6} cm^2 s^{-1} (n = 4), respectively, assuming a 100 % elution efficiency. There was good agreement between the diffusion coefficients measured by the two methods. For this work, diffusive gels, iron-oxide gels and iron-oxide from different batches were used. The good agreement between diffusion coefficients from different experiments indicates good reproducibility in the preparation of the gels and iron-oxide adsorbent. In addition, some experiments were carried out with gels (both diffusive and adsorbent gels) that had been prepared up to 6 months earlier. The good agreement in diffusion coefficients obtained indicates that gels can be kept for at least 6 months without a change in performance. Furthermore, there was no difference in performance of the gel adsorbent that was prepared with fresh iron-oxide, or iron-oxide that had been prepared 6 months earlier.

The diffusion coefficients measured using DGT devices were used in the remainder of work for this thesis. There may be small differences in the effective diffusion coefficients for the

diffusion cell and DGT devices, especially when As^{III} is concerned, due to uptake at the iron-oxide adsorbent and/or elution of As^{III}.

The presence of the membrane filter had no significant effect on the mass of As^{III} accumulated by DGT; this was not examined for As^{V} as the largest difference between results in this thesis and those of Zhang and co-workers[44] was observed for the As^{III} diffusion coefficients. The membrane pore size, preparation of the membrane and the type of membrane had no significant effect on the mass of As^{V} accumulated by DGT. Therefore, any differences observed between diffusion coefficients from work in this thesis and other work is unlikely to be due to the membrane filter or its preparation procedure.

4.6 References

1. Scally, S.; Davison, W.; Zhang, H., Diffusion coefficients of metals and metal complexes in hydrogels used in diffusive gradients in thin films. *Analytica Chimica Acta* **2006,** 558, (1-2), 222-229.

2. Garmo, O. A.; Royset, O.; Steinnes, E.; Flaten, T. P., Performance study of diffusive gradients in thin films for 55 elements. *Analytical Chemistry* **2003,** 75, (14), 3573-3580.

3. Chang, L. Y.; Davison, W.; Zhang, H.; Kelly, M., Performance characteristics for the measurement of Cs and Sr by diffusive gradients in thin films (DGT). *Analytica Chimica Acta* **1998,** 368, (3), 243-253.

4. Zhang, H.; Davison, W., Diffusional characteristics of hydrogels used in DGT and DET techniques. *Analytica Chimica Acta* **1999,** 398, (2-3), 329-340.

5. Davison, W.; Zhang, H., In-situ speciation measurements of trace components in natural-waters using thin-film gels. *Nature* **1994,** 367, (6463), 546-548.

6. Sangi, M. R.; Halstead, M. J.; Hunter, K. A., Use of the diffusion gradient thin film method to measure trace metals in fresh waters at low ionic strength. *Analytica Chimica Acta* **2002,** 456, (2), 241-251.

7. Alfaro-De la Torre, M. C.; Beaulieu, P. Y.; Tessier, A., In situ measurement of trace metals in lakewater using the dialysis and DGT techniques. *Analytica Chimica Acta* **2000,** 418, (1), 53-68.

8. Scally, S.; Davison, W.; Zhang, H., In situ measurements of dissociation kinetics and labilities of metal complexes in solution using DGT. *Environmental Science & Technology* **2003,** 37, (7), 1379-1384.

9. Gimpel, J.; Zhang, H.; Hutchinson, W.; Davison, W., Effect of solution composition, flow and deployment time on the measurement of trace metals by the diffusive gradient in thin films technique. *Analytica Chimica Acta* **2001,** 448, (1-2), 93-103.

10. Peters, A. J.; Zhang, H.; Davison, W., Performance of the diffusive gradients in thin films technique for measurement of trace metals in low ionic strength freshwaters. *Analytica Chimica Acta* **2003,** 478, (2), 237-244.

11. Denney, S.; Sherwood, J.; Leyden, J., In situ measurements of labile cu, Cd and Mn in river waters using DGT. *Science of the Total Environment* **1999,** 239, (1-3), 71-80.

12. Twiss, M. R.; Moffett, J. W., Comparison of copper speciation in coastal marine waters measured using analytical voltammetry and diffusion gradient in thin-film techniques. *Environmental Science & Technology* **2002,** 36, (5), 1061-1068.

13. Zhang, H.; Davison, W., Performance-characteristics of diffusion gradients in thin-films for the in-situ measurement of trace-metals in aqueous-solution. *Analytical Chemistry* **1995,** 67, (19), 3391-3400.

14. Scally, S.; Zhang, H.; Davison, W., Measurements of lead complexation with organic ligands using DGT. *Australian Journal of Chemistry* **2004,** 57, (10), 925-930.

15. Sondergaard, J., In situ measurements of labile al and Mn in acid mine drainage using diffusive gradients in thin films. *Analytical Chemistry* **2007,** 79, (16), 6419-5423.

16. Dahlqvist, R.; Zhang, H.; Ingri, J.; Davison, W., Performance of the diffusive gradients in thin films technique for measuring Ca and Mg in freshwater. *Analytica Chimica Acta* **2002,** 460, (2), 247-256.

17. Downard, A. J.; Panther, J.; Kim, Y. C.; Powell, K. J., Lability of metal ion-fulvic acid complexes as probed by FIA and DGT: A comparative study. *Analytica Chimica Acta* **2003,** 499, (1-2), 17-28.

18. Jansen, B.; Kotte, M. C.; van Wijk, A. J.; Verstraten, J. M., Comparison of diffusive gradients in thin films and equilibrium dialysis for the determination of al, Fe(III) and Zn complexed with dissolved organic matter. *Science of the Total Environment* **2001,** 277, (1-3), 45-55.

19. Teasdale, P. R.; Hayward, S.; Davison, W., In situ, high-resolution measurement of dissolved sulfide using diffusive gradients in thin films with computer-imaging densitometry. *Analytical Chemistry* **1999,** 71, (11), 2186-2191.

20. Murdock, C.; Kelly, M.; Chang, L. Y.; Davison, W.; Zhang, H., DGT as an in situ tool for measuring radiocesium in natural waters. *Environmental Science & Technology* **2001,** 35, (22), 4530-4535.

21. Docekalova, H.; Divis, P., Application of diffusive gradient in thin films technique (DGT) to measurement of mercury in aquatic systems. *Talanta* **2005,** 65, (5), 1174-1178.

22. French, M. A.; Zhang, H.; Pates, J. M.; Bryan, S. E.; Wilson, R. C., Development and performance of the diffusive gradients in thin-films technique for the measurement of technetium-99 in seawater. *Analytical Chemistry* **2005,** 77, (1), 135-139.

23. Mason, S.; Hamon, R.; Nolan, A.; Zhang, H.; Davison, W., Performance of a mixed binding layer for measuring anions and cations in a single assay using the diffusive gradients in thin films technique. *Analytical Chemistry* **2005,** 77, (19), 6339-6346.

24. Zhang, H.; Davison, W.; Gadi, R.; Kobayashi, T., In situ measurement of dissolved phosphorus in natural waters using DGT. *Analytica Chimica Acta* **1998,** 370, (1), 29-38.

25. Fitz, W. J.; Wenzel, W. W.; Zhang, H.; Nurmi, J.; Stipek, K.; Fischerova, Z.; Schweiger, P.; Kollensperger, G.; Ma, L. Q.; Stingeder, G., Rhizosphere characteristics of the arsenic hyperaccumulator *Pteris vittata* L. and monitoring of phytoremoval efficiency. *Environmental Science & Technology* **2003,** 37, (21), 5008-5014.

26. Motelica-Heino, M.; Naylor, C.; Zhang, H.; Davison, W., Simultaneous release of metals and sulfide in Lacustrine sediment. *Environmental Science & Technology* **2003,** 37, (19), 4374-4381.

27. Naylor, C.; Davison, W.; Motelica-Heino, M.; Van Den Berg, G. A.; Van Der Heijdt, L. M., Simultaneous release of sulfide with Fe, Mn, Ni and Zn in marine harbour sediment measured using a combined metal/sulfide DGT probe. *Science of the Total Environment* **2004,** 328, (1-3), 275-286.

28. Li, W.; Zhao, H.; Teasdale, P. R.; John, R.; Zhang, S., Synthesis and characterisation of a polyacrylamide-polyacrylic acid copolymer hydrogel for environmental analysis of Cu and Cd. *Reactive & Functional Polymers* **2002,** 52, (1), 31-41.

29. Li, W.; Zhao, H.; Teasdale, P. R.; John, R., Preparation and characterisation of a poly(acrylamidoglycolic acid-coacrylamide) hydrogel for selective binding of Cu^{2+} and application to diffusive gradients in thin films measurements. *Polymer* **2002,** 43, (17), 4803-4809.

30. Li, W. J.; Zhao, H. J.; Teasdale, P. R.; Wang, F. Y., Trace metal speciation measurements in waters by the liquid binding phase DGT device. *Talanta* **2005,** 67, (3), 571-578.

31. Li, W.; Zhao, H.; Teasdale, P. R.; John, R.; Zhang, S., Application of a cellulose phosphate ion exchange membrane as a binding phase in the diffusive gradients in thin films technique for measurement of trace metals. *Analytica Chimica Acta* **2002,** 464, (2), 331-339.

32. Li, W. J.; Zhao, J. J.; Li, C. S.; Kiser, S.; Cornett, R. J., Speciation measurements of uranium in alkaline waters using diffusive gradients in thin films technique. *Analytica Chimica Acta* **2006,** 575, (2), 274-280.

33. Li, W. J.; Teasdale, P. R.; Zhang, S. Q.; John, R.; Zhao, H. J., Application of a poly(4-styrenesulfonate) liquid binding layer for measurement of Cu^{2+} and Cd^{2+} with the diffusive gradients in thin-films technique. *Analytical Chemistry* **2003,** 75, (11), 2578-2583.

34. Westrin, B. A.; Axelsson, A.; Zacchi, G., Diffusion measurement in gels. *Journal of Controlled Release* **1994,** 30, (3), 189-199.

35. Warnken, K. W.; Zhang, H.; Davison, W., Accuracy of the diffusive gradients in thin-films technique: Diffusive boundary layer and effective sampling area considerations. *Analytical Chemistry* **2006,** 78, (11), 3780-3787.

36. Warnken, K. W.; Zhang, H.; Davison, W., Performance characteristics of suspended particulate reagent-iminodiacetate as a binding agent for diffusive gradients in thin films. *Analytica Chimica Acta* **2004,** 508, (1), 41-51.

37. Ona-Nguema, G.; Morin, G.; Juillot, F.; Calas, G.; Brown, G. E., EXAFS analysis of arsenite adsorption onto two-line ferrihydrite, hematite, goethite, and lepidocrocite. *Environmental Science & Technology* **2005,** 39, (23), 9147-9155.

38. Wilkie, J. A.; Hering, J. G., Adsorption of arsenic onto hydrous ferric oxide: Effects of adsorbate/adsorbent ratios and co-occurring solutes. *Colloids and Surfaces A-Physicochemical and Engineering Aspects* **1996,** 107, 97-110.

39. Larner, B. L.; Seen, A. J., Evaluation of paper-based diffusive gradients in thin film samplers for trace metal sampling. *Analytica Chimica Acta* **2005,** 539, (1-2), 349-355.

40. Dixit, S.; Hering, J. G., Comparison of arsenic(V) and arsenic(III) sorption onto iron oxide minerals: Implications for arsenic mobility. *Environmental Science & Technology* **2003,** 37, (18), 4182-4189.

41. Stilwell, K. *Arsenic speciation by diffusive gradients in thin films*. M.Sc. Thesis, University of Canterbury, New Zealand, 2003.

42. Li, Y. H.; Gregory, S., Diffusion of ions in sea-water and in deep-sea sediments. *Geochimica et Cosmochimica Acta* **1974,** 38, (5), 703-714.

43. Warnken, K. W.; Zhang, H.; Davison, W., Trace metal measurements in low ionic strength synthetic solutions by diffusive gradients in thin films. *Analytical Chemistry* **2005,** 77, (17), 5440-5446.

44. Zhang, H., unpublished results, 2006.

Chapter 5

Method development for As^{V} and As^{III} accumulation by DGT

5.1 Introduction

For DGT to be applied with confidence when determining As concentrations in waters, a number of factors were investigated to examine their effect on the DGT measurement. These factors were related to the performance of the iron-oxide adsorbent under various conditions, and the actual As species being accumulated. Experiments were undertaken to investigate competition between As^{V} and As^{III} for adsorption sites on the iron-oxide, competition between As and other adsorbing cation and anion species, effects of pH on both As^{V} and As^{III} adsorption and diffusion, effect of fulvic acid on As^{V} and As^{III} adsorption (including the potential formation of complexes between As and fulvic acid in solution), and the effect of Fe^{III} colloids on the fraction of As^{V} measured by DGT. In addition, the capacity of the iron-oxide adsorbent was determined.

5.1.1 Capacity of the adsorbent used in DGT

DGT has the potential to be used for long-term deployments. However, the capacity of the adsorbent may be a limiting factor. The quantitative relationship in the DGT equation will only apply if the capacity of the adsorbent is not exceeded. If the capacity of the adsorbent is exceeded unknowingly during a DGT deployment, then this would result in an underestimation of the concentration determined by DGT. It is common practice to determine the capacity of the adsorbent used in DGT; this has been carried out with a variety of analytes and adsorbents.[1-8] Furthermore, competitive capacities have also been determined;[2-4] in a natural water there will be a variety of species adsorbing in addition to the analyte of interest.

5.1.2 Adsorption of As by iron-oxides

Arsenic is known to adsorb to a variety of metal oxides. These include Fe, Al, and Mn oxides.[9, 10] Adsorption is one of the reactions that controls the mobility and bioavailability of As.[11, 12] Iron-oxides are important solids for the adsorption of As; they can be present as discrete particles or as coatings on other mineral surfaces.[9] There are a variety of iron-oxides including ferrihydrite, goethite, and hematite.[13] These iron-oxides differ in their composition and their crystal structure.[14] Goethite and hematite are extremely stable iron-oxides which have a defined crystal structure, whereas ferrihydrite is poorly crystalline.[13] The surface areas of ferrihydrite, goethite, and hematite range from 100 to 400, 8 to 200, and 2 to 90 $m^2\ g^{-1}$, respectively.[13] The large surface area makes ferrihydrite a good adsorbent; this is the iron-oxide that was used for the work in this thesis.

The As^V and As^{III} species adsorb to iron-oxides through inner-sphere complexation via replacement of hydroxyl functional groups on the iron-oxide surface.[15-19] Inner-sphere complexes are defined as covalent linkages between the adsorbed ion and the reactive surface, with no water of hydration between the adsorbed ion and the surface functional group.[16] A variety of co-ordination modes have been characterized (Figure 5.1). Ona-Nguema *et al.*,[17] using x-ray absorption fine structure spectroscopy (EXAFS), found that As^{III} forms bidentate mononuclear and bidentate binuclear complexes with ferrihydrite and hematite, whereas for goethite the dominant complex was bidentate binuclear with minor amounts of monodentate complexation. The bidentate mononuclear complex was absent in goethite. Manning *et al.*[16] also used EXAFS to examine As^{III} complexation by goethite. They found that As^{III} formed bidentate binuclear complexes; there was no evidence to suggest monodentate complexation was occurring.

Waychunas *et al.*,[19] Fendorf *et al.*,[15] and Sherman and Randall[18] have all used EXAFS to examine complexation of As^V by iron-oxides. Waychunas *et al.*[19] found that As^V adsorbs on ferrihydrite mainly as a binuclear bidentate complex. They also observed monodentate complexation; this corresponded to ~ 30 % of all Fe-As interactions. Fendorf *et al.*[15] found monodentate and bidentate binuclear complexation of As^V by goethite. The monodentate complexes were more pronounced at low As^V surface coverage. At high surface coverage, the bidentate complexes predominate. In contrast to Waychunas *et al.*[19] and Fendorf *et al.*,[15] Sherman and Randall[18] found that complexation of As^V by goethite, hematite, and

ferrihydrite occurred only via bidentate binuclear complexation. They did not find any evidence of bidentate mononuclear or monodentate complexation.

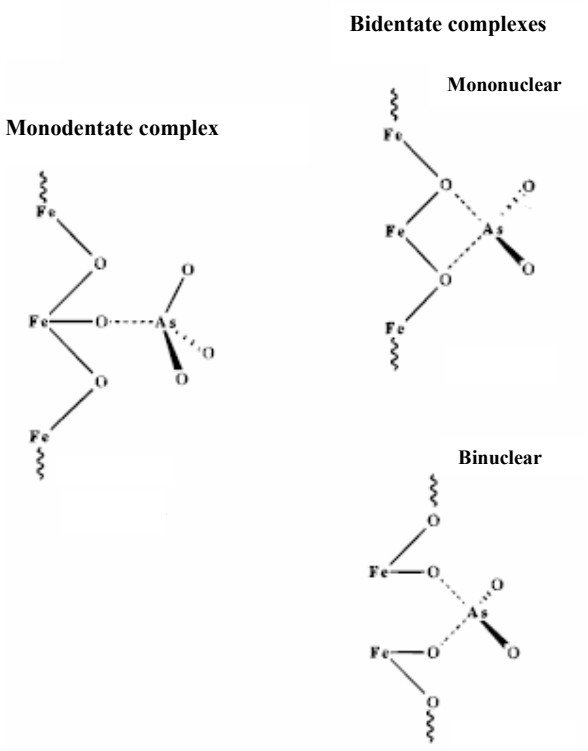

Figure 5.1 Schematic illustrations of co-ordination modes of As with iron-oxides. Figure adapted from Fendorf *et al*.[15]

5.1.2.1 Effect of pH on As adsorption

One of the most important factors affecting adsorption of As^{V} and As^{III} to iron-oxides is pH; pH has a major influence on As protonation, and on the composition of surface functional groups of the iron-oxide through protonation and de-protonation reactions.[9] The surface of an iron-oxide can have a positive or negative charge depending on the pH.[13] Protonation of surface hydroxy groups leads to a positively charged functional group (equation 5.1), whereas de-protonation leads to a negatively charged functional group (equation 5.2).

$$\equiv FeOH + H^{+} \rightleftharpoons \equiv FeOH_2^{+} \qquad \textbf{(5.1)}$$

$$\equiv FeOH \rightleftharpoons \equiv FeO^{-} + H^{+} \qquad \textbf{(5.2)}$$

The pH at which the positive charge on the iron-oxide surface, due to protonated groups, equals the negative charge on the surface, due to de-protonated groups, is pH_{pzc}, where pzc is the point of zero charge.[20] At this pH the net charge on the surface is zero. It is important to note that negative, positive, and neutral functional groups will exist on the iron-oxide surface simultaneously.[13] At pH < pH_{pzc}, the ≡ $FeOH_2^+$ groups predominate over the ≡ FeO^- groups; this gives the surface an overall positive charge, however, some ≡ FeO^- groups will still exist.[13] The opposite is observed at pH > pH_{pzc}. Iron-oxides have a pH_{pzc} in the pH range 6 to 10.[13] Jain *et al*.[21] determined a pH_{pzc} for ferrihydrite of 8.5. The pH_{pzc} of a surface can change with adsorption of anions or cations.[21]

Arsenic speciation is affected by pH. The pK_a values for As^V are 2.20, 6.97 and 11.53; for As^{III} the values are 9.22, 12.13 and 13.40.[22] Figure 5.2 shows speciation diagrams for As^V and As^{III} species as a function of pH. The decrease in As^V adsorption at high pH has been attributed to electrostatic interactions between negatively charged As^V species and the negatively charged iron-oxide surface.[11, 22]

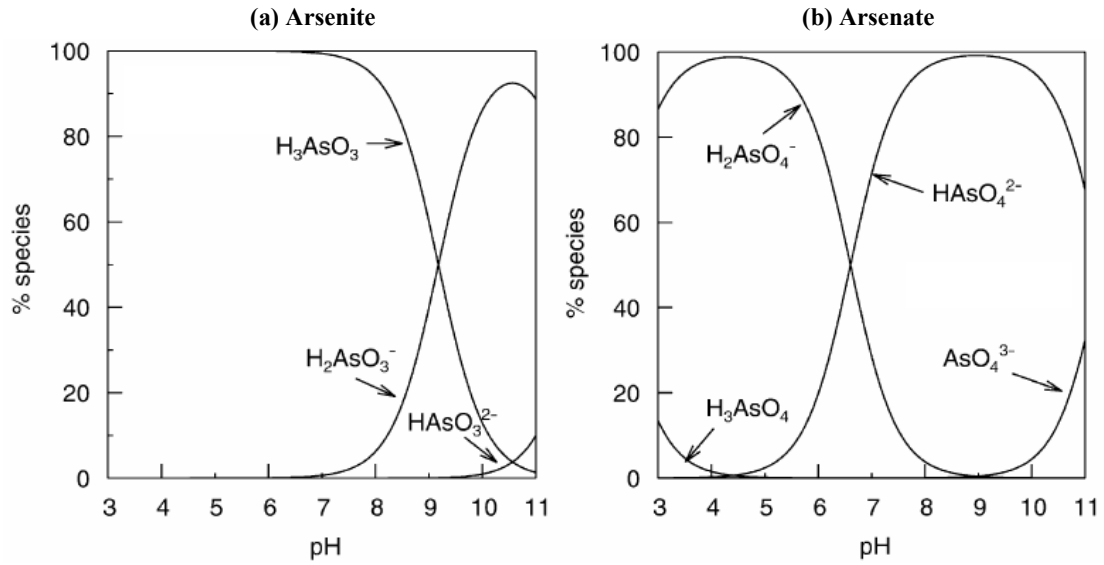

Figure 5.2 Arsenite (a) and arsenate (b) speciation as a function of pH. From Smedley and Kinniburgh.[23]

5.1.2.2 Anion and cation adsorption on iron-oxides

Iron-oxides adsorb a variety of both cations and anions.[13, 24] These include the cations Pb^{2+}, Zn^{2+}, Cd^{2+}, Cu^{2+}, Ni^{2+}, Co^{2+}, Ca^{2+}, Sr^{2+} Cr^{3+} and Ag^+;[13, 24] and the anions PO_4^{3-}, VO_4^{3-}, SO_4^{2-},

SeO_4^{2-}, SeO_3^{2-} and CrO_4^{2-}.[13, 24] The adsorption process involves interaction of the cation or anion with the surface hydroxyl groups of the iron-oxide.[13]

The adsorption of cations can be specific or non-specific.[13] Specific adsorption involves co-ordination of the cation with iron-oxide surface hydroxyl groups to form monodentate (equation 5.3) and bidentate (equation 5.4) inner-sphere surface complexes.[13] Non-specific cation adsorption (equation 5.5) involves ion-pair formation where the adsorbing species retains its primary hydration sphere.[13] Non-specific adsorption is strongly dependent on ionic strength,[13, 25] whereas specific adsorption shows little ionic strength dependence.[25]

$$\equiv FeOH + M^{z+} \rightleftharpoons \equiv FeOM^{(z-1)+} + H^+ \quad \textbf{(5.3)}$$

$$\equiv (FeOH)_2 + M^{z+} \rightleftharpoons \equiv (FeO)_2M^{(z-1)+} + 2H^+ \quad \textbf{(5.4)}$$

$$\equiv FeO^- + M^{z+} \rightleftharpoons \equiv FeO^-M^{z+} \quad \textbf{(5.5)}$$

The alkali cations adsorb non-specifically; the alkaline earth cations and transition metals adsorb specifically.[13] For cations, adsorption on iron-oxides increases with pH;[13, 24] generally adsorption increases from 0 to 100 % over a narrow range of 1 to 2 pH units.[13]

The adsorption of anions onto iron-oxide surfaces can also be specific or non-specific.[13] Specific adsorption involves replacement of the surface hydroxyl groups of an iron-oxide by the adsorbing anion to form monodentate (equation 5.6) and bidentate (equation 5.7) complexes. Anions that adsorb specifically on iron-oxides include phosphate, silicate, selenite, arsenate, chloride, fluoride, citrate and oxalate.[13]

$$\equiv FeOH + L^- + H^+ \rightleftharpoons \equiv FeL + H_2O \quad \textbf{(5.6)}$$

$$\equiv (FeOH)_2 + L^- + 2H^+ \rightleftharpoons \equiv Fe_2L^+ + 2H_2O \quad \textbf{(5.7)}$$

Non-specific adsorption involves ion-pair formation; these anions are easily exchanged by other anions at higher concentrations in solution.[13] Anions that adsorb non-specifically include nitrate and perchlorate; sulfate and selenate can be considered as intermediate

between non-specifically and specifically adsorbed anions.[13] In general, anion adsorption is at a maximum at low pH and decreases with increasing pH.[13, 24] For non-specifically adsorbing anions, adsorption is negligible above the pH_{pzc} of the iron-oxide due to the increasing negative behaviour of the iron-oxide surface with increasing pH.[13]

A variety of anions have been shown to inhibit adsorption of As^{V} and As^{III} by iron-oxides under a range of conditions and concentrations.[22, 26-31] The major anions that affect adsorption include phosphate,[22, 27, 28, 31] sulfate,[22, 26, 27] and silicate.[27, 29, 30]

5.1.3 Adsorption of fulvic acid by iron-oxides

5.1.3.1 Fulvic acid

Humic substances are naturally occurring, heterogeneous, organic acids that are widely distributed in soils, natural waters, and sediments.[32] They are derived from the decomposition of terrestrial and aquatic animal and plant debris.[33] Humic substances can be sub-divided into three categories based on their solubility:[20] humin, the fraction of humic substance that is insoluble in water at all pH values; humic acid, the fraction that is insoluble at pH 2 but becomes soluble at high pH; and fulvic acid, which is soluble at all pH values.

Humic and fulvic acids are general terms that cover a wide range of individual compounds.[20] The exact structures of these compounds have not been eludicated.[20] Figure 5.3 shows a model of a fulvic acid that has been derived from various experimental results.

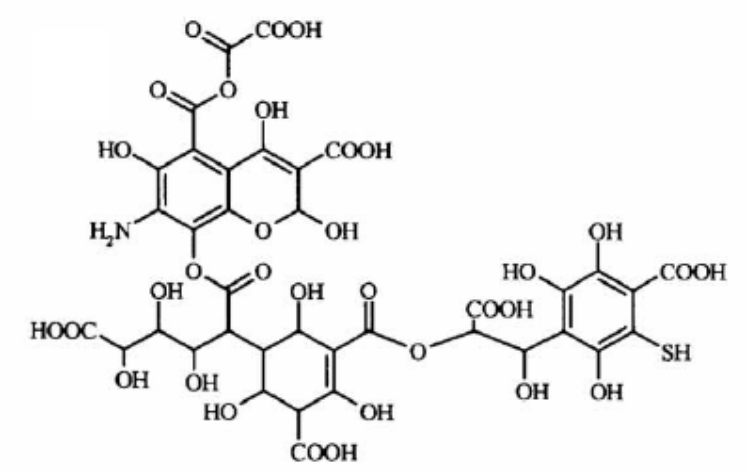

Figure 5.3 Model of a fulvic acid. Figure from Alvarex-Puebla *et al*.[34]

Humic and fulvic acids have a similar structure, but they differ in molecular weight and elemental and functional group compostions.[35] The general molecular weight range of fulvic acids is 500 to 2000 Daltons, and that of humic acids is 2000 to 10^6 or more Daltons.[20] Fulvic acids contain higher oxygen and lower carbon contents than humic acids.[32] Almost all oxygen in fulvic acid can be accounted for by functional groups (COOH, OH, C=O) whereas a high portion of oxygen in humic acid occurs as structural components (e.g. in ether and ester linkages).[32]

Fulvic acids are able to form stable complexes with many metal cations including Fe^{3+}, Al^{3+}, Pb^{2+}, Cu^{2+}, Zn^{2+}, Pb^{2+}, Ca^{2+}, Mn^{2+} and Mg^{2+}.[33, 36] The ability of humic substances to form complexes is attributed to their high content of oxygen-containing functional groups, including carboxylic, phenolic, hydroxy, and carbonyl structures of various types.[32] Amino groups may also be important.[32]

Concentrations of humic substances are conveniently expressed in terms of the mass of their carbon per unit volume. Concentrations of humic substances in rivers and lakes range from 2 to 15 mg C L^{-1}, with a mean of 4 to 6 mg C L^{-1}; in groundwater the concentrations are below 2 mg C L^{-1}, with an average value of 0.7 mg C L^{-1}; and seawater ranges from 0.3 to 2.0 mg C L^{-1}, with an average of 1 mg C L^{-1}.[20]

5.1.3.2 Adsorption of fulvic acid by iron-oxides

Fulvic acids have been shown to adsorb to iron-oxides such as goethite,[37] hematite[12] and ferrihydrite;[38] they are proposed to adsorb onto these surfaces via ligand exchange between carboxyl/hydroxyl functional groups of fulvic acid and the hydroxyl groups of metal hydroxides.[33] This is shown schematically in equation 5.8. Hydrogen bonding and electrostatic interactions may also be important.[37]

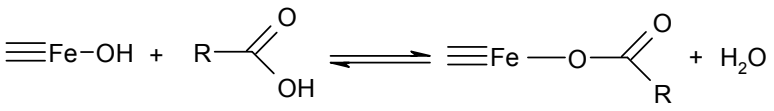

(5.8)

Furthermore, fulvic acid has been shown to decrease the adsorption of As^V and As^{III} on a variety of iron-oxides; these include ferrihydrite,[38, 39] goethite[37] and hematite.[12] It is suggested that fulvic acid may displace As that is already adsorbed to the iron-oxide, or it

may block adsorption sites within the pores of the iron-oxide, making sites inaccessible to As species. This is illustrated in Figure 5.3.

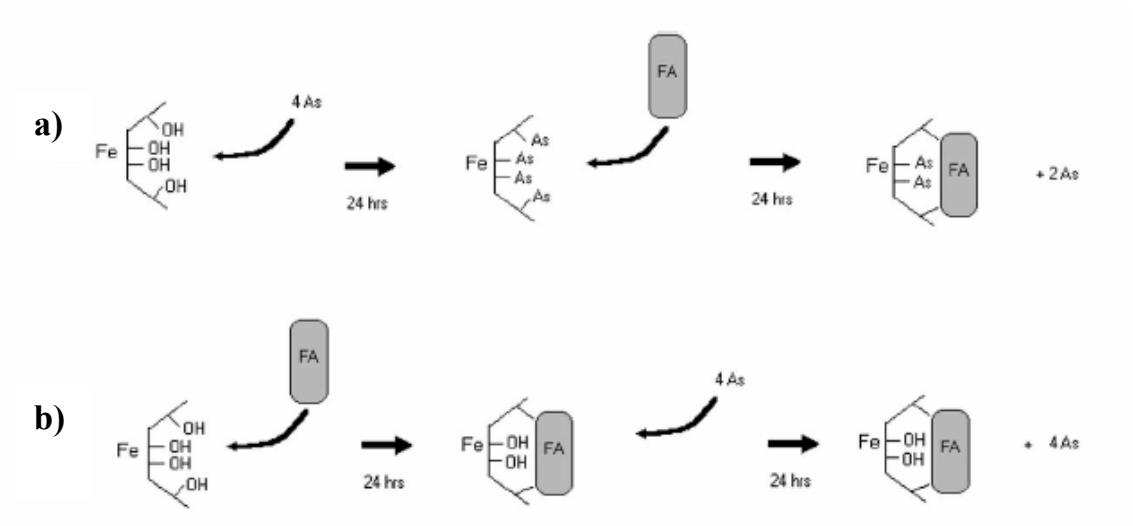

Figure 5.4 Schematic diagram of the proposed effect of fulvic acid on As adsorption by iron-oxide. Scheme (a) represents addition of As before fulvic acid; scheme (b) represents addition of As after fulvic acid. In scheme (a) fulvic acid is shown to remove previously adsorbed As; in scheme (b) fulvic acid is shown to block available adsorption sites for As. Figure adapted from Simeoni *et al.*[39]

5.1.4 Interactions between As and fulvic acid

5.1.4.1 As-Fe^{III}-fulvic acid complexes

It has been reported that As can form complexes with fulvic acid.[12, 40-42] The nature of these interactions is not well understood. It is proposed that negatively charged As^{V} species and neutral As^{III} species associate with the negatively charged fulvic acid by metal bridging mechanisms;[12, 41, 42] Fe^{III} and Al^{III} are important ions in this process.[12, 41, 42] It has also been proposed that Fe^{III}-fulvic acid colloids may be providing binding sites for the adsorption of As rather than the formation of a non-colloidal As-Fe^{III}-fulvic acid complex.[42]

The possibility of non-colloidal As-Fe^{III}-fulvic acid complexes has implications for the concentration of As measured by the DGT method. If such an As complex was non-labile, then the concentration determined by DGT would be less than the total concentration of As in solution, as the complexed fraction of As would not be taken up by the DGT device. Alternatively, if the non-colloidal As-Fe^{III}-fulvic acid complex does exist and the complex is

labile, then the concentration determined by DGT (using the diffusion coefficient of 'free' As) would be less than the total concentration of As in solution. This is because fulvic acids have lower diffusion coefficients than 'free' As species.[43-45] Diffusion coefficients of fulvic acid through polyacrylamide gels in the presence of metal ions are ~ 2 x 10^{-6} cm^2 s^{-1}.[43-45] This is ~ 2.5 times lower than the diffusion coefficient of As^V and ~ 3 times lower than the diffusion coefficient of As^{III}.

5.1.4.2 As reduction and oxidation in the presence of fulvic acid

Fulvic acid has been shown to play a role in both the oxidation and reduction of As.[12, 46] Redman *et al.*[12] examined the oxidation of As^{III} and reduction of As^V in the presence of 6 different fulvic acids. While only one fulvic acid reduced As^V to As^{III} to some extent, all of the fulvic acid samples oxidized As^{III} to As^V; the amount of oxidation depended on the fulvic acid sample. Redman *et al.*[12] suggest that the oxidation/reduction properties of fulvic acid was due to quinone or other functional groups that had been previously oxidized or reduced in their natural environment. In the absence of fulvic acid, oxidation or reduction of As did not occur.

Tongesayi and Smart[46] examined the reduction of As^V in the presence of fulvic acid at various pH, fulvic acid concentrations, Fe^{III} concentration, and in light and dark conditions. They found that in the presence of fulvic acid there was significant reduction of As^V to As^{III} and that the reduction was a function of time. They also found that reduction occurred in both dark and light conditions and that Fe^{III} increased the rate of the reduction reaction. It was suggested that Fe^{III} may be acting as a catalyst by shuttling electrons between fulvic acid and As^V. Reduction of As^V was significant at all pH values investigated (3.5, 6, 7 and 8). Tongesayi and Smart[46] also observed some oxidation of As^{III} at pH 2 in the presence of fulvic acid, whereas, at pH 6, the oxidation of As^{III} was not as significant.

5.1.5 Chapter outline

This chapter is mainly concerned with examining the effect of pH, anions and cations, fulvic acid, and Fe^{III} on (i) the diffusion coefficients of As^V and As^{III}, and (ii) the adsorption of As^V and As^{III} by the iron-oxide adsorbent. In addition, the capacity of the iron-oxide adsorbent and the effect of varying the $[As^V]/[As^{III}]$ concentration ratio was examined.

Many of the results in this chapter are reported as the mass of As accumulated by DGT. The accumulated mass is compared to the predicted mass. The predicted mass has been calculated using the DGT equation, experimental parameters, and the diffusion coefficients of As^{V} and As^{III} measured at pH 5 (chapter 4). Furthermore, many of the results are expressed as a ratio of accumulated mass of As to predicted mass of As. A ratio of 1.0 implies that there is no significant difference between the accumulated and predicted masses and therefore the parameter investigated has no significant effect on the DGT measurement (i.e. diffusion or adsorption of the As species is not affected). A ratio > 1.0 implies an increase in diffusion coefficient or adsorption of the As species; a ratio < 1.0 implies a decrease in diffusion coefficient or adsorption of the As species.

5.2 Experimental

All experiments in this chapter were concerned with deployment of DGT devices. Therefore the general procedure for measuring pH and temperature, retrieving DGT devices, removing and eluting the adsorbent, and the collection of samples from the deployment solutions, will be described now, rather than in each of the following sections. This is the same procedure as described in chapter 4, but has also been included here for convenience.

After DGT devices were retrieved, they were placed in Milli-Q water and then washed thoroughly before disassembling and removal of the iron-oxide gel adsorbent. The iron-oxide adsorbent was rinsed with Milli-Q water and excess water was removed from the adsorbent by carefully dabbing on Durx™ clean room wipes. The iron-oxide gel adsorbent was placed in acid-cleaned plastic centrifuge tubes and eluted with 2 mL of concentrated HCl for 24 h on an orbital shaker. After 24 h, 8 mL of Milli-Q water was added to the eluent and left for 16 to 24 h on an orbital shaker before the As concentration in the eluent solution was measured using HG-AAS. Immediately prior to sampling the eluent, the plastic centrifuge tube was given a brief but vigorous shake by hand.

Samples were removed from the As deployment solutions at the start and end of the experiment to confirm that the As concentration had not changed significantly over this time. These samples were stabilized by adding concentrated HCl to give a final concentration of 1.1 mol L^{-1} HCl and analysed at the same time as the DGT eluents. The As concentrations determined from these samples were used to predict the mass of As adsorbed onto the iron-

oxide adsorbent for the DGT experiments. In addition, an As^{III} analysis was carried out on the deployment solution at the end of the experiment to confirm that reduction of As^{V} (for As^{V} experiments) or oxidation of As^{III} (for As^{III} experiments) had not occurred. For all experiments, there was no evidence of either As^{III} oxidation or As^{V} reduction. A 100 % elution efficiency was assumed for all DGT calculations.

All DGT experiments were carried out in a solution volume of 4 L. The volume of solution was sufficiently large to avoid significant depletion of As by the DGT devices. Using this volume, the amount of As removed from solution was < 3 %.

The DGT devices were assembled and deployed as described in chapter 2. The membrane filters used for this work were 0.025 μm cellulose nitrate membrane filters (Schleicher & Schuell). The membrane filters were firstly soaked in Milli-Q water for 24 h and cleaned in 5 % v/v HNO_3 for 24 h; they were then rinsed with Milli-Q water and stored in 0.01 mol L^{-1} $NaNO_3$.

The pH of the As deployment solutions was measured at the start and end of each experiment. The temperature of the solution was measured immediately prior to deployment of DGT devices, after DGT devices were removed, and approximately halfway through the experiment. It is the average of these temperature and pH measurements that is reported in the results section.

5.2.1 Capacity of iron-oxide adsorbent

The capacity of the iron-oxide gel adsorbent was determined by deploying DGT devices in an As^{V} solution for various times until maximum adsorption had occurred. The As^{V} deployment solution was prepared by diluting 40 mL of 1 mol L^{-1} $NaNO_3$, 100 mL of 1 mol L^{-1} sodium acetate (pH 5.0), and 85 mL of 1000 ppm As^{V}, to 4 L. The final concentrations of $NaNO_3$, sodium acetate, and As^{V} in the deployment solution, were 0.01 mol L^{-1}, 0.025 mol L^{-1}, and ~ 21.5 ppm, respectively. A small volume of 1 mol L^{-1} NaOH was added to adjust the pH to ~ 5.0. The solution was left to stand for ~ 1 h before DGT devices were deployed. Eighteen DGT devices were deployed in the well-stirred solution (stirring rate was 620 rpm; unless stated otherwise this stirring rate was used for all experiments in this chapter) and removed at various stages during the experiment to give deployment times from ~ 0.5 to 40 h. The exact

deployment times were recorded. Duplicate DGT devices were deployed and retrieved to give total deployment times of ~ 1, 2.5, 6, 10, and 16 h. Triplicate DGT devices were deployed to give a total deployment time of 40 h. For all other times, single DGT devices were deployed and retrieved. For this work, a 100 % elution efficiency was assumed even though the mass of As accumulated on the iron-oxide adsorbent was larger than the mass loadings used for the elution efficiency experiment (section 4.2.1).

The Fe content of the iron-oxide adsorbent gel was also determined. This was carried out by eluting 10 iron-oxide gel disks using the standard elution procedure. The concentration of Fe in the eluent was determined using electrothermal atomic absorption spectroscopy (ETAAS). The ETAAS parameters for Fe measurements are described in section 2.4.1. A 1000 ppm Fe^{III} atomic absorption (AA) standard was used to prepare standard solutions.

5.2.2 Adsorption of total As at various $[As^V]/[As^{III}]$ ratios

To examine if As^V or As^{III} affected the adsorption of the other species, DGT devices were deployed in solutions containing various $[As^V]/[As^{III}]$ ratios. The mass of As^V and As^{III} accumulated within DGT devices was compared to the predicted mass using the As^V and As^{III} diffusion coefficients measured in chapter 4. The As deployment solutions were prepared by diluting 40 mL of 1 mol L^{-1} $NaNO_3$, 100 mL of 1 mol L^{-1} sodium acetate (pH 5.0), and appropriate volumes of 10 ppm As^V and 10 ppm As^{III}, to 4 L. The final concentrations of $NaNO_3$, sodium acetate, and total As in the deployment solutions were 0.01 mol L^{-1}, 0.025 mol L^{-1}, and ~ 60 ppb. A small volume of 1 mol L^{-1} NaOH was added to adjust the pH to ~ 5.0. The solutions were left to stand for ~1 h before DGT devices were deployed in the well-stirred solutions and removed after ~ 30 h. The exact deployment times were recorded.

Table 5.1 below shows the various $[As^V]/[As^{III}]$ ratios used for these experiments along with the total As concentrations, solution pH, deployment times, and temperature for each experiment. For these experiments, the concentrations of As^{III} and total As were determined at the start and end of the experiment. The concentration of As^V was determined by the difference between the two measurements. The measured As^V to As^{III} ratio, and the total concentration of As in samples removed at the start of the experiment (and stabilized using concentrated HCl) were used to calculate the predicted total mass of As accumulated by DGT.

Experiment	Total [As]	% As^V	% As^{III}	Time[a]	Temperature[b]	Devices[c]	pH
1	61 ± 2 ppb	83	17	32.6 h	24.0 ± 0.5 °C	6	4.9
2	66 ± 3 ppb	50	50	32.5 h	24.0 ± 0.5 °C	4	5.1
3	50 ± 2 ppb	17	83	31.9 h	24.0 ± 0.5 °C	5	5.0
4	65 ± 5 ppb	67	33	31.4 h	24.0 ± 0.5 °C	6	5.1
5	63 ± 5 ppb	33	67	31.9 h	24.0 ± 0.5 °C	6	5.0

Table 5.1 $[As^V]/[As^{III}]$ ratios and experimental conditions and parameters used. The uncertainty associated with the concentration of As is the standard deviation of the mean from at least duplicate HG-AAS measurements.

[a]Deployment time of DGT devices

[b]Average temperature of deployment solution

[c]Number of DGT devices deployed

5.2.3 Effect of pH on mass of As^V and As^{III} accumulated by DGT

The effect of pH on the mass of As accumulated by DGT was examined by measuring the mass of As^V or As^{III} (depending on the experiment) accumulated within DGT devices at pH ~ 3 and ~ 7. The mass of As accumulated within DGT devices was compared to the predicted mass of As using the As^V or As^{III} diffusion coefficients measured at pH 5 (chapter 4). The As deployment solutions were prepared by diluting 40 mL of 1 mol L^{-1} $NaNO_3$, 100 mL of 1 mol L^{-1} sodium acetate (pH 5.0) and 24 mL of either 10 ppm As^V or 10 ppm As^{III} (depending on the experiment), to 4 L. The final concentrations of $NaNO_3$, sodium acetate, and As in the deployment solutions were 0.01 mol L^{-1}, 0.025 mol L^{-1} and ~ 60 ppb, respectively. Concentrated HNO_3 was added to adjust the pH of the deployment solution to ~ 3; 1 mol L^{-1} NaOH was added to adjust the pH to ~ 7.0, depending on the experiment that was carried out. The deployment solutions were left to stand for ~ 1 h before DGT devices were deployed in the well-stirred solutions for > 22 h. The exact deployment times were recorded.

5.2.4 Effect of anions and cations on mass of As^V and As^{III} accumulated by DGT

The effect that major anions and cations have on the mass of As^V and As^{III} accumulated by DGT was examined by deploying DGT devices in a simulated natural water and measuring the mass of As accumulated. This was carried out separately for solutions containing As^V or As^{III}. The accumulated mass of As was compared to the predicted mass of As using the As^V and As^{III} diffusion coefficients measured in chapter 4. The deployment solutions were

prepared by diluting 40 mL of 1 mol L^{-1} $NaNO_3$, 100 mL of 1 mol L^{-1} sodium acetate (pH 5.0), 10 mL of 0.4 mol L^{-1} NaCl, 2 mL of 0.4 mol L^{-1} KNO_3, 15 mL of 0.4 mol L^{-1} $Ca(NO_3)_2$, 5.8 mL of 0.4 mol L^{-1} $MgSO_4$, 4.2 mL of 0.004 mol L^{-1} KH_2PO_4, 200 mL of 0.0166 mol L^{-1} Na_2SiO_3, and 24 mL of either 10 ppm As^V or 10 ppm As^{III} (depending on the experiment), to 4 L. A small volume of 1 mol L^{-1} NaOH was added to adjust the pH to ~ 5.0. The solutions were left for ~ 1 h before DGT devices were deployed in the well-stirred solutions for > 23 h. The exact deployment times were recorded.

Table 5.2 shows the approximate concentrations of anions, cations, and As present in the deployment solutions. The typical concentrations of anions and cations present in a river water were obtained from Langmuir,[47] Morel and Hering[36] and Smith *et al.*[48] These concentrations were scaled by a factor of 4 to give a more realistic ratio of anions and cations to the concentration of As used in these experiments.

Anion or cation	Concentration
Cl^-	35 ppm
K^+	7.8 ppm
Ca^{2+}	60 ppm
Mg^{2+}	14 ppm
SO_4^{2-}	56 ppm
Si^{4+}	23 ppm
PO_4^{3-}	400 ppb
As	60 ppb

Table 5.2 Concentrations of anions and cations present in the As^V and As^{III} deployment solutions

5.2.5 Effect of fulvic acid on mass of As^V and As^{III} accumulated by DGT

The effect of fulvic acid on the mass of As^V and As^{III} accumulated by DGT was examined. This experiment examined the competitive effects of fulvic acid on the iron oxide adsorbent by measuring the mass of As accumulated within DGT devices from an As^V or As^{III} solution containing 5 ppm fulvic acid. The accumulated mass was compared to the predicted mass using the diffusion coefficients measured in chapter 4. The experiment was carried out separately for solutions containing As^V or As^{III}. The DGT deployment solutions were prepared by diluting 40 mL of 1 mol L^{-1} $NaNO_3$, 100 mL of 1 mol L^{-1} sodium acetate (pH

5.0), 80 mL of 250 ppm fulvic acid, and 24 mL of either 10 ppm As^{V} or 10 ppm As^{III} (depending on the experiment), to 4 L. The final concentrations of $NaNO_3$, sodium acetate, fulvic acid, and As were 0.01 mol L^{-1}, 0.025 mol L^{-1}, 5 ppm, and ~ 60 ppb, respectively. A small volume of 1 mol L^{-1} NaOH was added to adjust the pH to ~ 5.0. The solution was equilibrated for 24 h before DGT devices were deployed in the well-stirred solutions for > 23 h. The exact deployment times were recorded.

The fulvic acid (FAG1) employed for this work was isolated from the B_h horizon of a gley podsol soil by Gregor *et al*.[49] using the acid pyrophosphate/XAD-7 method. It contained 0.01 % Fe and 0.03 % Al by mass.[49] A fulvic acid containing low amounts of Fe and Al is critical as it is possible that Fe or Al bound to fulvic acid may bind As, hence lowering the diffusion coefficient of this As fraction; this would reduce the amount of As accumulated by DGT. For the As^{V} and As^{III} deployment solutions prepared above, the concentration of Fe measured by ETAAS (using the conditions and parameters described in section 2.4.1) was 1.8 x 10^{-8} mol L^{-1}. A 60 ppb As solution corresponds to 8 x 10^{-7} mol L^{-1}, therefore if there is any complexation of As by fulvic acid, and assuming a 1:1 stoichiometry,[40] then only ~ 2.2 % of the As would be complexed, having an insignificant effect on the mass of As accumulated.

5.2.6 Combined effect of fulvic acid and Fe^{III} on the mass of As^{V} accumulated by DGT

The effect that soluble Fe-fulvic acid complexes have on the mass of As^{V} accumulated by DGT was examined by deploying DGT devices in As^{V} solutions containing 5 ppm fulvic acid and various concentrations of Fe^{III}. The accumulated mass was compared to the predicted mass using the As^{V} diffusion coefficients measured in chapter 4. The DGT deployment solutions were prepared by diluting 40 mL of $NaNO_3$, 100 mL of sodium acetate (pH 5.0), 80 mL of 250 ppm fulvic acid (FAG1), various volumes of 1000 ppm $Fe(NO_3)_3$ AA standard (to give final Fe^{III} concentrations of 2.78, 0.38, and 0.24 μmol L^{-1}), and 24 mL of 10 ppm As^{V}, to 4 L. The Fe concentrations were determined by ETAAS using the conditions and parameters described in section 2.4.1. The final concentrations of $NaNO_3$, sodium acetate, fulvic acid, and As^{V} were 0.01 mol L^{-1}, 0.025 mol L^{-1}, 5 ppm and ~ 60 ppb, respectively. A small volume of 1 mol L^{-1} NaOH was added to adjust the pH to ~ 5.0. The solution was equilibrated for 24 h before DGT devices were deployed in the well-stirred solutions for > 22 h. The exact deployment times were recorded.

The metal complexation capacity of the fulvic acid used in this work was unknown and was not determined. The Al^{3+} complexation capacities of similar fulvic acids have been measured in this laboratory;[45] they range from 0.6 to 0.9 mmol Al^{3+} g^{-1} fulvic acid. Therefore a Fe^{III} complexation capacity of 0.6 mmol Fe^{3+} g^{-1} fulvic acid was assumed for calculations involved in this work. For all these experiments, the concentrations of Fe^{III} were lower than the estimated Fe^{III} complexation capacity of the fulvic acid. This was to ensure the formation of colloidal iron would be limited.

It was assumed that under the conditions used for these experiments, Fe^{III}-fulvic acid complexes were formed.

5.2.7 Effect of colloidal Fe in the presence and absence of fulvic acid on mass of As^V accumulated by DGT

The effect that colloidal Fe, in the presence and absence of fulvic acid, has on the mass of As^V accumulated by DGT was examined by deploying DGT devices in As^V solutions containing various concentrations of Fe^{III} and fulvic acid. The concentration of As^V in solution determined by DGT was compared with the concentration determined directly using HG-AAS. For the HG-AAS measurements, samples were filtered through a 0.025 μm membrane prior to analysis to remove colloidal iron.

For experiments that examined the effect of colloidal Fe in the absence of fulvic acid, the DGT deployment solution was prepared in the following way: appropriate volumes of 1000 ppm $Fe(NO_3)_3$ AA standard were added to ~ 3700 mL of Milli-Q water. This solution was stirred vigorously and titrated with 0.25 mol L^{-1} NaOH until a pH between 7.2 and 7.4 was obtained; NaOH was added slowly to ensure that the pH did not rise above 8. This solution was left for ~ 1 h before addition of 40 mL of 1 mol L^{-1} $NaNO_3$ and 100 mL of 1 mol L^{-1} sodium acetate (pH 5.0). This solution was left for a further 48 h before 24 mL of 10 ppm As^V was added. A small volume of 1 mol L^{-1} NaOH was added to adjust the pH to ~ 5.0. The final volume was 4 L. This solution was left for a further 24 h to equilibrate before DGT devices were deployed in the well-stirred solution for > 29 h. The exact deployment times were recorded. The stirring rate used was 700 rpm; this is a faster rate than that used for other experiments due to the need to suspend the iron colloids in solution. The concentrations of As^V and Fe^{III} used in these experiments are summarized in Table 5.3.

For experiments that examined the effect of colloidal Fe in the presence of fulvic acid, the DGT deployment solution was prepared as above except that after addition of $NaNO_3$ and sodium acetate, the solution was left for 24 h before appropriate volumes of fulvic acid were added and left for a further 24 h. After this time, 24 mL of 10 ppm As^V was added and the pH adjusted to ~ 5 using 1 mol L^{-1} NaOH. The final volume was 4 L. This solution was left for a further 24 to 48 h to equilibrate before DGT devices were deployed in the well-stirred solution > 27 h. The exact deployment times were recorded. The stirring rate was 700 rpm. The concentrations of As^V, Fe^{III} and fulvic acid used in these experiments are summarised in Table 5.3.

Experiment	[Fe^{III}]/ppm	[Fulvic acid]/ppm
1	2.5	0
2	1	0
3	5	5
4	2	5
5	2	1

Table 5.3 Table showing various Fe^{III} and fulvic acid concentrations used for the experiments in this section.

For experiments 2, 4, and 5, 40 mL of the As deployment solution was filtered through a filter membrane at the start of the experiment. The mass of As on the filter membrane was measured after eluting the filter membrane with concentrated HCl. The same elution procedure as that used for the iron-oxide adsorbent was used to elute As from the filter membrane. This was carried out to examine if the concentration of dissolved As in solution and the mass of As adsorbed to iron-oxide in solution agreed with the total amount of As added.

5.3 Results

5.3.1 Capacity of iron-oxide adsorbent

The capacity of the iron-oxide adsorbent was determined by deploying DGT devices in an As^V solution for various times until maximum adsorption had occurred. The As^V iron-oxide capacity plot is illustrated in Figure 5.5. The total capacity of the iron-oxide gel adsorbent was ~ 100,000 ng of As. However, the linear capacity (i.e. capacity in which As is adsorbed to the adsorbent linearly and therefore behaves according to the DGT theory) of the iron-oxide gel adsorbent was ~ 30,000 ng.

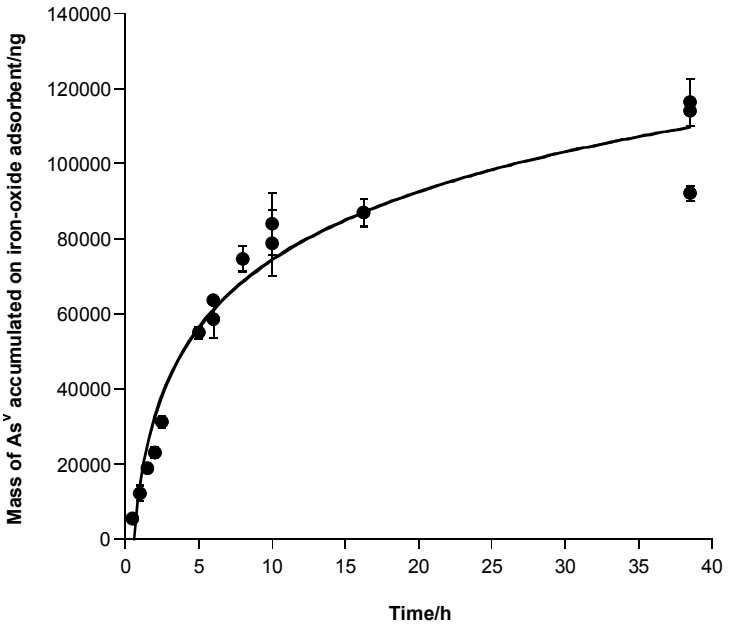

Figure 5.5 Mass of As^V accumulated on the iron-oxide adsorbent within DGT devices *vs*. time. The uncertainty associated with each datum point is the standard deviation of the mean for at least duplicate HG-AAS measurements. The concentration of As^V, $NaNO_3$, and sodium acetate were 21.5 ppm, 0.01 mol L^{-1}, and 0.025 mol L^{-1}, respectively. The average temperature during the experiment was 23.0 ± 0.5 ^oC. The pH was 5.0.

If the data up to 2.5 h (i.e. ~ 30,000 ng of As accumulated, Figure 5.6 (a)) are used to determine the As^V diffusion coefficient, a value of (4.65 ± 0.50) x 10^{-6} cm^2 s^{-1} (pH 5.0, 23 ± 0.5 ^oC) is obtained when using the following parameters: slope = 12610 ng h^{-1}; Δg = 0.09 cm; C = 21500 ppb and A = 3.14 cm^2. This value agrees within experimental uncertainty with the previously determined average As^V diffusion coefficient of (4.90 ± 0.05) x 10^{-6} cm^2 s^{-1} (pH

5.0, 24.5 ± 0.5 ^{o}C) (section 4.3.3.1). If the datum point at 5 h (i.e. ~ 55,000 ng of As accumulated, Figure 5.6 (b)) is included to calculate the slope, then the effective As^{V} diffusion coefficient decreases to (4.10 ± 0.40) x 10^{-6} cm^2 s^{-1} when using the same parameters as above, but with slope = 11049 ng h^{-1}. In addition, a positive y-intercept for the latter plot is obtained. A negative intercept is expected due to the time required to establish a linear concentration gradient through the diffusive gel. Lastly, if the data up to 8 h (~ 75,000 ng of As accumulated, Figure 5.6 (c)) is used to calculate the slope, then an effective As^{V} diffusion coefficient of (3.45 ± 0.40) x 10^{-6} cm^2 s^{-1} is obtained when using the same parameters as above but with slope = 9355 ng h^{-1}. Furthermore, the y-intercept becomes more positive. These later calculations confirm that the assumptions in DGT theory are valid only for accumulation masses ≤ 30, 000 ng.

The uncertainties associated with the diffusion coefficients calculated above are a combination of the uncertainty of the slope of the DGT plot (i.e. standard deviation of slope), the thickness of the diffusive gel, and the initial concentration of As^{V} present in the deployment solution.

The average amount of Fe per gel disk was 0.45 ± 0.05 mg. The uncertainty associated with this value is the standard deviation of the mean from 10 iron-oxide gel disks.

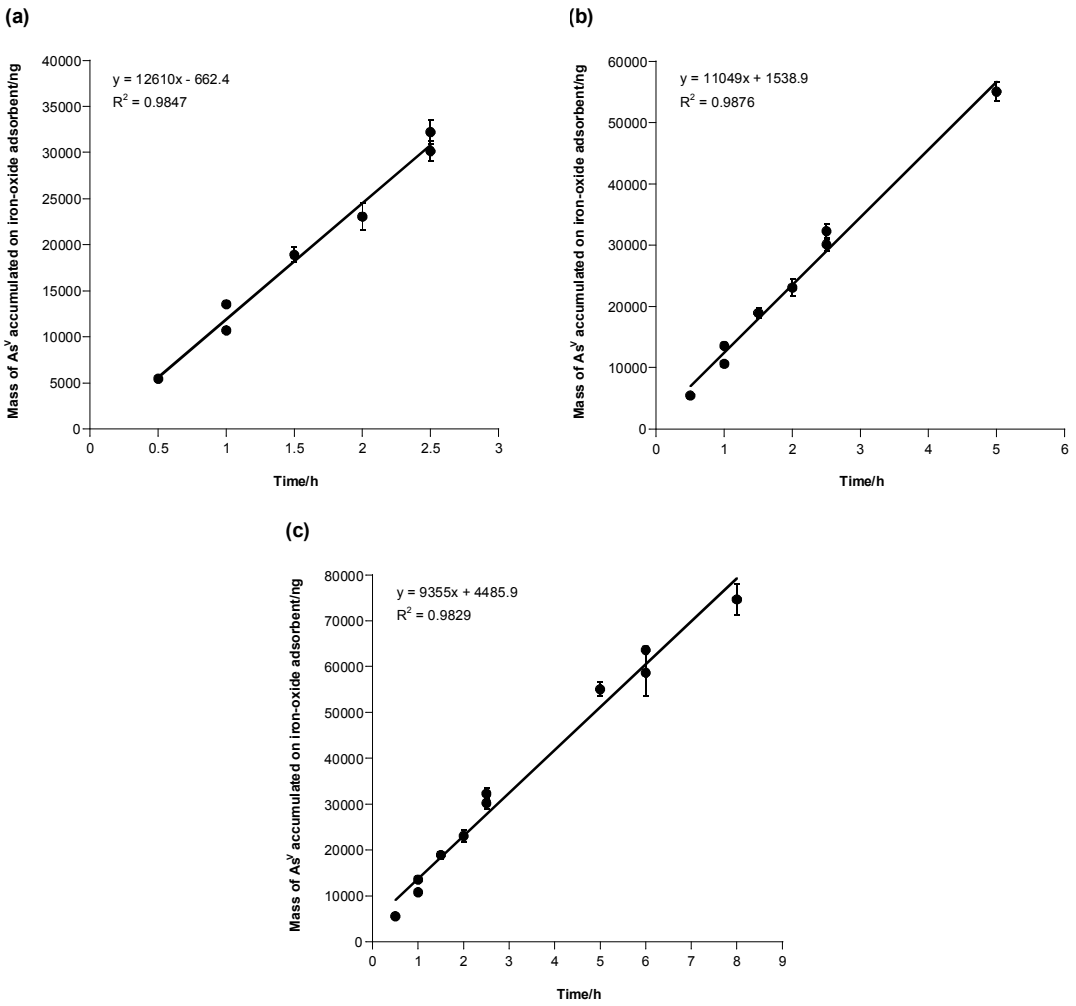

Figure 5.6 Mass of As^V accumulated on the iron-oxide adsorbent within the DGT devices at various times for data up to (a) 2.5 h, (b) 5 h, and (c) 8 h. These plots are enlargements of certain sections of Figure 5.1.

5.3.2 Adsorption of total As at various $[As^V]/[As^{III}]$ ratios

Arsenic solutions with various $[As^V]/[As^{III}]$ ratios were used to establish if As^V or As^{III} affected the adsorption of the other species at the iron-oxide adsorbent. The measured mass of total As accumulated within DGT devices was compared to the predicted mass of As and is illustrated in Table 5.4 and Figure 5.7. The predicted mass of As was calculated by using the As^{III} and As^V diffusion coefficients that were determined in chapter 4, and using the DGT equation.

Experiment	Total [As]	% As^V	Accumulated Mass	Predicted mass	A-Mass/P-Mass[a]
1	61 ± 2 ppb	83	1430 ± 40 ng (n = 6)	1265 ± 75 ng	1.13 ± 0.10
2	66 ± 3 ppb	50	1525 ± 60 ng (n = 4)	1460 ± 105 ng	1.04 ± 0.10
3	50 ± 2 ppb	17	1115 ± 80 ng (n=5)	1155 ± 85 ng	0.97 ± 0.10
4	65 ± 25ppb	67	1185 ± 65 ng (n=6)	1345 ± 130 ng	0.88 ± 0.15
5	63 ± 5 ppb	33	1340 ± 40 ng (n=6)	1415 ± 115 ng	0.95± 0.10

Table 5.4 Comparison of accumulated mass of As with predicted mass of As for solutions containing various concentrations of As^V and As^{III}. The uncertainty associated with the predicted mass is a combination of the uncertainty of the thickness of the diffusive gel, the initial concentration of total As present in solution and the As^V and As^{III} diffusion coefficients. The uncertainty associated with the accumulated mass is the standard deviation of the mean of replicate DGT deployments. Note than 'n' denotes the number of DGT devices deployed. Experimental conditions are given in the caption for Table 5.1.

[a]accumulated mass/predicted mass

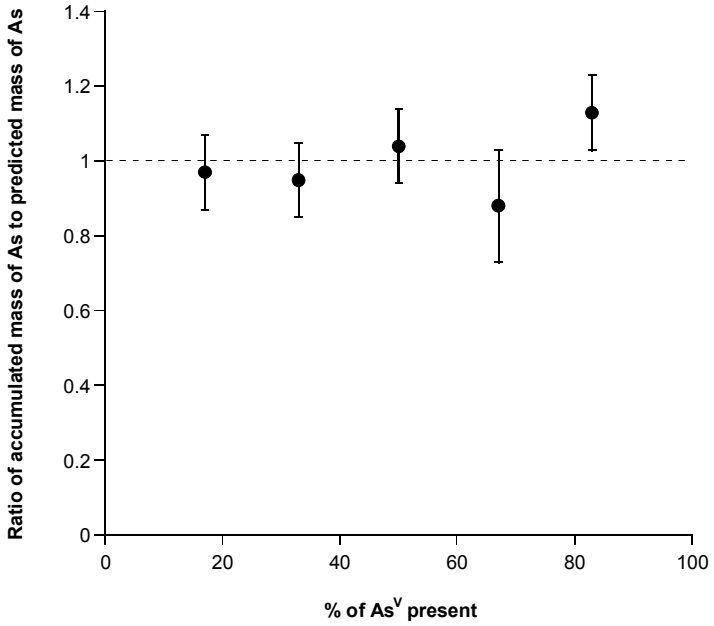

Figure 5.7 Ratio of accumulated mass of As to predicted mass of As for solutions containing various $[As^V]/[As^{III}]$ ratios, expressed as % of As^V present. The dotted line indicates a ratio of 1 (i.e. the accumulated mass and predicted mass of As are the same). The uncertainty associated with each datum point is a combination of the uncertainty associated with the accumulated and predicted masses of As.

Reasonable agreement between the total mass of As accumulated within the DGT devices and the predicted mass of As, was obtained for all experiments. For only one experiment the predicted and accumulated masses did not agree within experimental uncertainty. The relative standard deviations of replicate DGT deployments were generally < 5 %.

5.3.3 Effect of pH on mass of As^{V} and As^{III} accumulated by DGT

The effect of pH on the mass of As accumulated by DGT was examined by measuring the mass of As^{V} and As^{III} accumulated within DGT devices at pH ~ 3 and ~ 7. The mass accumulated was compared to the predicted mass (assuming pH 5 diffusion coefficients); the results are presented in Table 5.5 and Figure 5.8.

Experiment	Arsenic species	pH	Accumulated Mass	Predicted mass	A-Mass/P-Mass[a]
1[b]	As^{III}	3.0	1000 ± 90 ng (n = 5)	1070 ± 70 ng	0.93 ± 0.15
2[c]	As^{III}	7.1	1385 ± 90 ng (n = 4)	1320 ± 140 ng	1.05 ± 0.15
3[e]	As^{V}	3.0	1130 ± 85 ng (n = 6)	1035 ± 60 ng	1.09 ± 0.15
4[e]	As^{V}	6.9	960 ± 65 ng (n = 6)	905 ± 50 ng	1.06 ± 0.10

Table 5.5 Comparison of accumulated mass of As with predicted mass of As at pH 3 and 7 for As^{III} and As^{V}. The uncertainty associated with the predicted mass is a combination of the uncertainties of the thickness of the diffusive gel, the initial concentration of As present in solution, and the As diffusion coefficients. The uncertainty associated with the accumulated mass is the standard deviation of the mean of replicate DGT deployments. Note that 'n' denotes the number of DGT devices deployed.

[a]accumulated mass/predicted mass

[b][As] = 60 ± 3 ppb, time = 23.9 h, temperature = 25.5 ± 1 ºC

[c][As] = 65 ± 5 ppb, time = 27.0 h, temperature = 25.0 ± 1 ºC

[d][As] = 61 ± 2 ppb, time = 27.6 h, temperature = 25.0 ± 1 ºC

[e][As] = 59 ± 2 ppb, time = 25.1 h, temperature = 24.0 ± 1 ºC

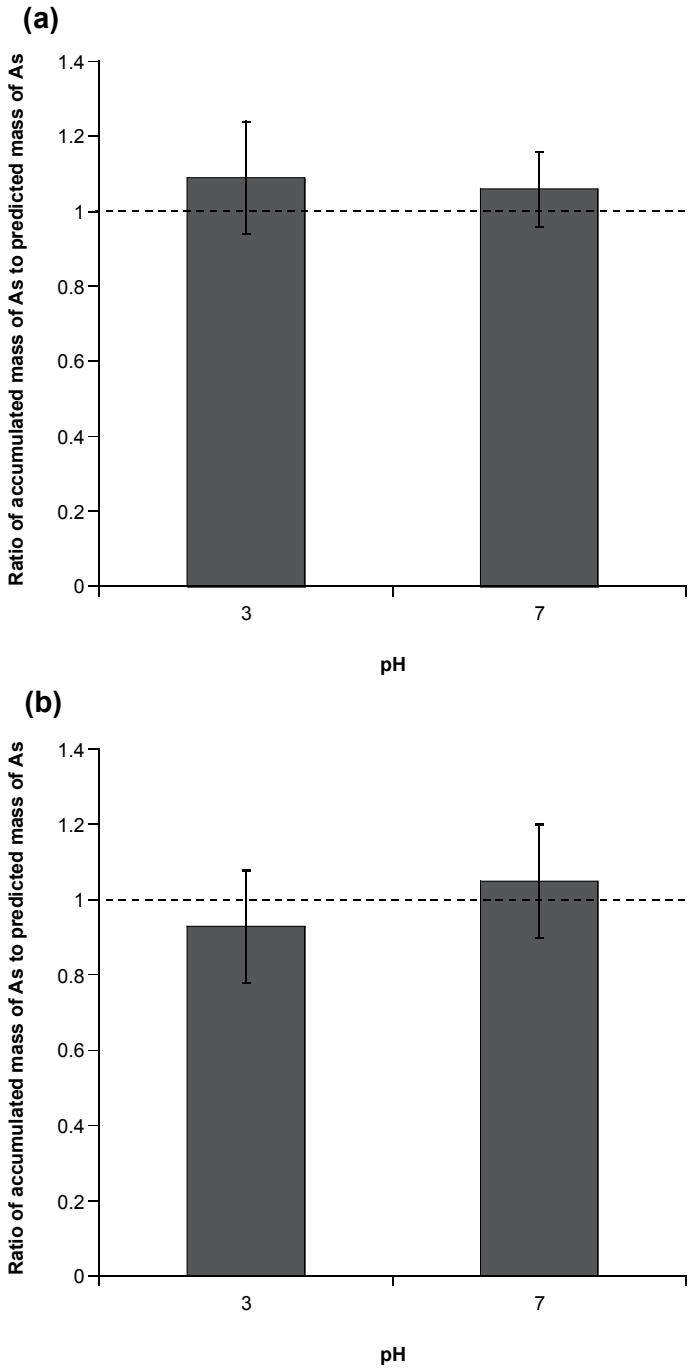

Figure 5.8 Ratio of accumulated mass of As to predicted mass of As at pH 3 and 7 for (a) As^{V}, and (b) As^{III}. The dotted line represents a ratio of 1. The uncertainty associated with the data is a combination of the uncertainty associated with the accumulated and predicted masses of As. Experimental conditions are given in the caption for Table 5.5.

For all experiments, the mass of As accumulated within the DGT devices agrees within experimental uncertainty with the mass of As predicted. The relative standard deviations of replicate DGT deployments were < 10 %.

5.3.4 Effect of anions and cations on mass of As^V and As^{III} accumulated by DGT

The effect that anions and cations have on the mass of As^V and As^{III} accumulated by DGT was examined by deploying DGT devices in As^V and As^{III} solutions containing anions and cations that simulated a freshwater. For As^V, the measured mass of As accumulated by DGT was 1320 ± 60 ng (n = 5, pH 5.0, 24.0 ± 1.0 ^oC, t = 30.5 h, [As^V] = 69 ± 2 ppb). The predicted mass of As^V was 1290 ± 65 ng. For As^{III}, the measured mass accumulated within DGT devices was 1015 ± 95 ng (n = 5, pH 5.0, 24.5 ± 1.0 ^oC, t = 23.5 h, [As^{III}] = 60 ± 2 ppb). The predicted mass of As^{III} was 1050 ± 80 ng. The uncertainty associated with the predicted mass and accumulated mass are the same as described as in section 5.3.2. These results are also illustrated in Figure 5.9 as the ratio of accumulated mass of As to predicted mass of As.

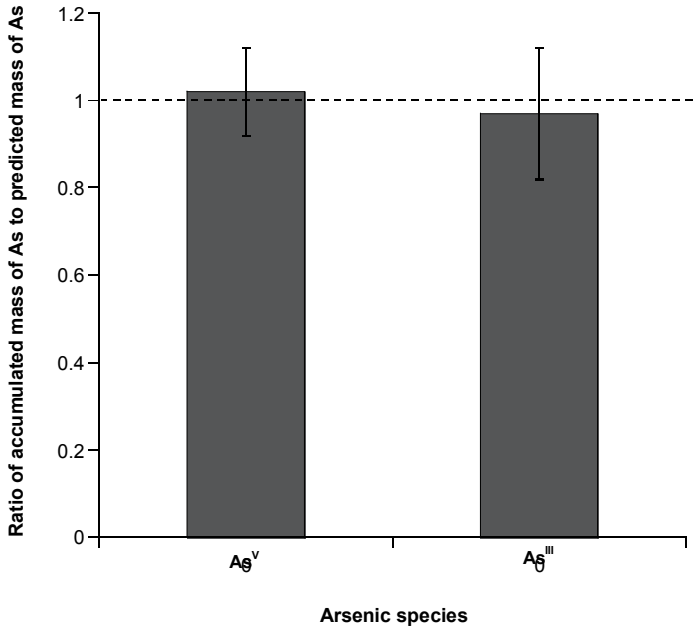

Figure 5.9 Ratio of accumulated mass of As to predicted mass of As for As^V and As^{III} in the presence of anions and cations. The dotted line represents a ratio of 1. The uncertainty associated with the data is a combination of the uncertainty associated with the accumulated and predicted masses. Experimental conditions are given in the text above.

For both the As^V and As^{III} experiments, the mass of As accumulated by DGT agrees within experimental uncertainty with the mass of As predicted. The relative standard deviations for replicate DGT deployments for the As^V and As^{III} experiments were < 5 % and <10 %, respectively.

5.3.5 Effect of fulvic acid on mass of As^V and As^{III} accumulated by DGT

The effect of fulvic acid on the mass of As^V and As^{III} accumulated by DGT was examined by deploying DGT devices in As^V and As^{III} solutions containing 5 ppm fulvic acid; the accumulated mass of As was compared with the predicted mass of As. For As^V, the measured mass accumulated within DGT devices was 1250 ± 70 ng (n = 5, pH 5.0, 24.5 ± 0.5 ^oC, [As^V] = 65 ± 4 ppb, t = 30.6 h). The predicted mass of As^V was 1230 ± 95 ng. For As^{III}, the measured mass accumulated within DGT devices was 1145 ± 100 ng (n = 6, pH 5.0, 24.0 ± 0.5 ^oC, [As^{III}] = 66 ± 3 ppb, t = 23.7 h). The predicted mass of As^{III} was 1170 ± 95 ng. The uncertainty associated with the predicted and accumulated masses have been described in section 5.3.2. These results are also illustrated in Figure 5.10, expressed as the ratio of accumulated mass of As to the predicted mass of As.

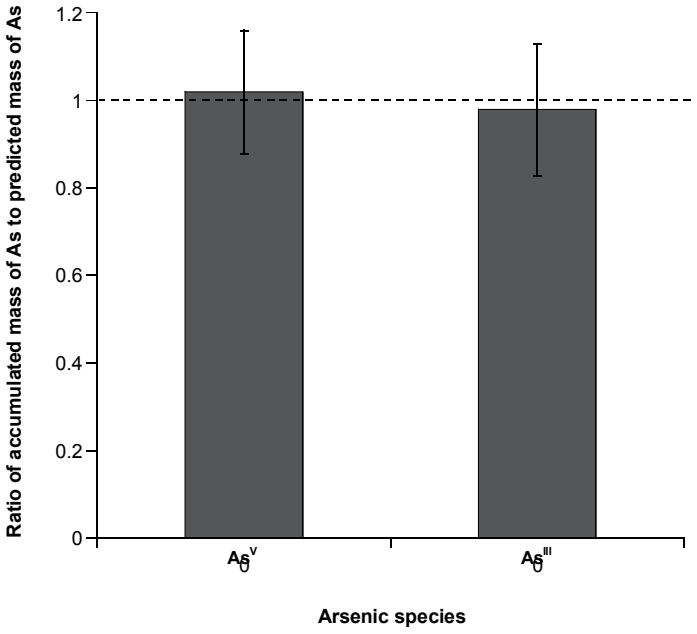

Figure 5.10 Ratio of accumulated mass of As to predicted mass of As for As^V and As^{III} in the presence of 5 ppm fulvic acid. The dotted line represents a ratio of 1. The uncertainty associated with the data is a combination of the uncertainty associated with the accumulated and predicted masses. Experimental conditions are given in the text above.

For both the As^{V} and As^{III} experiments, the mass of As accumulated by DGT agrees within experimental uncertainty with the mass of As predicted. The relative standard deviations for replicate DGT deployments were < 10 %.

5.3.6 Combined effect of fulvic acid and Fe^{III} on the mass of As^{V} accumulated by DGT

The effect that soluble Fe^{III}-fulvic acid complexes have on the mass of As^{V} accumulated by DGT was examined by deploying DGT devices in As^{V} solutions containing 5 ppm fulvic acid and various concentrations of Fe^{III}. The accumulated mass of As was compared to the predicted mass of As. The results are shown in Table 5.6, and are also illustrated in Figure 5.11 as the ratio of accumulated mass of As to the predicted mass of As.

Experiment	$[Fe^{III}]$/µmol L^{-1}	Accumulated mass	Predicted mass
1[a]	2.80	1205 ± 65 ng (n = 5)	1175 ± 75 ng
2[b]	0.38	890 ± 70 ng (n = 6)	885 ± 90 ng
3[c]	0.24	900 ± 95 ng (n = 5)	870 ± 50 ng

Table 5.6 Comparison of accumulated mass of As with predicted mass of As for solutions containing 5 ppm fulvic acid and various Fe^{III} concentrations. The uncertainty associated with the predicted mass is a combination of the uncertainties of the thickness of the diffusive gel, the initial concentration of As present in solution, and the As diffusion coefficients. The uncertainty associated with the accumulated mass is the standard deviation of the mean of replicate DGT deployments. Note that 'n' denotes the number of DGT devices deployed.

[a][As] = 66 ± 3 ppb, time = 29.0 h, temperature = 24.0 ± 0.5 °C, pH 5.1

[b][As] = 64 ± 6 ppb, time = 22.3 h, temperature = 24.0 ± 0.5 °C, pH 5.1

[c][As] = 54 ± 2 ppb, time = 26.1 h, temperature = 24.0 ± 0.5 °C, pH 5.0

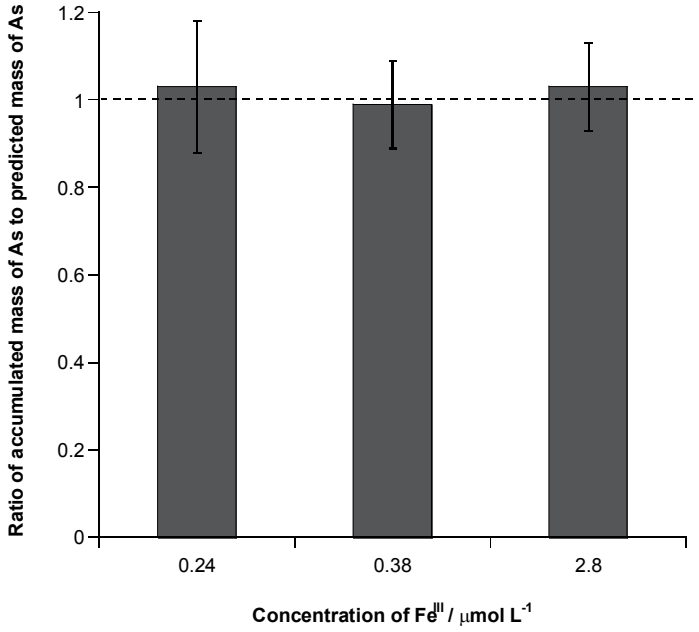

Figure 5.11 Ratio of accumulated mass of As to predicted mass of As for As^V in the presence of 5 ppm fulvic acid and 0.24, 0.38 and 2.8 μmol L^{-1} Fe^{III}. The dotted line represents a ratio of 1. The uncertainty associated with the data is a combination of the uncertainty associated with the accumulated and predicted masses. Experimental conditions are given in the caption for Table 5.6.

For all experiments there was excellent agreement between the mass of As accumulated by DGT and the mass of As predicted assuming insignificant sequestration of As^V by soluble Fe^{III}-fulvic acid complexes. The relative standard deviations for replicate DGT deployments were < 10 % for all experiments.

5.3.7 Effect of colloidal Fe in the presence and absence of fulvic acid on mass of As^V accumulated by DGT

The effect of colloidal Fe (in the presence and absence of fulvic acid) on the distribution of As^V species in solution was examined by deploying DGT devices in As^V solutions containing various concentrations of Fe^{III} and fulvic acid. The concentration of As^V in solution determined by DGT was also compared with the concentration in filtered samples determined directly by HG-AAS at the start ($[As]_{int}$) and end ($[As]_{end}$) of the experiment. The results are illustrated in Table 5.7.

Experiment	$[As^V]$/ppb	[Fe]/ppm	[FA]/ppm	C_{DGT}/ppb	$[As]_{Int}$ (HG-AAS)/ppb	$[As]_{End}$ (HG-AAS)/ppb
1[a]	60	2.5	0	0.7 ± 0.1 (n = 3)	0.8 ± 0.1 ppb	nd[*]
2[b]	60	1	0	8.7 ± 0.7 (n = 6)	8.6 ± 0.8	5.4 ± 0.6
3[c]	60	5	5	7.2 ± 0.9 (n = 6)	9.4 ± 1.3	5.3 ± 0.2
4[d]	60	2	5	38.5 ± 2.5 (n = 5)	33.9 ± 0.2	35.3 ± 0.1
5[e]	60	2	1	14.2 ± 1.9 (n = 6)	13.2 ± 0.7	9.8 ± 0.9

Table 5.7 Effect of Fe^{III} and fulvic acid on the concentration of dissolved As in solution as measured by DGT and HG-AAS. The uncertainty associated with the concentration determined by DGT is a combination of the uncertainties of replicate DGT deployments (standard deviation of the mean), the thickness of the diffusive gel, and the As^V diffusion coefficient. The uncertainty associated with the HG-AAS measurements is the standard deviation of the mean of at least duplicate measurements. Note that 'n' denotes the number of DGT devices deployed.

[a]Time = 29.2 h, temperature = 25.0 ± 1.0 ºC, pH 5.0

[b]Time = 29.8 h, temperature = 25.0 ± 0.5 ºC, pH 5.0

[c] Time = 29.4 h, temperature = 23.0 ± 1.0 ºC, pH 5.0

[d]Time = 27.2 h, temperature = 24.0 ± 1.0 ºC, pH 5.0, after the addition of As^V the solution was equilibrated for 48 h; whereas for all other experiments an equilibration time of 24 h was used.

[e]Time = 28.1 h, temperature = 25.0 ± 1.0 ºC, pH 4.9

[*]Not determined

For all experiments except number 4, the concentration determined by DGT agreed within experimental uncertainty with the concentration of As determined at the start of the experiment using HG-AAS. Interestingly, for only one experiment (number 4) the concentration of As determined by HG-AAS at the start of the experiment agreed with the concentration at the end of the experiment, also measured by HG-AAS. For all experiments the relative standard deviation for replicate DGT deployments was < 10 %.

Table 5.8 shows the mass of As on the filter membrane, after filtering 40 mL of the As DGT deployment solutions, and the mass of As in the filtrate for samples measured at the start of experiments 2,4, and 5. Good agreement between the total mass of As and the mass of As expected in 40 mL of solution was obtained which implies that all of the As is accounted for during these experiments and no significant adsorption is occurring on the glass surface of the filtering apparatus.

Experiment	Mass of As in 40 mL of filtrate[a]	Mass of As on filter membrane	Total mass of As	Ratio of total mass of As to As_{int} mass[b]
2	345 ± 30 ng	2020 ± 110 ng	2365 ± 335 ng	0.99 ± 0.20
4	1355 ± 10 ng	1090 ± 40 ng	2445 ± 104 ng	1.02 ± 0.10
5	530 ± 30 ng	2000 ± 170 ng	2530 ± 360 ng	1.05 ± 0.20

Table 5.8 Mass of As in filtrate and on the filter membrane after filtering 40 mL of As deployment solution through a 0.025 μm filter membrane. The uncertainty associated with the mass of As in the filtrate and on the membrane are the standard deviation of the mean from duplicate samples.

[a] This was calculated using the $[As]_{int}$ value from Table 5.7

[b] As_{int} mass is the mass of As in 40 ml of solution as determined by the concentration of As initially in solution. This was estimated to be 2400 ± 120 ng.

5.4 Discussion

5.4.1 Capacity of iron-oxide adsorbent

The capacity of the iron-oxide adsorbent was determined by deploying DGT devices in an As^V solution for various times until maximum adsorption had occurred. The linear capacity of the iron-oxide adsorbent used in this DGT method was determined to be ~ 30,000 ng of As. The good linearity between mass of As accumulated and time (for mass up to 30,000 ng) and the good agreement between the As^V diffusion coefficient calculated for mass of As ≤ 30,000 ng ((4.65 ± 0.50) x 10^{-6} cm^2 s^{-1}) with the previously determined As^V diffusion coefficient ((4.90 ± 0.05) x 10^{-6} cm^2 s^{-1}), indicates that the DGT equation can be applied when total As on the adsorbent is ≤ 30,000 ng. The decrease in the calculated effective As^V diffusion coefficient as the mass of As on the adsorbent increased above > 30,000 ng of As indicates that the DGT equation does not hold in this region. The decrease in the slope of the plot of mass of As accumulated *vs*. time indicates that the rate of As adsorption decreases at As loadings above 30,000 ng. Reduction in the rate of analyte adsorbed with increasing mass loadings has been observed by other workers for phosphate adsorption on ferrihydrite.[5, 8]

Kinetics of adsorption are controlled by the availability and accessibility of surface sites, the relative charges of the surface and adsorbing species, and the rate of complexation of the dissolved species with surface sites.[12] The reason for the reduction in the rate of As adsorption at higher masses of As in this work is likely due to a reduction in the surface iron-oxide sites that are available to react with As. Consequently, As may need to diffuse further

into the gel adsorbent to react with non-surface iron-oxide sites. This has the effect of increasing the length of the diffusion path and decreasing the steepness of the concentration gradient through the diffusive gel. Hence, the mass of As diffusing to the adsorbent would decrease. In addition, the surface charge of the iron-oxide may have an effect on As^V adsorption. Jain *et al*.[21] have reported that adsorption of As^V on ferrihydrite resulted in a reduction in surface charge (i.e. the surface becomes more negative). Electrostatic interactions between the negatively charged As^V species and increasingly negative iron-oxide surface, may result in the reduction of As^V adsorption with increasing mass of As^V adsorbed to the iron-oxide. Electrostatic interactions are one of the reasons suggested for lower amounts of As^V adsorption on iron-oxides at high pH compared to low pH.[11, 22]

Using the linear capacity of ~ 30,000 ng of As, the maximum deployment time for these DGT devices in a water can be calculated. For a 0.8 mm thick diffusive gel, DGT could be deployed in a water that contained ~ 10 ppb As^V for 6.5 months before the linear capacity would be exceeded. This estimate is based on the assumption that the performance of the diffusive gel and adsorbent gel is unaffected during long-term DGT deployments and the water is ~ 25 ^oC. In many situations the temperature of a natural water will be lower than this and the As species will diffuse more slowly giving a longer maximum deployment time. If longer deployment times were used (e.g. 12 months) then the solution concentration of As would be underestimated by ~ 12 % (if the diffusion coefficient established in chapter 4 was applied), due to the lower effective diffusion coefficient calculated for adsorbed As masses > 30,000 ng. If required, the deployment time may be increased without exceeding the linear capacity by increasing the thickness of the diffusive gel and/or decreasing the area available for diffusion. Alternatively, the amount of iron-oxide incorporated into the gel could be increased. However, larger amounts of iron-oxide were found to hinder casting procedures and setting of the gel. This affect has also been observed by other workers.[5]

Another contributing factor that can limit the deployment time of DGT is other adsorbing species that are present in natural waters. The capacity for As may be reduced due to competition for the adsorbent by anions, cations, and other adsorbing species; this is likely to be more of an issue for polluted waters. If approximate concentrations of those adsorbing species are known, then by using diffusion coefficients established in the literature, a 'competitive' adsorbent capacity could be estimated. However, the maximum deployment

time is likely to be limited by microbial attack and biofouling by algae and bacteria.[50] Biofoluing of DGT devices has been observed in a number of studies in which DGT has been applied to natural waters in the field.[6, 51-54] It is suggested that biofilms can form within 2 days and be as thick as 0.5 mm.[52] Biofouling causes an extension of the diffusion path;[8, 55] therefore Δg in the DGT equation is actually the thickness of the diffusive gel and biofilm. This means that the concentration measured by DGT would be underestimated if only the thickness of the diffusive gel was used in the DGT calculation. However, the diffusion coefficient of the analyte through the biofilm may be different from that in the diffusive gel, and if an analyte cannot diffuse through the biofilm, then the exposed surface area, A, may also be smaller.[51] Furthermore, biofilms may act as an adsorbent for the analyte.[6] The effects of biofouling are likely to depend on the characteristics of the natural water.

The triplicate deployment of DGT devices at 38.5 h showed poorer reproducibility (RSD ~ 12.5 %) than previously observed. At this time, the mass of As ranged from ~ 90,000 to ~ 115,000 ng. This may indicate that the distribution of iron-oxide throughout a sheet of iron-oxide gel is not uniform. Therefore, when the gel is cut into disks to be assembled in DGT devices, some gel disks may contain more iron-oxide than others, and hence have different capacities. However, as long as the linear capacity is not exceeded this should not be a problem.

Using the average mass of As accumulated at 38.5 h (i.e. 108000 ± 13000 ng) and the average mass of Fe contained within an iron-oxide gel disk (i.e. 0.45 ± 0.05 mg), a value for the moles of As adsorbed per mole of Fe can be calculated. This value was 0.18 ± 0.04 mol_{As} mol_{Fe}^{-1}. This is in reasonable agreement with the As^{V} adsorption maxima reported by Raven *et al*.[11] at pH 4.6 (0.25 mol_{As} mol_{Fe}^{-1}), Dixit and Hering[31] at pH 4.0 (0.24 mol_{As} mol_{Fe}^{-1}) and within the range 0.16 to 0.25 mol_{As} mol_{Fe}^{-1} reported by Wilkie and Hering.[26]

5.4.2 Adsorption of total As at various $[As^{V}]/[As^{III}]$ ratios

Arsenic solutions with various $[As^{V}]/[As^{III}]$ ratios were used to establish if As^{V} or As^{III} affected the adsorption of the other species at the iron-oxide adsorbent. The good agreement between the total mass of As accumulated within DGT devices and the predicted mass, for various $[As^{V}]/[As^{III}]$ ratios, implies that the presence of one As species does not measurably affect adsorption of the other. Therefore, under the conditions used in this study, no

competitive adsorption effect between the As^{V} species, $H_2AsO_4^-$, and As^{III} species, H_3AsO_3, for binding sites on the iron-oxide gel adsorbent, was observed. This is not surprising as the total mass of As on the adsorbent was < 5 % of the linear capacity, and < 1.5 % of the total capacity, of the iron-oxide gel adsorbent.

Goldberg[25] investigated competitive adsorption of As^{V} and As^{III} on a variety of oxides and clay minerals, including ferrihydrite. Goldberg[25] examined the adsorption of As^{III} (1.5 ppm) and As^{V} (1.5 ppm) separately on ferrihydrite (500 ppm) over the pH range 2 to 11; this was compared to adsorption on ferrihydrite when both As^{III} and As^{V} were each present at 1.5 ppm. There was no evidence of any competitive effect in this system; the adsorption-pH profiles were indistinguishable between the single species (As^{V} or As^{III}) and dual-species (As^{V} and As^{III}) experiments.

Jain and Loeppert[22] examined the competitive adsorption of As^{V} and As^{III} on ferrihydrite in the pH range 4 to 9.5 for a variety of total As concentrations. Jain and Loeppert[22] found similar behaviour to that described by Goldberg[25] for the relatively low As concentrations investigated. Using an As^{V} and As^{III} concentration of 75 ppm and ferrihydrite concentration of 2 g L^{-1}, the effect of As^{III} on adsorption of As^{V} was insignificant at pH < 8; above this pH, As^{III} decreased the adsorption of As^{V} presumably due to competition of As^{III} for As^{V} adsorption sites. It is suggested that As^{III} was able to compete and reduce adsorption of As^{V} due to electrostatic repulsion of the negatively charged As^{V} species, $HAsO_4^{2-}$, by the negatively charged surface of ferrihydrite (pH_{pzc} = 8.1). The effect of As^{V} on adsorption of As^{III} was minor. At pH 4 the amount of As^{III} adsorbed in the presence of As^{V} was ~ 97 % of that when As^{V} was absent. The amount of As^{III} adsorbed in the presence of As^{V} increased with pH. The greater adsorption of As^{III} at high pH was partially attributed to the more favourable electrostatic interaction for adsorption of H_3AsO_3 and $H_2AsO_3^-$ *vs*. $HAsO_4^{2-}$ to the negatively charged surface of ferrihydrite at high pH compared with the adsorption of $H_2AsO_4^-$ *vs*. H_3AsO_3 to the positively charged surface at low pH. In general, the results of Jain and Loeppert[22] show that the competitive effect of As^{V} on As^{III} adsorption by ferrihydrite at low As concentrations was more pronounced than the effect of As^{III} on As^{V} adsorption. At higher total concentrations of As, Jain and Loeppert[22] found more severe competition between As^{V} and As^{III} for adsorption sites on ferrihydrite; this may have been

due to capacity effects. The results from Jain and Loeppert[22] and Goldberg[25] agree with the results from the work in this thesis.

5.4.3 Effect of pH on mass of As^V and As^{III} accumulated by DGT

The effect of pH on the mass of As accumulated by DGT was examined by measuring the mass of As^V and As^{III} accumulated separately within DGT devices at pH ~ 3 and ~ 7. The good agreement between the mass of As accumulated within DGT devices and the predicted mass for both As^V and As^{III} at pH ~ 3 and ~ 7, implies that pH has little effect on the mass of As accumulated by DGT. For all experiments the predicted and accumulated mass agreed within experimental uncertainty.

Varying the pH may affect the DGT measurement in more than one way. The pH dictates which species of As^V or As^{III} will be present (Figure 5.2); these species may have different diffusion coefficients and/or different adsorption efficiencies on the iron-oxide adsorbent. In addition, the properties of the iron-oxide adsorbent will also change as the surface gains a more negative charge with increasing pH. Over the pH range examined (3 to 7), As^{III} exists almost exclusively as the H_3AsO_3 species. Therefore the only effect that pH is likely to have would originate from changes in the iron-oxide adsorbent. In contrast, the speciation of As^V varies significantly with pH. At pH 5, As^V exists almost entirely as the $H_2AsO_4^-$ species. At pH 3, As^V exists as ~ 83 % $H_2AsO_4^-$ and ~ 17 % H_3AsO_4. If it is assumed that the uncharged As^V species, H_3AsO_4, has a similar diffusion coefficient to H_3AsO_3 (which is larger than the diffusion coefficient of $H_2AsO_4^-$), then it might be expected that the ratio of accumulated mass of As to predicted mass of As will be > 1 for As^V at pH 3, (when using the diffusion coefficient of $H_2AsO_4^-$, measured at pH 5.0, to calculate the predicted mass). However, a ratio of 1.09 ± 0.15 was obtained, which agrees within experimental uncertainty with a ratio of 1.

At pH 7, As^V exists as 44 % $HAsO_4^{2-}$ and 56 % $H_2AsO_4^-$. If it is assumed that $HAsO_4^{2-}$ has a smaller diffusion coefficient than $H_2AsO_4^-$, due to its larger charge and therefore likely increase in hydration, then at pH 7 it would not be unreasonable if the ratio of the accumulated mass of As to predicted mass of As is < 1; however, a ratio of 1.06 ± 0.10 was obtained which agrees within experimental uncertainty with a ratio of 1. Considering that the diffusion coefficient of HPO_4^{2-} in water (7.34×10^{-6} cm^2 s^{-1})[56] is less than the diffusion

coefficient of $H_2PO_4^-$ in water (8.46 x 10^{-6} cm^2 s^{-1}),[56] then the assumption that the diffusion coefficient of $HAsO_4^{2-}$ would be less than $H_2AsO_4^-$ seems valid.

These results suggest that any change in the diffusion coefficient of As^V or its adsorption to iron-oxide, as a result of changes in pH, is minor, or that the effects are opposite and counter-balance. Similar results have been observed for phosphate adsorption on ferrihydrite.[5] Mason *et al*.[5] examined the effect of pH on phosphate measurements by DGT. The pH was varied from 3 to 8. Over this entire pH range, Mason *et al*.[5] obtained good agreement between the concentration of P in solution determined by DGT and ICP-MS. Similar to As^V, the speciation of P will change with pH. Mason *et al*.[5] used the diffusion coefficient of $H_2PO_4^-$ for interpreting the results over this pH range. At pH 3, P exists as 88 % $H_2PO_4^-$ and 12 % H_3PO_4; at pH 8, P exists as 86 % HPO_4^{2-} and 14 % $H_2PO_4^-$. Even though the diffusion coefficient of HPO_4^{2-} in water is ~ 85 % of the diffusion coefficient of $H_2PO_4^-$,[56] and assuming a similar ratio in the diffusive gel, Mason *et al*.[5] still obtained good agreement in the P concentration measured by DGT and ICP-MS. This is a similar result to that observed in this thesis for As.

The observation that As adsorption is not significantly affected within the pH range 3 to 7 agrees with the work of Goldberg,[25] Jain and Loppert,[22] Dixit and Hering[31] and Raven *et al*.,[11] who studied the effect of pH on adsorption of As^V and As^{III} by ferrihydrite in solution. They found that for As^{III} and As^V concentrations in the ppm range (0.75 to 75 ppm), pH did not significantly affect adsorption of either As^V or As^{III}. Even though the concentrations of As used by these workers are greater than the concentration of As used in the experiments carried out in this thesis, they also used higher concentration of ferrihydrite. At higher As concentrations, Jain and Loeppert,[22] Dixit and Hering[31] and Raven *et al*.[11] found that pH had more of an affect on the adsorption of As^V and As^{III}. The As^V species was affected to a greater extent than As^{III}.

5.4.4 Effect of anions and cations on mass of As^V and As^{III} accumulated by DGT

The effect of anions and cations on the mass of As^V and As^{III} accumulated by DGT was examined by deploying DGT devices in As^V and As^{III} solutions containing competing anions and cations; the accumulated mass of As was compared to the predicted mass of As. The

good agreement between the mass of As accumulated by DGT and the predicted mass, for both As^{V} and As^{III}, indicates that the presence of anions and cations do not have a significant affect on the DGT measurement. This implies that anions and cations, at concentrations typically found in natural waters, have a negligible effect on either diffusion of As^{V} or As^{III}, or the adsorption of As^{V} or As^{III} by the iron-oxide adsorbent, under the conditions used in this study. However, it is important to note that longer deployment times, higher concentrations of ions or a change in pH may have an effect on the DGT measurement with regards to reduced adsorption by the iron-oxide adsorbent within the DGT device.

Many authors have reported the interference to As^{V} and As^{III} adsorption onto iron-oxides by various anions. Jain and Loeppert[22] examined the effect of PO_4^{3-} and SO_4^{2-} on As^{III} and As^{V} adsorption by ferrihydrite. The As species (As^{V} or As^{III}) were added at the same time as the interfering species (SO_4^{2-} or PO_4^{3-}) to a 2 g L^{-1} ferrihydrite suspension and equilibrated for 24 h. The effect of PO_4^{3-} and SO_4^{2-} on As^{III} and As^{V} adsorption was dependent upon pH and the concentration of PO_4^{3-} and SO_4^{2-}.

For all experiments carried out by Jain and Loeppert[22] the concentration of As was 150 ppm and the concentration of the ferrihydrite suspension was 2 g L^{-1}. Phosphate resulted in a significant decrease in As^{V} and As^{III} adsorption over the pH range investigated (3.5 to 10.5). At [As]:[PO_4^{3-}] concentration (ppm) ratios of 1:1, 1:10, and 1:50, the adsorption of As^{V} by ferrihydrite at pH 5 decreased by ~ 5, ~ 40 and ~ 90 %, respectively; for As^{III} the decrease in adsorption was ~ 10, ~ 40, and ~ 65 %, respectively. Dixit and Hering[31] observed similar behaviour with regards to As adsorption on ferrihydrite in the presence of PO_4^{3-}. At pH 4.0, As^{V} adsorption was decreased from > 95 % to ~ 80 % in the presence of PO_4^{3-}; As^{III} adsorption decreased from ~ 75 % to undetectable. The concentration of As was 750 ppb, the concentration of PO_4^{3-} was 9500 ppb and the concentration of ferrihydrite was 0.03 g L^{-1}. They also obtained similar results for adsorption on goethite. The [As]:[PO_4^{3-}] ratio used in the work for this thesis was ~ 1:6, however no significant effect on adsorption of As^{V} or As^{III} was observed. Jain and Loeppert[22] report that the adsorption maximum for As^{V} on ferrihydrite at pH 4.6 is 0.25 mol_{As} mol_{Fe}^{-1}. At [As^{V}]:[PO_4^{3-}] concentration ratios of 1:1, 1:10 and 1:50, the total anion concentrations in the system used by Jain and Loeppert[22] were 0.2, 1.1 and 5.1 mol_{As+P} mol_{Fe}^{-1}; therefore, its is likely that the reason Jain and Loeppert[22] observed a significant decrease in As adsorption in the presence of PO_4^{3-} was due to the

ferrihydrite capacity being exceeded; this may also be a reason for the decrease in adsorption observed by Dixit and Hering.[31]

For the work carried out in this thesis, the amount of PO_4^{3-} adsorbed on the iron-oxide adsorbent within the DGT device can be estimated using the diffusion coefficient of $H_2PO_4^-$ through the diffusive gel (6.05×10^{-6} cm^2 s^{-1}).[8] Thus an estimation of the total amounts of As and PO_4^{3-} adsorbed onto the iron-oxide during these experiments can be obtained. It is estimated that the total amount of As and PO_4^{3-} adsorbed by ferrihydrite is < 10 % and < 30 % of the total and linear capacity of the adsorbent, respectively; therefore any effects of PO_4^{3-} inhibition on As adsorption would be minimal.

Jain and Loeppert[22] also found that sulfate had no significant effect on As^V adsorption over the entire pH range, even at an $[As^V]:[SO_4^{2-}]$ concentration ratio of 1:50. For As^{III}, at $[As^{III}]:[SO_4^{2-}]$ concentration ratios of 1:1, 1:10 and 1:50, the adsorption decrease at pH 5 was ~ 3, ~ 5 and ~ 8 %, respectively. The $[As]:[SO_4^{2-}]$ concentration ratios used in the work for this thesis was 1:930. Our results and those of Jain and Loeppert[22] may indicate that SO_4^{2-} is only weakly adsorbed to ferrihydrite.

Swedlund and Webster[29] examined the adsorption and polymerisation of SiO_4^{4-} on ferrihydrite and its effect on As adsorption. They proposed that the interaction between SiO_4^{4-} and ferrihydrite depends on the mole ratio of Si to Fe on the ferrihydrite. At low Si:Fe mole ratios, SiO_4^- appears to be adsorbed as monomeric silicate in the ferrihydrite surface; when the Si:Fe mole ratio is high, SiO_4^{4-} appears to be associated with the ferrihydrite via siloxane linkages (Si-O-Si), essentially polymerising to form a separate silica phase. The Si:Fe mole ratio in which polymerization becomes important is suggested to lie between 0.05 to 0.2.

Swedlund and Webster[29] used ~ 55 ppm Fe and 4 ppm As for their experiments. They found that As^V and As^{III} adsorption was not significantly affected by the presence of SiO_4^{4-} (9 ppm) at pH < 8. At pH > 9, As^V adsorption was inhibited. At higher SiO_4^{4-} concentrations (165 ppm) adsorption of As^V was not affected at pH < 6 but at pH > 6 the higher concentrations of SiO_4^{4-} had a more significant effect than lower concentrations of SiO_4^{4-}. For As^{III}, adsorption on ferrihydrite was significantly affected by SiO_4^{4-} at all pH values. At pH 5 the adsorption of As^{III} was only 60 % of the adsorption in the absence of SiO_4^{4-}. It was believed that

polymerisation was important at the higher SiO_4^{4-} concentrations, as modelled predictions did not agree with experimental results. The modelling slightly underestimated the effect of SiO_4^{4-} on As^{III} and As^{V} adsorption at high SiO_4^{4-} concentration as the model did not take account of surface polymerisation of SiO_4^{4-}, which could inhibit As adsorption by steric effects or by decreasing the surface potential; polymerisation of SiO_4^{4-} makes the ferrihydrite surface more negatively charged. The concentration of SiO_4^{4-} used for the experiments in this thesis was 56 ppm, which is within the concentration range used by Swedlund and Webster.[29]

Waltham and Fick[30] examined the effect of SiO_4^{4-} on the kinetics of As^{v} and As^{III} adsorption on goethite. The concentration of As was 7.5 ppm and goethite was 1.0 g L^{-1}. They showed that SiO_4^{4-} adsorption on goethite can reduce the rate and the total quantity of As^{V} and As^{III} adsorbed at various pH and SiO_4^{4-} concentrations. Waltham and Fick[30] found that the total quantity of As^{V} adsorbed remained nearly constant from pH 4 to 8 at 9.2 and 92 ppm SiO_4^{4-}. However the rate of adsorption was slower in the presence of SiO_4^{4-} and depended on the SiO_4^{4-} concentration. For As^{III}, the presence of SiO_4^{4-} decreased the rate of adsorption and the total quantity of As^{III} adsorbed; as the concentration of SiO_4^{4-} increased the extent of interference on As^{III} adsorption, with regards to kinetics and total amount of As^{III} adsorbed, increased. At pH 4, the presence of 9.2 ppm SiO_4^{4-} resulted in ~ 15 % decrease in adsorption, at 92 ppm SiO_4^{4-} this decrease was ~ 35 %. At pH 6, the presence of 9.2 ppm SiO_4^{4-} resulted in ~ 4 % decrease in adsorption; at 92 ppm the decrease was ~ 35 %. The results from this thesis showed no observable effect of 56 ppm SiO_4^{4-} on the adsorption of As^{V} or As^{III} at As concentrations of 60 ppb. The [As]/[SiO_4^{4-}] ratio used in the work for this thesis was higher than that used by Swedlund and Webster[29] and Waltham and Fick.[30]

5.4.5 Effect of fulvic acid on mass of As^{V} and As^{III} accumulated by DGT

The effect that fulvic acid has on the ability of the iron-oxide adsorbent to adsorb As was examined by deploying DGT devices in As^{V} and As^{III} solutions containing 5 ppm fulvic acid. The assumption was that fulvic acid diffusing to the adsorbent could block sites for As adsorption. The good agreement between the mass of As accumulated within DGT devices and the predicted As mass for As^{V} and As^{III} experiments, indicates that fulvic acid is not significantly affecting the amount of As accumulated on the iron-oxide adsorbent, under the conditions used in this study. Since it has been shown that fulvic acid adsorbs to iron-oxides,[12, 37, 38] and fulvic acid affects the adsorption of As to iron-oxides,[12, 37-39] it is likely

that in the experiments carried out for this work, adsorption of fulvic acid on the iron-oxide adsorbent was occurring, however, fulvic acid diffusion and adsorption was not significant enough to affect the adsorption of As. Furthermore, results from section 5.3.7, show that the particular fulvic acid used in the work for this thesis does affect the amount of As adsorbed to colloidal iron-oxide in solution, presumably by its adsorption to the iron-oxide. Longer deployment times and/or higher concentrations of fulvic acid may affect the mass of As adsorbed by the iron-oxide adsorbent within DGT devices. However, deployment of DGT in a natural water containing ~ 10 ppm fulvic acid resulted in the concentration determined by DGT to be the same as the concentration determined by HG-AAS (chapter 7). This indicates that even for fulvic acid concentrations as high as 10 ppm, there is no significant effect on adsorption of As^{III} or As^{V} by iron-oxide in the DGT devices; and hence the DGT measurement is not affected.

A number of research groups have studied the effect of fulvic acid on the adsorption of As^{V} and/or As^{III}. Redman *et al*.[12] examined the effect of As^{III} and As^{V} adsorption onto hematite in the presence of 6 different fulvic acids. In the absence of fulvic acid, adsorption of As^{III} and As^{V} was rapid, attaining equilibrium within ~ 1 h for As^{V} and 6 h for As^{III}. At these times, all of the As in solution had been adsorbed to the hematite. However, coating the hematite with fulvic acid prior to adsorption of As^{V} and As^{III}, dramatically slowed the attainment of equilibrium from less than 6 h to ~ 100 h for both As species. The adsorption of As^{III} was affected more than the adsorption of As^{V}. At 20 h, ~ 25 % of As^{III} and ~ 20 % of As^{V} still remained in solution. The increase in equilibrium time was attributed to either: (i) occupation and/or obstruction of adsorption sites by fulvic acid which would slow the rate at which As species encountered favourable sites; (ii) coagulation of hematite particles by fulvic acid, further reducing the number of available sites; or (iii) dependence of As adsorption on fulvic acid desorption to reveal favourable surface sites.

In addition to these kinetic experiments, Redman *et al*.[12] also carried out equilibrium experiments in which As and fulvic acid were sequentially introduced into a solution containing suspended hematite. This was carried out for 6 fulvic acid samples. As^{V} and As^{III} were allowed to adsorb individually onto colloidal hematite, reaching nearly 100 % adsorption before the addition of fulvic acid. The solution was left for a further 100 h to re-equilibrate. Analysis of the aqueous phase showed that the fulvic acid desorbed between 1

and 20 % of As^{V} from the hematite; this depended on the particular fulvic acid sample used. For As^{III}, 4 to 12 % of As was desorbed due to the addition of fulvic acid. Overall, As^{III} was desorbed to a greater extent than As^{V} by every fulvic acid sample except one. Redman *et al*.[12] also found evidence of complexation of the dissolved As by fulvic acid. This suggests that the total As mobilised by fulvic acid was much greater than indicated by measuring free As alone. For example, for one of the fulvic acid samples that desorbed As, the free As concentration in solution was ~ 0.3 ppb, however, the total As concentration (i.e. free As plus As complexed by fulvic acid) in solution was ~ 6.5 ppb. The inverse of the above experiment (i.e. addition of As to hematite that had been pre-adsorbed with fulvic acid) showed similar results. In the experiments carried out by Redman *et al*.[12] the concentration of hematite was 300 mg L^{-1}, the concentration of fulvic acid was 10 mg C L^{-1}, and the concentration of As^{V} or As^{III} was 75 ppb. The pH was 6.

Grafe *et al*.[37] showed that fulvic acid, humic acid, and citric acid adsorbs to goethite over the pH range 3 to 11. Humic acid and fulvic acid reduced adsorption of both As^{V} and As^{III}; citric acid only reduced adsorption of As^{III}. The effect of fulvic acid on As^{V} adsorption was dependent on pH. The amount of As^{V} adsorbed on goethite, in the presence of fulvic acid, was reduced by ~ 20 % at pH 3 and at pH 8 the reduction was ~ 15 %. For As^{III} the effect of fulvic acid was also more significant at low pH. At pH 3 the amount of As^{III} adsorbed to goethite was reduced by ~ 20 %; whereas at pH 8 the reduction was ~ 8 %. The adsorption behaviour of As on goethite was independent of the order in which As was added (i.e. if As was added before or after fulvic acid). Grafe *et al*.[37] also found that the adsorption of fulvic acid was hindered by the presence of both As^{V} and As^{III}. In the experiments carried out by Grafe *et al*.[37] the concentration of goethite was 2.5 g L^{-1}, the fulvic acid concentration was 12 mg C L^{-1}, and the concentration of As^{V} and As^{III} were 75 ppm.

The same group also examined the adsorption of As^{V} and As^{III} on ferrihydrite in the presence and absence of fulvic acid.[38] Fulvic acid was shown to adsorb on ferrihydrite, however in contrast to the work carried out using goethite, fulvic acid did not affect adsorption of As^{V} significantly on ferrihydrite between pH 3 and 8. Adsorption of As^{III} was affected by fulvic acid but not to the extent that was observed on goethite. The adsorption behaviour of As on ferrihydrite was independent of the order in which As was added. Both As^{V} and As^{III} affected the adsorption of fulvic acid on ferrihydrite. In these experiments the concentration of

goethite was 1 g L^{-1}, the fulvic acid concentration was 12 mg C L^{-1} and the concentration of As^{V} and As^{III} were 75 ppm.

Simeoni *et al*.[39] also examined whether the order in which As^{V} and fulvic acid were added influenced the adsorption of As^{V} on ferrihydrite. For experiments in which As^{V} was adsorbed onto ferrihydrite 24 h prior to the addition of fulvic acid, the amount of As^{V} desorbed was dependent on the concentration of fulvic acid and pH. The concentration of fulvic acid ranged from 0 to 60 ppm, the concentration of As^{V} was 4 ppm and the concentration of ferrihydrite was 22 mg L^{-1}. At pH 4, there was little change in As^{V} adsorption up to 6 ppm fulvic acid; increasing the concentration of fulvic acid led to an increase in the desorption of As^{V}, with ~ 15 % of As desorbed at 60 ppm fulvic acid. At pH 6 , addition of fulvic acid resulted in a ~ 5 % desorption over the entire fulvic acid concentration range and at pH 8 only ~ 6 % desorption was observed.

For experiments in which fulvic acid was added to ferrihydrite 24 h prior to the addition of As^{V}, adsorption of As^{V} was significantly less at higher fulvic acid concentrations than when As^{V} was adsorbed first. At pH 4, there was no significant difference in adsorption at a fulvic acid concentration of ~ 6 ppm compared to experiments in the absence of fulvic acid. At 60 ppm fulvic acid the decrease in As^{V} adsorption was ~ 27 %. At pH 6 and 8 this decrease was ~ 9 and ~ 30 %, respectively, at 60 ppm fulvic acid.

It is likely that in the experiments carried out for the work in this thesis, the capacity of the adsorbent was sufficiently high that fulvic acid was not effecting adsorption of As^{V} or As^{III} to the iron-oxide adsorbent, within the DGT device. Redman *et al*.[12] found that equilibrium had been reached after 4 h for the adsorption of fulvic acid on hematite. After this time < 5 % of the fulvic acid had adsorbed to hematite; this indicates that only a small fraction of the fulvic acid may be adsorbing. In addition, for DGT, if adsorption of fulvic acid by the iron-oxide is slow then the drive for diffusion of fulvic acid to the adsorbent would be lessened due to a small concentration gradient.

As the above discussion shows, fulvic acid can affect the adsorption of both As^{V} and As^{III} on different iron-oxides at various As, fulvic acid, and iron-oxide concentrations, as well as pH. Differences in experimental conditions and the fact that in DGT the iron-oxide is

immobilized in a gel, in which adsorption can only occur via diffusion of species through the diffusion layer, may be reasons why in the work for this thesis no significant effect of fulvic acid on As adsorption was observed. In addition, because As and fulvic acid are potentially adsorbing onto iron-oxide simultaneously, then obstruction or blocking of adsorption sites by fulvic acid may be less of a factor for the DGT technique.

5.4.6 Combined effect of fulvic acid and Fe^{III} on the mass of As^{V} accumulated by DGT

The effect that soluble Fe-fulvic acid complexes have on the mass of As^{V} accumulated by DGT was examined by deploying DGT devices in As^{V} solutions containing 5 ppm fulvic acid and various concentrations of Fe^{III}. The accumulated mass of As was compared to the predicted mass of As. The good agreement between the mass of As accumulated by DGT and the predicted mass of As^{V} for each experiment, indicates that As^{V} is not complexed by Fe^{III}-fulvic acid in solution to any significant extent under the conditions used in these experiments. If As^{V} was associating with fulvic acid then the accumulated mass would be less than the predicted mass due to the slower diffusion of fulvic acid species relative to 'free' As^{V}.

Potential complexation of As by Fe-fulvic acid species has been reported in the literature. Akoitai[40] examined the interaction between Fe^{III}-fulvic acid complexes and As^{V}; an XAD-4 resin was used to separate As associated with the fulvic acid fraction from solution. This resin did not retain As^{V} in the absence of fulvic acid. The concentration of fulvic acid used was 17 ppm and the concentration of Fe^{III} was varied from 0 to 500 ppb. Akoitai[40] found that as the concentration of Fe^{III} bound to fulvic acid increased, the amount of complexed As^{V} also increased. For the five Fe^{III} concentrations examined, the ratio of moles of Fe^{III} complexed by fulvic acid to moles of As^{V} bound to the Fe^{III}-fulvic acid was ~ 1. This suggests that As^{V} forms a 1:1 complex with Fe^{III}-fulvic acid. In the absence of Fe^{III} but using the same concentrations of fulvic acid and As^{V}, only a small amount of As^{V} was retained by fulvic acid. This was assumed to be due to residual Fe^{III} already present in the fulvic acid sample.

Lin *et al.*[41] examined the interaction between As^{V} and organic substances in a water extract of compost (WEC). They used ion chromatography to separate 'free' As from complexed As and found that 30 to 50 % of the added As^{V} had reacted with the WEC. Lin *et al.*[41] also confirmed this result using dialysis, in which a dialysis bag with a molecular weight cut off of

1000 was used; the As^V-WEC solution was placed in the dialysis bag and dialyzed against a large volume of water. The binding of As by dissolved organic carbon (DOC) was identified through the As concentration difference across the dialysis membrane. The membrane allows passage of 'free' As but not large NOM-As complexes. They found that ~ 55 % of As^V was associated with the WEC fraction, suggesting that As^V is complexed by DOC of the WEC to form As-DOC complexes. Lin *et al.*[41] proposes that Ca, Mg, and especially Fe, Al, and Mn, act as bridging cations for complexation between As^V and DOC in the WEC. They observed that when As^V was reacted with WEC that had been purified by removal of cations, there was no evidence of complexation between the WEC and As^V. For the experiments carried out by Lin *et al.*,[41] the concentrations of Al and Fe in the WEC was 630 and 90 ppb, respectively, the concentration of As^V was 2 ppm and the concentration of DOC in the WEC was 70 ppm.

Redman *et al.*[12] examined complexation between As species and fulvic acid in water samples that contained various concentrations of cations. They used an anion-exchange resin to separate organically-complexed As (retained on the resin) from 'free' As. The As^V and As^{III} species were added to the water samples containing fulvic acid separately and equilibrated for 90 h at pH 6. Three out of the 6 water samples lowered the free As^V concentration in solution, indicating that complexation between fulvic acid in the water samples and As^V had occurred. For As^{III}, 3 out of the 6 water samples also lowered the free As^{III} concentration in solution, again indicating complexation between As^{III} and fulvic acid in the water samples. However, one of the samples that did not show evidence of As^V complexation, surprisingly showed evidence of As^{III} complexation. In addition, one sample that showed As^{III} complexation did not show As^V complexation.

Redman *et al.*[12] found that the water samples that contained the highest concentration of cations exhibited the greatest complexation with As^V and As^{III}, however there were some exceptions and this relationship between the extent of complexation and the cation concentration of the samples was not statistically significant. Redman *et al.*[12] propose that metal bridging appears to be a potential mechanism for complexation of As by fulvic acid. For the experiments carried out by Redman *et al.*[12] the concentration of fulvic acid was 10 mg C $L^{-1}$and the concentration of As was 75 ppb. It is possible that due to the high concentrations of Al and Fe in some of the fulvic acid water samples used by Redman *et al.*,[12] that the complexation was actually As adsorbing to colloids in solution. The water sample

that showed the most extensive complexation contained 6.9 ppm Fe, 0.13 ppm Al, and 0.23 ppm Mn.

Ritter *et al*.[42] examined the association between natural organic matter (NOM) and As^V using dialysis and carried out experiments to identify the interaction that is occurring between As and fulvic acid. They examined three different NOM samples. Results from two out of the three NOM samples were consistent with binding of As^V by NOM. The two samples that showed complexing behavior towards As^V had higher concentrations of Fe^{III} (280 and 500 ppb) compared to the other sample, in which the Fe^{III} concentration was below the detection limit. Ritter *et al*.[42] also carried out experiments in which the NOM was spiked with Fe^{III}. The solutions were allowed to equilibrate for 24 h and filtered using a 0.45 μm membrane (supposedly to remove colloidal Fe^{III}) before addition of As^V. They found significantly more As^V in the dialysis bags for the Fe-spiked samples, indicating the importance of Fe^{III} in As^V-NOM interactions. When the experiments were carried out without the addition of NOM (i.e. just iron in the dialysis bag) an increase of As^V concentration in the dialysis bag was not observed; this implies that the As content in the dialysis bag when NOM is present is not due to an inorganic colloidal Fe^{III}-As^V interaction.

In further experiments, Ritter *et al*.[42] added Fe^{III} incrementally to one of the NOM samples before addition of As^V. They found a clear relationship between the concentration of Fe and the concentration of As^V inside the dialysis bag (i.e. complexed As). Increasing the concentration of Fe from 0 to 0.2 mmol L^{-1} resulted in the concentration of As^V increasing within the dialysis bag. An r^2 value of 0.97 was obtained, indicating a strong relationship between the Fe^{III} concentration and the amount of complexed As. The slope of the plot was 0.2, indicating an Fe/As mole ratio of 5 which is higher than the Fe/As mole ratio used in the experiments for this thesis (the highest Fe/As mole ratio was 3.5), and higher than the Fe/As mole ratio of 1 reported by Akoitai[40] for As^V complexation.

Ritter *et al*.[42] proposed that the NOM retains the added Fe^{III} in solution through the formation of non-colloidal NOM-Fe complexes and/or through colloidal Fe^{III}-NOM interactions. The NOM-suspended iron then serves as binding sites for As^V, resulting in the formation of dissolved, non-colloidal As^V-Fe^{III}-NOM complexes and/or a NOM-suspended Fe^{III}-As^V colloidal association. However, they found a significant proportion of the Fe was present as

colloids at all Fe/C ratios. At an Fe/C ratio of 0.001 (lowest ratio used), 23 % of the 'dissolved' iron (i.e. iron in solution after filtration at 0.45 μm) was present as colloids between the size range of 0.1 and 0.45 μm. At an Fe/C molar ratio of 0.12, 84 % of the 'dissolved' iron was present within the 0.1 to 0.45 μm size fraction. These colloids may be NOM-stabilized iron hydroxide or formed by Fe-induced coagulation of NOM. This indicates that the association of fulvic acid and As may be due to colloidal interaction and not to the formation of a dissolved As-Fe^{III}-fulvic acid complex. Because the experiments carried out for this thesis contained low Fe concentrations, it is unlikely that colloidal iron would be formed.

5.4.7 Effect of colloidal Fe in the presence and absence of fulvic acid on mass of As^V accumulated by DGT

The effect of colloidal Fe (in the presence and absence of fulvic acid) on the 'dissolved' (non-colloidal) concentration of As^V was examined by deploying DGT devices in As^V solutions containing various concentrations of Fe^{III} and fulvic acid. The results showed that in the presence of colloidal Fe, the concentration of As determined by DGT was less than the total concentration of As^V present due to the adsorption of As^V by iron-oxide in solution. This fraction of As^V is not available to be measured by DGT. Experiments 1 and 2 (Table 5.7, section 5.3.7) show the effect of increasing the Fe^{III} concentration and therefore the concentration of colloidal Fe^{III} in solution. Increasing the Fe^{III} concentration from 1 to 2.5 ppm resulted in a decrease in the dissolved As^V concentration, as determined by DGT, from 8.7 ± 0.7 ppb to 0.7 ± 0.1 ppb. This corresponds to 85 % and > 98 % of the total As^V being associated with colloidal material at 1 ppm and 2 ppm Fe^{III}, respectively. Comparing the results from experiments 1, 4, and 5 (which all have similar total Fe^{III} concentrations) shows that fulvic acid had a significant affect on the amount of As^V adsorbed to Fe^{III} colloids in solution. Increasing the concentration of fulvic acid resulted in an increase of the dissolved fraction of As^V. For an Fe^{III} concentration of 2 ppm and a fulvic acid concentration of 1 ppm, the concentration of As measured by DGT is 14.2 ± 1.9 ppb; at 2 ppm Fe^{III} and 5 ppm fulvic acid, the concentration of As^V measured by DGT is 38.5 ± 2.5 ppb. Therefore, as the concentration of fulvic acid is increased from 1 to 5 ppm (in the presence of 2 ppm As Fe^{III}) the amount of As adsorbed to colloidal Fe^{III} is ~ 75 % and ~ 35 % of the total As present in solution, respectively.

Comparing the results from experiments 3 and 4 shows that at constant fulvic acid concentration (i.e. 5 ppm), the concentration of Fe^{III} affects the dissolved concentration of As^{V}. At 5 ppm fulvic acid and 5 ppm Fe^{III}, the dissolved As concentration was 7.2 ± 0.9 ppb, as measured by DGT. At 5 ppm fulvic acid and 2 ppm Fe^{III}, the dissolved concentration determined by DGT is 38.5 ± 2.5 ppb. This corresponds to ~ 88 % and ~ 35 % of the total amount of As being associated with iron-oxide in solution at 5 ppm and 2 ppm Fe, respectively, at 5 ppm fulvic acid. These results clearly show that fulvic acid is capable of reducing the amount of As^{V} adsorbed by iron-oxide in solution; therefore increasing the dissolved fraction of As^{V}.

Only three [Fe]/[fulvic acid] concentration ratios were investigated in this work. At [Fe]/[Fulvic acid] ratios of 2, 1 and 0.4, the dissolved As concentrations measured by DGT were 14.2, 7.2 and 38.5 ppb. It was expected that as the [Fe]/[fulvic acid] concentration ratio decreased the dissolved As^{V} concentration would increase, however this was not observed. It follows that the actual concentrations of Fe and fulvic acid are important rather than the ratio of Fe to fulvic acid.

Grafe *et al*.,[37] Grafe *et al*.,[38] Simeoni *et al*.,[39] and Redman *et al*.[12] have all found that fulvic acid affects the adsorption of As^{V} and/or As^{III} to iron-oxides in solution. This may be due to competition between As and fulvic acid for adsorption sites on the iron-oxide, or as discussed by Simeoni *et al*.,[39] it may be due to the obstruction of potential As adsorption sites on the iron-oxide.

Generally, good agreement was obtained between the concentration of As measured by DGT and the concentration of As initially measured in solution by HG-AAS after 0.025 μm membrane filtration. However, the concentration of dissolved As in solution at the completion of each experiment was consistently lower than the concentration of dissolved As in solution at the start of the experiment, both determined by HG-AAS. This phenomenon was not observed for experiment 4. The concentration of dissolved As determined at the completion of experiments 1, 2, 3, and 5 was between 26 to 44 % lower than the concentration at the start of the experiment. For these experiments, As was added 24 h before DGT devices were deployed. It is possible that 24 h was not long enough for the system to reach equilibrium; therefore there is a difference between the concentrations of As

determined at the start and completion of the experiment. This explanation is supported by the results from experiment 4 in which an equilibrium time of 48 h was used. For this experiment, good agreement between the concentrations of As measured at the start and completion of the experiment were obtained. However, if the system had not reached equilibrium after 24 h, it is surprising that good agreement between the concentration of As measured by DGT and the concentration of As measured by HG-AAS at the start of the experiment. The DGT technique measures a time-averaged concentration over the deployment period. Assuming that the decrease in the dissolved As concentration over the deployment time is linear, due to the system having not reached equilibrium, then one might expect that the average of the concentrations of As at the start and at the completion of the experiment (determined by HG-AAS) would give a value closer to that obtained by DGT. Table 5.9 shows a comparison between the concentration of As determined by DGT and the average of the As concentration at the start and completion of the experiments, measured by HG-AAS after filtration. The concentration determined by DGT is consistently higher for three of the experiments than the average concentration of As.

Experiment	C_{DGT}	[As] (HGAAS)[a]	Ratio[b]
2	8.7 ± 0.7 ppb	7.0 ± 0.7 ppb	1.25
3	7.2 ± 0.9 ppb	7.4 ± 0.8 ppb	1.00
4	38.5 ± 2.5 ppb	34.6 ± 0.2 ppb	1.10
5	14.2 ± 1.9 ppb	11.5 ± 0.8 ppb	1.25

Table 5.9 Comparison of the concentration of As measured by DGT and the average concentration of As determined at the start and completion of the DGT experiments.

[a] Average concentration of As determined at the start and end of the experiment

[b] $C_{DGT}/[As]_{HG\text{-}AAS}$ ratio

Even for the experiment (number 4) in which it seems that equilibrium had been reached, the concentration determined by DGT was still higher than the concentration determined by HG-AAS after filtration. It is possible that the concentrations of As determined by HG-AAS after filtration are lower than the actual concentrations of As in solution; this may be due to some dissolved As being retained within or on the filter membrane during the filtration process. Therefore, the actual concentration of As would be higher, and the average of these two measurements would also be higher and closer to the concentration determined by DGT. If retention of dissolved As within or on the membrane is responsible for the difference between

C_{DGT} and the concentrations of As measured by HG-AAS after filtration, then this highlights the importance of an in-situ method like DGT over a laboratory based method that involves filtration. Problems associated with filtering samples have been observed. These include: adsorption/desorption of trace elements from the filter or from solids retained by it; inclusion/exclusion of colloidal associated trace metals; filter clogging; and contamination.[57]

5.5 Conclusion

The results from this chapter suggest that the DGT method for total As determinations should be able to be used in a straight-forward manner in a variety of environmental situations and conditions. The mass of As accumulated within DGT devices at pH 3 and 8 were not significantly different from that measured at pH 5 for As^{V} and As^{III} experiments; this suggests that the DGT method for total As determinations should be capable of measuring total As in a variety of waters with varying pH. Anions and cations, present at concentration ratios typical of those expected in an unpolluted water, showed no significant effect on the As^{V} or As^{III} measurements by DGT, and the adsorption of As to the iron-oxide adsorbent was unaffected by the presence of fulvic acid and dissolved Fe^{III}. The discrepancy in some of the results obtained in the work for this thesis and those from the literature may be attributed to differences in experimental conditions used; especially in the concentrations of reactants and reaction times used. The difference in concentration of various reactants such as As, Fe, fulvic acid, and various anions and cations, complicates direct comparisons of results with those from this thesis.

The presence of colloidal Fe in solution significantly reduced the dissolved concentration of As determined by DGT, indicating that the colloidal fraction of As is not available to be measured by DGT. In addition, the presence of fulvic acid affected the adsorption of As onto colloidal Fe in solution. For the Fe colloid experiments, reasonable agreement was obtained between the concentration of As measured by DGT and that measured by HG-AAS after filtration. Furthermore, there was evidence to suggest that the dissolved concentration determined by HG-AAS after filtration may be underestimated due to adsorption losses during the filtration step; this highlights the advantages of in-situ methods for determining As.

There is no evidence that the uptake of As^{V} by DGT devices is affected by the presence of As^{III}, and vice versa. The total capacity of the iron-oxide adsorbent in the DGT device was

determined to be ~ 100,000 ng of As, however the linear capacity at which the DGT equation holds was ~ 30,000 ng.

5.6 References

1. Chang, L. Y.; Davison, W.; Zhang, H.; Kelly, M., Performance characteristics for the measurement of Cs and Sr by diffusive gradients in thin films (DGT). *Analytica Chimica Acta* **1998,** 368, (3), 243-253.

2. Li, W.; Zhao, H.; Teasdale, P. R.; John, R., Preparation and characterisation of a poly(acrylamidoglycolic acid-coacrylamide) hydrogel for selective binding of Cu^{2+} and application to diffusive gradients in thin films measurements. *Polymer* **2002,** 43, (17), 4803-4809.

3. Li, W.; Zhao, H.; Teasdale, P. R.; John, R.; Zhang, S., Synthesis and characterisation of a polyacrylamide-polyacrylic acid copolymer hydrogel for environmental analysis of Cu and Cd. *Reactive & Functional Polymers* **2002,** 52, (1), 31-41.

4. Li, W.; Zhao, H.; Teasdale, P. R.; John, R.; Zhang, S., Application of a cellulose phosphate ion exchange membrane as a binding phase in the diffusive gradients in thin films technique for measurement of trace metals. *Analytica Chimica Acta* **2002,** 464, (2), 331-339.

5. Mason, S.; Hamon, R.; Nolan, A.; Zhang, H.; Davison, W., Performance of a mixed binding layer for measuring anions and cations in a single assay using the diffusive gradients in thin films technique. *Analytical Chemistry* **2005,** 77, (19), 6339-6346.

6. Murdock, C.; Kelly, M.; Chang, L. Y.; Davison, W.; Zhang, H., DGT as an in situ tool for measuring radiocesium in natural waters. *Environmental Science & Technology* **2001,** 35, (22), 4530-4535.

7. Zhang, H.; Davison, W., Performance-characteristics of diffusion gradients in thin-films for the in-situ measurement of trace-metals in aqueous-solution. *Analytical Chemistry* **1995,** 67, (19), 3391-3400.

8. Zhang, H.; Davison, W.; Gadi, R.; Kobayashi, T., In situ measurement of dissolved phosphorus in natural waters using DGT. *Analytica Chimica Acta* **1998,** 370, (1), 29-38.

9. Stollenwerk, K. G., Geochemical processes controlling transport of arsenic in groundwater: A review of adsorption. In *Arsenic in groundwater: Geochemistry and occurrence,*Welch, A. H.; Stollenwerk, K. G., Eds. Kluwer Academic Publishers: Boston, 2002.

10. Plant, J. A.; Kinniburgh, D. G.; Smedley, P. L.; Fordyce, F. M.; Klinck, B. A., Arsenic and selenium In *Treatise on geochemistry,*Holland, H. D.; Turekian, K. K.; Lollar, B. S., Eds. Elsevier Science: Oxford, 2004; Vol. 9.

11. Raven, K. P.; Jain, A.; Loeppert, R. H., Arsenite and arsenate adsorption on ferrihydrite: Kinetics, equilibrium, and adsorption envelopes. *Environmental Science & Technology* **1998,** 32, (3), 344-349.

12. Redman, A. D.; Macalady, D. L.; Ahmann, D., Natural organic matter affects arsenic speciation and sorption onto hematite. *Environmental Science & Technology* **2002,** 36, (13), 2889-2896.

13. Cornell, R. M.; Schwertmann, U., *The iron oxides: Structure, properties, reactions, occurrence and uses*. VCH Publishers: New York, 1996.

14. Schwertmann, U.; Cornell, R. M., *Iron oxides in the laboratory: Preparation and characterization*. VCH Publishers: New York, 1991.

15. Fendorf, S.; Eick, M. J.; Grossl, P.; Sparks, D. L., Arsenate and chromate retention mechanisms on goethite .1. Surface structure. *Environmental Science & Technology* **1997,** 31, (2), 315-320.

16. Manning, B. A.; Fendorf, S. E.; Goldberg, S., Surface structures and stability of arsenic(III) on goethite: Spectroscopic evidence for inner-sphere complexes. *Environmental Science & Technology* **1998,** 32, (16), 2383-2388.

17. Ona-Nguema, G.; Morin, G.; Juillot, F.; Calas, G.; Brown, G. E., EXAFS analysis of arsenite adsorption onto two-line ferrihydrite, hematite, goethite, and lepidocrocite. *Environmental Science & Technology* **2005,** 39, (23), 9147-9155.

18. Sherman, D. M.; Randall, S. R., Surface complexation of arsenic(V) to iron(III) (hydr)oxides: Structural mechanism from ab initio molecular geometries and EXAFS spectroscopy. *Geochimica et Cosmochimica Acta* **2003,** 67, (22), 4223-4230.

19. Waychunas, G. A.; Rea, B. A.; Fuller, C. C.; Davis, J. A., Surface-chemistry of ferrihydrite .1. EXAFS studies of the geometry of coprecipitated and adsorbed arsenate. *Geochimica et Cosmochimica Acta* **1993,** 57, (10), 2251-2269.

20. Drever, J. I., *The geochemistry of nautral waters: Surface and groundwater environments*. 3rd ed.; Prentice Hall: New Jersey, 1997.

21. Jain, A.; Raven, K. P.; Loeppert, R. H., Arsenite and arsenate adsorption on ferrihydrite: Surface charge reduction and net OH^- release stoichiometry. *Environmental Science & Technology* **1999,** 33, (8), 1179-1184.

22. Jain, A.; Loeppert, R. H., Effect of competing anions on the adsorption of arsenate and arsenite by ferrihydrite. *Journal of Environmental Quality* **2000,** 29, (5), 1422-1430.

23. Smedley, P. L.; Kinniburgh, D. G., A review of the source, behaviour and distribution of arsenic in natural waters. *Applied Geochemistry* **2002,** 17, (5), 517-568.

24. Dzombak, D. A.; F.M.M, M., *Surface complexation modeling: Hydrous ferric oxide*. John Wiley & Sons, Inc.: New York, 1990.

25. Goldberg, S., Competitive adsorption of arsenate and arsenite on oxides and clay minerals. *Soil Science Society of America Journal* **2002,** 66, (2), 413-421.

26. Wilkie, J. A.; Hering, J. G., Adsorption of arsenic onto hydrous ferric oxide: Effects of adsorbate/adsorbent ratios and co-occurring solutes. *Colloids and Surfaces A-Physicochemical and Engineering Aspects* **1996,** 107, 97-110.

27. Zhang, W.; Singh, P.; Paling, E.; Delides, S., Arsenic removal from contaminated water by natural iron ores. *Minerals Engineering* **2004,** 17, (4), 517-524.

28. Gao, Y.; Mucci, A., Acid base reactions, phosphate and arsenate complexation, and their competitive adsorption at the surface of goethite in 0.7 m NaCl solution. *Geochimica et Cosmochimica Acta* **2001,** 65, (14), 2361-2378.

29. Swedlund, P. J.; Webster, J. G., Adsorption and polymerisation of silicic acid on ferrihydrite, and its effect on arsenic adsorption. *Water Research* **1999,** 33, (16), 3413-3422.

30. Waltham, C. A.; Eick, M. J., Kinetics of arsenic adsorption on goethite in the presence of sorbed silicic acid. *Soil Science Society of America Journal* **2002,** 66, (3), 818-825.

31. Dixit, S.; Hering, J. G., Comparison of arsenic(V) and arsenic(III) sorption onto iron oxide minerals: Implications for arsenic mobility. *Environmental Science & Technology* **2003,** 37, (18), 4182-4189.

32. Aiken, G. R.; McKnight, D. M.; Wershaw, R. L.; Maccarthy, P., An introduction to humic substances in soil, sediment, and water. In *Humic substances in soil, sediment, and water: Geochemistry, isolation, and chracterization,*Aiken, G. R.; McKnight, D. M.; Wershaw, R. L.; Maccarthy, P., Eds. John Wiley & Sons Inc.: New York, 1985.

33. Wang, S. L.; Mulligan, C. N., Effect of natural organic matter on arsenic release from soils and sediments into groundwater. *Environmental Geochemistry and Health* **2006,** 28, (3), 197-214.

34. Alvarez-Puebla, R. A.; Valenzuela-Calahorro, C.; Garrido, J. J., Theoretical study on fulvic acid structure, conformation and aggregation - a molecular modelling approach. *Science of the Total Environment* **2006,** 358, (1-3), 243-254.

35. Evangelou, V. P., *Environmental soil and water chemistry: Principles and applications*. John Wiley & Sons, Inc.: New York, 1998.

36. Morel, F. M.; Hering, J. G., *Principles and applications of aquatic chemistry*. John Wiley & Sons, Inc.: New York, 1993.

37. Grafe, M.; Eick, M. J.; Grossl, P. R., Adsorption of arsenate (V) and arsenite (III) on goethite in the presence and absence of dissolved organic carbon. *Soil Science Society of America Journal* **2001,** 65, (6), 1680-1687.

38. Grafe, M.; Eick, M. J.; Grossl, P. R.; Saunders, A. M., Adsorption of arsenate and arsenite on ferrihydrite in the presence and absence of dissolved organic carbon. *Journal of Environmental Quality* **2002,** 31, (4), 1115-1123.

39. Simeoni, M. A.; Batts, B. D.; McRae, C., Effect of groundwater fulvic acid on the adsorption of arsenate by ferrihydrite and gibbsite. *Applied Geochemistry* **2003,** 18, (10), 1507-1515.

40. Akoitai, S. A. *Arsenic in leachates from mine waste rocks*. Ph.D. Thesis, University of Canterbury, New Zealand, 2000.

41. Lin, H. T.; Wang, M. C.; Li, G. C., Complexation of arsenate with humic substance in water extract of compost. *Chemosphere* **2004,** 56, (11), 1105-1112.

42. Ritter, K.; Aiken, G. R.; Ranville, J. F.; Bauer, M.; Macalady, D. L., Evidence for the aquatic binding of arsenate by natural organic matter-suspended Fe(III). *Environmental Science & Technology* **2006,** 40, (17), 5380-5387.

43. Scally, S.; Davison, W.; Zhang, H., Diffusion coefficients of metals and metal complexes in hydrogels used in diffusive gradients in thin films. *Analytica Chimica Acta* **2006,** 558, (1-2), 222-229.

44. Scally, S.; Zhang, H.; Davison, W., Measurements of lead complexation with organic ligands using DGT. *Australian Journal of Chemistry* **2004,** 57, (10), 925-930.

45. Downard, A. J.; Panther, J.; Kim, Y. C.; Powell, K. J., Lability of metal ion-fulvic acid complexes as probed by FIA and DGT: A comparative study. *Analytica Chimica Acta* **2003,** 499, (1-2), 17-28.

46. Tongesayi, T.; Smart, R. B., Arsenic speciation: Reduction of arsenic(V) to arsenic(III) by fulvic acid. *Environmental Chemistry* **2006,** 3, (2), 137-141.

47. Langmuir, D., *Aqueous environmental geochemistry*. Prentice-Hall, Inc.: New York, 1997.

48. Smith, E.; Hamilton-Taylor, J.; Davison, W.; Fullwood, N. J.; McGrath, M., The effect of humic substances on barite precipitation-dissolution behaviour in natural and synthetic lake waters. *Chemical Geology* **2004,** 207, (1-2), 81-89.

49. Gregor, J. E.; Powell, H. K. J.; Town, R. M., Evidence for aliphatic mixed-mode coordination in copper(II)-fulvic acid complexes. *Journal of Soil Science* **1989,** 40, (3), 661-673.

50. Davison, W.; Zhang, H., In-situ speciation measurements of trace components in natural-waters using thin-film gels. *Nature* **1994,** 367, (6463), 546-548.

51. Cleven, R.; Nur, Y.; Krystek, P.; Van den Berg, G., Monitoring metal speciation in the rivers Meuse and Rhine using DGT. *Water Air and Soil Pollution* **2005,** 165, (1-4), 249-263.

52. Webb, J. A.; Keough, M. J., Quantification of copper doses to settlement plates in the field using diffusive gradients in thin films. *Science of the Total Environment* **2002,** 298, (1-3), 207-217.

53. Webb, J. A.; Keough, M. J., Measurement of environmental trace-metal levels with transplanted mussels and diffusive gradients in thin films (DGT): A comparison of techniques. *Marine Pollution Bulletin* **2002,** 44, (3), 222-229.

54. Li, W. J.; Zhao, H. J.; Teasdale, P. R.; John, R.; Wang, F. Y., Metal speciation measurement by diffusive gradients in thin films technique with different binding phases. *Analytica Chimica Acta* **2005,** 533, (2), 193-202.

55. Dunn, R. J. K.; Teasdale, P. R.; Warnken, J.; Schleich, R. R., Evaluation of the diffusive gradient in a thin film technique for monitoring trace metal concentrations in estuarine waters. *Environmental Science & Technology* **2003,** 37, (12), 2794-2800.

56. Li, Y. H.; Gregory, S., Diffusion of ions in sea-water and in deep-sea sediments. *Geochimica Et Cosmochimica Acta* **1974,** 38, (5), 703-714.

57. Gimpel, J.; Zhang, H.; Davison, W.; Edwards, A. C., In situ trace metal speciation in lake surface waters using DGT, dialysis, and filtration. *Environmental Science & Technology* **2003,** 37, (1), 138-146.

Chapter 6

Measurement of As^{III} and As^{V} diffusion coefficients through a Nafion membrane and method development for As speciation by DGT

6.1 Introduction

For DGT to be used to speciate As, it needs to be developed so that only one As species is selectively accumulated. Preliminary results from work in this laboratory established that a negatively charged Nafion membrane may be used to slow the diffusion of As^{V} relative to As^{III}.[1] Between pH 4 and 8, As^{III} exists as an uncharged species, H_3AsO_3, which can diffuse through the Nafion membrane and accumulate on the iron-oxide adsorbent within the DGT device. In contrast, As^{V} exists as negatively charged species, $H_2AsO_4^-$ and $HAsO_4^{2-}$, and these species are repelled by the negatively charged Nafion membrane. This dramatically slows diffusion of As^{V} to the adsorbent and provides a basis for differentiation between As species. Therefore As^{III} should be selectively accumulated by DGT in the presence of As^{V}.

6.1.1 Structure of Nafion

Nafion is a perfluorosulfonated ionomer. It consists of a perfluorinated polymer backbone with side chains containing sulfonic acid groups.[2] The sulfonic acid groups dissociate in water to give SO_3^- end groups;[2] this gives the Nafion membrane its negative charge. The general structure of Nafion is illustrated in Figure 6.1.

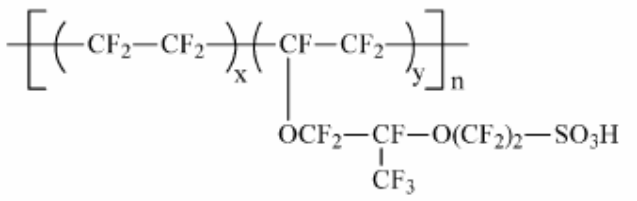

Figure 6.1 Chemical structure of Nafion; *x* and *y* represent molar compositions and do not imply a sequence length. Figure adapted from Hickner *et al*.[3]

Nafion is a non-crossed-linked polymer,[4, 5] however it still has a highly ordered structure.[5] The presence of both hydrophilic groups and hydrophobic fluorinated chains in the same polymer leads to micro-phase separation.[2, 6, 7] The hydrophobic sub-phase is formed by the perfluorinated polymer backbones and by the side chains, except for their SO_3^- end groups.[2, 7] The hydrophilic sub-phase is formed by water, mobile counterions, and SO_3^- groups.[2, 7] The sulfonate groups form ion-clusters.[6] The clusters which are 30 to 40 Å in diameter, are interconnected by narrow channels (10 Å diameter).[6, 8] It is these SO_3^--lined channels that are responsible for the transport of positively charged species but rejection of negatively charged ions.[9] The channel structure of Nafion is illustrated schematically in Figure 6.2.

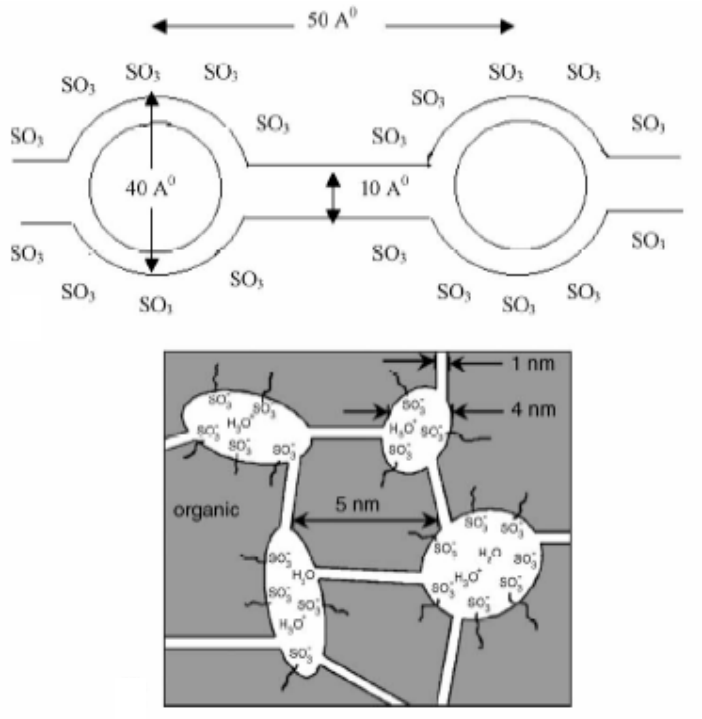

Figure 6.2 Schematic structure of a Nafion membrane. Figure adapted from Smitha *et al*.[8]

The Nafion membrane used in the work for this thesis was Nafion 112. Nafion 112 has an equivalent weight of 1100. The equivalent weight is the number of grams of dry Nafion per mole of sulfonic acid groups when the Nafion membrane is in the acid form.[9] This corresponds to ~ 7 % of the Nafion membrane being sulfonate groups by mass. Nafion 117 and 112 membranes have the same equivalent weight but different thickness.[3] Lower equivalent weight Nafion membranes are also available.[3]

6.1.2 Use of Nafion to exclude anionic species

The negatively charged properties of the Nafion membrane have been utilized to prevent diffusion of negatively charged species to an electrode or adsorbent.[10-14] Nafion-coated electrodes have been used to prevent adsorption of interfering negatively charged natural organic matter (NOM) on the electrode surface.[10-12] Furthermore, it has also been shown that a negatively charged Nafion-coated electrode can exclude negatively charged metal complexes of ethylenediaminetetraacetic acid (EDTA), nitrilotriacetic acid (NTA), and oxine-5-sulfonate;[12] whereas neutral and positively charged complexes show similar behavior to that at uncoated electrodes.[12] In addition, Nafion has also been shown to exclude complexes due to size.[12]

Nafion-coated electrodes have also been used for selective determination of species of biological interest.[13, 14] A Nafion-coated electrode has been used to exclude both uric acid and ascorbic acid for glucose determination at pH 7. At pH 7, both uric acid and ascorbic acid are negatively charged and are repelled by the Nafion membrane. In addition, a Nafion-coated electrode has been used to selectively measure the concentration of uric acid in the presence of ascorbic acid.[13] At pH 5, ascorbic acid is negatively charged and is repelled by the Nafion membrane;[13] in contrast, uric acid is uncharged and is allowed to pass through the Nafion membrane to the electrode surface and be measured.[13]

A Nafion coating on a membrane filter has also been used in a passive sampling device, similar to DGT, to prevent transport of metal-bound NOM to the adsorbent.[15] However, surprisingly the Nafion coating did not prevent the transport of smaller negatively charged metal complexes such as those of NTA and oxine-5-sulfonate.[15] This is in contrast to the application of Nafion described above.

6.1.3 Chapter Outline

This chapter is concerned with the measurement of As^{III} and As^{V} diffusion coefficients through a Nafion 112 membrane using a specifically designed diffusion cell and modified DGT devices. This was carried out to ascertain if the ratio of the As^{III} and As^{V} diffusion coefficients was large enough to allow As^{III} to be selectively accumulated in the presence of As^{V}. In addition, the effect that pH, anions, and cations have on the mass of As accumulated by DGT with a Nafion membrane was examined. Furthermore, the effect of pre-treatment of the Nafion membrane was examined when using DGT to determine As concentrations in a solution containing major anions and cations.

6.2 Experimental

Nafion 112 (described in section 2.3.7) was used for all experiments. The Nafion membranes were firstly soaked in Milli-Q water and then cleaned in 5 % v/v HNO_3 for 24 h. The Nafion was then rinsed in Milli-Q water and stored in a solution containing 0.01 mol L^{-1} $NaNO_3$ and 0.025 mol L^{-1} sodium acetate (pH 5.0). Unless otherwise stated, this pre-treatment procedure was used for all Nafion membranes. The Nafion membranes were re-used after cleaning and pre-treating as described above. Throughout this work there was no evidence to suggest that re-using Nafion membranes affected their performance.

Two samples of Nafion 112 were used for the work in this thesis. Nafion membrane 1 refers to Nafion that had been purchased ~ 2 years before use. It was stored in water until it was used. Nafion membrane 2 was purchased more recently. It was soaked in Milli-Q water for a week before it was subjected to pre-treatment, as described above. The diffusion coefficients of As^{V} and As^{III} were measured through both Nafion membrane 1 and Nafion membrane 2 to examine if the 'age' of the membrane had an effect on the diffusion properties of the membrane and/or if the membrane manufacturing process was reproducible (therefore providing a similar Nafion membrane and similar As diffusion coefficients). All diffusion cell experiments used Nafion membrane 1. The measurement of As diffusion coefficients by DGT devices used both Nafion membrane 1 and Nafion membrane 2. For subsequent DGT experiments, no distinction between the two membranes was made.

It has been shown that there is a difference in the thickness of Nafion 117 membranes in their dry and wet states.[4, 6, 16, 17] The thickness of the wet state of the membrane is ~ 1.10 to 1.25

times larger than the dry state of the membrane.[4, 6, 16, 17] Presumably, there is also a difference between the dry and wet states of Nafion 112 membrane, however, the thickness of the dry Nafion 112 membrane (0.005 cm) was used for all diffusion coefficient calculations.

6.2.1 Measurement of As^{III} and As^{V} diffusion coefficients through a Nafion membrane at pH 5 using a diffusion cell

Measurement of diffusion coefficients of As^{III} and As^{V} through the Nafion membrane were carried out by placing a piece of Nafion in the opening that separates the two sides of the diffusion cell. A diffusive gel was not used in this work. These experiments were carried out using a diffusion cell that was specially designed to accommodate the thin Nafion membrane (see section 2.3.3.2).

6.2.1.1 As^{III} diffusion coefficients

The measurement of As^{III} diffusion coefficients through the Nafion membrane was carried out in duplicate. For the first measurement, both sides of the diffusion cell contained 1 mL of 1 mol L^{-1} $NaNO_3$, 2.5 mL of 1 mol L^{-1} sodium acetate (pH 5.0), 94.5 mL of Milli-Q water, and 2.5 ml of 1 mol L^{-1} NaOH; 2 mL of 1000 ppm As^{III} was added to compartment A and 2 ml of 'solution A' (containing 0.025 mol L^{-1} NaOH and 1.21 mol L^{-1} HCl) was added to compartment B of the diffusion cell. 'Solution A' was added to compartment B to match the matrix of the As standard added to compartment A. The final concentrations of $NaNO_3$ and sodium acetate in both sides of the diffusion cell were 0.01 and 0.025 mol L^{-1}, respectively. The concentration of As^{III} in compartment A was ~ 20 ppm. The NaOH was added to adjust the pH to ~ 5.0.

The pH was measured at the end of the experiment to make sure that it had not changed significantly. Both sides of the diffusion cell were stirred using small magnetic followers. Samples of solution were removed from compartment B of the diffusion cell (2 to 0.2 mL) every 10 to 15 mins so that the As concentration could be determined after appropriate dilution. An equivalent volume was also removed from compartment A to maintain the same volume in each side of the diffusion cell. Replicate samples were removed and analysed from compartment B of the diffusion cell for at least 2 sampling times to determine reproducibility. The temperature in compartment A of the diffusion cell was measured at the start and end of the experiment. In addition, whenever replicate samples were removed for analysis, the

temperature was also measured. It is the average of these temperature measurements that is reported in the results section.

Samples were removed from compartment A of the diffusion cell at the start and end of the experiment to determine the actual (rather than calculated) concentration of As^{III} initially present and to make sure that the As concentration had not changed significantly during the experiment. The measured As^{III} concentration is used to determine the As^{III} diffusion coefficient. All samples removed during the experiments were analysed within 2 h.

For the duplicate As^{III} diffusion cell experiment, there was a slight variation in the diffusion cell solutions used. Both sides of the diffusion cell contained 1 mL of 1 mol L^{-1} $NaNO_3$, 2.5 mL of 1 mol L^{-1} sodium acetate (pH 5.0), 94.5 mL of Milli-Q water, and 1 mL of 1 mol L^{-1} NaOH; 1 mL of 1000 ppm As^{III} was added to compartment A and 1 ml of 'solution A' was added to compartment B of the diffusion cell. The concentration of As^{III} in compartment A was ~ 10 ppm. All other procedures (i.e. pH measurements, sampling, and temperature measurements) were the same as for the first experiment.

6.2.1.2 As^{V} diffusion coefficients

The measurement of the As^{V} diffusion coefficient through the Nafion membrane was carried out once. Both sides of the diffusion cell contained 1 mL of 1 mol L^{-1} $NaNO_3$, 2.5 mL of 1 mol L^{-1} sodium acetate (pH 5.0), 94 mL of Milli-Q water, and 2.75 ml of 1 mol L^{-1} NaOH; 2.5 mL of 10,000 ppm As^{V} was added to compartment A and 2.5 ml of 'solution B' (containing 1.21 mol L^{-1} HCl) was added to compartment B of the diffusion cell. 'Solution B' was added to compartment B to match the matrix of the As^{V} standard added to compartment A. The final concentrations of $NaNO_3$ and sodium acetate in both sides of the diffusion cell were 0.01 and 0.025 mol L^{-1}, respectively. The concentration of As^{III} in compartment A was ~ 250 ppm. The NaOH was added to adjust the pH to 5.

A procedure similar to that outlined above for the measurement of As^{III} diffusion coefficients (i.e. pH measurements, sampling, and temperature measurements) was used for this experiment.

6.2.2 Measurement of As^{III} and As^{V} diffusion coefficients through a Nafion membrane at pH 5 using DGT devices

The diffusion coefficients of As^{III} and As^{V} through the Nafion membrane were measured using the modified DGT devices described in section 2.3.4.2. This was carried out by deploying DGT devices in As^{III} and As^{V} solutions for set times and measuring the mass of As accumulated on the iron-oxide adsorbent. Using the DGT equation, the diffusion coefficient was calculated. The DGT devices were assembled and deployed as described in chapter 2; a diffusive gel was not used in this work.

6.2.2.1 As^{III} diffusion coefficients

The diffusion coefficient of As^{III} was measured through the Nafion membrane 1 once and the Nafion membrane 2 twice.

The As^{III} deployment solutions were prepared by diluting 40 mL of 1 mol L^{-1} $NaNO_3$, 100 mL of 1 mol L^{-1} sodium acetate (pH 5.0) and 24 mL of 10 ppm As^{III}, to 4 L. The final concentrations of $NaNO_3$, sodium acetate and As^{III} in the deployment solutions were 0.01 mol L^{-1}, 0.025 mol L^{-1}, and ~ 60 ppb, respectively. A small volume of 1 mol L^{-1} NaOH was added to adjust the pH to ~ 5. The pH of the As^{III} deployment solutions was measured at the start and end of the experiments. The temperature of the As^{III} solutions was measured at the start, end, and at least one other time during the experiment. The average of these temperatures is reported in the results section. The solutions were left to stand for ~ 1 h before DGT devices were deployed in the well-stirred solutions (stirring rate of 630 rpm was used for all DGT experiments in this chapter) for > 25 h. The exact deployment times were recorded. After retrieval, DGT devices were placed in Milli-Q water and then washed thoroughly before disassembling and removal of the iron-oxide gel adsorbent. The same elution and analysis procedure was used as described in chapters 4 and 5.

Samples were removed from the As^{III} deployment solutions at the start and end of the experiment to confirm that the As concentration had not changed significantly over this time. These samples were stabilized by adding concentrated HCl to give a final concentration of 1.1 mol L^{-1} HCl and analysed at the same time as the DGT eluents. The As concentrations and masses determined from these samples were used to calculate the As^{III} diffusion coefficients. In addition, an As^{III} analysis was carried out on the deployment solution at the

end of the experiment to confirm that oxidation of As^{III} had not occurred during the experiments. When calculating the As^{III} diffusion coefficients using DGT devices, a 100 % elution efficiency was assumed.

6.2.2.2 As^{V} diffusion coefficients

The diffusion coefficient of As^{V} was measured through the 'Nafion 1' membrane once and the 'Nafion 2' membrane once.

The As^{V} deployment solutions were prepared by diluting 40 mL of 1 mol L^{-1} $NaNO_3$, 100 mL of 1 mol L^{-1} sodium acetate (pH 5.0), and 12 mL of 1000 ppm As^{V}, to 4 L. The final concentrations of $NaNO_3$, sodium acetate, and As^{V} in the deployment solutions were 0.01 mol L^{-1}, 0.025 mol L^{-1}, and ~ 3000 ppb respectively. A small volume of 1 mol L^{-1} NaOH was added to adjust the pH to ~ 5. The solutions were left to stand for ~ 1 h before DGT devices were deployed in the well-stirred solutions for > 26 h. The exact deployment times were recorded.

A similar procedure to that outlined above for the measurement of As^{III} diffusion coefficients using DGT devices (i.e. pH measurements, temperature measurements, sampling and DGT devices retrieval and elution) was used for the As^{V} experiments, except that an As^{III} analysis was not carried out on the deployment solution.

6.2.3 Effect of pH on mass of As^{III} and As^{V} accumulated by DGT with a Nafion membrane

The effect of pH on the mass of As accumulated by DGT in the presence of a Nafion membrane was examined by measuring the mass of As^{III} or As^{V} (depending on the experiment) accumulated within DGT devices at pH ~ 3 and ~ 7 for As^{III} experiments and at pH ~ 3 for As^{V} experiments. The mass of As accumulated within DGT devices was compared to the predicted mass of As which was calculated using the As^{V} or As^{III} diffusion coefficients that were measured with DGT devices at pH 5.0 (section 6.3.2). The DGT devices were assembled and deployed as described in chapter 2. The As deployment solutions were prepared by diluting 40 mL of 1 mol L^{-1} $NaNO_3$, 100 mL of 1 mol L^{-1} sodium acetate (pH 5.0), and either 24 mL of 10 ppm As^{III} or 12 mL of 1000 ppm As^{V} (depending on the experiment), to 4 L. The final concentrations of $NaNO_3$ and sodium acetate in the deployment

solutions were 0.01 mol L^{-1} and 0.025 mol L^{-1}, respectively. The final concentration of As in the deployment solution was ~ 60 ppb for As^{III} experiments and ~ 3000 ppb for As^{V} experiments. Concentrated HNO_3 was added to adjust the pH of the deployment solution to ~ 3; 1 mol L^{-1} NaOH was added to adjust the pH to ~ 7.0, depending on the experiment that was carried out. The solutions were left to stand for ~ 1 h before DGT devices were deployed in the well-stirred solutions for > 22 h. The exact deployment times were recorded. The same elution and analysis procedure to that described previously (section 6.2.2) was used.

Samples were removed from the As deployment solution at the start and end of the experiment to confirm that the As concentration had not changed significantly over this time. These samples were stabilized by adding concentrated HCl to give a final concentration of 1.1 mol L^{-1} HCl and analyzed at the same time as the DGT eluents. The As concentration determined from the samples was used to calculate the predicted mass. For the As^{III} experiments, an As^{III} analysis was carried out on the deployment solution at the end of the experiment to make sure that oxidation of As^{III} had not occurred.

6.2.4 Effect of anions and cations on mass of As^{III} and As^{V} accumulated by DGT with a Nafion membrane

The effect that major anions and cations have on the mass of As^{III} and As^{V} accumulated by DGT in the presence of a Nafion membrane was examined using a synthetic natural water. This was carried out by measuring the mass of As accumulated from an As^{V} or As^{III} solution (depending on the experiment) containing anions and cations, and comparing it to the predicted mass of As, which was calculated using the As^{III} and As^{V} diffusion coefficients measured using DGT devices (section 6.3.2). These experiments were carried out separately for solutions containing As^{V} or As^{III}. The DGT devices were assembled and deployed as described in chapter 2. The As deployment solutions were prepared by diluting 40 mL of $NaNO_3$, 100 mL of sodium acetate (pH 5.0), 10 mL of 0.1 mol L^{-1} NaCl, 2 mL of 0.1 mol L^{-1} KNO_3, 15 mL of 0.1 mol L^{-1} $Ca(NO_3)_2$, 5.6 mL of 0.1 mol L^{-1} $MgSO_4$, and either 24 mL of 10 ppm As^{III} or 12 mL of 1000 ppm As^{V} (depending on the experiment), to 4 L. The final concentration of As in the deployment solution was ~ 60 ppb for As^{III} experiments and ~ 3000 ppb for As^{V} experiments. A small volume of 1 mol L^{-1} NaOH was added to adjust the pH to ~ 5. The solutions were left for ~ 1 h before DGT devices were deployed in the well-

stirred solutions for > 25 h. The exact deployment times were recorded. The same elution and analysis procedure to that described previously (section 6.2.2) was used.

Samples were removed from the As deployment solution at the start and end of the experiment to confirm that the As concentration had not change significantly over this time. These samples were stabilized by adding concentrated HCl to give a final concentration of 1.1 mol L^{-1} HCl and analysed at the same time as the DGT eluents. The As concentration determined from the samples was used to calculate the predicted mass. For the As^{III} experiments, an As^{III} analysis was carried out on the deployment solution at the end of the experiment to make sure that oxidation of As^{III} had not occurred.

Table 6.1 shows the approximate concentrations of anions and cations present in the deployment solutions. The typical concentrations of anions and cations present in river water were obtained from Langmuir,[18] Morel and Hering[19] and Smith *et al*.[20]

Anion or cation	Concentration
Cl^-	8.8 ppm
K^+	2.0 ppm
Ca^{2+}	15.0 ppm
Mg^{2+}	3.5 ppm
SO_4^{2-}	14 ppm

Table 6.1 Concentrations of anions and cations present in the As^{V} and As^{III} deployment solutions

Pre-treatment of the Nafion membrane was also examined. After cleaning the membrane with 5 % v/v HNO_3, the Nafion membranes were placed in 1 of 3 pre-treatment solutions for at least 24 h. The Nafion membranes were stored in their corresponding pre-treatment solutions until use. Pre-treatment solution A contained 0.01 mol L^{-1} $NaNO_3$ and 0.025 mol L^{-1} sodium acetate (pH 5.0). Pre-treatment solution B contained 0.01 mol L^{-1}, 0.025 mol L^{-1} sodium acetate (pH 5.0), and 0.38 mmol L^{-1} $Ca(NO_3)_2$. Pre-treatment solution C contained 0.01 mol L^{-1} $NaNO_3$, 0.025 mol L^{-1} sodium acetate (pH 5.0), 0.38 mmol L^{-1} $Ca(NO_3)_2$, 0.25 mmol L^{-1} NaCl, 0.05 mmol L^{-1} KNO_3, and 0.l4 mmol L^{-1} $MgSO_4$; this pre-treatment solution has the same composition as the DGT deployment solutions except it did not contain As.

For the As^{III} experiments, 3 DGT devices containing membranes that were pre-treated using solution B, 2 DGT devices containing membranes that were pre-treated using solution A, and 2 DGT devices containing membranes that were pre-treated using solution C, were deployed. For the As^{V} solution, 2 DGT devices containing Nafion membranes that were pre-treated in each solution were deployed.

6.3 Results

6.3.1 Measurement of As^{III} and As^{V} diffusion coefficients through a Nafion membrane at pH 5 using a diffusion cell

6.3.1.1 As^{III} diffusion coefficients

The result from one As^{III} diffusion cell experiment is illustrated in Figure 6.3; it shows the mass of As^{III} in compartment B of the diffusion cell *vs*. time after addition of As^{III} to compartment A. Good linearity is observed between the mass of As^{III} diffused through the Nafion membrane and time. The As^{III} diffusion coefficient through the Nafion membrane was calculated from the slope of the plot in Figure 6.3 and using the DGT equation. The As^{III} diffusion coefficient was calculated to be $(2.60 \pm 0.10) \times 10^{-7}$ cm^2 s^{-1} (pH 5.0, 24.5 ± 0.5 ^{o}C) using the following parameters: slope = 213.34 ng min^{-1}; Δg = 0.005 cm; C = 21920 ppb; and A = 3.14 cm^2.

A duplicate experiment gave a diffusion coefficient of $(2.70 \pm 0.10) \times 10^{-7}$ cm^2 s^{-1} (pH 4.9, 25.5 ± 0.5 ^{o}C) using the following parameters: slope = 110.74 ng min^{-1}; Δg = 0.005 cm; C = 10895 ppb; and A = 3.14 cm^2. This value agrees within experimental uncertainty with the first measured diffusion coefficient. The uncertainty associated with the diffusion coefficients is a combination of the uncertainties in the slope of the diffusion cell plot (i.e. standard deviation of slope) and the initial concentration of As present in compartment A of the diffusion cell. Averaging the two calculated values and reporting an uncertainty of 1 standard deviation gives an As^{III} diffusion coefficient through the Nafion membrane of $(2.65 \pm 0.05) \times 10^{-7}$ cm^2 s^{-1}.

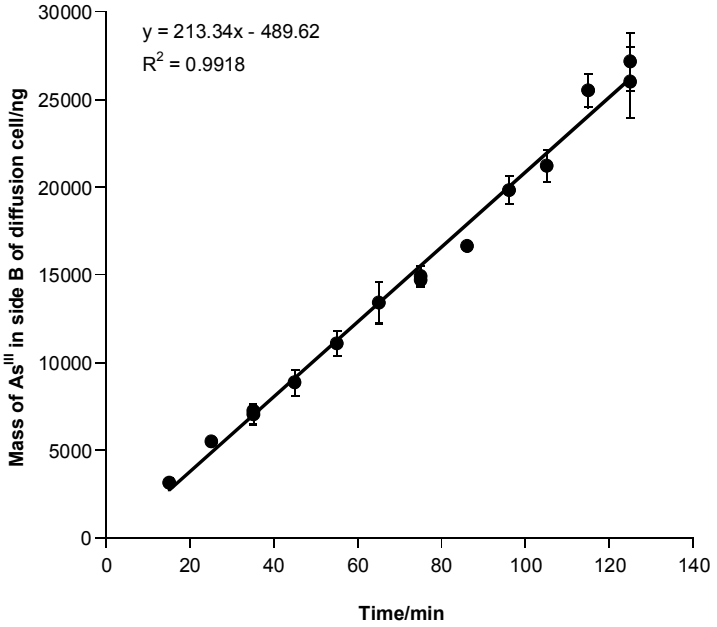

Figure 6.3 Mass of As^{III} diffused through Nafion membrane 1 with time during an As^{III} diffusion cell experiment. The uncertainty associated with each datum point is the standard deviation of the mean for at least two HG-AAS measurements. The concentrations of As^{III}, $NaNO_3$, and sodium acetate were 21920 ppb, 0.01 mol L^{-1}, and 0.025 mol L^{-1}, respectively. The average temperature during the experiment was 24.5 ± 0.5 ^{o}C. The pH was 5.0.

6.3.1.2 As^{V} diffusion coefficients

The result from the As^{V} diffusion cell experiment is illustrated in Figure 6.4; it shows the mass of As^{V} in compartment B of the diffusion cell *vs.* time after addition of As^{V} to compartment A. Reasonable linearity between the mass of As^{V} diffused through the Nafion membrane and time is observed. The As^{V} diffusion coefficient through the Nafion membrane was calculated from the slope of the plot in Figure 6.4 and using the DGT equation. The diffusion coefficient was calculated to be (4.25 ± 0.45) x 10^{-9} cm^2 s^{-1} (pH 5.0, 24.5 ± 0.5 ^{o}C) using the following parameters: slope = 40.465 ng min^{-1}; Δg = 0.005 cm; C = 253545 ppb; and A = 3.14 cm^2. The uncertainty associated with the As^{V} diffusion coefficient is derived from the same factors as for the As^{III} diffusion coefficient.

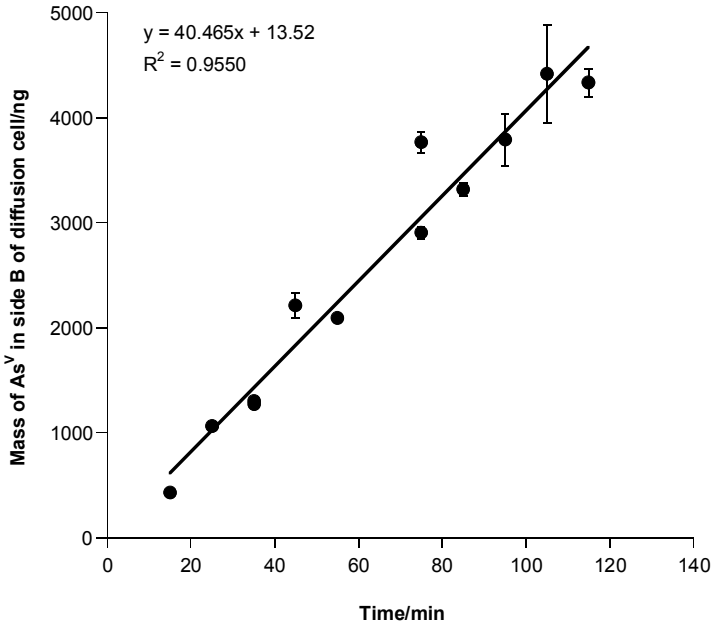

Figure 6.4 Mass of As^{V} diffused through Nafion membrane 1 with time during an As^{V} diffusion cell experiment. The uncertainty associated with each datum point is the standard deviation of the mean for at least two HG-AAS measurements. The concentrations of As^{V}, $NaNO_3$, and sodium acetate were 253545 ppb, 0.01 mol L^{-1}, and 0.025 mol L^{-1}, respectively. The average temperature during the experiment was 24.5 ± 0.5 ^{o}C. The pH was 5.0

Figure 6.4 shows a small positive y-intercept; however, if the standard deviation of the y-intercept (195 ng) is taken into account, the y-intercept may be negative

6.3.2 Measurement of As^{III} and As^{V} diffusion coefficients through a Nafion membrane at pH 5 using DGT devices

6.3.2.1 As^{III} diffusion coefficients

The diffusion coefficient of As^{III} through Nafion membranes 1 and 2 was determined by deploying modified DGT devices in an As^{III} solution and measuring the mass of As^{III} accumulated on the iron-oxide adsorbent. The diffusion coefficient of As^{III} was measured through Nafion membrane 1 and Nafion membrane 2 giving the values shown in Table 6.2. The diffusion coefficients were calculated using the DGT equation.

Experiment	Nafion[a]	Time[b]	[As^{III}][c]	Mass of As[d]	As^{III} diffusion coefficient
1	1	31.0 h	61 ± 4 ppb	1040 ± 105 ng (n = 3)	(2.45 ± 0.30) x 10^{-7} cm^2 s^{-1}
2	2	25.7 h	51 ± 3 ppb	685 ± 50 ng (n = 4)	(2.30 ± 0.20) x 10^{-7} cm^2 s^{-1}
3	2	25.7 h	59 ± 2 ppb	760 ± 50 ng (n = 3)	(2.20 ± 0.15) x 10^{-7} cm^2 s^{-1}

Table 6.2 As^{III} diffusion coefficients measured through a Nafion membrane using DGT devices. All experiments were carried out at pH 5.0 and 25.0 ± 1.0 °C. Note that 'n' refers to the number of DGT devices deployed. The other parameters used to determine the As^{III} diffusion coefficients were Δg = 0.005 cm and A = 3.14 cm^2. The uncertainty associated with the mass of As is the standard deviation of the mean mass of As accumulated from replicate DGT deployments. The uncertainty in the concentration of As^{III} initially in solution is the standard deviation of the mean for at least two HG-AAS measurements. The uncertainty associated with the diffusion coefficients are a combination of the uncertainty of the initial concentration of As^{III} present in the deployment solution and the mass of As accumulated on the iron oxide adsorbent. The relative standard deviation of replicate DGT deployments were < 10 % for all As^{III} experiments.

[a]Nafion membrane as described in the experimental section of this chapter

[b]Deployment time

[c]Concentration of As^{III} initially in solution

[d]Mass of As accumulated on iron-oxide adsorbent within DGT device

All of the DGT As^{III} diffusion coefficients agree within experimental uncertainty. Averaging the three calculated diffusion coefficients from Table 6.1 and reporting an uncertainty of 1 standard deviation, gives an As^{III} diffusion coefficient through the Nafion membrane of (2.30 ± 0.15) x 10^{-7} cm^2 s^{-1}.

6.3.2.2 As^{V} diffusion coefficients

The diffusion coefficient of As^{V} through Nafion membrane 1 and 2 was determined by deploying modified DGT devices in an As^{V} solution and measuring the mass of As^{V} accumulated on the iron-oxide adsorbent. The diffusion coefficient of As was calculated using the DGT equation. Table 6.3 shows the diffusion coefficients that were measured through the Nafion membrane.

Experiment	Nafion[a]	Time[b]	$[As^{V}]$[c]	Mass of As[d]	As^{V} diffusion coefficient
1	1	30.0 h	3025 ± 85 ppb	815 ± 85 ng (n = 2)	(3.95 ± 0.10) x 10^{-9} cm^2 s^{-1}
2	2	26.6 h	3185 ± 150 ppb	715 ± 55 ng (n = 4)	(3.75 ± 0.35) x 10^{-9} cm^2 s^{-1}

Table 6.3 As^{V} diffusion coefficients measured through a Nafion membrane. All experiments were carried out at pH 5.0 and 25.0 ± 1.0 ^{o}C. Note that 'n' refers to the number of DGT devices deployed. The other parameters used to determine the As^{III} diffusion coefficients were Δg = 0.005 cm and A = 3.14 cm^2. The uncertainties associated with the concentration of As^{V}, mass of As^{V}, and the diffusion coefficients have been derived from the same factors as described in the caption for Table 6.1. The relative standard deviation of replicate DGT deployments were < 10 % for all experiments.

[a]Nafion membrane as described in the experimental section of this chapter

[b]Deployment time

[c]Concentration of As^{V} initially in solution

[d]Mass of As accumulated on iron-oxide adsorbent within DGT device

The two As^{V} diffusion coefficients agree within experimental uncertainty. Averaging the two calculated diffusion coefficients from Table 6.3 and reporting an uncertainty of 1 standard deviation, gives an As^{V} diffusion coefficient through Nafion of (3.85 ± 0.15) x 10^{-9} cm^2 s^{-1}.

6.3.3 Effect of pH on mass of As^{III} and As^{V} accumulated by DGT with a Nafion membrane

The mass of As^{III} and As^{V} accumulated separately within DGT devices with a Nafion membrane was measured at pH ~ 3 and ~ 7 for As^{III}, and pH ~ 3 for As^{V}. The mass of As accumulated was compared with the predicted mass of As; the results are illustrated in Table 6.4 and the results for the As^{III} experiments are also illustrated in Figure 6.5.

For the As^{III} experiments, the mass of As accumulated within the DGT devices agrees within experimental uncertainty with the mass of As predicted at pH ~ 3 and ~ 7. For As^{V} at pH 3, the mass of As accumulated is ~ 11 times higher than the mass of As predicted. At pH 3, there will be ~ 17 % of the H_3AsO_4 species present; this will have a larger diffusion coefficient through Nafion than $H_2AsO_4^-$ because it is uncharged, hence an increase in mass of As on the iron-oxide is observed.

Experiment	Arsenic species	pH	Accumulated Mass of As	Predicted Mass of As	A-Mass/P-Mass[a]
1[b]	As^{III}	3.0	850 ± 60 ng (n = 6)	805 ± 55 ng	1.06 ± 0.15
2[c]	As^{III}	7.0	945 ± 25 ng (n = 5)	850 ± 80 ng	1.11 ± 0.13
3[d]	As^{V}	3.0	8035 ± 670 ng (n = 2)	730 ± 30 ng	11.0 ± 1.4

Table 6.4 Comparison of accumulated mass of As with predicted mass of As at pH ~ 3 and ~ 7 for As^{III} and pH ~ 3 for As^{V}. Note that 'n' refers to the number of DGT devices deployed. The uncertainty associated with the predicted mass is a combination of the uncertainties in the initial concentration of As present in solution and the As diffusion coefficients. The uncertainty associated with the mass of As accumulated is the standard deviation of the mean mass of As accumulated from replicate DGT deployments. The relative standard deviation of replicate DGT deployments were < 10 % for all experiments.

[a]accumulated mass/predicted mass

[b][As] = 58 ± 1 ppb, time = 26.8 h, temperature = 25.5 ± 1.0 °C

[c] [As] = 60 ± 4 ppb, time = 27.3 h, temperature = 24.5 ± 0.5 °C

[d] [As] = 3185 ± 45 ppb, time = 26.3 h, temperature = 25.0 ± 1.0 °C

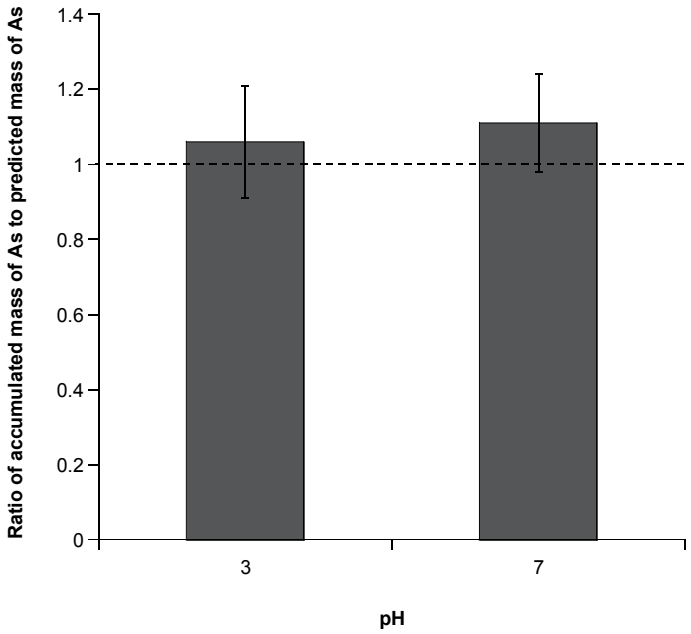

Figure 6.5 Ratio of accumulated mass of As^{III} to predicted mass of As^{III} at pH 3 and 7. The dotted line represents a ratio of 1.0. The uncertainty associated with the data is a combination of the uncertainty associated with the accumulated and predicted masses of As. Experimental conditions are described in the caption for Table 6.3.

6.3.4 Effect of anions and cations on mass of As^{III} and As^{V} accumulated by DGT with a Nafion membrane

The effect that anions and cations have on the mass of As^{III} and As^{V} accumulated by DGT with a Nafion membrane was examined by deploying DGT devices in As^{V} and As^{III} solutions containing anions and cations. The accumulated mass of As was compared with the predicted mass of As. In addition, membrane pre-treatment was also examined. The results are summarized in Table 6.5 and illustrated in Figure 6.6.

As species	Nafion pre-treatment	Accumulated mass of As	Predicted mass of As	A-Mass/P-Mass[a]
As^{III} [b]	A	765 ± 35 ng (n =2)	795 ± 55 ng	0.96 ± 0.11
	B	735 ± 85 ng (n =3)	795 ± 55 ng	0.92 ± 0.17
	C	805 ± 50 ng (n =2)	795 ± 55 ng	1.01 ± 0.13
As^{V} [c]	A	945 ± 40 ng (n =2)	765 ± 50 ng	1.24 ± 0.13
	B	875 ± 40 ng (n =2)	765 ± 50 ng	1.14 ± 0.13
	C	1035 ± 35 ng (n =2)	765 ± 50 ng	1.35 ± 0.14

Table 6.5 Effect of anions and cations and pre-treatment of Nafion membrane on mass of As^{III} and As^{V} accumulated by DGT in the presence of a Nafion membrane. Note that 'n' refers to the number of DGT devices deployed. The pre-treatment solutions were as follows: (A) 0.01 mol L^{-1} $NaNO_3$ and 0.025 mol L^{-1} sodium acetate (pH 5); (B) 0.01 mol L^{-1}, 0.025 mol L^{-1} sodium acetate (pH 5) and 0.38 mmol L^{-1} $Ca(NO_3)_2$; (C) 0.01 mol L^{-1} $NaNO_3$, 0.025 mol L^{-1} sodium acetate (pH 5), 0.38 mmol L^{-1} $Ca(NO_3)_2$, 0.25 mmol L^{-1} NaCl, 0.05 mmol L^{-1} KNO_3 and 0.l4 mmol L^{-1} $MgSO_4$. The uncertainties associated with the predicted and accumulated masses of As are derived from the same factors as described in the caption for Table 6.3. The relative standard deviations for replicate DGT deployments for the As^{V} and As^{III} experiments were < 5 % and < 10 % respectively.

[a]Accumulated mass/predicted mass

[b][As] = 58 ± 1 ppb, time = 26.8 h, temperature = 25.0 ± 1.0 °C, pH 5.0

[c] [As] = 3405 ± 195 ppb, time = 25.8 h, temperature = 25.0 ± 1.0 °C, pH 5.0

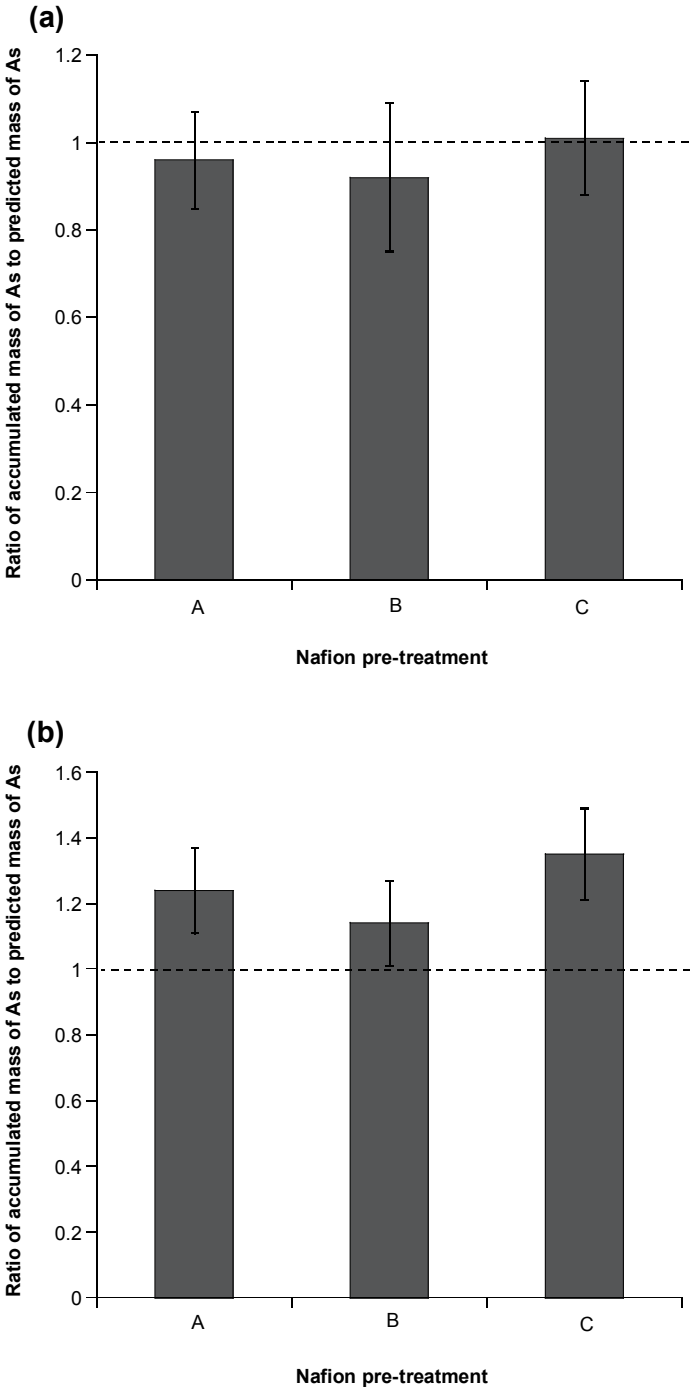

Figure 6.6 Ratio of accumulated mass of As to predicted mass of As for (a) As^{III} and (b) As^{V} in the presence of anions and cations for various Nafion pre-treatments. The dotted line represents a ratio of 1.0. The pre-treatments are described in the caption for Table 6.4. The uncertainty associated with the data is a combination of the uncertainty associated with the accumulated and predicted mass of As. Experimental conditions are described in the caption for Table 6.4.

For the As^{III} experiments, the mass of As accumulated for each Nafion pre-treatment procedure agreed within experimental uncertainty. In addition, the mass of accumulated As agreed within experimental uncertainty with the predicted mass of As for each pre-treatment procedure. For the As^{V} experiments, the mass of As accumulated for Nafion pre-treatment procedure A, B and C agreed within experimental uncertainty when the uncertainty in the predicted mass is taken into account. For the As^{V} experiments, none of the accumulated masses agreed within experimental uncertainty with the predicted mass of As.

6.4 Discussion

6.4.1 Measurement of As^{III} and As^{V} diffusion coefficients through a Nafion membrane at pH 5 using a diffusion cell and DGT devices

This section discusses the results from section 6.3.1 (measurement of As^{III} and As^{V} diffusion coefficients through Nafion using a diffusion cell at pH 5) and section 6.3.2 (measurement of As^{III} and As^{V} diffusion coefficients through Nafion using DGT devices at pH 5).

The As^{III} and As^{V} diffusion coefficients through the Nafion membrane were measured using a diffusion cell and DGT devices. The average As^{III} diffusion coefficient measured through a Nafion membrane by the use of a diffusion cell was $(2.65 \pm 0.05) \times 10^{-7}$ cm^2 s^{-1} (n = 2). The average As^{III} diffusion coefficient measured by the use of DGT devices was $(2.30 \pm 0.15) \times 10^{-7}$ cm^2 s^{-1} (n = 3). These values are in reasonable agreement with one another even though they do not agree within experimental uncertainty. For As^{V}, the diffusion coefficient measured through a Nafion membrane using a diffusion cell was $(4.25 \pm 0.45) \times 10^{-9}$ cm^2 s^{-1}. The average As^{V} diffusion coefficient measured by the use of DGT devices was $(3.85 \pm 0.15) \times 10^{-9}$ cm^2 s^{-1} (n = 2). These values agree within experimental uncertainty. For future work in this thesis, the diffusion coefficients measured using DGT devices will be used in all calculations.

It is important to note that if there was As^{III} present in the As^{V} solutions, the As^{V} diffusion coefficient would be overestimated as the As^{III} diffusion coefficient is much larger than that for As^{V}. It is difficult to perform an accurate As^{III} analysis on the As^{V} solutions as the concentration of As^{V} is high and causes interference with the As^{III} analysis, even when using optimized HG-AAS conditions. If 1 % As^{III} was present this would result in the As^{V} diffusion coefficient being overestimated by ~ 40 %; at 0.2 % As^{III}, the As^{V} diffusion coefficient would

be overestimated by ~ 10 %. The amount of As^{III} present in the As^{V} DGT solutions was < 0.5 % of the total As present. Hence the As^{V} diffusion coefficient could be overestimated by as much as 25 %.

The As^{III} and As^{V} diffusion coefficients were measured at pH 5.0. At this pH, As^{III} exists almost exclusively as H_3AsO_3, whereas As^{V} exists as ~ 99 % $H_2AsO_4^-$, 0.8 % $HAsO_4^{2-}$ and 0.2 % H_3AsO_4. The measured As^{V} diffusion coefficient is actually an average diffusion coefficient of the three As^{V} species. It is expected that the As^{V} species diffusion coefficients through the Nafion membrane would decrease in the order $H_3AsO_4 > H_2AsO_4^- > HAsO_4^{2-}$ due to the increase in charge of the As^{V} species. Even though only 0.2 % of H_3AsO_4 would be present, it could contribute a significant percentage of the total mass of As accumulated on the iron-oxide adsorbent within the DGT device or in compartment B of the diffusion cell, during the measurement of the As^{V} diffusion coefficients. If it is assumed that the diffusion coefficient of H_3AsO_4 through the Nafion membrane is similar to the diffusion coefficient of H_3AsO_3 through the Nafion membrane, then it is estimated that ~ 12 % of the mass of As^{V} accumulated within the DGT device or diffused through to compartment B of the diffusion cell, at pH 5, is due to the 0.2 % of uncharged As^{V} species, H_3AsO_4. Therefore the actual diffusion coefficient of $H_2AsO_4^-$ may be lower than the average As^{V} diffusion coefficient measured in the work for this thesis (i.e. $(3.85 \pm 0.15) \times 10^{-9}$ cm^2 s^{-1}). However, this small percentage of uncharged As^{V} would lead to a correspondingly small amount of As^{V} contributing to the measured 'As^{III}' concentration when using DGT with a Nafion membrane.

The reasonable agreement between the diffusion coefficients measured using the diffusion cell and DGT devices indicates that the modified diffusion cell and modified DGT devices, that were specially designed to measure diffusion coefficients through Nafion, function as intended. There was no evidence of a significant DBL in the diffusion cell relative to the DGT devices due to poorer stirring of solution within the diffusion cell. In addition, good linearity was obtained for all diffusion cell experiments.

For the measurement of As^{III} and As^{V} diffusion coefficients using DGT devices, different Nafion samples were used. The difference between the Nafion membranes, as described in section 6.2.2, was the time at which they were purchased. The good agreement in both the As^{III} and As^{V} diffusion coefficients measured through the two membranes implies that the 'age' of the membrane or its long-term storage, does not affect the diffusion coefficient of

either As^{III} or As^{V} significantly. In addition, the good agreement between the different Nafion membranes indicates good reproducibility in the membrane manufacturing process.

The lower diffusion coefficient measured for As^{V} ((3.85 ± 0.15) x 10^{-9} cm^2 s^{-1}) compared to As^{III} ((2.30 ± 0.15) x 10^{-7} cm^2 s^{-1}) is expected due to the repulsion between the negatively charged As^{V} species ($H_2AsO_4^-$) and the negatively charged sulfonate groups within the Nafion membrane. The diffusion coefficient of As^{V} is ~ 60 times lower than the diffusion coefficient of the uncharged As^{III} species (H_3AsO_3) due to electrostatic repulsion; however this ratio may be higher if As^{III} was contributing to the As^{V} diffusion coefficient measurements. The diffusion coefficient of As^{III} through the Nafion membrane ((2.30 ± 0.15) x 10^{-7} cm^2 s^{-1}) is ~ 25 times lower than the diffusion coefficient of As^{III} through the polyacrylamide diffusive gel ((5.85 ± 0.30) x 10^{-6} cm^2 s^{-1}). This suggests that the Nafion membrane also inhibits the free diffusion of As^{III} to an extent. This may be due to different porosities, water content, or pore size between the Nafion membrane and the diffusive gel. Another contributing factor may be the negative charge associated with the Nafion membrane which slows the diffusion of the As^{III} species due to its polarity.

The diffusion coefficients of As^{III} and As^{V} through a Nafion 117 membrane have been measured previously in our laboratory using a diffusion cell (in the presence of a polyacrylamide diffusive gel) and DGT devices (in the presence of a filter membrane).[1] This is a different Nafion product from the one used in the work for this thesis (i.e. Nafion 112). The thickness of the Nafion 117 membrane is 0.018 cm; the thickness of the Nafion 112 membrane is 0.005 cm.

Stillwell[1] made three measurements of the As^{III} diffusion coefficient through a Nafion membrane and a polyacrylamide gel using a diffusion cell in a 0.01 $NaNO_3$ mol L^{-1} medium. The values obtained by Stillwell[1] were: (7.53 ± 0.12) x 10^{-7} cm^2 s^{-1}, (6.65 ± 0.67) x 10^{-7} cm^2 s^{-1} and (4.56 ± 0.20) x 10^{-7} cm^2 s^{-1}. None of these values agrees within experimental uncertainty. The diffusion coefficient of As^{III} through the Nafion membrane and filter membrane using DGT devices was measured from a single experiment in which DGT devices were deployed for various times. The medium used was 0.0125 mol L^{-1} sodium acetate (pH 5.0). The diffusion coefficient calculated from this method was (4.64 ± 0.37) x 10^{-7} cm^2 s^{-1}. The poor reproducibility obtained by Stillwell[1] for the diffusion cell experiments may be due to leakage of solution from one side of the diffusion cell to the other, due to a

poor seal with the Nafion membrane. Stillwell[1] used a different diffusion cell from that employed in the work for this thesis. In addition, poor contact between the Nafion membrane and the diffusive gel may result in poor reproducibility. The As^{III} diffusion coefficients through the Nafion membrane are of the same magnitude as those measured in the work for this thesis.

The As^{V} diffusion coefficients measured by Stillwell[1] using a diffusion cell were calculated using one datum point as the amount of As^{V} diffused through the Nafion membrane was too low to measure as a function of time. For this work the composition of the diffusion cell solution medium was 0.01 mol L^{-1} $NaNO_3$ and 0.05 sodium acetate (pH 5.0). The measured values were: $(8.82 \pm 0.13) \times 10^{-9}$ cm^2 s^{-1}, $(1.09 \pm 0.05) \times 10^{-9}$ cm^2 s^{-1} and $(2.64 \pm 0.14) \times 10^{-8}$ cm^2 s^{-1}. For these As^{V} experiments, Stillwell[1] observed leakage in the diffusion cell. The diffusion coefficient of As^{V} through the Nafion membrane is very low and hence very minor leakage in the diffusion cell would contribute significantly to the measured mass of As^{V} in compartment B. The diffusion coefficient of As^{V} through Nafion and a membrane filter using DGT devices could not be measured by Stillwell[1] due to the mass of As^{V} on the adsorbent being less than the detection limit of the instrument used to determine As. The As^{V} diffusion coefficients measured by Stillwell[1] using a diffusion cell are of the same magnitude as those measured in the work for this thesis.

The higher diffusion coefficients measured by Stillwell,[1] in comparison to the diffusion coefficients measured in the work for this thesis, may be due to the use of a different Nafion membrane (Nafion 117 *vs*. Nafion 112) or to leakage of solution due to a poor seal in the diffusion cell and DGT devices. In addition, Stillwell[1] used the thickness of the diffusive gel and the Nafion membrane to calculate the As diffusion coefficients that were determined from diffusion cell experiments; it may have been more appropriate to use only the thickness of the Nafion membrane. The Nafion membrane would control the overall rate of mass transport of As to the adsorbent within the DGT device due to the diffusion coefficient being ~ 25 times lower in the Nafion membrane than the diffusive gel for As^{III}, and ~ 1300 times lower for As^{V}. Using the thickness of the Nafion membrane and diffusive gels for calculation of the As diffusion coefficients would result in an overestimation of the diffusion coefficient. This agrees with the observation that, with one exception, the diffusion coefficients through the Nafion membrane measured by Stillwell[1] are larger than those measured in the work for this thesis. Stillwell[1] also measured a smaller As^{III} diffusion coefficient through the Nafion

membrane than through the diffusive gel which agrees with the results from the work in this thesis. Considering the use of Nafion 112 *vs*. 117, the thickness of the Nafion 112 membrane is also an advantage over the 117 membrane which is 0.18 mm thick (~ 3.6 times thicker than the Nafion 112 membrane). For a 24 h DGT deployment in a 60 ppb As^{III} solution using a Nafion 117 membrane, and assuming a similar diffusion coefficient to that in the Nafion 112 membrane, then the mass of As accumulated would be ~ 200 ng. (c.f. ~ 730 ng for the Nafion 112 membrane). Better sensitivity is obtained using a thinner Nafion membrane.

Instead of using a Nafion membrane to slow diffusion of the As^{V} species, it may be possible to use a negatively charged gel in the same way as a diffusive gel is used in DGT. This idea was briefly considered as a way to provide a good seal for a diffusion cell and DGT devices that had not been modified. Negatively charged gels containing sulfonic acid groups have been synthesized.[21-26] These are based on the use of 2-acrylamido-2-methylpropane sulfonic acid (AMPS) as a co-monomer. An advantage of using a sulfonate gel, may be the ability to control the amount of negative charge within the gel by varying the amount of AMPS used. This may allow greater difference in the As^{III} and As^{V} diffusion coefficients than the ~ 60 times difference obtained with the Nafion membrane. However a number of drawbacks to the use of such a gel were identified. Firstly, it may be difficult to reproduce the exact gel composition each time the gel is synthesized. A second difficultly is that if the gel was the same thickness as the diffusive gel typically used in DGT (0.8 mm) and the As^{III} diffusion coefficient was similar to that for the Nafion membrane, only very small amounts of As^{III} would be accumulated. For example, 24 h deployment in a 60 ppb As^{III} solution would yield ~ 45 ng of As^{III} compared with ~ 730 ng accumulated through a 0.05 mm thick Nafion membrane. Sensitivity may be improved by using a thinner sulfonate diffusive gel or longer deployment times. However, it may be difficult to prepare an intact gel of 0.05 mm thickness due to poor mechanical strength; longer deployment times may be impractical or may be affected by bio-fouling. Hence this approach was not pursued.

6.4.2 Effect of pH on mass of As^{III} and As^{V} accumulated by DGT with a Nafion membrane

The effect of pH on the mass of As^{III} and As^{V} accumulated by DGT with a Nafion membrane was examined by measuring the mass of As^{III} accumulated by DGT at pH ~ 3 and ~ 7 and measuring the mass of As^{V} accumulated by DGT at pH ~ 3. The accumulated mass of As was

compared to the predicted mass of As. The good agreement between the measured and predicted mass of As^{III} indicates that pH has minimal effect on the mass of As^{III} accumulated by DGT, and hence it is concluded that varying the pH between 3 and 7 does not measurably affect the diffusion coefficient of As^{III} through the Nafion membrane. Over the pH range investigated, the As^{III} species exists almost exclusively as H_3AsO_3 and no change in the diffusion coefficient is expected. The pH would also have very little effect on the composition of the Nafion membrane. Kreuer[27] reports that the pK_a of Nafion is ~ -6; Ma *et al*.[16] reports that the pK_a of Nafion is ~ -3.1, which is between the pK_a for methane sulfonic acid (pK_a = -1.0) and triflic acid (pK_a = -5.1).[16] Therefore, over the pH range 3 to 7, the sulfonate groups within the Nafion membrane would be 100 % deprotonated and interactions between the membrane and H_3AsO_3 should be independent of pH.

For As^{V} at pH 3.0, the accumulated mass was ~ 11 times higher than the predicted mass which was calculated using the As^{V} diffusion coefficient at pH 5. At pH 5, ~ 99 % of As^{V} exists as $H_2AsO_4^-$. However at pH 3.0, As^{V} exists as 83 % $H_2AsO_4^-$ and 17 % H_3AsO_4. If it is assumed that the uncharged As^{V} species (H_3AsO_4) has a similar diffusion coefficient through Nafion as the uncharged As^{III} species (H_3AsO_3), then a more realistic predicted mass is calculated. Using these assumptions, the predicted mass was calculated to be ~ 8000 ± 800 ng. This is in good agreement with the accumulated mass of 8035 ± 670 ng. This result indicates that there is significant diffusion of As^{V} through the Nafion membrane at low pH due to the presence of the uncharged As^{V} species (H_3AsO_4). This has implications for the use of DGT with a Nafion membrane to selectively accumulate As^{III} at low pH and the feasibility of this approach would depend on the As^{V} to As^{III} ratio.

6.4.3 Effect of anions and cations on mass of As^{III} and As^{V} accumulated by DGT with a Nafion membrane

The effect that anions and cations have on the mass of As^{III} and As^{V} accumulated with DGT devices incorporating a Nafion membrane was examined by deploying DGT devices in As^{V} and As^{III} solutions containing anions and cations. The accumulated mass was compared to the predicted mass. In addition, various pre-treatments of the membrane were examined.

For the As^{III} experiments, the accumulated mass of As agreed within experimental uncertainty with the predicted mass for every Nafion pre-treatment. This suggest that

deployment of DGT devices with a Nafion membrane in a solution containing anions and cations, at concentrations typical for an unpolluted water, does not affect the mass of As^{III} accumulated by DGT with a Nafion membrane. If cations are associating with the negatively charged sulfonate groups within the Nafion membrane it does not significantly affect the diffusion of As^{III}. In addition, there does not seem to be any significant advantage in the use of different pre-treatment procedures of the Nafion membrane, as all of the accumulated masses for the various pre-treatments agreed within experimental uncertainty.

In contrast for the As^{V} experiments, the accumulated mass of As did not agree within experimental uncertainty with the predicted mass for any of the Nafion pre-treatment procedures. The accumulated mass of As was between 1.14 to 1.35 times higher than the predicted mass. The Nafion membrane that was pre-treated by immersing in a solution containing all major anions and cations (i.e. the same composition as the deployment solution) resulted in the largest mass of As^{V} accumulated. These results suggest that cations in solution such as Ca^{2+} and Mg^{2+} are associating with the negatively charged sulfonate groups. This would have the effect of shielding the negatively charged As^{V} species ($H_2AsO_4^-$) from the negatively charged sulfonate groups within the Nafion membrane. Therefore, because the negatively charged As^{V} species experience less electrostatic repulsion from the negatively charged sulfonate groups, within the Nafion membrane, the diffusion coefficient is increased. This leads to an increase in mass of As^{V} accumulated on the adsorbent within the DGT device. It has been suggested that a variety of cations,[4, 6, 28-31] including Mg^{2+}, Ca^{2+}, K^+ and Na^+,[4, 30, 31] can associate with a Nafion membrane via ion-exchange. However, the membranes that were pre-treated with only $NaNO_3$ and sodium acetate resulted in a higher mass of As accumulated than when the Nafion membrane was pre-treated in $NaNO_3$, sodium acetate, and $Ca(NO_3)_2$.

It is also possible that complexation of $H_2AsO_4^-$ by Ca^{2+} and Mg^{2+} in solution is occurring and therefore an increase in mass accumulated is observed as the As^{V} complexes formed are not negatively charged. For the concentrations of Ca^{2+} and As^{V} used in the work for this thesis, it was calculated that at pH 5, 0.25 % of $[CaHAsO_4]$ and 1 % of $[CaH_2AsO_4]^+$ would be present in solution. Assuming that the uncharged $[CaHAsO_4]$ species has a similar diffusion coefficient to H_3AsO_3 through the Nafion membrane, then the presence of 0.25 % $[CaHAsO_4]$ may contribute up to 12 to15 % of the mass of As^{V} accumulated on the adsorbent within the DGT devices. The contribution of the $[CaH_2AsO_4]^+$ species is unclear; it is

positively charged and is likely to partition with the negatively charged sulfonate groups within the Nafion membrane.

The increase in mass of As^{V} accumulated in a water containing anions and cations at typical concentrations as in an unpolluted water, would have only minor implications for the measurement of As^{III} concentration using DGT with a Nafion membrane. The As^{III} concentration would be slightly overestimated; this point will be addressed in more detail in chapter 7 (applications of DGT to natural waters).

For all further work involving DGT with a Nafion membrane, pre-treatment A was used. This is the pre-treatment procedure that has been used for all experiments other than in this section of work. This procedure, as described in section 6.2, involved soaking the Nafion membrane in Milli-Q water for at least 24 h and then cleaning in 5 % v/v HNO_3 for 24 h; the membrane was rinsed in Milli-Q water and stored in a solution containing 0.01 mol L^{-1} $NaNO_3$ and 0.025 mol L^{-1} sodium acetate (pH 5).

Various pre-treatment and cleaning procedures for Nafion membranes have been reported in the literature.[4, 17, 28-30, 32-35] These procedures usually involve the use of reagents such as HNO_3,[4, 28, 29, 34, 35] HCl,[4, 17, 29, 30, 32, 35] H_2SO_4,[33, 34] NaOH,[4, 29, 30, 32] and H_2O_2[17, 33-35] at various concentrations, temperatures, and pre-treatment times. Hydrogen peroxide and HNO_3 are used to oxidise any small molecular contaminants that have been introduced into the Nafion membrane during the manufacturing process;[4, 33, 35] such impurities may block the ion-conduction channels of the Nafion membrane.[35] The pre-treatment procedures remove the discolouration of the Nafion membrane to give a colourless membrane.[33, 35] These pre-treatments were briefly investigated in the work for this thesis. Boiling the Nafion membrane sequentially in 3 % H_2O_2 for 1 h, 6 mol L^{-1} HNO_3 for 1 h, and Milli-Q water for 1 h, produced a colourless membrane, indicating the removal of coloured impurities. However, the shape of the membrane disk changed from round to oval. Since these membranes had been pre-cut they could no longer be used in DGT devices due to the change in shape. More importantly the change of shape must correspond to a change in membrane structure. As a consequence this type of pre-treatment was not investigated further and the good reproducibility obtained for the diffusion coefficients of both As^{III} and As^{V} suggests that pre-treatment and extensive cleaning of the Nafion membrane with reagents such as H_2O_2 and HNO_3 is not critical for their application in DGT.

6.5 Conclusion

The As^{III} and As^{V} diffusion coefficients through Nafion were measured using a diffusion cell and DGT devices that were specially designed to accommodate Nafion and prevent solution leakage. The As^{III} and As^{V} diffusion coefficients measured through a Nafion 112 membrane using a diffusion cell were $(2.65 \pm 0.05) \times 10^{-7}$ cm^2 s^{-1} (n = 2) and $(4.25 \pm 0.45) \times 10^{-9}$ cm^2 s^{-1} (n = 1), respectively. Using DGT devices, the As^{III} and As^{V} diffusion coefficients through a Nafion 112 membrane were $(2.30 \pm 0.15) \times 10^{-7}$ cm^2 s^{-1} (n = 3) and $(3.85 \pm 0.10) \times 10^{-9}$ cm^2 s^{-1} (n = 2), respectively, assuming a 100 % elution efficiency. Reasonable agreement between the diffusion coefficients measured by the two methods was obtained. The diffusion coefficient of As^{III} through the Nafion membrane is ~ 60 times larger than the diffusion coefficient of As^{V}. This will allow selective accumulation of As^{III} in the presence of As^{V}, within certain limits, and hence the speciation of As. These limits are discussed in chapter 7.

The effect of pH on the mass of As^{III} accumulated was minimal as indicated by the good agreement between the predicted and accumulated As masses at pH 3, 5 and 7. For As^{V} at pH 3, the accumulated mass of As was ~ 11 times higher than that predicted using the diffusion coefficients measured at pH 5.0. This is due to protonation of the As^{V} species to form H_3AsO_4 which is less hindered by the negatively charged sulfonate groups within the Nafion membrane compared to $H_2AsO_4^-$. Therefore the selective accumulation of As^{III} in the presence of As^{V} will be dependent on pH.

The results from this chapter indicate that anions and cations in solution had no significant effect on the mass of As^{III} accumulated by DGT with a Nafion membrane. For As^{V}, there was evidence that an increase in diffusion coefficient had occurred due to cations shielding the negatively charged As^{V} species from the negatively charged sulfonate groups within the Nafion membrane, or due to complexation of the negatively charged As^{V} species. Pre-treatment of the Nafion membrane in solutions containing various anions and cations prior to DGT deployment did not offer any significant advantage for the diffusion of either As^{V} or As^{III} when compared to the general pre-treatment procedure that had been used for previous Nafion work.

.

6.6 References

1. Stilwell, K. *Arsenic speciation by diffusive gradients in thin films*. M.Sc. Thesis, University of Canterbury, New Zealand, 2003.

2. Ioselevich, A. S.; Kornyshev, A. A.; Steinke, J. H. G., Fine morphology of proton-conducting ionomers. *Journal of Physical Chemistry B* **2004,** 108, (32), 11953-11963.

3. Hickner, M. A.; Ghassemi, H.; Kim, Y. S.; Einsla, B. R.; McGrath, J. E., Alternative polymer systems for proton exchange membranes (PEMs). *Chemical Reviews* **2004,** 104, (10), 4587-4611.

4. Goswami, A.; Acharya, A.; Pandey, A. K., Study of self-diffusion of monovalent and divalent cations in Nafion-117 ion-exchange membrane. *Journal of Physical Chemistry B* **2001,** 105, (38), 9196-9201.

5. Sondheimer, S. J.; Bunce, N. J.; Fyfe, C. A., Structure and chemistry of Nafion-H - a fluorinated sulfonic-acid polymer. *Journal of Macromolecular Science-Reviews in Macromolecular Chemistry and Physics* **1986,** C26, (3), 353-413.

6. Dalla Costa, R. F.; Ferreira, J. Z.; Deslouis, C., Electrochemical study of the interactions between trivalent chromium ions and Nafion (R) perfluorosulfonated membranes. *Journal of Membrane Science* **2003,** 215, (1-2), 115-128.

7. Vishnyakov, A.; Neimark, A. V., Molecular dynamics simulation of microstructure and molecular mobilities in swollen Nafion membranes. *Journal of Physical Chemistry B* **2001,** 105, (39), 9586-9594.

8. Smitha, B.; Sridhar, S.; Khan, A. A., Solid polymer electrolyte membranes for fuel cell applications - a review. *Journal of Membrane Science* **2005,** 259, (1-2), 10-26.

9. Mauritz, K. A.; Moore, R. B., State of understanding of Nafion. *Chemical Reviews* **2004,** 104, (10), 4535-4585.

10. Hurst, M. P.; Bruland, K. W., The use of Nafion-coated thin mercury film electrodes for the determination of the dissolved copper speciation in estuarine water. *Analytica Chimica Acta* **2005,** 546, (1), 68-78.

11. Murimboh, J.; Lam, M. T.; Hassan, N. M.; Chakrabarti, C. L., A study of Nafion-coated and uncoated thin mercury film-rotating disk electrodes for cadmium and lead speciation in model solutions of fulvic acid. *Analytica Chimica Acta* **2000,** 423, (1), 115-126.

12. Morrison, G. M. P.; Florence, T. M., Electrochemical speciation analysis of metals at membrane-coated electrodes. *Electroanalysis* **1989,** 1, (6), 485-491.

13. Zen, J. M.; Jou, J. J.; Ilangovan, G., Selective voltammetric method for uric acid detection using pre-anodized Nafion-coated glassy carbon electrodes. *Analyst* **1998,** 123, (6), 1345-1350.

14. Liu, H. Y.; Deng, J. Q., Amperometric glucose sensor using tetrathiafulvalene in Nafion gel as electron shuttle. *Analytica Chimica Acta* **1995,** 300, (1-3), 65-70.

15. Blom, L. B.; Morrison, G. M.; Roux, M. S.; Mills, G.; Greenwood, R., Metal diffusion properties of a Nafion-coated porous membrane in an aquatic passive sampler system. *Journal of Environmental Monitoring* **2003,** 5, (3), 404-409.

16. Ma, C. S.; Zhang, L.; Mukerjee, S.; Ofer, D.; Nair, B. D., An investigation of proton conduction in select PEM's and reaction layer interfaces-designed for elevated temperature operation. *Journal of Membrane Science* **2003,** 219, (1-2), 123-136.

17. Saito, M.; Arimura, N.; Hayamizu, K.; Okada, T., Mechanisms of ion and water transport in perfluorosulfonated ionomer membranes for fuel cells. *Journal of Physical Chemistry B* **2004,** 108, (41), 16064-16070.

18. Langmuir, D., *Aqueous environmental geochemistry*. Prentice-Hall, Inc.: New York, 1997.

19. Morel, F. M.; Hering, J. G., *Principles and applications of aquatic chemistry*. John Wiley & Sons, Inc.: New York, 1993.

20. Smith, E.; Hamilton-Taylor, J.; Davison, W.; Fullwood, N. J.; McGrath, M., The effect of humic substances on barite precipitation-dissolution behaviour in natural and synthetic lake waters. *Chemical Geology* **2004,** 207, (1-2), 81-89.

21. Abdel-Azim, A. A. A.; Farahat, M. S.; Atta, A. M.; Abdel-Fattah, A. A., Preparation and properties of two-component hydrogels based on 2-acrylamido-2-methylpropane sulphonic acid. *Polymers for Advanced Technologies* **1998,** 9, (5), 282-289.

22. Atta, A. M.; Abdel-Azim, A. A., Synthesis of polymeric hydrogels containing sulfonate group. *Polymers for Advanced Technologies* **1999,** 10, (3), 187-194.

23. Durmaz, S.; Okay, O., Acrylamide/2-acrylamido-2-methylpropane sulfonic acid sodium salt-based hydrogels: Synthesis and characterization. *Polymer* **2000,** 41, (10), 3693-3704.

24. Travas-Sejdic, J.; Easteal, A. J., Effect of crosslink density and amount of charges on poly(acrylamide-co-2-acrylamido-2-methyl-1-propanesulphonic acid) gel structure. *Polymer* **2000,** 41, (7), 2535-2542.

25. Zaroslov, Y. D.; Philippova, O. E.; Khokhlov, A. R., Change of elastic modulus of strongly charged hydrogels at the collapse transition. *Macromolecules* **1999,** 32, (5), 1508-1513.

26. Zhang, C.; Easteal, A. J., Study of poly(acrylamide-co-2-acrylamido-2-methylpropane sulfonic acid) hydrogels made using gamma radiation initiation. *Journal of Applied Polymer Science* **2003,** 89, (5), 1322-1330.

27. Kreuer, K. D., On the development of proton conducting polymer membranes for hydrogen and methanol fuel cells. *Journal of Membrane Science* **2001,** 185, (1), 29-39.

28. Huang, K. L.; Holsen, T. M.; Selman, J. R., Impurity diffusion through Nafion and ceramic separators used for electrolytic purification of spent chromium plating solutions. *Journal of Membrane Science* **2003,** 221, (1-2), 135-146.

29. Logette, S.; Eysseric, C.; Pourcelly, G.; Lindheimer, A.; Gavach, C., Selective permeability of a perfluorosulphonic membrane to different valency cations. Ion-exchange isotherms and kinetic aspects. *Journal of Membrane Science* **1998,** 144, (1-2), 259-274.

30. Rollet, A. L.; Simonin, J. P.; Turq, P., Study of self-diffusion of alkali metal cations inside a Nafion membrane. *Physical Chemistry Chemical Physics* **2000,** 2, (5), 1029-1034.

31. Steck, A.; Yeager, H. L., Water sorption and cation-exchange selectivity of a perfluorosulfonate ion-exchange polymer. *Analytical Chemistry* **1980,** 52, (8), 1215-1218.

32. Suresh, G.; Scindia, Y. M.; Pandey, A. K.; Goswami, A., Isotopic and ion-exchange kinetics in the Nafion-117 membrane. *Journal of Physical Chemistry B* **2004,** 108, (13), 4104-4110.

33. Fang, C.; Wu, B. L.; Zhou, X. Y., Nafion membrane electrophoresis with direct and simplified end-column pulse electrochemical detection of amino acids. *Electrophoresis* **2004,** 25, (2), 375-380.

34. Berezina, N. P.; Timofeev, S. V.; Kononenko, N. A., Effect of conditioning techniques of perfluorinated sulphocationic membranes on their hydrophylic and electrotransport properties. *Journal of Membrane Science* **2002,** 209, (2), 509-518.

35. Sumner, J. J.; Creager, S. E.; Ma, J. J.; DesMarteau, D. D., Proton conductivity in Nafion (R) 117 and in a novel bis[(perfluoroalkyl)sulfonyl]imide ionomer membrane. *Journal of the Electrochemical Society* **1998,** 145, (1), 107-110.

Chapter 7

Application of DGT to natural waters

7.1 Introduction

The overall aim for the DGT work in this thesis was to develop a method to enable speciation of dissolved inorganic As in water samples, allowing the concentrations of both As^{V} and As^{III} to be determined. When deploying DGT devices without the Nafion membrane, the mass of As accumulated is given by equation 7.1, where $M_{Non\text{-}Nafion}$ is the mass of As accumulated by the DGT device without the Nafion membrane; $C_{As(III)}$ and $C_{As(V)}$ are the concentrations of As^{III} and As^{V} in solution, respectively; ${}^{g}D_{As(III)}$ and ${}^{g}D_{As(V)}$ are the As^{III} and As^{V} diffusion coefficients through the diffusive gel, respectively; and ${}^{g}\Delta g$ is the thickness of the diffusive gel. When deploying DGT devices with the Nafion membrane, the mass of As accumulated is given by equation 7.2, where M_{Nafion} is the mass of As accumulated by the DGT device with the Nafion membrane; $C_{As(III)}$ and $C_{As(V)}$ are the concentrations of As^{III} and As^{V} in solution, respectively; ${}^{N}D_{As(III)}$ and ${}^{N}D_{As(V)}$ are the As^{III} and As^{V} diffusion coefficients through the Nafion membrane, respectively; and ${}^{N}\Delta g$ is the thickness of the Nafion membrane.

$$M_{Non-Nafion} = \frac{(C_{As(III)}\,{}^{g}D_{As(III)} + C_{As(V)}\,{}^{g}D_{As(V)})At}{{}^{g}\Delta g} \qquad \textbf{(7.1)}$$

$$M_{Nafion} = \frac{(C_{As(III)}\,{}^{N}D_{As(III)} + C_{As(V)}\,{}^{N}D_{As(V)})At}{{}^{N}\Delta g} \qquad \textbf{(7.2)}$$

Deploying DGT devices with and without Nafion membranes, simultaneously, allows the accurate measurement of the concentrations of As^{III} and As^{V} by solving equations 7.1 and 7.2 simultaneously. The concentration of total dissolved As can be calculated by the addition of the As^{V} and As^{III} concentrations. This method of determining As concentrations (i.e. by solving equations 7.1 and 7.2) will be referred to as the "simultaneous equation DGT approach" in this chapter.

If a measurement of total dissolved inorganic As was only required then the DGT device without the Nafion membrane could be deployed alone to accumulate both As^{V} and As^{III}. However, the question arises as to which As diffusion coefficient should be used when determining the total As concentration from the mass of As accumulated within the DGT device. This question is addressed in section 7.1.1 below. Measuring the total dissolved inorganic As concentration by using only the non-Nafion DGT device will be referred to as a "direct" approach in this chapter.

Furthermore, the DGT device with the Nafion membrane can potentially be used for measuring dissolved inorganic As^{III} concentrations directly, within the limits of the device. However, if this approach is used then the following questions would need to be addressed:

- what is the limiting $[As^{V}]/[As^{III}]$ ratio that allows successful application of DGT to the selective accumulation of As^{III} in the presence of As^{V} (see section 7.1.2)?
- what is the pH limit that allows successful application of DGT to the selective accumulation of As^{III} in the presence of As^{V} (see section 7.1.3)?
- does the effect that major cations have on the diffusion coefficient of As^{V} through the Nafion membrane (i.e. increase in As^{V} diffusion coefficient) significantly influence the concentration of As^{III} determined by DGT with a Nafion membrane (see section 7.1.4)?

Measuring the dissolved inorganic As^{III} concentration by using only the Nafion DGT device will be referred to as a "direct" approach in this chapter.

7.1.1 Diffusion coefficient of As for determining the total As concentration directly using only a DGT device without a Nafion membrane

The results from chapter 4 showed that the diffusion coefficient of As^{III} through a polyacrylamide diffusive gel ($(5.95 \pm 0.30) \times 10^{-6}$ cm^2 s^{-1}) is ~ 20 % higher than the diffusion coefficient of As^{V} ($(4.90 \pm 0.05) \times 10^{-6}$ cm^2 s^{-1}) through a polyacrylamide diffusive gel. When deploying DGT in a water containing As^{V} and As^{III}, the total mass of As accumulated by DGT is a weighted average which depends on the concentrations of As^{V} and As^{III} present in solution, and their respective diffusion coefficients. Therefore, when only using a non-Nafion DGT device to measure the total dissolved inorganic As directly, there is some ambiguity as to which diffusion coefficient of As should be used when calculating the concentration of As,

from the mass of As accumulated within the DGT device. The As^V, the As^{III}, or the average diffusion coefficient ($D_{As(V)}$, $D_{As(III)}$, or D_{Ave}, respectively) could be used when calculating the total As concentration using the DGT equation. Table 7.1 shows the theoretical effect of using these three diffusion coefficients to calculate the apparent concentration of total dissolved As in solution at various $[As^V]/[As^{III}]$ ratios.

$[As^V]/[As^{III}]$	$D_{As(V)}$ [a]	D_{Ave} [b]	$D_{As(III)}$ [c]
100	0.2 %	-9 %	-17 %
10	2 %	-8 %	-15 %
5	3 %	-7 %	-14 %
1	10 %	0 %	-8 %
0.1	18 %	8 %	-2 %
0.01	20 %	9 %	-0.2 %

Table 7.1 Theoretical effect of using $D_{As(V)}$, D_{Ave}, and $D_{As(III)}$ to calculate the concentration of total As in solution at various $[As^V]/[As^{III}]$ ratios at pH 5. The values show the percentage of under or over estimation of the total As concentration from using the various diffusion coefficients. A negative value implies that the total concentration of As would be underestimated; a positive value implies that the total concentration of As would be overestimated.

[a]Diffusion coefficient of As^V through polyacrylamide gel (4.90×10^{-6} cm^2 s^{-1})

[b]Average As diffusion coefficient (i.e. $(D_{As(V)} + D_{As(III)})/2 = 5.45 \times 10^{-6}$ cm^2 s^{-1})

[c]Diffusion coefficient of As^{III} through polyacrylamide gel (5.95×10^{-6} cm^2 s^{-1})

Table 7.1 clearly shows that if the average As diffusion coefficient is used to calculate the total As concentration, for solutions containing $[As^V]/[As^{III}]$ ratios between 100 and 0.01, then the result will always be within 10 % of the actual total As concentration in solution. If As^V dominates As speciation then more accurate results are obtained when using the As^V diffusion coefficient, and vice versa for As^{III}.

7.1.2 $[As^V]/[As^{III}]$ ratio limit for the successful direct measurement of the As^{III} concentration using only a DGT device with a Nafion membrane

The results from chapter 6 showed that the diffusion coefficient of As^{III} ($(2.30 \pm 0.15) \times 10^{-7}$ cm^2 s^{-1}) through the Nafion membrane is at least 60 times larger than the diffusion coefficient of As^V ($(3.85 \pm 0.15) \times 10^{-9}$ cm^2 s^{-1}), through the Nafion membrane. Application of the

Nafion DGT method to measure the concentration of inorganic As^{III} directly assumes that all of the As on the iron-oxide adsorbent originates from As^{III} in solution. However, the negatively charged As^{V} species still diffuses through the negatively charged Nafion membrane; in many environmental situations the concentration of As^{V} in solution will be greater than the concentration of As^{III}. The suitability of the DGT method, with a Nafion membrane, to 'selectively' accumulate As^{III} in the presence of As^{V} will depend on the $[As^{V}]/[As^{III}]$ ratio. The larger the $[As^{V}]/[As^{III}]$ ratio, the greater the contribution that the mass of As^{V} will have on the As^{III} measurement and therefore the greater the extent to which the concentration of As^{III} determined by DGT would be overestimated. Table 7.2 shows the calculated effect that the $[As^{V}]/[As^{III}]$ ratio has on the apparent As^{III} concentration measured by DGT with a Nafion membrane at pH 5.

$[As^{V}]/[As^{III}]$	$[As^{III}]_{DGT}$ [a]	$R_{DGT/Sol}$ [b]
1	10.2 ppb	1.02
2	10.3 ppb	1.03
5	10.8 ppb	1.08
10	11.7 ppb	1.17
20	13.3 ppb	1.33
100	26.7 ppb	2.67

Table 7.2 Calculated effect of $[As^{V}]/[As^{III}]$ ratio on the concentration of As^{III} (10 ppb) directly measured by DGT with a Nafion membrane at pH 5.

[a]Calculated apparent concentration of As^{III} determined by DGT with a Nafion membrane using the As^{III} and As^{V} diffusion coefficients through Nafion

[b]Ratio of the concentration of As^{III} determined by DGT to the concentration of As^{III} in solution

Table 7.2 shows that for every $[As^{V}]/[As^{III}]$ ratio illustrated, the apparent concentration of As^{III} measured by DGT with a Nafion membrane is an overestimation of the actual As^{III} concentration. These calculations suggest that the use of DGT with a Nafion membrane, to directly measure the As^{III} concentration, could be applied for $[As^{V}]/[As^{III}]$ ratios up to ~ 10; higher ratios would significantly affect the accuracy of the As^{III} measurement.

7.1.3 pH limit for the successful direct measurement of the As^{III} concentration using only a DGT device with a Nafion membrane

The results from chapter 6 showed that when the solution pH was decreased from 5 to 3, the effective As^{V} diffusion coefficient increased significantly due to the presence of the

uncharged H_3AsO_4 species, whereas the diffusion coefficient of As^{III} through the Nafion membrane was not significantly affected between pH 3 and 7. Furthermore, calculations suggested that the diffusion coefficient of H_3AsO_4 through the Nafion membrane was similar to the diffusion coefficient of H_3AsO_3. These results imply that the use of the DGT method, with a Nafion membrane, to 'selectively' accumulate As^{III} at low pH will be significantly affected by the presence of As^{V}. Table 7.3 shows the theoretical effect that pH has on the concentration of As^{III} (10 ppb) determined by DGT at various $[As^{V}]/[As^{III}]$ ratios.

$[As^{V}]/[As^{III}]$	$[As^{III}]_{DGT\ pH\ 3.5}$[a] /ppb	$[As^{III}]_{DGT\ pH\ 4.0}$[b] /ppb	$[As^{III}]_{DGT\ pH\ 4.5}$[c] /ppb	$[As^{III}]_{DGT\ pH\ 5.0}$[d] /ppb
0.1	10.1 (1.01)	10.0 (1.00)	10.0 (1.00)	10.0 (1.00)
1	10.8 (1.08)	10.4 (1.04)	10.3 (1.03)	10.2 (1.02)
5	13.7 (1.37)	11.8 (1.18)	11.1 (1.11)	10.8 (1.08)
10	17.6 (1.76)	13.7 (1.37)	12.3 (1.23)	11.7 (1.17)

Table 7.3 Theoretical effect of pH on the concentration of As^{III} in solution (10 ppb) directly measured by DGT with a Nafion membrane at various $[As^{V}]/[As^{III}]$ ratios. It is assumed that the diffusion coefficient of H_3AsO_4 through the Nafion membrane is similar to the diffusion coefficient of H_3AsO_3. The diffusion coefficient of As through the Nafion membrane at pH 5 was used for these calculations. The values in brackets are the ratios of $[As^{III}]_{DGT}$ to the concentration of As^{III} in solution (i.e. 10 ppb).

[a] $[As^{III}]$ measured by DGT at pH 3.5 assuming ~94 % of As^{V} exists as $H_2AsO_4^-$ and ~6 % exists as H_3AsO_4

[b] $[As^{III}]$ measured by DGT at pH 4.0 assuming ~98 % of As^{V} exists as $H_2AsO_4^-$ and ~2 % exists as H_3AsO_4

[c] $[As^{III}]$ measured by DGT at pH 4.5 assuming ~99 % of As^{V} exists as $H_2AsO_4^-$ and ~0.64 % exists as H_3AsO_4

[d] $[As^{III}]$ measured by DGT at pH 5.0 using As^{V} and As^{III} diffusion coefficients measured at pH 5.

Note that solution speciation of As was calculated using the computer program SPECIES

Table 7.3 shows that as pH decreases the As^{III} concentration measured by DGT would increasingly be overestimated due to the uncharged As^{V} species, H_3AsO_4, contributing significantly to the total mass of As accumulated on the iron-oxide adsorbent within the DGT device.

7.1.4 Influence of cations present in solution on the successful direct measurement of the As^{III} concentration using only a DGT device with a Nafion membrane

The results from chapter 6 showed that the As^V diffusion coefficient through the Nafion membrane increased by ~ 25 % when cations were present in solution at concentrations typical of fresh waters. This would have the effect of increasing the mass of As^V diffused through the Nafion membrane and can further overestimate the As^{III} concentration measured directly by DGT with a Nafion membrane. Table 7.4 shows the theoretical effect that an increase in the As^V diffusion coefficient of ~ 25 % would have on the concentration of As^{III} measured by DGT with a Nafion membrane at pH 5.

$[As^V]/[As^{III}]$	$[As^{III}]_{DGT}$ [a] ($D_{As(V)}$ = 3.85 x 10^{-9} cm^2 s^{-1})	$[As^{III}]_{DGT}$ [b] ($D'_{As(V)}$ = 4.75 x 10^{-9} cm^2 s^{-1})	$R_{[As^{III}]_{D'}/[As^{III}]_D}$ [C]
10	11.6 ppb	12.0 ppb	1.03
5	10.8 ppb	11.0 ppb	1.02
1	10.2 ppb	10.2 ppb	1.00
0.1	10.0 ppb	10.0 ppb	1.00

Table 7.4 Theoretical effect of a ~ 25 % increase in As^V diffusion coefficient through the Nafion membrane on the concentration of As^{III} in solution (10 ppb) directly measured by DGT with a Nafion membrane at various As^V to As^{III} ratios.

[a]Calculated concentration of As^{III} using $D_{As(V)}$ = 3.85 x 10^{-9} cm^2 s^{-1}

[b]Calculated concentration of As^{III} using $D'_{As(V)}$ = 4.75 x 10^{-9} cm^2 s^{-1} (i.e. $D' = D$ x 1.25)

[c]Ratio of $[As^{III}]_{DGT}$ concentration measured using $D_{As(V)}$ = 3.85 x 10^{-9} cm^2 s^{-1} to $[As^{III}]_{DGT}$ concentration measured using $D'_{As(V)}$ = 4.75 x 10^{-9} cm^2 s^{-1}

Table 7.4 shows that the ~ 25 % increase in diffusion coefficient of As^V in the presence of cations (at the concentrations used for the study in chapter 6) has a very minor affect on the concentration of As^{III} directly measured by DGT when the As^V to As^{III} ratio is varied between 0.1 and 10. However, higher cation concentrations may affect the As^V diffusion coefficient to a greater extent than the concentrations examined in the work for this thesis.

7.1.5 Chapter outline

This chapter is concerned with the determination of total As, As^{III}, and As^V concentrations in two well water samples and a river water spiked with two $[As^V]/[As^{III}]$ ratios.

The presence of cations, anions, and fulvic acid showed no significant effect on the mass of As^{V} and As^{III} accumulated by DGT from synthetic solutions (chapter 5), however cumulative affects were not investigated. In addition, there will be species that are present in the natural water samples that were not present in the prepared synthetic solutions. Therefore, if good agreement between the As concentrations measured by DGT and HG-AAS are obtained for the natural water samples then this is a definitive result that a 'true' natural water has little effect on the DGT measurement for As.

A comparison of the concentrations of dissolved As^{III} and total dissolved As (i.e. As^{V} + As^{III}) measured by the simultaneous equation DGT approach will be compared with the total As and As^{III} concentrations measured by HG-AAS after filtration. In addition, the concentrations of dissolved As^{III} and total dissolved As measured by the simultaneous equation DGT approach will be compared with the direct DGT measurement of total As (using DGT without Nafion membrane) and As^{III} (DGT with a Nafion membrane).

7.2 Experimental

7.2.1 Sample collection

Two well water samples and one river water sample were collected for As analysis and as a medium to spike with As. The well water samples (M34/0758 (well water 1) and O31/0156 (well water 2)) were collected in acid-washed 5 L plastic containers by Phil Abraham (Environment Canterbury). Well water O31/0136 was collected on 13/06/06 from a well near Lyell Creek, Hawthrone Road, Kaikoura. Well water M34/0758 was collected on 12/06/06 from a well located near Watties Road, Amberley. The well water samples were refrigerated immediately after collection. The river water sample was collected in acid-washed 20 L plastic containers. The sample was collected on 05/09/06 from Molloy Creek, Moana, West-Coast, New Zealand. The sampling site was adjacent to the Molloy Creek bridge. During transport, the river water samples were chilled in ice; the samples were refrigerated within 4 h of collection.

The water samples were not filtered before DGT deployments as the laboratory did not have facilities to filter large volumes of water relatively quickly; no attempt was made to preserve the samples other than refrigeration. All samples were stored in a refrigerator until analysis.

7.2.2 Determining fulvic acid concentration of Molloy Creek sample

The fulvic aid concentration of the Molloy Creek sample was determined by measuring the absorbance at 265 nm using a Varian Cary 50 UV-Visible spectrophotometer. Standards from 0 to 30 ppm were prepared from a 250 ppm fulvic acid (FAG1) stock solution.

7.2.3 Deployment of DGT with and without Nafion membranes in natural waters

The DGT devices were assembled and deployed as described in chapter 2. All experiments were carried out in a solution volume of 4 L. This volume of solution was sufficiently large to avoid significant depletion of As by the DGT devices. Using this volume, the amount of As removed from solution was < 3 %. The membrane filters used for this work were 0.025 μm cellulose nitrate membranes (Schleicher & Schuell). The membrane filters were pre-treated as described in section 2.3.6. The stirring rate used for all experiments in this chapter was 630 rpm. After the DGT devices were retrieved from solution they were placed in H_2O and then washed thoroughly before dissembling and removal of the iron-oxide gel adsorbent. The same elution and analysis procedure to that used for previous DGT experiments was adopted. The pH and temperature of the DGT deployment solutions were measured at the start and end of the experiments.

Samples were removed from the deployment solutions at the start and end of the experiment to confirm that the total As concentration had not changed significantly over this time. The samples were filtered through a 0.025 μm cellulose nitrate membrane (Schleicher & Schuell) and stabilized by adding concentrated HCl to give a final concentration of 1.1 mol L^{-1} HCl; these samples were analysed at the same time as the DGT eluents. An As^{III} analysis was carried out on the deployment solution at the start of the experiment using HG-AAS. The total As concentration and the As^{III} concentration measured by HG-AAS were compared to those measured by DGT (i.e. the simultaneous equation approach).

7.2.3.1 Well water

The concentrations of total As and As^{III} were measured in the two well water samples by deploying DGT devices without and with Nafion membranes in 4 L of the well-stirred sample solutions for > 28 h. The exact deployment times were recorded.

7.2.3.1 River water

The river water sample was spiked with As^{III} and As^{V} and the concentrations of As^{III} and total As were measured by DGT. This was carried out for two $[As^{V}]/[As^{III}]$ ratios. For the first experiment, 100 ml of sodium acetate (pH 5), 36 ml of 10 ppm As^{V}, and 4 ml of 10 ppm As^{III} were added to 4 L of the river water sample. This gave an $[As^{V}]/[As^{III}]$ ratio of ~ 9.0. For the second experiment, 100 ml of sodium acetate (pH 5), 32 ml of 10 ppm As^{V}, and 8 ml of 10 ppm As^{III} were added to 4 L of the river water sample. This gave an $[As^{V}]/[As^{III}]$ ratio of ~ 4.0. The solutions were left for ~ 24 h before DGT devices were deployed for > 25 h. The exact deployment times were recorded. Sodium acetate was added to the DGT deployment solutions as the addition of As caused a significant decrease in pH of the solution due to the acidity of the As standards. The pH of the river water samples before the addition of As was 6.8.

7.3 Results

7.3.1 Deployment of DGT with and without Nafion membranes in natural water

DGT devices with and without Nafion membranes were deployed in two well waters, and a river water (that contained 10 ppm fulvic acid) that was spiked with two $[As^{V}]/[As^{III}]$ ratios in the laboratory. The concentration of total As and As^{III} measured by the simultaneous equation DGT approach was compared to the concentration of total As and As^{III} measured by HG-AAS. In addition, The concentration of total As and As^{III} measured by the simultaneous equation DGT approach was compared to the direct measurement of total As (using DGT without Nafion membrane) and As^{III} (DGT with a Nafion membrane).

7.3.1.1 Comparison of concentrations of total As and As^{III} determined by the simultaneous equation DGT approach and HG-AAS

Table 7.5 shows the comparison between the concentration of total As and As^{III} determined by DGT and the concentration of total As and As^{III} measured by HG-AAS. The accumulated masses from Table 7.6 have been used to calculate the solution concentrations of As^{V} and As^{III} using equation 7.1 and 7.2. The concentration of total As determined by DGT was obtained by addition of the As^{III} and As^{V} concentrations.

Water sample	$[As_T]_{DGT}$[a] /ppb	$[As_T]_{HG-AAS}$ /ppb	DGT/HG-AAS ($[As_T]$)[b]	$[As_{As(III)}]_{DGT}$[c] /ppb	$[As_{As(III)}]_{HG-AAS}$ /ppb	DGT/HG-AAS ($[As_{III}]$)[d]
Well 1[e]	7.9 ± 1.6	8.3 ± 0.4	0.95 ± 0.22	0.6 ± 0.1	0.3 ± 0.1	2.00 ± 1.00
Well 2[f]	31.9 ± 4.0	38.2 ± 0.6	0.84 ± 0.11	2.0 ± 0.3	0.75 ± 0.1	2.66 ± 0.75
River 1[g]	110.0 ± 8.2	100.5 ± 8.4	1.09 ± 0.17	9.5 ± 1.2	10.1 ± 0.5	0.95 ± 0.17
River 2[h]	97.2 ± 8.1	91.5 ± 5.7	1.06 ± 0.15	18.5 ± 1.7	18.3 ± 0.9	1.01 ± 0.15

Table 7.5 Comparison of the concentrations of total As and As^{III} determined by the simultaneous equation DGT approach with the concentrations of total As and As^{III} measured by HG-AAS. The number of DGT devices deployed for each experiment was between 4 to 6.

[a]Total concentration of As determined by addition of the concentrations of As^{V} and As^{III} obtained by solving equations 7.1 and 7.2 simultaneously.

[b]Ratio of the concentration of total As measured by DGT to the concentration of total As measured by HG-AAS.

[c]Concentration of As^{III} determined by solving equations 7.1 and 7.2 simultaneously.

[d]Ratio of the concentration of As^{III} measured by DGT to the concentration of As^{III} measured by HG-AAS.

[e]Time = 33.1 h, temperature = 25.0 ± 1.0 °C, pH_{start} 7.45, pH_{end} 8.30

[f]Time = 28.8 h, temperature = 24.5 ± 0.5 °C, pH_{start} 7.15, pH_{end} 8.30

[g]Time = 29.8 h, temperature = 25.0 ± 1.0 °C, pH 4.95

[h]Time = 25.6 h, temperature = 25.0 ± 0.5 °C, pH 4.95

For the river water samples, the concentrations of total As and As^{III} determined by DGT agreed within experimental uncertainty with the concentrations of total As and As^{III} measured by HG-AAS. For well water 1, the total As concentration determined by DGT and the total As concentration measured by HG-AAS agreed within experimental uncertainty. For well water 2, the total concentration of As determined by DGT was ~ 16 % lower than that measured by HG-AAS. For both well water samples, the concentration of As^{III} determined by DGT was significantly higher than that measured by HG-AAS.

Due to the discrepancies between $[As_T]_{DGT}$ and $[As_T]_{HG-AAS}$ for well water 2 and between $[As^{III}]_{DGT}$ and $[As^{III}]_{HG-AAS}$ for well water 1 and 2, the results were examined more closely. The predicted masses of As accumulated in DGT devices with ($DGT_{As(III)}$) and without (DGT_{Total}) a Nafion membrane were calculated. These predicted masses are compared with accumulated masses in Table 7.6 and will be referred to in the discussion section of this chapter.

Water sample	Accumulated Mass/ng ($DGT_{Non-Nafion}$)[a]	Predicted Mass/ng ($DGT_{Non-Nafion}$)[b]	A/P[c]	Accumulated Mass/ng (DGT_{Nafion})[d]	Predicted Mass/ng (DGT_{Nafion})[e]	A/P[f]
Well 1	164 ± 19 ng (n = 5)	170 ± 12 ng	0.96 ± 0.18	12 ± 1 ng (n = 3)	8 ± 1 ng	1.50 ± 0.31
Well 2	574 ± 25 ng (n = 4)	681 ± 53 ng	0.84 ± 0.10	38 ± 5 ng (n = 2)	21 ± 2 ng	1.81 ± 0.41
River 1	2072 ± 70 ng (n =5)	1894 ± 132 ng	1.09 ± 0.11	174 ± 15 ng (n = 5)	185 ± 35 ng	0.94 ± 0.26
River 2	1594 ± 16 ng (n =4)	1516 ± 128 ng	1.05 ± 0.10	264 ± 12 ng (n = 4)	260 ± 23 ng	1.02 ± 0.14

Table 7.6 Comparison of the accumulated mass of As to the predicted mass of As for water samples using DGT devices with (DGT_{Nafion}) and without ($DGT_{Non-Nafion}$) a Nafion membrane.

[a]Accumulated mass of As for DGT without Nafion membrane

[b]Predicted mass of As for DGT without Nafion membrane

[c]Ratio of accumulated mass of As to predicted mass of As for DGT without Nafion membrane

[d]Accumulated mass of As for DGT with Nafion membrane

[e]Predicted mass of As for DGT with Nafion membrane

[f]Ratio of accumulated mass of As to predicted mass of As for DGT with Nafion membrane

[*]River water 1 and 2 contained ~ 10 ppm fulvic acid

The pH of both well water samples increased significantly during the DGT deployments. The pH increased from 7.45 at the start of the experiment to 8.30 at the end for well water 1; for well water 2 the pH increased from 7.20 to 8.30. It has been shown that adsorption of As^{V} to ferrihydrite results in the net release of OH^{-}.[1]

7.3.1.2 Comparison of concentrations of total As and As^{III} determined by the simultaneous equation DGT approach with direct DGT measurement

The concentrations of total dissolved As and dissolved As^{III} measured by the simultaneous equation DGT approach was compared with the direct DGT measurement of total As (using DGT without Nafion membrane) and As^{III} (DGT with a Nafion membrane). Figure 7.1 shows the comparison of these two approaches for measuring the total dissolved As concentration in the two well water and river water samples, and Figure 7.2 shows the comparison of these two approaches for measuring the dissolved As^{III} concentration in the two river water samples. Reasonable agreement between the two DGT approaches was obtained for total As and As^{III} determinations.

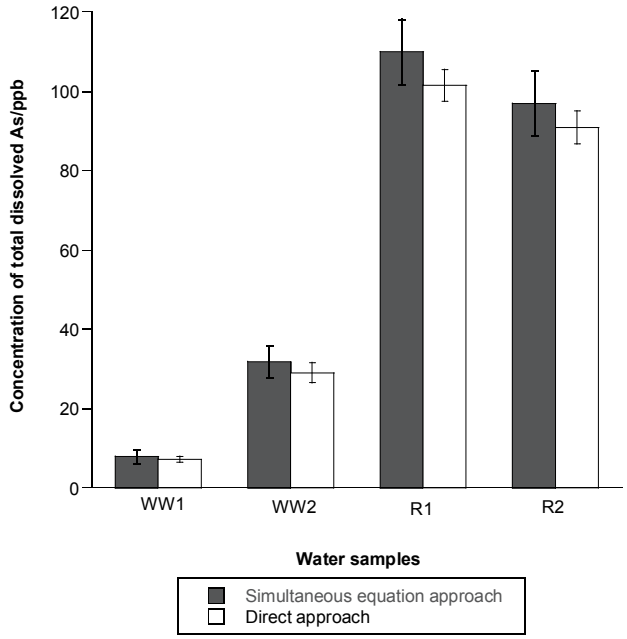

Figure 7.1 Comparison of the total concentration of As determined by the simultaneous equation approach and the direct approach for well water 1 (WW1), well water 2 (WW2), river water 1 (R1), and river water 2 (R2). Note that the average diffusion coefficient of As^{V} and As^{III} has been used to calculate the total As concentration for the direct approach method.

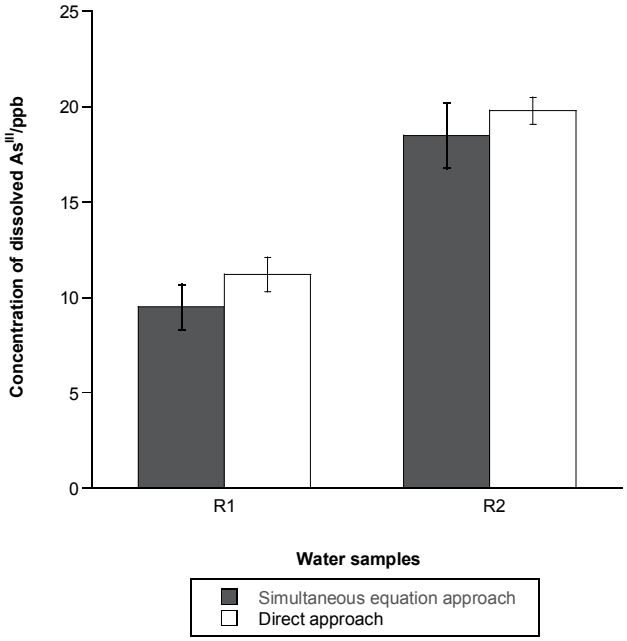

Figure 7.1 Comparison of the dissolved As^{III} concentration determined by the simultaneous equation approach and the direct approach for river water 1 (R1), and river water 2 (R2).

7.4 Discussion

7.4.1 Deployment of DGT with and without Nafion membranes in natural waters

DGT devices with and without Nafion membranes were deployed in two well waters and a river water spiked with two [As^{V}]/[As^{III}] ratios. The concentrations of As^{III} and total As measured by the simultaneous equation DGT approach were compared to those measured by HG-AAS. In addition, the concentrations of As^{III} and total As measured by the simultaneous equation DGT approach were compared with the direct measurement of total As (using DGT without Nafion membrane) and As^{III} (DGT with a Nafion membrane)

7.4.1.1 Comparison of concentrations of total As and As^{III} determined by the simultaneous equation DGT approach and HG-AAS for river water samples

For the river water samples the concentration of total As and As^{III} measured by the simultaneous equation DGT approach agrees within experimental uncertainty with the concentration of total As and As^{III} measured by HG-AAS. These results suggest that there are no species in the river water that affects the accumulation of As species by either DGT device.

7.4.1.2 Comparison of concentrations of total As and As^{III} determined by the simultaneous equation DGT approach and HG-AAS for well water samples

For well water 1, the concentration of total As determined by the simultaneous equation DGT approach (7.9 ± 1.6 ppb) agrees within experimental uncertainty with the concentration of total As measured by HG-AAS (8.3 ± 0.4), even though the concentration of As^{III} was overestimated.

For well water 2, the concentration of total As determined by the simultaneous equation DGT approach (31.9 ± 4.0 ppb) was lower than that measured by HG-AAS (38.2 ± 1.2 ppb). This discrepancy may be due to colloidal Fe^{III} in solution. The well water 2 sample showed evidence of colloidal material which had coagulated during the storage of the sample. Prior to deployment of DGT devices, the colloidal material was removed from solution by decanting. It is possible that there was some As adsorbed to Fe^{III} colloids that was not measured by the DGT technique but was measured by HG-AAS. The DGT technique does not measure As associated with colloids, but HG-AAS may measure this fraction if the colloidal material is dissolved during acidification of the HG-AAS samples. This colloidal fraction must be < 25

nm as the samples were filtered through a 0.025 μm membrane before the HG-AAS measurement. Therefore it is not unreasonable that the concentration of total As determined by HG-AAS is greater than that determined by DGT.

The concentrations of As^{III} determined by the simultaneous equation DGT approach for well water 1 and well water 2 were ~ 2.3 and ~ 3.3 times higher than the concentrations of As^{III} measured by HG-AAS, respectively. The mass of As accumulated by DGT with a Nafion membrane was ~ 1.5 and ~ 1.8 times higher than the predicted mass for the well water 1 and well water 2 samples, respectively. The mass of As measured on the iron-oxide adsorbent was 12 ± 1 and 38 ± 5 ng for well water 1 and well water 2, respectively. The mass of As predicted was 8 ± 1 and 21 ± 2 ng for well water 1 and well water 2, respectively. If the higher diffusion coefficient of As^{V} through the Nafion membrane in the presence of Ca^{2+} and Mg^{2+} is used (4.75×10^{-9} cm^2 s^{-1}), then the predicted mass of As for well water 1 and well water 2 would be 8.5 and 23 ng, respectively; these values still do not agree with the accumulated masses. Therefore another factor must be contributing to the difference between the predicted and accumulated masses.

The two well water samples contained higher concentrations of Ca^{2+} and Mg^{2+} (as measured by Environment Canterbury Laboratory) than the synthetic solutions in which the As^{V} diffusion coefficients through the Nafion membrane were measured (see chapter 6). The dissolved concentrations of Ca^{2+} and Mg^{2+} in well water 1 were 48 and 12 ppm; this corresponds to an increase in Ca^{2+} and Mg^{2+} concentrations of 3.2 and 3.4 times, respectively, compared to the synthetic solutions used in chapter 6 for measuring the diffusion coefficients of As^{V}. For well water 2, the dissolved concentrations of Ca^{2+} and Mg^{2+} were 30 and 8.8 ppm respectively; this corresponds to an increase in Ca^{2+} and Mg^{2+} concentrations of 2.0 and 2.5 times, respectively. The higher concentrations of Mg^{2+} and Ca^{2+} may contribute to the mass of As accumulated being greater than that predicted for DGT devices with a Nafion membrane. This may be due to an increase in shielding of the negatively charged As^{V} species from the negatively charged Nafion membrane due to Mg^{2+} and Ca^{2+} associating with the sulfonate groups within the Nafion membrane. The higher concentrations of Mg^{2+} and Ca^{2+} may cause an even larger increase in As^{V} diffusion coefficient than measured in chapter 6. In addition, the increase in As^{V} complexation by Ca^{2+} and Mg^{2+} may be a factor as the pH of the well water samples were > 7.0 which leads to greater complexation by Ca^{2+} than would occur at pH 5.0 (pH at which the measurements in chapter 6 were carried out to examine the effect

of Ca^{2+}). Speciation calculations showed that for well water 1, As^V would exist as 48 to 56 % $HAsO_4^{2-}$, 15 to 2 % $H_2AsO_4^-$ and 36 to 41 % $CaHAsO_4$. For well water 2, As^V would exist as 49 to 66 % $HAsO_4^{2-}$, 30 to 3 % $H_2AsO_4^-$ and 22 to 30 % $CaHAsO_4$. Therefore in both cases significant amounts of As^V would exist as the uncharged $CaHAsO_4$ complex which will be expected to have a larger diffusion coefficient than the $HAsO_4^{2-}$ or $HAsO_4^-$ species.

If it was assumed that $CaHAsO_4$ has a similar diffusion coefficient to H_3AsO_3 through the Nafion membrane, the predicted mass would be considerably larger than the accumulated mass (up to 4.6 x for well water 1 and 4.8 x for well water 2); this is assuming that the binding ability of the $CaHAsO_4$ species is the same as $HAsO_4^{2-}$ for the iron-oxide adsorbent within the DGT device.

7.4.1.1 Comparison of concentrations of total As and As^{III} determined by the simultaneous equation DGT approach with direct DGT measurement

Reasonable agreement was obtained between the concentration of total As and As^{III} when using the simultaneous equation DGT approach and the direct DGT approach methods. For the total As measurement, the direct approach underestimated the concentration of As, however, as expected it still agreed well with the simultaneous equation DGT approach, as the $[As^V]/[As^{III}]$ ratios were within the limits of the DGT device. River water 1 contained an $[As^V]/[As^{III}]$ ratio of ~ 9; river water 2 contained an $[As^V]/[As^{III}]$ ratio of ~ 4. Well water 1 and well water 2 contained $[As^V]/[As^{III}]$ ratios of ~ 28 and ~ 50, respectively. The underestimation of the total As concentration is due to the use of the average diffusion coefficient to calculate the As concentration in a system in which the concentration of As^V is greater than the concentration of As^{III} (as is the case for the four natural waters used in this work), the direct approach leads to an underestimation of total As. If the concentration of As^{III} was greater than the concentration of As^V, then the direct approach would lead to an overestimation of the total As concentration.

For the As^{III} measurements, the direct approach overestimates the concentration of As^{III}. This is expected as the presence of As^V contributes to the mass of As accumulated by the DGT device with a Nafion membrane. However, it still aggress well with that measured by the simultaneous equation approach for the river waters samples because the $[As^V]/[As^{III}] < 10$.

7.5 Conclusion

Good agreement between the total As and As^{III} concentrations determined by the simultaneous equation DGT approach and HG-AAS was obtained for both river water experiments; this indicates that in the river water sample there are no species present that significantly affect the measurement of total As and As^{III} by DGT. Good agreement was also obtained between the total As concentration determined by the simultaneous equation DGT approach and HG-AAS for well water 1 even though the concentration of As^{III} was overestimate relative to the HG-AAS measurement. For well water 2 the concentration of total As determined by DGT was lower than that for HG-AAS, presumably due to As adsorption by Fe^{III} colloids in solution. However for both well water samples, poor agreement was obtained for the As^{III} concentrations determined by DGT and by HG-AAS.

This may be due to the presence of Ca^{2+} and Mg^{2+} at higher concentrations than have been investigated previously; these cations may cause the As^{V} species to diffuse through the Nafion membrane faster than expected due to complexation with As^{V} or an increase in shielding of the As^{V} species from the negatively charged Nafion membrane.

Furthermore, good agreement was also obtained between the simultaneous equation DGT approach and the direct DGT approach.

7.6 References

1. Jain, A.; Raven, K. P.; Loeppert, R. H., Arsenite and arsenate adsorption on ferrihydrite: Surface charge reduction and net OH^- release stoichiometry. *Environmental Science & Technology* **1999,** 33, (8), 1179-1184.

Chapter 8

Kinetic fractionation of metals using ETAAS with a coupled microcolumn: Preliminary studies

8.1 Introduction

Flow systems involving adsorbents, accommodated within microcolumns, have been specifically used for measuring the labile fraction of metal in water samples.[1-5] For these methods the sample is passed across the adsorbent to capture both the free metal ion, and metal that is in labile complexes that dissociate while travelling across the microcolumn. The metal that is retained on the microcolumn (i.e. labile fraction) is eluted, and quantified by an appropriate analytical method to give a measurement of the labile metal fraction. The discriminatory criterion between labile and inert species is the contact time between the sample and the adsorbent. Therefore, measurement of the labile fraction is operationally defined and depends on factors that affect the contact time. Metal complexes that dissociate during this contact time will contribute to the fraction of metal measured. For example, Procopio *et al*.[4] used a microcolumn containing an ion-exchange adsorbent to fractionate Cu and Pb complexes into four lability categories by varying the time-scale of the measurement between 0.02 and 3 s. This was achieved by altering both the flow rate of sample across the microcolumn and the dimensions of the microcolumn. Work in this laboratory, by Adams *et al*.[1] and Simpson *et al*.,[5] has involved the use of microcolumns containing adsorbents in a flow injection manifold for speciation of Fe and Al, respectively. Both Adams *et al*.[1] and Simpson *et al*.[5] used contact times of 1.3 s to discriminate between labile and inert complexes. Bowles *et al*.[2] utilized a microcolumn filled with Chelex-100 resin, and a 0.25 s contact time, to distinguish labile complexes from inert complexes for a variety of metal-ligand systems.

Electrothermal atomic absorption spectrometry (ETAAS) is a widely applicable technique that is capable of determining both metals and semi-metals at very low concentrations; however in its conventional form ETAAS has limited speciation capabilities. One general approach to obtaining speciation information is by in-situ electrodeposition from metal complexes in the graphite furnace by application of selected potentials prior to analysis.[6] In another approach, ETAAS has been coupled to hydride generation flow systems in order to selectively determine a specific analyte oxidation state, for example to determine the As^{III} species in the presence of As^{V}.[7, 8] The third strategy is to couple ETAAS with on-line microcolumns, packed with an adsorbent, to pre-concentrate specific metal species.[3, 9-20] This is the approach investigated in this work and aspects of the method are be briefly reviewed in sections 8.1.1 and 8.1.2.

8.1.1 Adsorbents coupled to ETAAS for on-line metal speciation

Complex samples, such as sea-water and biological materials, can be difficult to analyze directly using ETAAS as they can pose severe matrix interferences and the background correction methods can be incapable of correcting for the very high background.[10, 16, 17, 19, 21] The low concentration of trace metals and the strong interference from the sample matrix can be overcome by the use of adsorbents; adsorbents can separate the analyte from the interfering species and can also preconcentrate the analyte.[3, 16, 17] The adsorbents that have been coupled on-line with ETAAS include: Chelex-100,[3, 11, 12] Muromac A-1,[10, 11, 16, 17] C_{18} silica gel,[11-13] polytetrafluoroethylene (PTFE) beads,[14, 15, 18] and PTFE turnings;[9] many other adsorbents have also been used.[19] The analyte metal can either adsorb directly to the adsorbent as is the case for the Chelex-100 and Muromac A-1 resins, or is reacted with a ligand prior to interacting with the adsorbent as in the case for the C_{18} and PTFE materials.

C_{18} and PTFE materials are hydrophobic and only retain non-charged compounds.[14] They have been used for adsorption of neutral complexes that have been formed by the reaction of metals and chelating reagents. Liu and Huang[13] used ammonium pyrrolidinedithiocarbamate (APDC) to complex Cu^{2+} and Cd^{2+} and adsorb these complexes onto a C_{18} adsorbent. The ligand APDC was also used by Anthemidis *et al*.[9] to complex Co^{2+}; the Co-PDC complex was adsorbed onto PTFE turnings. Diethyldithiophosphate (DDPA) has also been used to complex Cd^{2+} with adsorption of the complex onto PTFE beads.[14, 15, 18] For these systems the interaction between the adsorbent and the metal complex is hydrophobic in origin.

Chelating resins such as Chelex-100 and Muromac A-1, bind metal ions directly. Both of these adsorbents contain iminodiacetate functional groups which are responsible for the chelating properties of the adsorbent. The difference between Chelex-100 and Muromac A-1 is the polymeric support that the iminodiacetate functional groups are immobilised on. As a consequence, Chelex-100 resin swells and shrinks as it is converted from the basic form to the acidic form;[3, 11, 20, 22] (the Chelex-100 resin volume decreases by half when it is strongly acidified.[3, 22]), whereas Muromac A-1 does not shrink or swell below a pH of 4.5.[10] The continuous swelling and shrinking of the Chelex-100 resin complicates its use in microcolumns where the flow of solution predominantly in one direction can cause the resin to compact tightly. This increases backpressure in the microcolumn and creates void volume and thus affects the flow rate.[10, 11, 21, 22] However, this problem can be rectified by reversing the direction of flow across the microcolumn[3, 21, 22] and the variable void volume problem can be overcome by tightly compressing the resin between foam plugs; the foam plugs fill the void volume produced by the resin contracting and are compressed by the resin when it swells.[3]

As indicated earlier, the adsorbents are accommodated within a microcolumn. Microcolumns have been fabricated using both glass[3, 12] and PTFE tubing,[9, 10, 13, 14, 16-18] and the adsorbent can be held in place using materials such as polyethylene frits,[10, 13, 16, 17] polystyrene foam[3, 12] or glass wool.[14, 18] The location of the microcolumn is either within the tip of the autosampler sampling probe (known as column-in-tip design) or is located further back within the flow manifold (known as column-in-loop design).[11, 20]

8.1.2 On-line preconcentration and elution of metal ions from adsorbents for speciation by ETAAS

The analyte is preconcentrated by passing the sample across the adsorbent for a known time or using a known volume. After the preconcentration step, the metal ions are eluted from the absorbent and the eluent is directed into the graphite furnace of the ETAAS and analyzed. Elution of the metal from the adsorbent can be achieved using a variety of eluents; the chosen eluent can depend on the adsorbent used. Methanol,[13] ethanol,[14, 15, 18] HNO_3,[18] and isobutyl methyl ketone (IBMK)[9, 18] have been used to elute metals from the C_{18} and PTFE adsorbents; whereas HNO_3 is commonly used as the eluent for the Muromac A-1 and Chelex-100 adsorbents.[3, 10, 12, 17]

For many of the microcolumn-ETAAS systems, the preconcentration and elution steps are carried out using external pumps such as peristaltic or syringe pumps which push the sample and eluent across the microcolumn.[9, 10, 14-18] The eluent is propelled across the microcolumn and into the graphite furnace of the ETAAS via the autosampler which is placed in the graphite furnace dosing hole.[9, 10, 14-18] In some systems the preconcentration step is carried out using a peristaltic pump but the elution step uses the autosampler in its normal mode.[3, 12] However, none of these systems utilizes the full capabilities of the autosampler and in all systems additional pumps are required. For many of the systems, all steps in the preconcentration and elution procedures are automated.

8.1.3 Strategy for fractionation of metals using ETAAS with coupled microcolumn within the autosampler

The aim of this work is to incorporate a microcolumn containing Chelex-100 within the autosampler of the ETAAS instrument so that additional pumps are not required. This arrangement is illustrated in Figure 8.1 which shows a schematic diagram of the non-microcolumn autosampler (i.e. normal system) and the autosampler with a microcolumn inserted (i.e. microcolumn-in-tip system). In this chapter the use of the autosampler without the microcolumn will be referred to as the 'normal' system; the use of the autosampler with the inserted microcolumn will be referred to as the 'microcolumn' system.

This chapter describes the preliminary development of a new laboratory-based method for obtaining lability speciation information about metal-ligand systems in environmental samples.

The microcolumn would enable two fractions of metal from a water sample to be delivered sequentially to the ETAAS for analysis. The first fraction, as would result from normal sample pick up and delivery approach of the autosampler, would contain metal bound in inert complexes (not retained by the adsorbent). The second fraction, as would result from pick up of HNO_3 eluent and delivery to the furnace, would contain metal from labile complexes (retained by the adsorbent after dissociating while travelling across the Chelex-100 microcolumn). This procedure is schematically illustrated in Figure 8.2.

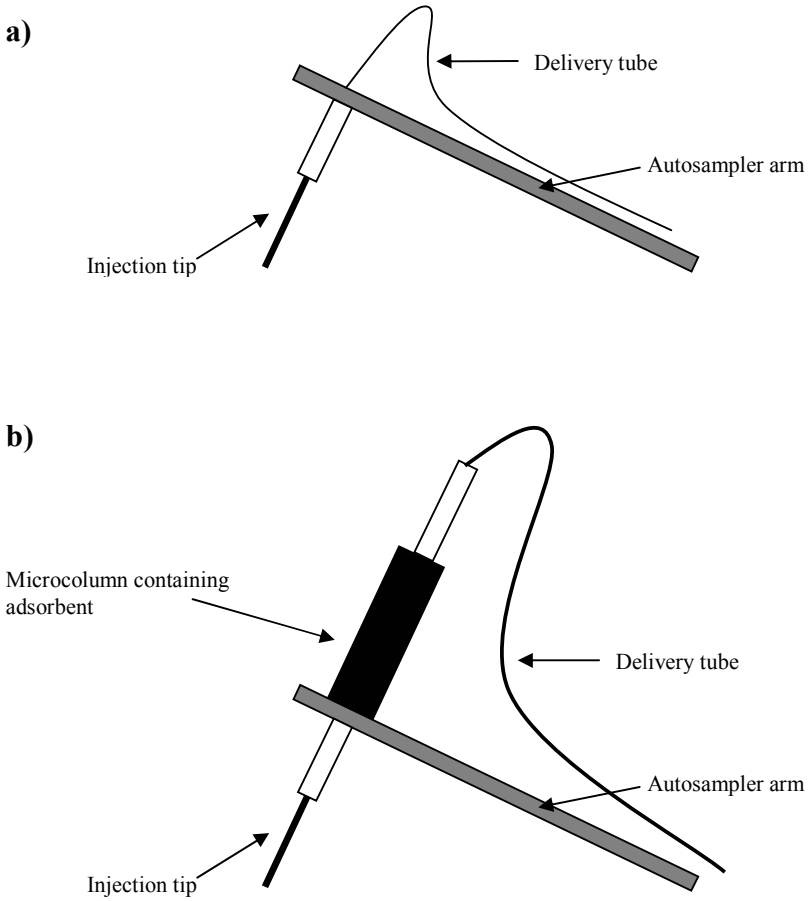

Figure 8.1 Schematic diagrams of (a) normal autosampler system and (b) microcolumn autosampler system.

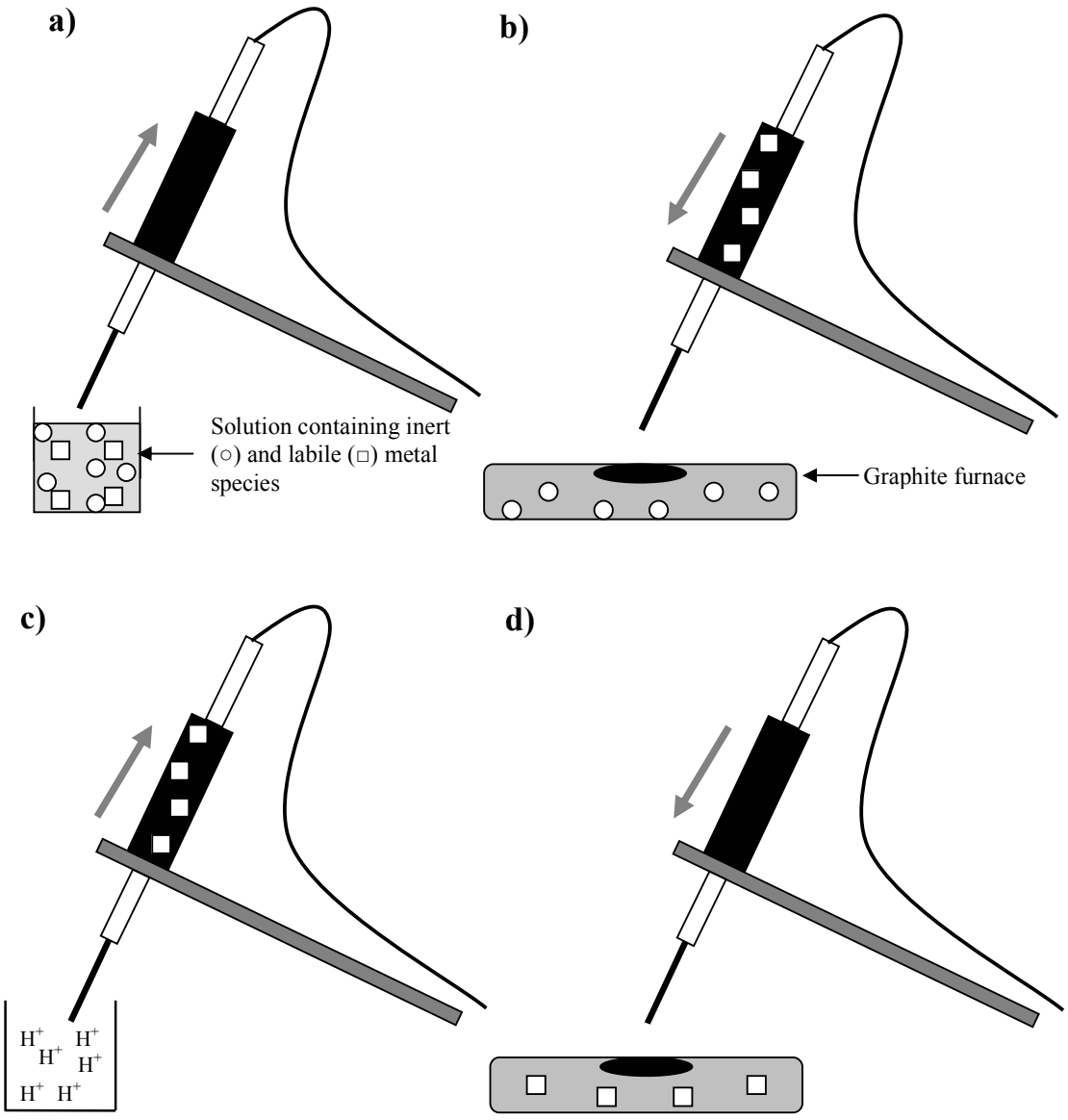

Figure 8.2 Schematic diagram showing procedure for ETAAS with coupled microcolumn. (a) A solution containing both inert (○) and labile (□) metal species is passed through the microcolumn containing Chelex 100 resin; (b) the microcolumn retains the labile metal species (□); the inert metal species (○) are injected into the graphite furnace and atomized and measured; (c) acid is passed across the microcolumn to elute the retained labile metal species (□); the eluted labile metal species (□) are injected into the graphite furnace and atomized and measured. After the elution step the microcolumn would be converted back to its basic form using an appropriate buffer so that steps (a) to (d) could be repeated. The grey arrows indicate the direction of flow across the microcolumn.

8.1.4 Chapter outline

This chapter is concerned with the preliminary investigation and development of a system that coupled a Chelex-100 microcolumn with the ETAAS instrument for kinetic speciation of metal complexes. The issues and parameters investigated include: (i) the adsorption of Cu to various microcolumn materials in the presence and absence of fulvic acid; (ii) the selection of an appropriate buffer to convert the Chelex-100 resin, within the microcolumn, from the acidic to the basic form after elution; and (iii) the investigation of metal uptake efficiency by the Chelex-100 resin (this includes the effect of buffer concentration, ionic strength and washing of the Chelex-100 resin).

8.2 Experimental

The set-up of the microcolumn within the autosampler of the ETAAS, and the procedures and materials used, are fully described in section 2.4.3. Both Cu and Cd analytes and Teflon and polycarbonate microcolumns were used for various sections of this work. The Cu and Cd ETAAS temperature programs are described in section 2.4.1. Experiments in this chapter were carried out using both the normal autosampler system and the microcolumn autosampler system. When using the microcolumn system, Milli-Q water is also passed across the microcolumn both before and following uptake of the sample or acid aliquot. The Milli-Q water aliquot (10 μL) before the sample or acid aliquot ensured that all of the sample or acid would be completely removed from within the pore volume of the Chelex-100 resin during injection into the graphite furnace; the Milli-Q water aliquot (25 to 35 μL) following the sample or acid aliquot ensured that the sample or acid would pass completely across the microcolumn. The sample or acid aliquot and both Milli-Q water aliquots are injected into the graphite furnace and analyzed.

8.2.1 Adsorption of Cu^{II} to microcolumn materials and tubing in the presence and absence of fulvic acid

The adsorption of Cu^{II} to the surface of the Teflon and polycarbonate microcolumns and various tubing was examined. After the microcolumns and tubing were cleaned with 1 mol L^{-1} HNO_3 they were buffered by pumping 0.05 mol L^{-1} sodium acetate/HNO_3 (pH 5.0) across the microcolumn for 3 min; this was followed by pumping Milli-Q water across the microcolumn and tubing for 3 min to remove any residual buffer.

All of the experiments in this section used an empty microcolumn that was not packed with Chelex-100 resin.

8.2.1.1 Adsorption of Cu^{2+} to Teflon and polycarbonate microcolumns

The extent of Cu^{2+} adsorption to the surface of the Teflon and polycarbonate microcolumns was examined by injecting an aliquot of Cu^{2+} into the graphite furnace using both the normal system and the microcolumn system and comparing the absorbance obtained after analysis. In addition, 1 mol L^{-1} HNO_3 was used to remove Cu^{2+} that had adsorbed to the microcolumn surfaces during various adsorption experiments; this eluent fraction was injected into the graphite furnace and analyzed for Cu. The concentration of Cu^{2+} used in this work was 10 ppb; it was prepared in 0.005 mol L^{-1} sodium acetate (pH 5.0). The pH of the Cu^{2+} standard was adjusted to 5.0 using 1 mol L^{-1} NaOH.

8.2.1.2 Adsorption of Cu^{2+} to various tubing

Various Teflon and tygon tubing were incorporated into the autosampler system by directly connecting to the Teflon delivery tubing or using tygon tubing of various diameters as connectors. The location of the tubing within the autosampler system is schematically shown in Figure 8.3.

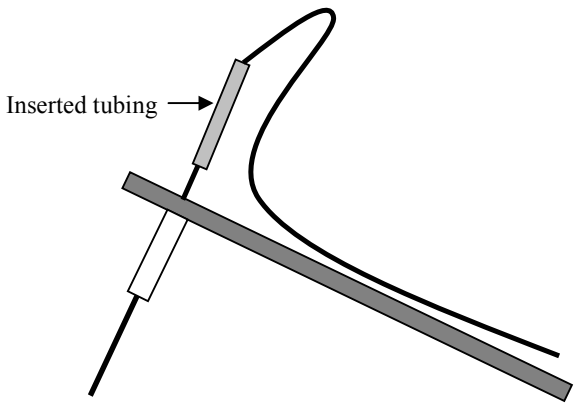

Figure 8.3 Schematic diagram showing location of 'microcolumn' tubing within the autosampler system.

The dimensions of the various tubing used to construct the 'microcolumn' are shown in Table 8.1 and are compared to the dimensions of the Teflon and polycarbonate microcolumns used previously.

Tubing/Material	Length/cm	Internal diameter/cm	Volume/µL
Tygon tubing 1	2.8	0.08	12.7
Tygon tubing 2	1.0	0.21	33.3
Teflon tubing 1	1.3	0.15	23.0
Teflon Tubing 2	2.8	0.100	22.0
Teflon microcolumn	1.3	0.12	14.7
Polycarbonate microcolumn	1.5	0.14	23.1

Table 8.1 Dimensions of tubing used to simulate a 'microcolumn' and dimensions of fabricated Teflon and polycarbonate microcolumns.

After the tubing was incorporated into the autosampler it was cleaned with 400 µL of 1 mol L^{-1} HNO_3, buffered for 3 min with 0.05 mol L^{-1} sodium acetate/HNO_3 (pH 5.0) and washed with Milli-Q water for 3 min. Four aliquots of a 10 ppb Cu^{2+} standard (30 µL) were passed completely across the tubing; Cu^{2+} that had adsorbed to the tubing was eluted using 1 mol L^{-1} HNO_3 (35 µL) and injected into the graphite furnace and analyzed for Cu.

The Cu^{2+} standard was prepared in 0.005 mol L^{-1} sodium acetate/HNO_3 buffer (pH 5.0); the pH of the standard was adjusted to 5.0 using 1 mol L^{-1} NaOH.

8.2.1.3 Adsorption of Cu^{II} to Teflon and polycarbonate microcolumns in the presence of fulvic acid

The extent of Cu adsorption to the surface of the Teflon and polycarbonate microcolumns was examined in the presence of fulvic acid. Experiments were carried out using Cu concentrations of 10 and 1.5 ppb and using a fulvic acid concentration of 20 ppm. The fulvic acid sample (B1F) used in this work was previously isolated by Powell and Fenton[23] from International Humic Substance Society reference peat by an acid pyrophosphate-XAD-7 method analogous to that of Gregor and Powell.[24] The Cu-fulvic acid solutions were prepared in 0.005 mol L^{-1} sodium acetate buffer (pH 5.0); the pH was adjusted to 5.0 using 1 mol L^{-1} NaOH. Similar experiments to those above (section 8.2.1.1) were carried out to examine the

adsorption of Cu, in the presence of fulvic acid, to the Teflon and polycarbonate microcolumns.

8.2.2 Investigation of background absorbance associated with the use of sodium acetate to buffer the Chelex-100 microcolumn

This section is concerned with the investigation of background absorbance (interference) that is present when sodium acetate/HNO_3 is used to buffer the Chelex-100 microcolumn. Unless otherwise stated, all of the experiments in this section involved the use of the Teflon microcolumn packed with Chelex-100 resin.

8.2.2.1 Effect of background absorbance on Cd signal

The effect that the use of sodium acetate buffer has on the Cd signal was investigated by buffering and washing the Chelex-100 microcolumn with 0.05 mol L^{-1} sodium acetate/HNO_3 and Milli-Q water for 3 min, respectively; this was followed by 10 µL of a 6.25 ppb Cd^{2+} standard (prepared in 1 mol L^{-1} HNO_3) which was passed across the Chelex-100 microcolumn and injected into the graphite furnace and measured. A second aliquot of Cd^{2+} was also passed across the Chelex-100 microcolumn and measured. The background (interfering species) and analyte signal absorbance were monitored at the 228.8 nm Cd line.

8.2.2.2 Washing of Chelex-100 resin after buffering with sodium acetate

The length of the washing step was varied from 0 to 10 min to examine if the observed interference could be removed by more extensive washing of the Chelex-100 resin within the microcolumn. Sodium acetate/HNO_3 buffer (0.05 mol L^{-1}, pH 5.0) was pumped across the Chelex-100 microcolumn for 3 min followed by Milli-Q water (if washing was required) for between 3 to 10 min. The Chelex-100 resin was eluted using 35 µL of 1 mol L^{-1} HNO_3 and injected into the graphite furnace and analyzed. The background absorbance was monitored at the 228.8 nm Cd line.

8.2.2.3 Ashing temperature and time

The ashing temperature was varied between 400 and 1400 ^{o}C to examine if the background absorbance could be removed by volatilization of the problem species. The ashing step is step 4 in the ETAAS temperature program for Cd determinations (see section 2.4.1). Sodium acetate/HNO_3 buffer (0.05 mol L^{-1}, pH 5.0) was pumped across the Chelex-100 microcolumn

for 3 min followed by Milli-Q water for a further 3 min. The Chelex-100 resin was eluted using 13 μL of 1 mol L^{-1} HNO_3 and injected into the graphite furnace and atomized using various ETAAS temperature programs in which the ashing temperature was varied. The background absorbance was monitored at the 228.8 nm Cd line. The effect of ashing temperature on the Cd signal was also examined by directly injecting 13 μL of a 10 ppb Cd^{2+} standard (1 % v/v HNO_3) into the graphite furnace.

In addition, the effect that ashing temperature has on the background absorbance associated with $NaNO_3$ was examined. Sodium nitrate (15 μL of 0.1 mol L^{-1}) was injected directly into the graphite furnace and analyzed; the background absorbance was monitored at the 228.8 nm Cd line.

8.2.2.4 Examination of different buffers and a different adsorbent

A variety of buffers were examined to investigate the possibility of using an alternative buffer to sodium acetate which did not show a significant background absorbance when eluted with HNO_3. The buffers examined were calcium acetate, 2-(N-morpholino)ethanesulphonic acid (MES), and ammonium acetate. The concentration of all buffers was 0.05 mol L^{-1} unless otherwise stated; their preparation procedures are described in section 2.2.4. The buffer was pumped across the Chelex-100 microcolumn for 3 min followed by Milli-Q water for a further 3 min. The Chelex-100 resin was eluted using 13 μL of 1 mol L^{-1} HNO_3 and injected into the graphite furnace and analyzed. The background absorbance was monitored at the 228.8 nm Cd line.

In addition, various metal salts (sodium acetate, calcium acetate, ammonium acetate, KCl, KOH, KNO_3, NaCl, NaOH, $NaNO_3$, NH_4Cl, and NH_4NO_3) were injected directly into the graphite furnace and their backgrounds examined. The concentrations of $NaNO_3$, NaCl, NaOH, KNO_3, KCl, NH_4Cl, NH_4NO_3, and KOH were 0.1 mol L^{-1}; the concentrations of calcium acetate, sodium acetate, ammonium acetate, and MES were 0.05 mol L^{-1}. The background absorbance was monitored at the 228.8 nm Cd line.

Controlled pore glass derivatised with 8-hydroxyquinoline as the chelating agent (CPG-8HQ) was also investigated briefly to see if a background was present when this adsorbent was used in conjunction with sodium acetate/HNO_3 buffer. The same procedure as above was used to

examine the background except that measurements were carried out using sodium acetate/HNO_3 at pH 5.0 and 8.2.

8.2.3 Investigation of Cd uptake by Chelex-100 microcolumn

This section is concerned with the investigation of Cd uptake by the Chelex-100 resin. The parameters investigated that may affect uptake include: effect of washing the Chelex-100 resin with water after buffering, and concentration of ammonium acetate, and NH_4NO_3 in solution.

8.2.3.1 Washing of Chelex-100 resin after buffering with sodium acetate

The importance of the washing step was investigated to see if it was necessary to wash the Chelex-100 microcolumn with Milli-Q water following buffering with ammonium acetate. The Chelex-100 microcolumn was buffered for 3 min using either 0.05 or 1 mol L^{-1} ammonium acetate/HNO_3. If a washing step was required, the Chelex-100 microcolumn was washed for 3 or 12 min with Milli-Q water before a 6.25 ppb Cd^{2+} standard (10 μL) was passed across the microcolumn and injected into the graphite furnace and analyzed. This was followed by 10 μL of 1 mol L^{-1} HNO_3 which was passed across the microcolumn (to elute Cd retained on the Chelex-100 microcolumn) and injected into the graphite furnace and analyzed. Further HNO_3 elutions were carried out to ensure all of the Cd had been removed from the Chelex-100 microcolumn. The uptake efficiency for experiments involving a washing step was compared to the uptake efficiency for experiments which did not involve a washing step.

The Cd^{2+} standard was prepared in 0.005 mol L^{-1} ammonium acetate (pH 5.0); the pH was adjusted to 5.0 using 1 mol L^{-1} NH_3.

8.2.3.2 Concentration of ammonium acetate/HNO_3 buffer in solution

The concentration of ammonium acetate/HNO_3 buffer (pH 5.0) in the Cd^{2+} standard solution was varied from 0.0005 to 0.05 mol L^{-1} to examine the effect of buffer concentration on uptake efficiency. The Cd^{2+} standards (18.75 ppb) were prepared by diluting 0.75 mL of 2.5 ppm Cd^{2+} and either 5, 1, 0.5, 0.1, or 0.05 mL of 1 mol L^{-1} ammonium acetate/HNO_3 buffer (pH 5.0), to 100 mL; this gave Cd^{2+} standards containing 0.05, 0.01, 0.005, 0.001, and 0.0005 mol L^{-1} ammonium acetate, respectively. The pH was adjusted to 5.0 using 1 mol L^{-1} NH_3.

Before each measurement the Chelex-100 microcolumn was buffered for 3 min with 0.05 mol L^{-1} ammonium acetate; this was followed by a 3 min washing step with Milli-Q water. The appropriate Cd^{2+} solutions (10 µL) were passed across the microcolumn and injected into the graphite furnace and analyzed. This was followed by 10 µL of 1 mol L^{-1} HNO_3 (to remove Cd that had been retained by the Chelex-100 microcolumn) which was injected into the graphite furnace and analyzed.

8.2.3.3 Concentration of NH_4NO_3 in solution

The effect of ionic strength on the uptake efficiency of Cd^{2+} was examined by varying the concentration of NH_4NO_3 in the Cd^{2+} standard solution from 0 to 0.095 mol L^{-1}. The Cd^{2+} standards (18.75 ppb) were prepared by diluting 0.75 mL of 2.5 ppm Cd^{2+}, 0.5 mL of 1 mol L^{-1} ammonium acetate/HNO_3 buffer (pH 5.0), and either 0, 0.5, 2.5, 4.5 or 9.5 mL of 1 mol L^{-1} NH_4NO_3, to 100 mL; this gave Cd standards containing 0, 0.005, 0.025, 0.045 and 0.095 mol L^{-1} NH_4NO_3, respectively. The pH was adjusted to 5.0 using 1 mol L^{-1} NH_3. The volume of the Cd^{2+} standard passed across the microcolumn was 10 µL.

The preparation of the Chelex-100 microcolumn and procedure for passing the Cd^{2+} standard and HNO_3 across the microcolumn were the same as in section 8.2.3.2.

8.3 Results

8.3.1 Adsorption of Cu^{II} to microcolumn materials and tubing in the presence and absence of fulvic acid

Preliminary experiments involving adsorption of Cu^{2+} to Chelex-100 resin (packed within the Teflon microcolumn) and elution using 1 mol L^{-1} HNO_3, showed inconsistent and variable results for both uptake and elution. To investigate the origin of these effects, the resin was removed from the microcolumn and the system was used to introduce aliquots of a Cu^{2+} standard into the graphite furnace to examine if good reproducibility for the Cu signal could be obtained. Good reproducibility would indicate that the microcolumn design was suitable. However, during this preliminary work there was evidence of Cu adsorption to the Teflon microcolumn; therefore various adsorption experiments were carried out to examine this phenomenon.

Many of the experiments in this section of work were carried out using a Cu^{2+} standard prepared in 0.005 mol L^{-1} sodium acetate/HNO_3 buffer (pH 5.0). Due to the absence of a complexing agent in solution or acidification, adsorption of Cu^{2+} to the container walls was a concern and therefore fresh standards were prepared for each section of work and used immediately. The choice of this solution to examine adsorption of Cu^{2+} to the microcolumn was based on plans for subsequent experiments. After the method had been developed and optimized, it could be validated by carrying out a complexation capacity experiment using EDTA as the complexing ligand. When the Cu concentration is in excess of the EDTA concentration there will be 'free' Cu in solution and hence it was necessary to examine possible adsorption of free Cu^{2+}, to the microcolumn, from non-acidified solutions.

Unless otherwise stated the uncertainty associated with results in this chapter are the standard deviation of the mean from replicate measurements. The number of replicate measurements is denoted by 'n'.

8.3.1.1 Adsorption of Cu^{2+} to Teflon and polycarbonate microcolumns

The results from a variety of experiments suggested that Cu^{2+} was adsorbing to the surface of the Teflon and polycarbonate microcolumns. There was a significant difference between the absorbance obtained when Cu^{2+} (35 μL) was injected into the graphite furnace and analyzed using the microcolumn system and that obtained when using the normal system (i.e. microcolumn absent). As a typical example, in one experiment the average absorbance was 0.637 ± 0.009 (n = 4) when the Teflon microcolumn was absent; when the Teflon microcolumn was present the average absorbance was 0.308 ± 0.010 (n = 4). Replicate experiments, carried out at a latter date, showed similar results; overall the absorbance obtained for the Teflon microcolumn system was 53 ± 9 % (n = 6) lower than that obtained for the normal system. These results suggest that adsorption of Cu^{2+} to the Teflon microcolumn may be occurring, giving a lower absorbance. Similar results were also obtained using a polycarbonate microcolumn; the absorbance obtained for the polycarbonate microcolumn system was 49 ± 3 % (n = 3) lower than that obtained for the normal system.

The discrepancy observed with and without the microcolumn was not due to differences in the volume of the Cu^{2+} standard removed or dispensed by the two systems. Calibration showed that there were no significant differences in these volumes of solution removed or dispensed when using the microcolumn system compared to the normal system. Furthermore,

injection of an acidified Cu^{2+} standard (1 % HNO_3) using the Teflon microcolumn system showed similar absorbance to that obtained using the normal system; this indicates that there is not a design problem with the Teflon microcolumn.

Multiple Cu^{2+} injections were made using the Teflon microcolumn system to examine if the absorbance increased with the number of Cu^{2+} injections. The absorbance may increase as possible adsorption sites on the microcolumn become saturated; resulting in less loss of Cu^{2+} on the microcolumn. These results are illustrated in Figure 8.4.

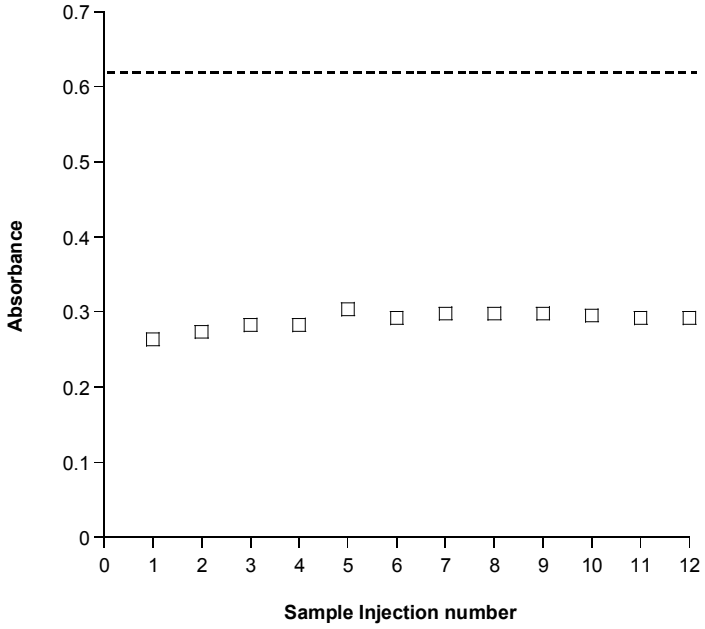

Figure 8.4 Absorbances from multiple injections of a 10 ppb Cu^{2+} standard (35 µL) using the Teflon microcolumn system. The dotted line (-----) represents the absorbance (i.e. 0.620) obtained for the injection of 35 µL of a 10 ppb Cu^{2+} standard using the normal system.

Figure 8.4 shows that there was no measurable difference in absorbance as the number of Cu sample injections increased. After 12 injections, 35 µL of 1 mol L^{-1} HNO_3 was passed completely across the microcolumn and injected into the graphite furnace and analyzed. An absorbance > 1.0 was obtained which indicated significant Cu in the HNO_3 eluent. Further HNO_3 injections were made and only the absorbance associated with the HNO_3 blank was obtained. This result indicates that HNO_3 was quantitatively removing adsorbed Cu from the

Teflon microcolumn. A duplicate of this experiment, in which nine Cu^{2+} injections were carried out and then eluted with 1 mol L^{-1} HNO_3, gave an absorbance of 0.880. Similar results were also obtained when using the polycarbonate microcolumn.

The amount of Cu^{2+} adsorbed to the Teflon microcolumn from one Cu^{2+} injection (instead of multiple injections as for the previous experiments) was examined by passing an aliquot of Cu^{2+} (30 µL) across the microcolumn followed by multiple aliquots of HNO_3 (30 µL) to elute adsorbed Cu^{2+}. This was carried out in triplicate. The results are shown in Table 8.2.

Injection	Absorbance Experiment 1	Absorbance Experiment 2	Absorbance Experiment 3
Cu^{2+}	0.436	0.457	0.428
HNO_3	0.125	0.144	0.128
HNO_3	0.0	0.0	0.0
HNO_3	0.0	0.0	0.0

Table 8.2 Absorbance from a single Cu^{2+} injection (30 µl of 10 ppb Cu^{2+}) followed by multiple HNO_3 injections to remove Cu adsorbed to the Teflon surface. The concentration and volume of HNO_3 used to elute adsorbed Cu were 1 mol L^{-1} and 30 µL, respectively.

The results illustrated in Table 8.2 indicate that between 22 to 24 % of Cu^{2+} is adsorbing to the Teflon microcolumn when one aliquot of a Cu^{2+} standard was passed across the microcolumn; hence this fraction is measured in the HNO_3 eluent. Addition of the absorbance obtained from the Cu^{2+} injection and the first HNO_3 injection, for all 3 experiments, agrees well with the absorbance (i.e. 0.545 ± 0.007) obtained when 30 µL of a 10 ppb Cu^{2+} standard was injected into the graphite furnace using the normal system. This experiment was repeated at various times during the work for this thesis using the same conditions; overall the amount of Cu^{2+} adsorbing to the Teflon microcolumn was 28 ± 10 % (n = 7). Similar experiments involving a polycarbonate microcolumn showed that 31 ± 2 % (n = 2) of Cu^{2+} was adsorbing to the microcolumn. Throughout this work there was no evidence of Cu^{2+} adsorbing to the Teflon delivery tubing.

8.3.1.2 Adsorption of Cu^{2+} to various tubing

The adsorption of Cu^{2+} to various tubing was examined to see if an alternative material could be used to construct a microcolumn. If the tubing was appropriate it could be packed with an adsorbent and used as a microcolumn. Multiple aliquots of a 10 ppb Cu^{2+} (35 µL) standard were passed across the various tubing and any adsorbed Cu^{2+} was eluted with 1 mol L^{-1} HNO_3 (35 µL) and injected into the graphite furnace and analyzed. Table 8.3 shows the absorbance obtained when adsorbed Cu^{2+} was eluted from the various tubing.

	Absorbance					
HNO_3 elution	**Tygon tubing 1**	**Tygon tubing 2**	**Teflon tubing 1**	**Teflon tubing 2**	**Teflon microcolumn**	**Polycarbonate microcolumn**
1	0.020	0.031	0.025	0.037	0.955	1.498
2	0.008	0.009	0.003	0.016	0.065	0.064
3	0.009	0.001	0.007	0.006	0.008	0.027
4	0.0	0.0	0.0	0.0	0.0	0.0

Table 8.3 Adsorption of Cu^{2+} to various materials. Absorbances were obtained when 1 mol L^{-1} HNO_3 (35 µL) was passed across the various tubing and fabricated microcolumns to remove Cu^{2+} that had been adsorbed from passing 4 aliquots of a 10 ppb Cu^{2+} standard (30 µL) completely across the tubing or microcolumns.

Table 8.3 shows that the adsorption of Cu^{2+} to the various tubing was minor compared to the Teflon and polycarbonate microcolumns.

8.3.1.3 Adsorption of Cu^{II} to Teflon and polycarbonate microcolumns in the presence of fulvic acid

The results from a variety of experiments suggested in addition to adsorption from a non-complexing medium, Cu also adsorbed to the surface of the Teflon and polycarbonate microcolumns when fulvic acid was present in solution. There was a significant difference between the absorbances obtained when 30 µL of a Cu-fulvic acid solution (10 ppb Cu and 20 ppm fulvic acid) was injected into the graphite furnace and analyzed using the microcolumn system and that obtained when using the normal system (i.e. column absent). For one of the experiments the average absorbance was 0.602 ± 0.006 (n = 6) when the Teflon microcolumn was absent; when the Teflon microcolumn was present the average absorbance was 0.315 ± 0.024 (n = 5). The results show that the absorbance when the Teflon

microcolumn is used was 48 % lower than when the normal system was used to introduce an aliquot of Cu-fulvic acid solution into the graphite furnace. This suggests that adsorption of a Cu-fulvate complex to the Teflon microcolumn may be occurring, giving a lower absorbance. Replicate experiments, carried out at a latter date, showed similar results to that above; overall the absorbance obtained for the Teflon microcolumn system was 42 ± 6 % (n = 5) lower than that obtained for the normal system. Similar results were also obtained using a polycarbonate microcolumn; the absorbance obtained for the microcolumn system was 55 ± 5 % (n = 3) lower than that obtained for the normal system.

After the above measurements were carried out using the Cu-fulvic acid solution and the Teflon and polycarbonate microcolumns, 1 mol L^{-1} HNO_3 (35 µL) was passed across the microcolumn to elute any adsorbed Cu. The eluent was injected into the graphite furnace and analyzed. For both the Teflon and polycarbonate microcolumns the absorbance for the first HNO_3 elution was > 1.0; further HNO_3 elutions were made and only the absorbance associated with the HNO_3 blank was obtained. This indicates significant Cu in the first HNO_3 eluent originating from Cu that had been adsorbed on the microcolumns in the presence of fulvic acid.

Similar experiments to those above were carried out using a 20 ppm fulvic acid solution that contained 1.5 ppb Cu (instead of 10 ppb Cu). Five aliquots of the Cu-fulvic acid solution were passed across either the Teflon or polycarbonate microcolumns. The average absorbance of the five aliquots for the Teflon microcolumn was 0.075 ± 0.003, for the polycarbonate microcolumn it was 0.062 ± 0.004. After the measurements were completed, 1 mol L^{-1} HNO_3 was used to elute any adsorbed Cu and the eluent injected into the graphite furnace. Figure 8.5 shows the absorbance obtained when passing 5 separate HNO_3 aliquots across the polycarbonate and Teflon microcolumns to remove adsorbed Cu. The first HNO_3 elutions gave relatively high absorbances indicating removal of adsorbed Cu from both the Teflon and polycarbonate micocolumns.

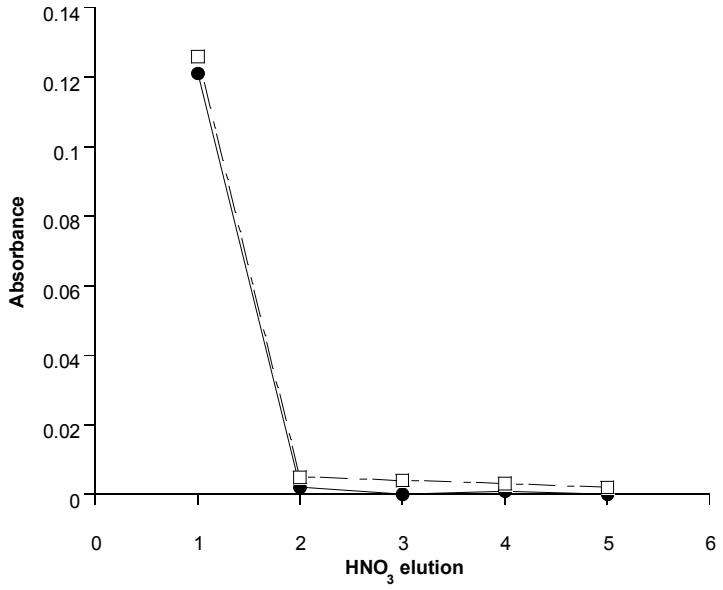

Figure 8.5 Absorbance obtained when 1 mol L^{-1} HNO_3 (30 µL) was passed across the Teflon (●) and polycarbonate (□) microcolumns to remove Cu that had been adsorbed from passing multiple aliquots (30 µL) of a Cu-fulvic acid solution (1.5 ppb Cu and 20 ppm fulvic acid) through the respective microcolumns.

The amount of Cu (from the Cu-fulvic acid system containing 10 ppb Cu and 20 ppm fulvic acid) adsorbed to the Teflon microcolumn from one Cu injection (instead of multiple injections as for previous experiments) was examined by passing an aliquot of the Cu-fulvic acid solution (30 µL) through the microcolumn, followed by multiple injections of HNO_3 to elute any adsorbed Cu. This was carried out in duplicate. The results are shown in Table 8.4.

Injection	Absorbance Experiment 1	Absorbance Experiment 2
Cu-fulvic acid	0.382	0.379
HNO_3	0.134	0.133
HNO_3	0.0	0.0
HNO_3	0.0	0.0

Table 8.4 Absorbance from a single Cu-fulvic injection (30 µl of Cu-fulvic acid solution containing 10 ppb Cu) followed by multiple HNO_3 injections to remove Cu adsorbed to the Teflon surface. The concentration and volume of HNO_3 used to elute adsorbed Cu were 1 mol L^{-1} and 30 µL, respectively.

The results illustrated in Table 8.4 indicate that 26 % of Cu is adsorbing to the Teflon microcolumn and hence this fraction is measured in the HNO_3 eluent. Addition of the absorbance obtained from the Cu-fulvic acid injection and the first HNO_3 injection for both experiments is in reasonable agreement with the absorbance obtained when 30 µL of a 10 ppb Cu-fulvic acid standard is injected into the graphite furnace using the normal system (i.e. 0.506 ± 0.015). Similar experiments involving a polycarbonate microcolumn showed that 34 ± 4 % (n = 2) of Cu was adsorbing to the microcolumn. In the absence of the microcolumn, the amount of Cu adsorbing to only the Teflon delivery tubing was 9 ± 3 %.

The Cu that adsorbed to the polycarbonate and Teflon microcolumns throughout this work did not arise from the sodium acetate buffer that is used to buffer the microcolumn. Buffering the microcolumn for 3 min using 0.05 mol L^{-1} sodium acetate/HNO_3 (pH 5.0) and passing acid through the microcolumn to remove any adsorbed Cu resulted in a signal that was not significantly different from the HNO_3 blank.

8.3.2 Investigation of background absorbance associated with the use of sodium acetate to buffer the Chelex-100 microcolumn

Sodium acetate was initially employed as the buffer to convert the Chelex-100 resin to the Na form after elution with HNO_3 in the previous step. However, when the eluent was injected into the graphite furnace and atomized, a large background absorbance was observed (Figure 8.6). This background was only observed for the 'first' elution of the Chelex-100 resin; successive elutions did not result in a significant background.

This section examines the background that is present when sodium acetate/HNO_3 (pH 5.0) is used to buffer the Chelex-100 microcolumn and investigates a number of parameters to resolve the background absorbance problem. These included introducing a longer washing step to remove sodium acetate that may be trapped within the pore volume of the Chelex-100 resin, changing the temperature program of the ETAAS in an attempt to volatilize the species causing the background, and the use of alternative buffers to convert the Chelex-100 resin from the acidic to the basic form.

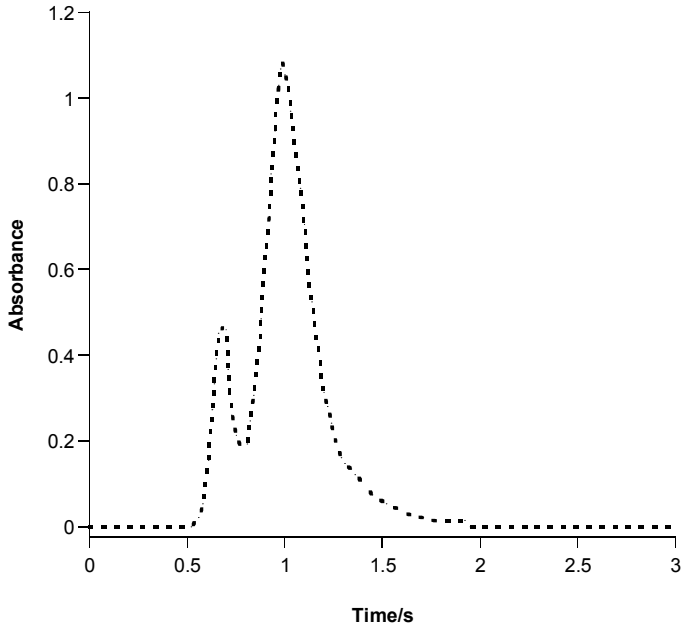

Figure 8.6 Background absorbance observed when 1 mol L^{-1} HNO_3 (30 µL) is passed across the Chelex-100 microcolumn and injected into the graphite furnace and atomized. The microcolumn was buffered by flushing with 0.05 mol L^{-1} sodium acetate/HNO_3 (pH 5.0) for 3 min; this was followed by pumping Milli-Q water across the microcolumn for 3 min to remove any residual buffer. The atomization temperature was 2600 ^oC; the ashing temperature and time were 400 ^oC and 5 s, respectively. The background was monitored at the 228.8 nm Cd line.

8.3.2.1 Effect of background absorbance on Cd signal

The effect that the background absorbance has on the Cd signal was investigated using the procedure outlined in section 8.2.2.1. This procedure was designed so that the first measurement would be affected by the background whereas the second measurement would not be. For the second measurement, the species that gives rise to the background has already been removed from the adsorbent during the first measurement due to the HNO_3 in the sample. Figure 8.7 shows the Cd signal in the presence (a and b) and absence (c and d) of a significant background absorbance. The background absorbance affects peak shape of the Cd signal and reduces sensitivity by between 35 to 42 %.

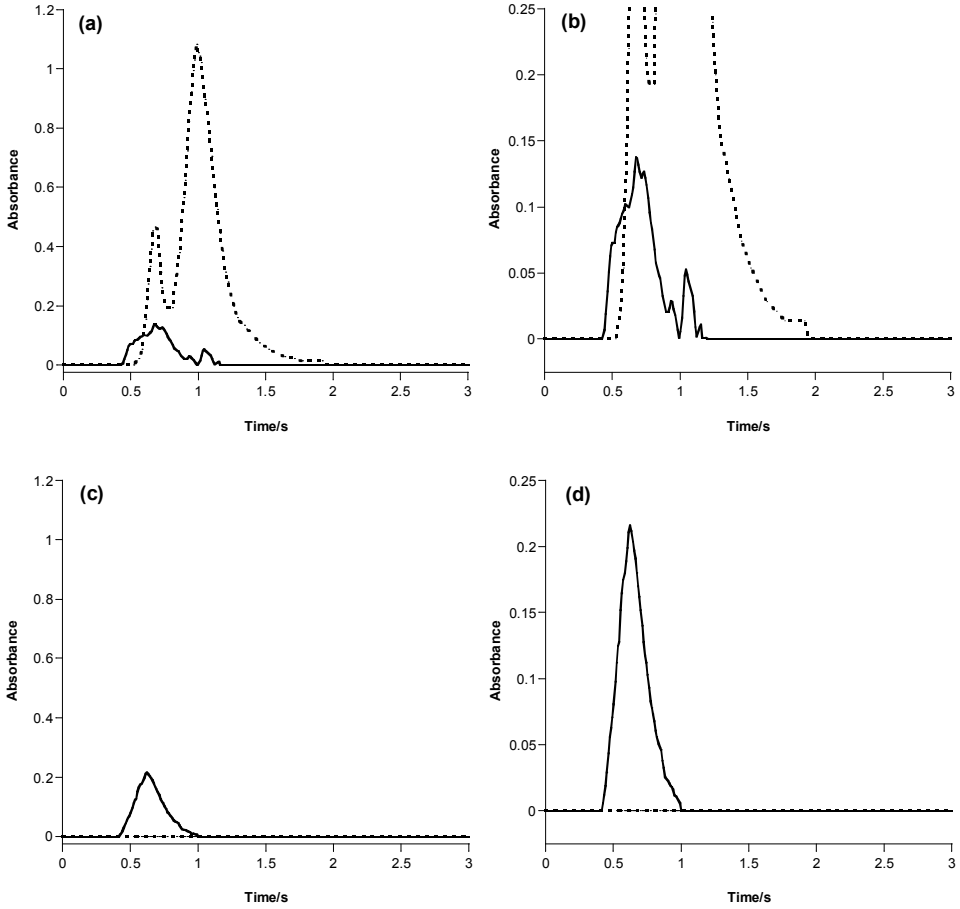

Figure 8.7 Effect of background absorbance (------) on Cd signal (——) with (a and b) and without (c and d) pre-buffering of the microcolumn. Plots (b) and (d) are enlargements of (a) and (c), respectively. The Chelex-100 microcolumn was buffered for 3 min with 0.05 mol L^{-1} sodium acetate (pH 5.0), washed for 3 min with Milli-Q water, and then 10 µL of a 6.25 ppb Cd^{2+} standard (prepared in 1 mol L^{-1} HNO_3) was passed across the microcolumn and injected into the graphite furnace of the ETAAS and atomized giving signals a/b; a replicate Cd^{2+} standard was then passed across the microcolumn and injected into the graphite furnace of the ETAAS and atomized giving signals c/d. The atomization temperature was 2600 ^oC; the ashing temperature and time was 400 ^oC and 5 s, respectively.

8.3.2.2 Washing of Chelex-100 resin with Milli-Q water after buffering with sodium acetate

The effect on the background absorbance of washing the microcolumn with Milli-Q water after buffering was examined for washing times of 0 to 10 min. Varying the washing time from 0 to 10 min had no significant effect on the background signal for the first elution (Table 8.5). However, washing the microcolumn eliminates the background absorbance of a second elution step. In the absence of a washing step a significant background absorbance is

observed for the second acid elution which is typically between 66 to 74 % of the background observed for the first elution. Washing the microcolumn removes residual buffer from within the tubing connected to the Chelex-100 microcolumn and hence eliminates the background absorbance associated with the second elution step. A large background absorbance for a second elution may be a problem if all of the metal retained by the Chelex-100 microcolumn cannot be removed in the first elution and a second elution is required.

Washing time/min	Background absorbance
0	0.848 ± 0.027
3	0.818 ± 0.032
5	0.780 ± 0.025
10	0.824 ± 0.038

Table 8.5 Effect of Milli-Q water washing time on background absorbance. The Chelex-100 microcolumn was flushed for 3 min with 0.05 mol L^{-1} sodium acetate (pH 5.0). The uncertainty associated with the background absorbance is the standard deviation of the mean from duplicate measurements.

8.3.2.3 Ashing temperature and time

The ashing temperature was varied from 400 to 1400 ^{o}C to examine if the species causing the background absorbance could be volatilized from the graphite furnace prior to the atomization step. Figure 8.8 shows the effect of ashing temperature on both the Cd signal (□) and background absorbance (●). It shows that increasing the temperature from 400 to 1000 ^{o}C does not significantly affect the background absorbance signal. At 1200 ^{o}C the background is reduced by over 50 %, however the background can not be removed by increasing the ashing temperature without decreasing the Cd signal. The Cd signal is significantly reduced at ashing temperatures > 400 ^{o}C. The ashing time for these experiments was 5 s; increasing the ashing time up to 40 s at 400 ^{o}C had no significant effect on background absorbance. Figure 8.8 also shows the effect of ashing temperature on the background absorbance when $NaNO_3$ (○) is injected directly into the graphite furnace and analyzed. At ashing temperatures below 1000 ^{o}C, $NaNO_3$ showed similar background absorbance behaviour to that observed when buffering the Chelex-100 column with sodium acetate and eluting.

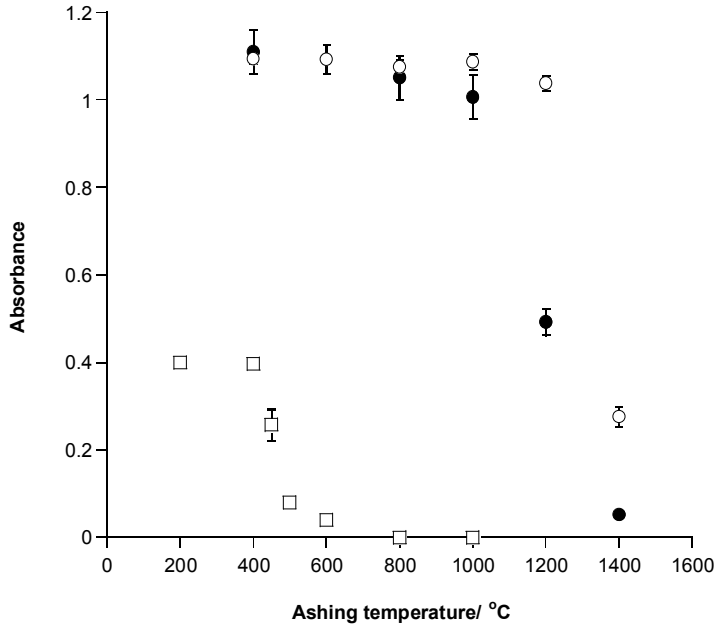

Figure 8.8 Effect of ashing temperature on background absorbance (●) and Cd signal (□). The effect of ashing temperature on the background absorbance associated with $NaNO_3$ (○) has been included for comparison. The concentration of the Cd^{2+} standard was 10 ppb; the concentration of $NaNO_3$ was 0.1 mol L^{-1}. The atomization temperature was 2600 °C; the ashing time was 5 s. The uncertainty associated with each datum point is the standard deviation of the mean from triplicate measurements.

8.3.2.4 Examination of different buffers and a different adsorbent

A variety of buffers were examined as alternatives to sodium acetate. The aim was to identify a buffer which did not show a significant background absorbance when the adsorbent was eluted with HNO_3. The buffers examined were MES, calcium acetate, and ammonium acetate.

The background absorbances from the various buffers are shown in Figure 8.10. The background absorbance associated with the MES buffer, (b), is similar to that of the sodium acetate/HNO_3 buffer (a), whereas for calcium acetate/HNO_3 (c) the maximum background absorbance is less and the absorbance-time profile is different. However, the best result was obtained with ammonium acetate/HNO_3 buffer (d) which did not show any significant background absorbance at concentrations of 0.05 and 1 mol L^{-1}.

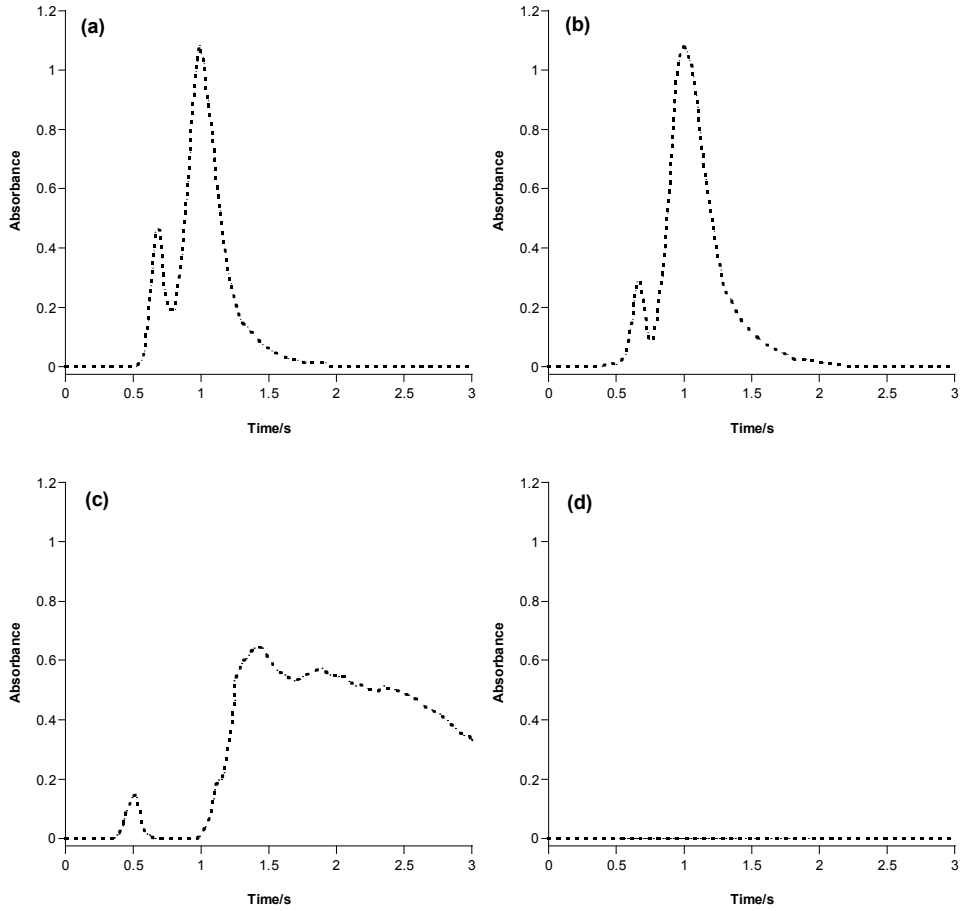

Figure 8.9 Background absorbance observed when 1 mol L^{-1} HNO_3 (30 µL) is passed across the Chelex-100 microcolumn and injected into the graphite furnace and atomized after the microcolumn has been buffered with 0.05 mol L^{-1} of (a) sodium acetate/HNO_3, (b) MES, (c) calcium acetate/HNO_3, and (d) ammonium acetate/HNO_3. After the buffering step the Chelex-100 microcolumn was washed for 3 min using Milli-Q water. The atomization temperature was 2600 ^oC; the ashing temperature and time were 400 ^oC and 5 s, respectively. The background was monitored at the 228.8 nm Cd line.

The background associated with the use of sodium acetate/HNO_3 (pH 5.0) could be completely removed if ammonium acetate/HNO_3 (pH 5.0) was passed across the Chelex-100 microcolumn after sodium acetate/HNO_3. However, passing sodium acetate followed by ammonium acetate and then sodium acetate across the Chelex-100 microcolumn, resulted in the normal background absorbance that is observed in the presence of sodium acetate alone.

Metal salts (40 µL) were directly injected into the graphite furnace and their backgrounds examined. For all of the ammonium salts (ammonium acetate, NH_4Cl and NH_4NO_3) no significant background was observed. However, Na, K and Ca salts (KOH, calcium acetate,

KCl, KNO_3, NaCl, NaOH, $NaNO_3$ and sodium acetate) all showed a significant background absorbance. The MES buffer also showed a significant background.

The effect of sodium acetate/HNO_3 buffer on the background absorbance when using CPG-8HQ as an alternative adsorbent was also examined. After buffering the microcolumn containing CPG-8HQ and elution with HNO_3, no background absorbance was observed. However when the pH of the sodium acetate solution was increased to 8.2 a significant background was evident (Table 8.6). When the CPG-8HQ adsorbent was converted to the basic form using 0.1 mol L^{-1} NaOH, instead of sodium acetate, the background absorbance was 0.280.

pH of sodium acetate/HNO_3 solution	Background absorbance
5.0	0.0
8.2	0.224

Table 8.6 Effect of pH of sodium acetate/HNO_3 on background absorbance when using CPG-8HGQ as the adsorbent. The microcolumn containing CPG-8HQ was buffered for 3 min with 0.05 mol L^{-1} sodium acetate and washed for 3 min with Milli-Q water. The atomization temperature was 2600 ^{o}C; the ashing temperature and time was 400 ^{o}C and 5 s, respectively. The background was monitored at the 228.8 nm Cd line.

8.3.3 Investigation of Cd uptake by Chelex-100 microcolumn

For all experiments in this section the results are presented as an uptake efficiency. The uptake efficiency is the % of total Cd retained by the Chelex-100 resin; it is calculated by determining the absorbance ratio of Cd eluted from the Chelex-100 resin to total Cd (i.e. Cd eluted + Cd not retained by Chelex-100 resin).

8.3.3.1 Washing of Chelex-100 resin after buffering with sodium acetate

The importance of the washing step on uptake efficiency of Cd was investigated to determine whether the Chelex-100 microcolumn should be washed with Milli-Q water after it had been buffered with ammonium acetate/HNO_3 (pH 5.0), prior to loading with Cd. The results are shown in Table 8.7.

Procedure	Uptake efficiency
0.05 mol L^{-1} buffer and 3 min wash step	94 ± 3 % (n = 4)
0.05 mol L^{-1} buffer and 12 min wash step	95 ± 1 % (n = 2)
1 mol L^{-1} buffer and 3 min wash step	94 ± 2 % (n = 2)
0.05 mol L^{-1} buffer and no wash step	65 ± 2 % (n = 3)
1 mol L^{-1} buffer and no wash step	48 ± 4 % (n = 2)

Table 8.7 Effect of washing step on uptake efficiency of Cd^{2+}. The concentration of Cd^{2+} was 6.25 ppb. The Chelex-100 microcolumn was buffered for 3 min using ammonium acetate/HNO_3 (pH 5.0). The uncertainties associated with the uptake efficiency are the standard deviation from replicate measurements.

The results show that washing the Chelex-100 microcolumn for 3 min with Milli-Q water significantly increases the subsequent Cd uptake efficiency when compared to experiments in which the washing step was absent. Washing the Chelex-100 microcolumn for > 3 min does not significantly affect the uptake efficiency. Furthermore, increasing the concentration of the ammonium acetate buffer from 0.05 to 1 mol L^{-1} (in the absence of a washing step) significantly reduces the uptake efficiency.

8.3.3.2 Concentration of ammonium acetate/HNO_3 buffer in solution

The concentration of ammonium acetate/HNO_3 buffer (pH 5.0) in the Cd^{2+} standard solution was varied from 0.0005 to 0.05 mol L^{-1} to examine the effect of buffer concentration on uptake efficiencies. These results are illustrated in Figure 8.10 and are compared to the predicted uptake efficiencies that have been calculated using the computer program SPECIES. The experimental results show that the uptake efficiency is not significantly affected when the ammonium acetate concentration in solution is varied from 0.0005 to 0.005 mol L^{-1}; however ammonium acetate concentrations > 0.005 mol L^{-1} resulted in a decrease in uptake efficiency. From the SPECIES calculations, uptake efficiency is predicted to show a decrease only at an ammonium acetate concentration of 0.05 mol L^{-1}.

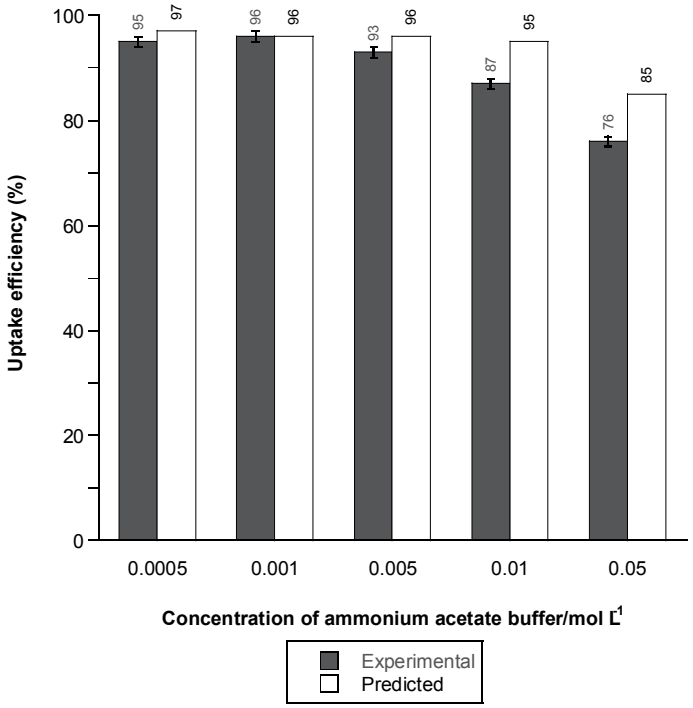

Figure 8.10 Effect of ammonium acetate/HNO_3 buffer concentration (pH 5.0) on experimental uptake efficiency of Cd^{2+}. The Chelex-100 microcolumn was buffered for 3 min using 0.05 mol L^{-1} ammonium acetate and washed for 3 min using Milli-Q water. The uncertainties associated with the uptake efficiency are the standard deviation from triplicate measurements. The predicted uptake efficiencies have been include for comparison. Note that the effect of NH_4^+ could not be included in the SPECIES calculations because of the lack of stability constant data.

8.3.3.3 Concentration of NH_4NO_3 in solution

The effect of ionic strength on the uptake efficiency of Cd^{2+} was examined by varying the concentration of NH_4NO_3 in the Cd^{2+} standard solution from 0 to 0.095 mol L^{-1}. These results are illustrated in Figure 8.11 and show that increasing the NH_4NO_3 concentration from 0.005 to 0.095 mol L^{-1} results in a decrease in uptake efficiency of Cd^{2+}.

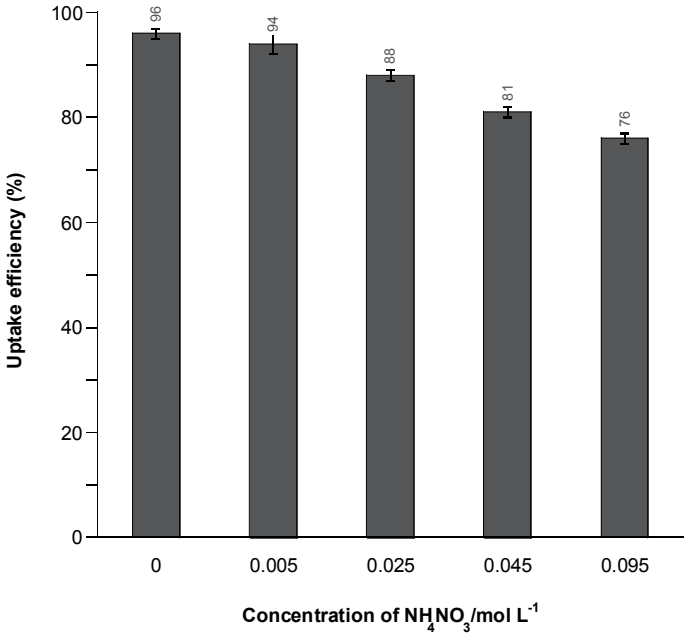

Figure 8.11 Effect of NH_4NO_3 concentration on uptake efficiency of Cd^{2+}. The concentration of Cd^{2+} was 18.75 ppb and the solution contained 0.005 mol L^{-1} ammonium acetate/HNO_3 buffer (pH 5.0). The Chelex-100 microcolumn was buffered for 3 min using 0.05 mol L^{-1} ammonium acetate and washed for 3 min using Milli-Q water. The uncertainties associated with the uptake efficiency are the standard deviation from triplicate measurements.

8.4 Discussion

8.4.1 Adsorption of Cu^{II} to microcolumn materials and tubing in the presence and absence of fulvic acid

8.4.1.1 Adsorption of Cu^{2+} to Teflon and polycarbonate microcolumns and various tubing

The extent of Cu^{2+} adsorption by Teflon and polycarbonate microcolumns, and various Teflon and tygon tubing, was examined using a 10 ppb Cu^{2+} standard that was prepared in 0.005 mol L^{-1} sodium acetate/HNO_3 (pH 5.0). The results from a variety of experiments suggested that Cu^{2+} was adsorbing to the surface of the Teflon and polycarbonate microcolumns.

When one aliquot of 10 ppb Cu^{2+} was passed across the Teflon microcolumn, 28 ± 10 % (n = 7) of Cu was adsorbed; for the polycarbonate microcolumn the adsorption was 31 ± 2 % (n = 2). The adsorption behaviour of Cu^{2+} to the Teflon and polycarbonate microcolumns could be overcome by acidification of the Cu^{2+} standard, presumably because protons compete for and

saturate possible adsorption sites on the surface of the Teflon and polycarbonate microcolumns. The adsorption of Cu^{2+} to Teflon and tygon tubing was relatively minimal.

Teflon containers and bottles are commonly used to store samples and solutions containing both metals and non-metals[25-30] due to Teflon's chemically inertness.[26, 27, 30] A number of studies have been carried out to examine the adsorption of metal ions at the ppb concentration level to Teflon materials.[26, 29, 31-33] Sekaly *et al*.[26] studied the adsorption of trace metals (Al, Cu, Pb, Ni, and Cd) onto the surface of Teflon containers from river water, rain, and melted snow. They found that the metal concentration in the dissolved phase for the melted snow and rain samples, stored in Teflon containers, remained constant during a 2 h experiment at pH 5.5; the same result was obtained for the river water sample at pH 8.1. These results imply that adsorption of metals to the Teflon containers from these media is minimal. Further experiments showed that there was no evidence of metal adsorption to Teflon containers after 24 h.

Massee and Maessen[33] examined the adsorption of Ag, Cd, and Zn onto the surface of Teflon containers in distilled H_2O and synthetic seawater (in which the pH had been adjusted using NaOH and HNO_3). For samples stored for up to 28 days, they found only minor adsorption (< 5 %) of Cd and Ag to the Teflon containers at pH 4 in both distilled H_2O and synthetic seawater. At pH 8.5, Massee and Maessen[33] found that ~ 36 % of Cd and 20 % of Zn had adsorbed to the surface of the Teflon containers after 30 min from distilled H_2O; however at pH 8.5 the adsorption of Cd and Zn from synthetic seawater was minimal. Similar results were obtained for Ag with an increase in adsorption from pH 4 to 8.5. Subramanian *et al*.[29] observed similar behaviour; they found that river water samples stored in Teflon containers showed no loss of Zn in the pH range 1.5 to 8.0 for at least 30 days.

Diaz-Cruz *et al*.[32] examined adsorption of Cd and Zn in various electrochemical cells including Teflon cells. They found significant adsorption of Cd and Zn to Teflon cells at pH > 6 for solutions containing 0.01 mol L^{-1} KNO_3; at pH < 6, adsorption of Cd and Zn to the cells was negligible.

In summary, the results from Sekaly *et al*,[26] Massee and Maessen,[33] Subramanian *et al*.,[29] and Diaz-Cruz *et al*.[32] all showed minor or no adsorption of various trace metals at pH ~ 5, the pH at which experiments for the work in this thesis were carried out.

Somewhat different results were obtained by Anderson *et al.*[31] who examined the adsorption of Cd, Cu, Ni, and Zn to a Teflon soil solution sampler cup from solutions containing 0.01 mol L^{-1} NaCl, 0.01 mol L^{-1} $CaCl_2$, and no electrolyte. They found significant adsorption of all four metal ions by the Teflon cup. At pH 5.8, > 50 % of the metal added adsorbed to the surface of the Teflon cup from a 0.01 mol L^{-1} NaCl matrix ; the adsorption of Cu was greater than that of Cd, Ni, and Zn. Adsorption of Cd, Cu, Ni, and Zn was also observed at pH 3.6, however it was less significant than at pH 5.8. Anderson *et al.*[31] found that when $CaCl_2$ was used to prepare the metal solutions, the adsorption of Cd, Ni and Zn was only minor compared to use of 0.01 mol L^{-1} NaCl, however the adsorption of Cu was still significant. Even though Anderson *et al.*[31] observed adsorption of trace metals to the Teflon cups, the timescale of their experiments and those carried out for the work in this thesis are vastly different. The contact time between the solutions and the Teflon cups for the experiments carried out by Anderson *et al.*[31] was 7 days; for the experiments carried out for the work in this thesis the contact time between the Cu^{2+} solution and the Teflon microcolumn was ~ 2 s. It has been shown that when trace metals adsorb to various bottle and container materials, that adsorption increases with storage time.[26, 29, 33] Furthermore, the Teflon cups used by Anderson *et al.*[31] consisted of two phases: Teflon and a mineral residue from quartz flour (which is used to produce the cup). The authors proposed that the mineral surface provides the adsorption sites for metal ions.[31]

The unexpected adsorption of Cu^{2+} to the Teflon and polycarbonate microcolumns observed in the work for this thesis may be due to the way in which the microcolumns are fabricated. It is reported that radicals are formed when polymeric materials such as Teflon and polycarbonate are mechanically fractured.[34-38] These radicals are know as mechanoradicals; they are defined as free radicals that are produced by mechanical action such as drilling and cutting of the polymer.[35] Mechanoradicals are formed when homolytic scission of a carbon-carbon bond occurs (equation 8.1).[37, 38]

$$C{-}C \longrightarrow C^{\cdot} + C^{\cdot} \qquad \textbf{(8.1)}$$

It is possible that if the radicals that form on the surface of the Teflon and polycarbonate microcolumns during construction of the microcolumn are long lived, they interact with Cu^{2+} leading to adsorption. Furthermore, mechanoanions and mechanocations can also form on the

surface of polymer materials when heterolytic scission of a carbon-carbon bond occurs (equation 8.2).[37]

$$C{-}C \longrightarrow C^{+} + C^{-} \qquad \textbf{(8.2)}$$

These anionic surface species would also provide possible adsorption sites for Cu^{2+}. The results from this thesis showed that various samples of Teflon tubing, which is unlikely to have been mechanically fractured or stressed, showed minimal adsorption.

8.4.1.2 Adsorption of Cu^{II} to Teflon and polycarbonate microcolumns in the presence of fulvic acid

The extent of Cu adsorption by Teflon and polycarbonate microcolumns in the presence of fulvic acid was examined. Two fulvic acid solutions were used in the work for this thesis; both contained the same concentration of fulvic acid (20 ppm) but varied in their Cu concentrations (10 and 1.5 ppb Cu). The amount of Cu in both fulvic acid solutions was less than the Cu complexation capacity of the fulvic acid sample (340 ± 40 μmol Cu (g FA)$^{-1}$).[39] For the Cu-fulvic acid solutions that contained 10 and 1.5 ppb Cu, the amount of Cu was ~ 40 times and ~ 250 times less than that required to reach the complexation capacity of the fulvic acid, respectively. The low Cu concentration, relative to fulvic acid, of both solutions suggests that Cu should be bound in inert complexes and hence there should be negligible free Cu to adsorb to the surface of the microcolumns. However, significant Cu adsorption was observed in both the Teflon and polycarbonate microcolumns. When one aliquot of the Cu-fulvic acid solution (containing 10 ppb Cu and 20 ppm fulvic acid) was passed across the Teflon microcolumn, 26 ± 1 % (n = 2) of Cu was adsorbed; for the polycarbonate microcolumn the adsorption was 34 ± 4 % (n =2). The difference in adsorption between the polycarbonate and Teflon microcolumns may be due to the reactivity of each material or the difference in internal surface areas of the two microcolumns. The internal surface areas of the Teflon and polycarbonate microcolumns were 0.49 and 0.66 cm^2, respectively. Significant adsorption of Cu from the Cu-fulvic acid solution containing 1.5 ppb Cu and 20 ppm fulvic acid was also observed.

The precise nature of Cu adsorption in the presence of fulvic acid is unknown. It may be due to 'free' Cu adsorbing to the Teflon and polycarbonate surface as described above. However because the concentration of Cu is much less than the Cu complexation capacity of the fulvic

acid sample, this seems unlikely. Another possible mechanism is a hydrophobic interaction between hydrophobic components of the fulvic acid sample and the hydrophobic Teflon surface, and to a lesser extent polycarbonate. Hydrophobic interactions have been used to adsorb a variety of non-charged metal complexes of pyrrolidinedithiocarbamate[9, 40, 41] and diethyldithiophosphate[14, 15, 18] to Teflon materials such as beads,[14, 15, 18, 42] tubing[18, 40, 42] and turnings.[9, 41] Furthermore, although fulvic acids are highly soluble in water, they are known to adsorb strongly to hydrophobic XAD resins.[24, 43-45] However, this occurs at low pH when the functional groups of fulvic acid are protonated and therefore adsorption to the surface of the resin can occur. Aiken *et al.*[45] studied the effect of pH on the adsorption of a fulvic acid on XAD-8 resin; they found adsorption increased as the pH was decreased from 7 to 2. The experiments for the work in this thesis were carried out at pH 5; hence the interaction between fulvic acid and a hydrophobic surface would be expected to be minimal, however complexation of the metal ion will reduce the net charge on the fulvic acid possibly promoting adsorption.

Adsorption of Cu-fulvic acid complexes to the microcolumns would significantly affect the measurement of both the labile and inert Cu fractions. In addition to the capture of 'free' Cu on the adsorbent, Cu-fulvic acid complexes would adsorb to the microcolumn material. The inert fraction would thus be underestimated whilst the labile fraction would be overestimated and therefore this method would be severely limited when applied to humic natural waters (which had been an objective of this work).

8.4.2 Investigation of background absorbance associated with the use of sodium acetate to buffer the Chelex-100 microcolumn

The background absorbance observed when using sodium acetate/HNO_3 (pH 5.0) to buffer the Chelex-100 microcolumn significantly affected the Cd signal. In the presence of the background causing species, Cd sensitivity was decreased by between 35 to 42 % (for a 6.25 ppb Cu^{2+} standard prepared in 1 mol L^{-1} HNO_3); in addition the profile of the absorbance-time signal was affected. The decrease in analyte sensitivity may be due to premature volatilization of Cd species from the graphite furnace during the ashing step, and/or the background correction method is incapable of compensating for the effect of the interfering matrix species from the buffer, when the Chelex-100 microcolumn is buffered with sodium acetate and eluted with HNO_3. The asymmetry of the Cd signal indicates the limited ability of

continuum source to correct accurately for background absorbing species. Because the Cd signal is reduced, the labile fraction of a sample would be significantly underestimated.

Background absorbance is due to molecular absorption and/or light scattering. It is proposed that the background absorbance observed in the work for this thesis is due to the initial presence of $NaNO_3$ in the graphite furnace. When the Chelex-100 microcolumn is buffered with sodium acetate, protons (from the previous elution step) are displaced from the adsorbent and replaced with Na^+. During elution of the adsorbent with HNO_3, Na^+ is displaced by H^+ and $NaNO_3$ is formed.

The results obtained here agree in general with those of other studies which have shown that metals salts such as NaCl, $MgCl_2$, $CaCl_2$, $NaNO_3$, $Mg(NO_3)_2$, Na_2SO_4, $MgSO_4$, and $CaSO_4$ give rise to significant background absorption in ETAAS and can interfere with the analyte signal.[46, 47]

This section discusses the affects of various conditions and parameters on the background absorbance signal. This includes washing of the Chelex-100 resin after the buffering step, varying the ashing temperature and time and using different buffers and a different adsorbent.

8.4.2.1 Washing of Chelex-100 resin with Milli-Q water after buffering with sodium acetate

Washing of the Chelex-100 resin with Milli-Q water (up to 10 min) after buffering with 0.05 mol L^{-1} sodium acetate/HNO_3 (pH 5.0) was examined to see if the species causing the background absorbance could be physically removed by using a longer washing step. Even though washing of the Chelex-100 microcolumn with Milli-Q water removed residual buffer from within the tubing connected to the microcolumn, it had no measurable effect on the background absorbance associated with the first Chelex-100 microcolumn elution. This indicates that the species that is causing the background is simply not occluded in the pore volume of the Chelex-100 resin.

8.4.2.2 Ashing temperature and time

The ashing temperature was varied from 400 to 1400 ^oC to examine if the species causing the background absorbance could be volatilized from the graphite furnace prior to the atomization step. The background decreased significantly at ashing temperatures > 1000 ^oC;

however at ashing temperatures > 400 ^{o}C the Cd signal significantly decreased indicating loss of volatile molecular Cd species from the graphite furnace. This implies that increasing the ashing temperature is not a practical way to overcome the background absorbance problem when Cd is the analyte. On the other hand, this may be an appropriate method for metals that are less volatile than Cd. Longer ashing times at an ashing temperature of 400 ^{o}C also had no significant effect on the background absorbance.

The effect of ashing temperature on the background associated with direct injection of 0.1 mol L^{-1} $NaNO_3$ showed similar behaviour to that obtained when the Chelex-100 microcolumn is buffered and eluted. The $NaNO_3$ background decreased at ashing temperatures > 1200 ^{o}C which is higher than that observed for the Chelex-100 microcolumn eluent background (i.e. > 1000 ^{o}C). Even though there is a discrepancy in the temperature at which the background is removed for the direct injection of $NaNO_3$ and for the background associated with the Chelex-100 microcolumn, this does not necessarily imply that $NaNO_3$ is not the cause of the Chelex-100 microcolumn background. These experiments were carried out at different times with different graphite furnaces. The age of the furnace may influence the ashing temperature at which background starts to be removed and also the amounts of $NaNO_3$ deposited into the graphite furnace may also have an effect.

It is reported that $NaNO_3$ decomposes to $NaNO_2$ at 380 ^{o}C;[48, 49] at temperatures > 800 ^{o}C $NaNO_2$ decomposes to Na_2O which has a melting point of 920 ^{o}C and sublimes at 1275 ^{o}C.[49] This sublimation temperature agrees well with the temperature at which the species which causes the background absorbance is volatilized from the furnace (1000-1200 ^{o}C) and is consistent with the involvement of $NaNO_3$ in the background absorbance.

8.4.2.3 Examination of different buffers and a different adsorbent

A variety of buffers (MES, calcium acetate, and ammonium acetate) were examined to investigate the possibility of using an alternative buffer to sodium acetate. A suitable buffer must not show a significant background absorbance when Chelex-100 is eluted with HNO_3. Ammonium acetate (at 0.05 or 1 mol L^{-1}) showed no significant background when used to buffer the Chelex-100 microcolumn whereas there was a significant background associated with both the MES and calcium acetate buffers. The background associated with the MES buffer was very similar to that for sodium acetate.

Employing ammonium acetate as the buffer to regenerate the Chelex-100 resin means that there is no opportunity for $NaNO_3$ to form. When the Chelex-100 resin is eluted, NH_4NO_3 is formed instead of $NaNO_3$; NH_4NO_3 shows no significant background. Confirming this interpretation, when NH_4NO_3 (40 µL of 0.1 mol L^{-1}) was directly injected into the graphite furnace and analyzed there was no significant background; however when $NaNO_3$ (40 µL of 0.1 mol L^{-1}) was injected directly into the graphite furnace and analyzed, the background observed was similar to that obtained when the Chelex-100 microcolumn is buffered with sodium acetate and eluted with HNO_3. All of the Na^+, K^+ and Ca^{2+} salts investigated showed a significant background when injected directly into the graphite furnace, whereas the NH_4^+ salts showed no significant background.

Ammonium acetate (pH 5.0) has previously been used as a washing solution to remove weakly bound major cations such as Ca^{2+}, Mg^{2+}, Na^+, and K^+ from chelating resins prior to elution.[3, 10, 12, 21, 50-53] At pH < 5.0, transition metals can also be eluted from the resin using ammonium acetate.[53] Ellis and Roberts[21] showed that if the washing step with ammonium acetate was not included then both sensitivity and precision is negatively affected due to the major cation species interfering with the Cu, Cd, Mn, and Pb signal. Chang *et al*.[10] observed a 33 % decrease in the Cd signal if a washing step with ammonium acetate was not used; they also found that the background absorbance decreased with increased volume of washing solution. The results from the present work, which show that the background associated with buffering the Chelex-100 microcolumn with sodium acetate can be overcome by washing with 0.05 mol L^{-1} ammonium acetate; agree with those from the literature.

The use of CPG-8HQ as an alternative adsorbent was also examined and showed no significant background when sodium acetate/HNO_3 (pH 5.0) was used to buffer the adsorbent. However if the pH of the sodium acetate/HNO_3 buffer was increased to 8.2 a significant background was observed (Absorbance = 0.224) which was similar to, but lower than, that obtained when Chelex-100 resin is used as the adsorbent (Absorbance > 0.8).

The structure of 8HQ is shown in Figure 8.12. The pK_a values for 8HQ are 5.06 and 9.81.[54] The pK_a value at 5.06 corresponds to proton dissociation from the N^+-H group and the pK_a value at 9.81 corresponds to the O-H group.[54] At pH 5.0 the O-H group would not be significantly deprotonated and when the CPG-8HQ adsorbent is buffered with sodium acteate/HNO_3 (pH 5.0), a Na^+ counter ion is not required. Therefore CPG-8HQ can be used

as an adsorbent in conjunction with sodium acetate/HNO_3 at pH 5.0 without problems of background absorbance. However, at higher pH deprotonation of the O-H group will occur and Na^+ will act as a counter ion for the 8HQ anion. Under these conditions, when eluted with HNO_3 the background absorbance would appear due to the presence of $NaNO_3$. This behaviour was observed at pH 8.2.

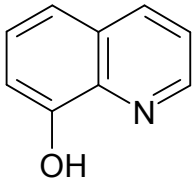

Figure 8.12 Structure of 8-hydroxyquinoline (8HQ).

There are some disadvantages to the use of CPG-8HQ. These include non-quantitative elution of some metals;[39, 50] it has been reported that both HNO_3 and HCl are required for quantitative elution.[50] Furthermore, CPG-8HQ is no longer commercially available.

8.4.3 Investigation of Cd uptake by Chelex-100 microcolumn

Throughout the work for this thesis the uptake efficiency for a Cd^{2+} standard (in the concentration range 6.25 to 18.75 ppb) ranged from 90 to 98 % when optimum conditions were used. The variability in the uptake efficiency may have been due to the swelling and shrinking effect of the Chelex-100 resin; at times during the work for this thesis the flow through the microcolumn seemed to be impeded. This problem was resolved by packing the microcolumn with new Chelex-100 resin every day.

The average uptake efficiency was 94 ± 2 % (n = 47). The uncertainty associated with the uptake efficiency is the standard deviation of the mean for the 47 determinations. The average uptake efficiency is in good agreement with the 96 % that was calculated using the SPECIES program. The elution efficiency (i.e. percentage of Cd removed from the Chelex-100 microcolumn during the elution step) using 10 μL of 1 mol L^{-1} HNO_3 was > 98 %.

8.4.3.1 Washing of Chelex-100 resin after buffering with sodium acetate

The importance of the washing step on uptake efficiency was investigated to see if the Chelex-100 microcolumn required to be washed after it had been buffered with ammonium acetate/HNO_3 (pH 5.0). The results showed that the washing step was critical in maintaining

high uptake efficiency and that in the absence of a washing step the uptake efficiency was dependent on the concentration of ammonium acetate/HNO_3 used to buffer the Chelex-100 microcolumn. Buffering the Chelex-100 microcolumn with 0.05 mol L^{-1} ammonium acetate in the absence of a washing step reduced the uptake efficiency from 94 ± 3 % (n = 4) to 65 ± 2 % (n = 3) and when 1 mol L^{-1} ammonium acetate/HNO_3 was used to buffer the Chelex-100 microcolumn in the absence of a washing step, the uptake efficiency was reduced from 94 ± 2 % (n = 2) to 48 ± 4 % (n = 2).

Clearly, ammonium acetate that is retained within the pore volume of the Chelex-100 resin has a significant effect on the uptake of Cd^{2+} by Chelex-100 resin. This may be due to a combination of competition between the Chelex-100 resin and the acetate ion for Cd^{2+} and competition between NH_4^+ and Cd^{2+} for binding sites on the Chelex-100 resin.

8.4.3.2 Concentration of ammonium acetate/HNO_3 buffer in solution

The concentration of ammonium acetate/HNO_3 (pH 5.0) in the Cd^{2+} standard was varied from 0.005 to 0.05 mol L^{-1} to examine the effect of buffer concentration on uptake efficiency. The results showed that the uptake efficiency decreased when the ammonium acetate concentration was > 0.005 mol L^{-1}. The predicted uptake efficiencies, which were calculated using the SPECIES computer program, indicated a decrease only at an ammonium acetate concentration of 0.05 mol L^{-1}. The decrease predicted by the SPECIES calculation is due to complexation of Cd^{2+} by acetate to form $CdCH_3COO^+$ and $Cd(CH_3COO)_2$ which is not adsorbed to the Chelex-100 resin. Reasonable agreement was obtained between the experimental results and those predicted for ammonium acetate concentrations ≤ 0.005 mol L^{-1}. At ammonium acetate concentrations > 0.005 mol L^{-1} the agreement between the experimental and predicted results was less satisfactory. However, the effect of NH_4^+ concentration could not be included in the SPECIES calculation because of the lack of stability constant data. For an ammonium acetate concentration of 0.01 mol L^{-1} the experimental uptake efficiency was 87 ± 1 % whereas the predicted uptake efficiency was 95 %; at an ammonium acetate concentration of 0.05 mol L^{-1} the experimental uptake efficiency was 76 ± 1 % whereas the predicted uptake efficiency was 85 %. The discrepancy between the experimental and predicted uptake efficiencies may be due to weak competition between NH_4^+ and Cd^{2+} for resin sites. At an ammonium acetate concentration of 0.05 mol L^{-1}, the concentration of NH_4^+ is 3 x 10^5 times higher than the concentration of Cd^{2+}.

Ellis and Roberts[21] examined the effect of ammonium acetate concentration on the uptake of Cu, Cd, Mn, and Pb by Chelex-100 resin. They found that increasing the ammonium acetate concentration from 0.125 to 2 mol L^{-1} resulted in a decrease in the uptake of metal ions by the resin. This result is in good agreement with the work in this thesis. Ellis and Roberts[21] proposed that the poor recovery of metal ions at high ammonium acetate concentration is due to the high concentration of NH_4^+ competing with the analyte for adsorption sites. Jimenez[50] examined the uptake of a variety of metal ions by Chelex-100 resin at ammonium acetate concentrations of 0.1, 0.25, 0.5, and 1 mol L^{-1}. They found the best recovery of metal ions at an ammonium acetate concentration of 0.1 mol L^{-1}; higher concentrations of ammonium acetate resulted in ion-exchange being dominated by NH_4^+.

Vassileva and Furuta[52] examined the retention of Bi, Mo, Pb, Tl and V by the chelating resin Muromac A-1 when ammonium acetate was being used to remove metals such as Ca, Mg, and Na from the resin. Muromac A-1 has the same chelating groups as Chelex-100 (i.e. iminodiacetate) except that these groups are immobilized on a different polymeric support. They found that Bi, Mo, Pb, Tl, and V were increasingly removed from the Muromac A-1 resin as the ammonium acetate concentration was increased from 0.04 to 1 mol L^{-1}; this indicates that uptake or retention of these metal ions by Muromac A-1 is affected by the ammonium acetate concentration.

8.4.3.3 Concentration of NH_4NO_3 in solution

The effect of ammonium concentration on the uptake efficiency of Cd^{2+} was examined by varying the concentration of NH_4NO_3 in the Cd^{2+} standard solution from 0 to 0.095. The results showed that the uptake efficiency was dependent on the NH_4NO_3 concentration in solution. The uptake efficiency decreased from 96 ± 1 % in the absence of NH_4NO_3 to 76 ± 1 % at an NH_4NO_3 concentration of 0.095 mol L^{-1}. The results confirm that the reduced uptake by Cd^{2+} at high ammonium acetate concentration is due to the high concentration of ammonium.

8.5 Conclusion

This chapter was concerned with the preliminary investigation of coupling a microcolumn packed with Chelex-100 resin with ETAAS for speciation measurements. The results

suggested that Cu^{2+} was adsorbing to the surface of both the Teflon and polycarbonate microcolumns; more importantly there was also evidence of adsorption of Cu-fulvic acid complexes to both microcolumns presumably via a hydrophobic interaction between fulvic acid and the microcolumn surface. Adsorption of complexes would significantly affect the measurement of both the labile and inert fractions of a sample.

The ETAAS background absorbance that was observed when the Chelex-100 microcolumn was buffered with 0.05 mol L^{-1} sodium acetate and eluted with HNO_3 was found to be due to the presence of $NaNO_3$. The background could not be removed by washing the Chelex-100 resin or varying the ETAAS temperature program to volatilize the species causing the background prior to atomization; however the background absorbance problem was solved by using ammonium acetate to buffer the Chelex-100 resin. Alternatively the CPG-8HQ adsorbent could be used in conjunction with sodium acetate at pH 5.0 and no significant background would observed, though there are some disadvantages to using CPG-8HQ.

Lastly, the effects of washing the Chelex-100 resin after buffering, and varying the concentrations of ammonium acetate buffer and NH_4NO_3, on the uptake efficiency of Cd^{2+}, were examined. It was shown that washing the Chelex-100 resin with Milli-Q water after buffering with ammonium acetate was critical in maintaining high uptake efficiency of Cd^{2+}; furthermore the highest uptake efficiencies were obtained at low ammonium acetate and NH_4NO_3 concentrations.

This preliminary study of on-line microcolumn fraction of metals showed promising results. High uptake and elution efficiencies were obtained when using optimum conditions, and use of ammonium acetate/HNO_3 to buffer the chelex-100 microcolumn led to no significant background. A significant weakness for this method (in relation to its intended application to environmental waters) was the possible adsorption of Cu-fulvic acid complexes to the microcolumn materials. Further work is required to assess the feasibility of this method. For comments on further work required see chapter 9 (conclusions and future work).

8.6 References

1. Adams, M. L.; Powell, K. J., Flow injection method for iron fractionation by reaction with oxine-derivatised fractogel. *Analytica Chimica Acta* **2001,** 433, (2), 289-297.

2. Bowles, K. C.; Apte, S. C.; Batley, G. E.; Hales, L. T.; Rogers, N. J., A rapid chelex column method for the determination of metal speciation in natural waters. *Analytica Chimica Acta* **2006,** 558, (1-2), 237-245.

3. Fernandez, F. M.; Stripeikis, J. D.; Tudino, M. B.; Troccoli, O. E., Fully automatic on-line separation preconcentration system for electrothermal atomic absorption spectrometry: Determination of cadmium and lead in sea-water. *Analyst* **1997,** 122, (7), 679-684.

4. Procopio, J. R.; Viana, M. D. M.; Hernandez, L. H., Microcolumn ion-exchange method for kinetic speciation of copper and lead in natural waters. *Environmental Science & Technology* **1997,** 31, (11), 3081-3085.

5. Simpson, S. L.; Powell, K. J.; Nilsson, N. H. S., Flow injection determination of Al^{3+} and $Al_{13}O_4(OH)_{24}(H_2O)_{12}^{7+}$ species using a 1.3-s reaction with 8-quinolinol-derivatised fractogel. *Analytica Chimica Acta* **1997,** 343, (1-2), 19-32.

6. Matousek, J. P.; Money, S. D.; Powell, K. J., Metal speciation by coupled in situ graphite furnace electrodeposition and electrothermal atomic absorption spectrometry. *Talanta* **2000,** 52, (6), 1111-1122.

7. Shraim, A.; Chiswell, B.; Olszowy, H., Speciation of arsenic by hydride generation-atomic absorption spectrometry (HG-AAS) in hydrochloric acid reaction medium. *Talanta* **1999,** 50, (5), 1109-1127.

8. Bermejo-Barrera, P.; Moreda-Pineiro, J.; Moreda-Pineiro, A.; Bermejo-Barrera, A., Selective medium reactions for the 'arsenic(III)', 'arsenic(V)', dimethylarsonic acid and monomethylarsonic acid determination in waters by hydride generation on-line electrothermal atomic absorption spectrometry with in situ preconcentration on Zr-coated graphite tubes. *Analytica Chimica Acta* **1998,** 374, (2-3), 231-240.

9. Anthemidis, A. N.; Zachariadis, G. A.; Stratis, J. A., Cobalt ultra-trace on-line preconcentration and determination using a PTFE turnings packed column and electrothermal atomic absorption spectrometry. Applications in natural waters and biological samples. *Journal of Analytical Atomic Spectrometry* **2002,** 17, (10), 1330-1334.

10. Chang, H. J.; Sung, Y. H.; Huang, S. D., Determination of ultra-trace amounts of cadmium, cobalt and nickel in sea-water by electrothermal atomic absorption spectrometry with on-line preconcentration. *Analyst* **1999,** 124, (11), 1695-1699.

11. Fang, Z. L., Trends and potentials in flow injection on-line separation and preconcentration techniques for electrothermal atomic absorption spectrometry. *Spectrochimica Acta Part B-Atomic Spectroscopy* **1998,** 53, (10), 1371-1379.

12. Fernandez, F. M.; Tudino, M. B.; Troccoli, O. E., Automatic on-line ultratrace determination of Cd species of environmental significance in natural waters by FI-ETAAS. *Journal of Analytical Atomic Spectrometry* **2000,** 15, (6), 687-695.

13. Liu, Z. S.; Huang, S. D., Automatic online preconcentration system for graphite-furnace atomic-absorption spectrometry for the determination of trace-metals in sea-water. *Analytica Chimica Acta* **1993,** 281, (1), 185-190.

14. Long, X. B.; Chomchoei, R.; Gala, P.; Hansen, E. H., Evaluation of a novel PTFE material for use as a means for separation and preconcentration of trace levels of metal ions in sequential injection (SI) and sequential injection lab-on-valve (SI-LOV) systems - determination of cadmium(II) with detection by electrothermal atomic absorption spectrometry (ETAAS). *Analytica Chimica Acta* **2004,** 523, (2), 279-286.

15. Miro, M.; Jonczyk, S.; Wang, J. H.; Hansen, E. H., Exploiting the bead-injection approach in the integrated sequential injection lab-on-valve format using hydrophobic packing materials for on-line matrix removal and preconcentration of trace levels of cadmium in environmental and biological samples via formation of non-charged chelates prior to etaas detection. *Journal of Analytical Atomic Spectrometry* **2003,** 18, (2), 89-98.

16. Sung, Y. H.; Huang, S. D., On-line preconcentration system coupled to electrothermal atomic absorption spectrometry for the simultaneous determination of bismuth, cadmium, and lead in urine. *Analytica Chimica Acta* **2003,** 495, (1-2), 165-176.

17. Sung, Y. H.; Liu, Z. S.; Huang, S. D., Automated on-line preconcentration system for electrothermal atomic absorption spectrometry for the determination of copper and molybdenum in sea-water. *Journal of Analytical Atomic Spectrometry* **1997,** 12, (8), 841-847.

18. Wang, J. H.; Hansen, E. H., Sequential injection on-line matrix removal and trace metal preconcentration using a PTFE beads packed column as demonstrated for the determination of cadmium by electrothermal atomic absorption spectrometry. *Journal of Analytical Atomic Spectrometry* **2002,** 17, (3), 248-252.

19. Alonso, E. V.; de Torres, A. G.; Pavon, J. M. C., Flow injection on-line electrothermal atomic absorption spectrometry. *Talanta* **2001,** 55, (2), 219-232.

20. Fang, Z.; Tao, G., Flow injection on-line solid-liquid separation and preconcentration atomic spectrometry. In *Flow analysis with atomic spectrometric detectors*, Sanz-Medel, A., Ed. Elesvier: New York, 1999.

21. Ellis, L. A.; Roberts, D. J., Determination of copper, cadmium, manganese and lead in saline water with flow injection and atom trapping atomic absorption spectrometry. *Journal of Analytical Atomic Spectrometry* **1998,** 13, (7), 631-634.

22. Fang, Z. L.; Ruzicka, J.; Hansen, E. H., An efficient flow-injection system with online ion-exchange preconcentration for the determination of trace amounts of heavy-metals by atomic-absorption spectrometry. *Analytica Chimica Acta* **1984,** 164, 23-39.

23. Powell, H. K. J.; Fenton, E., Size fractionation of humic substances: Effect on protonation and metal binding properties. *Analytica Chimica Acta* **1996,** 334, (1-2), 27-38.

24. Gregor, J. E.; Powell, H. K. J., Acid pyrophosphate extraction of soil fulvic-acids. *Journal of Soil Science* **1986,** 37, (4), 577-585.

25. Ariza, J. L. G.; Morales, E.; Sanchez-Rodas, D.; Giraldez, I., Stability of chemical species in environmental matrices. *Trac-Trends in Analytical Chemistry* **2000,** 19, (2-3), 200-209.

26. Sekaly, A. L. R.; Chakrabarti, C. L.; Back, M. H.; Gregoire, D. C.; Lu, J. Y.; Schroeder, W. H., Stability of dissolved metals in environmental aqueous samples: Rideau river surface water, rain and snow. *Analytica Chimica Acta* **1999,** 402, (1-2), 223-231.

27. Reimann, C.; Siewers, U.; Skarphagen, H.; Banks, D., Does bottle type and acid-washing influence trace element analyses by ICP-MS on water samples? A test covering 62 elements and four bottle types: High density polyethene (HDPE), polypropene (PP), fluorinated ethene propene copolymer(FEP) and perfluoroalkoxy polymer(PFA). *Science of the Total Environment* **1999,** 239, (1-3), 111-130.

28. Gasparon, M., Trace metals in water samples: Minimising contamination during sampling and storage. *Environmental Geology* **1998,** 36, (3-4), 207-214.

29. Subramanian, K. S.; Chakrabarti, C. L.; Sueiras, J. E.; Maines, I. S., Preservation of some trace-metals in samples of natural-waters. *Analytical Chemistry* **1978,** 50, (3), 444-448.

30. Batley, G. E.; Gardner, D., Sampling and storage of natural-waters for trace-metal analysis. *Water Research* **1977,** 11, (9), 745-756.

31. Andersen, M. K.; Raulund-Rasmussen, K.; Strobel, B. W.; Hansen, H. C. B., Adsorption of cadmium, copper, nickel, and zinc to a poly(tetrafluorethene) porous soil solution sampler. *Journal of Environmental Quality* **2002,** 31, (1), 168-175.

32. Diazcruz, J. M.; Esteban, M.; Vandenhoop, M.; Vanleeuwen, H. P., Stripping voltammetry of metal-complexes - interferences from adsorption onto cell components. *Analytical Chemistry* **1992,** 64, (17), 1769-1776.

33. Massee, R.; Maessen, F.; Degoeij, J. J. M., Losses of silver, arsenic, cadmium, selenium and zinc traces from distilled water and artificial sea-water by sorption on various container surfaces. *Analytica Chimica Acta* **1981,** 127, 181-193.

34. Tatar, L.; Kaptan, H. Y., Computer-simulation analysis of the ESR spectra of mechanoradicals in PMMA. *Journal of Polymer Science Part B-Polymer Physics* **1997,** 35, (14), 2195-2200.

35. Kaptan, H. Y.; Tatar, L., An electron spin resonance study of mechanical fracture of poly(methyl methacrylate). *Journal of Applied Polymer Science* **1997,** 65, (6), 1161-1167.

36. Shimada, S.; Suzuki, A.; Sakaguchi, M.; Hori, Y., Molecular motion of chain end peroxy radicals of polyethylene molecules tethered on a fresh surface of poly(tetrafluoroethylene). *Macromolecules* **1996,** 29, (3), 973-977.

37. Sakaguchi, M.; Shimada, S.; Kashiwabara, H., Mechanoions produced by mechanical fracture of solid polymer .6. A generation mechanism of triboelectricity due to the reaction of mechanoradicals with mechanoanions on the friction surface. *Macromolecules* **1990,** 23, (23), 5038-5040.

38. Sohma, J., Mechanochemistry of polymers. *Progress in Polymer Science* **1989,** 14, (4), 451-596.

39. Downard, A. J.; Panther, J.; Kim, Y. C.; Powell, K. J., Lability of metal ion-fulvic acid complexes as probed by FIA and DGT: A comparative study. *Analytica Chimica Acta* **2003,** 499, (1-2), 17-28.

40. Benkhedda, K.; Infante, H. G.; Ivanova, E.; Adams, F. C., Trace metal analysis of natural waters and biological samples by axial inductively coupled plasma time of flight mass spectrometry (ICP-TOFMS) with flow injection on-line adsorption preconcentration using a knotted reactor. *Journal of Analytical Atomic Spectrometry* **2000,** 15, (10), 1349-1356.

41. Anthemidis, A. N.; Zachariadis, G. A.; Stratis, J. A., On-line solid phase extraction system using PTFE packed column for the flame atomic absorption spectrometric determination of copper in water samples. *Talanta* **2001,** 54, (5), 935-942.

42. Wang, J. H.; Hansen, E. H., Coupling sequential injection on-line preconcentration using PTFE beads packed column to direct injection nebulization inductively coupled plasma mass spectrometry. *Journal of Analytical Atomic Spectrometry* **2002,** 17, (10), 1278-1283.

43. McDonald, S.; Bishop, A. G.; Prenzler, P. D.; Robards, K., Analytical chemistry of freshwater humic substances. *Analytica Chimica Acta* **2004,** 527, (2), 105-124.

44. Tatar, E.; Csintalan, E.; Mihucz, V. G.; Tompa, K.; Poppl, L.; Zaray, G., Determination of fulvic acids in water samples of Hungarian caverns. *Microchemical Journal* **2002,** 73, (1-2), 11-18.

45. Aiken, G. R.; Thurman, E. M.; Malcolm, R. L.; Walton, H. F., Comparison of XAD macroporous resins for the concentration of fulvic-acid from aqueous-solution. *Analytical Chemistry* **1979,** 51, (11), 1799-1803.

46. Chan, G. C. Y.; Chan, W. T., Determination of lead in a chloride matrix by atomic absorption spectrometry using electrothermal vaporization and capacitively coupled plasma atomization. *Journal of Analytical Atomic Spectrometry* **1998,** 13, (3), 209-214.

47. Cabon, J. Y.; LeBihan, A., Interference of salts on the determination of lead by electrothermal atomic absorption spectrometry. Ion chromatographic study. *Spectrochimica Acta Part B-Atomic Spectroscopy* **1996,** 51, (6), 619-631.

48. Chaudhry, M. M.; Littlejohn, D., Ion chromatographic study of the effect of ammonium-nitrate as a modifier in electrothermal atomic-absorption spectrometry. *Analyst* **1992,** 117, (4), 713-715.

49. Garbett, K.; Goodfellow, G. I.; Marshall, G. B., The application of atomic-absorption spectrometry in the analysis of metallic sodium .1. Volatilization characteristics of sodium-salts during electrothermal atomization. *Analytica Chimica Acta* **1981,** 126, 135-145.

50. Jimenez, M. S.; Velarte, R.; Castillo, J. R., Performance of different preconcentration columns used in sequential injection analysis and inductively coupled plasma-mass spectrometry for multielemental determination in seawater. *Spectrochimica Acta Part B-Atomic Spectroscopy* **2002,** 57, (3), 391-402.

51. Willie, S. N.; Lam, J. W. H.; Yang, L.; Tao, G., On-line removal of Ca, Na and Mg from iminodiacetate resin for the determination of trace elements in seawater and fish otoliths by flow injection ICP-MS. *Analytica Chimica Acta* **2001,** 447, (1-2), 143-152.

52. Vassileva, E.; Furuta, N., Application of iminodiacetate chelating resin Muromac A-1 in on-line preconcentration and inductively coupled plasma optical emission spectroscopy determination of trace elements in natural waters. *Spectrochimica Acta Part B-Atomic Spectroscopy* **2003,** 58, (8), 1541-1552.

53. Kingston, H. M.; Barnes, I. L.; Brady, T. J.; Rains, T. C.; Champ, M. A., Separation of 8 transition-elements from alkali and alkaline-earth elements in estuarine and seawater with chelating resin and their determination by graphite furnace atomic-absorption spectrometry. *Analytical Chemistry* **1978,** 50, (14), 2064-2070.

54. Tsakovski, S.; Benkhedda, K.; Ivanova, E.; Adams, F. C., Comparative study of 8-hydroxyquinoline derivatives as chelating reagents for flow-injection preconcentration of cobalt in a knotted reactor. *Analytica Chimica Acta* **2002,** 453, (1), 143-154.

Chapter 9

Conclusions and future work

This thesis examined aspects of environmental speciation using adsorbent-based techniques. The primary objectives of this thesis were to:

i) Investigate the use of DGT to measure total inorganic As.
ii) Develop the DGT method for selective As accumulation and hence inorganic As speciation.
iii) Investigate the use of ETAAS with a coupled microcolumn for kinetic speciation measurements.

9.1 DGT for total As determination

This objective was concerned with investigation of the DGT method for total inorganic As determinations (As^{V} + As^{III}). This objective involved the measurement of As^{V} and As^{III} diffusion coefficients through polyacrylamide gels and membrane filters, and examining a number of factors which may affect the use of DGT for total As measurements in a natural water. These factors included: capacity of the iron-oxide adsorbent, competition between As^{III} and As^{V} for adsorption sites on the iron-oxide adsorbent, and the effects that pH, anions and cations, fulvic acid, and colloidal Fe^{III} have on the uptake and/or diffusion of the individual As species.

9.1.1 Experimental findings

9.1.1.1 Measurement of As^{V} and As^{III} diffusion coefficients

The As^{V} and As^{III} diffusion coefficients through a polyacrylamide gel and membrane filter were measured using both a diffusion cell and DGT devices. Good agreement between the two methods was obtained. For As^{V}, the average diffusion coefficients measured using a diffusion cell and DGT devices were (4.85 ± 0.35) x 10^{-6} cm^2 s^{-1} and (4.90 ± 0.05) x 10^{-6} cm^2 s^{-1} at pH 5.0, respectively. For As^{III}, the average diffusion coefficients measured using a

diffusion cell and DGT devices were (6.40 ± 0.30) x 10^{-6} cm^2 s^{-1} and (5.95 ± 0.30) x 10^{-6} cm^2 s^{-1} at pH 5.0, respectively.

It was shown that the membrane filter (0.025 μm pore size) did not significantly affect the As^{III} diffusion coefficient. Further, the As^{V} diffusion coefficient was not affected by membrane type (Schleicher & Schuell *vs.* Millipore), membrane pore size (0.025 μm *vs.* 0.45 μm) or membrane pre-treatment (acid washed *vs*. non-acid washed).

The similar values for the As^{V} and As^{III} diffusion coefficients enables the average As diffusion coefficient (i.e. $(D_{As(V)} + D_{As(III)})/2$) to be used when calculating the total As concentration using the DGT equation, if the total As concentration is measured directly using the non-Nafion DGT device. .

9.1.1.2 Capacity of iron-oxide adsorbent and competition between As^{V} and As^{III} for adsorption sites

The total capacity of the iron-oxide adsorbent in the DGT device was determined to be ~ 100,000 ng of As; however the linear uptake range in which the DGT theory holds was ≤ 30,000 ng of As. This means that DGT can be deployed in a water containing 10 ppb As for ~ 6 months before the capacity of the adsorbent would be exceeded. However, deployment times of this length would be affected by competition from other adsorbing species in a natural water and biofouling of the DGT device.

There was no evidence that the uptake of As^{V} by the DGT adsorbent was affected by the presence of As^{III}, and vice versa.

9.1.1.3 Effects of pH, anions, cations and fulvic acid on DGT measurements

Over the pH range 3 to 7, pH had no significant influence on the As^{III} or As^{V} diffusion coefficients and did not significantly affect the uptake of As^{III} or As^{V} by the iron-oxide adsorbent. In addition, anions and cations present at concentrations typical of those expected in fresh water, showed no significant effect on the measurement of As^{V} or As^{III} concentrations using DGT at pH 5.0. Furthermore, As measurements were unaffected by the presence of 5 ppm fulvic acid. There was also no evidence of complexation between As^{V} and

Fe^{III}-fulvic acid species, an interaction that would significantly slow the diffusion of the As^{V} species to the iron-oxide adsorbent.

9.1.1.4 Effect of colloidal Fe^{III} and fulvic acid on DGT measurements

The presence of colloidal Fe^{III} in solution significantly reduced the concentration of dissolved As measured by DGT, indicating that the colloidal fraction of As is not available to be measured by the DGT technique. Reasonable agreement was obtained between the concentration of As measured by DGT and that measured by HG-AAS after filtration; however there was evidence to suggest that the dissolved concentration determined by HG-AAS may be underestimated due to adsorption losses during the filtration step. In addition, the presence of fulvic acid affected the adsorption of As onto colloidal Fe^{III} in solution due to competition for adsorption sites.

9.1.2 Utility of DGT for total As determinations

Collectively, the results above suggest that the DGT method for total As determinations should be able to be used in a straight-forward manner in a variety of environmental situations and conditions. However, some care should be taken when using this method as concentrations of phosphate, anions, cations, and fulvic acid, higher than those examined in this thesis, may affect the DGT measurement.

The in-situ capabilities of DGT are its greatest advantage for measuring total dissolved As concentrations as the distribution of As between the colloidal and dissolved phase may change considerably if a sample is collected and returned to the laboratory for analysis. In addition, many of the other methods described in this thesis for determining total As require reagents to be added prior to measurement; this may further comprise the distribution of As between the dissolved and colloidal phase. The preconcentration abilities of DGT will also be an advantage when measuring low concentrations of As, furthermore, the time-averaged capabilities would be useful in certain situations.

When the DGT technique is used directly to measure the total dissolved As concentration using the average As diffusion coefficient, accurate results to within 10 % should be obtained at all $[As^{V}]/[As^{III}]$ ratios.

9.2 DGT for inorganic As speciation

This objective was concerned with the development of a DGT device to selectively accumulate the As^{III} inorganic species in the presence of As^{V}. This was achieved by placing a negatively charged Nafion membrane at the front of the DGT device to repel the negatively charged As^{V} species ($H_2AsO_4^-$). This objective involved the measurement of As^{III} and As^{V} diffusion coefficients through the Nafion membrane, and the effects that pH, anions, and cations have on the diffusion of the individual As species. Lastly, DGT was applied to natural waters in the laboratory to determine total As, As^{III} and As^{V} concentrations.

9.2.1 Experimental findings

9.2.1.1 Measurement of As^{III} and As^{V} diffusion coefficients through Nafion

The As^{III} and As^{V} diffusion coefficients through the Nafion membrane were measured using both a diffusion cell and DGT devices that were specifically modified to accommodate the thin Nafion membrane. Good agreement between the two methods was obtained. For As^{III}, the average diffusion coefficients measured using a diffusion cell and DGT devices were $(2.65 \pm 0.05) \times 10^{-7}$ cm^2 s^{-1} and $(2.30 \pm 0.15) \times 10^{-7}$ cm^2 s^{-1} at pH 5.0, respectively. For As^{V}, the average diffusion coefficients measured using a diffusion cell and DGT devices were $(4.25 \pm 0.45) \times 10^{-9}$ cm^2 s^{-1} and $(3.85 \pm 0.10) \times 10^{-9}$ cm^2 s^{-1} at pH 5.0, respectively.

The diffusion coefficient of As^{III} is ~ 60 times larger than the diffusion coefficient of As^{V} through the Nafion membrane. This 60 times difference in diffusion coefficients limits the use of the Nafion DGT device for direct inorganic As speciation to $[As^{V}]/[As^{III}]$ ratios ≤ 10. At an $[As^{V}]/[As^{III}]$ ratio of 10, the concentration of As^{III} determined would be overestimated by ~ 17 %. Ratios > 10 would significantly affect the accuracy of the As^{III} measurement. However, as indicated in chapter 7, using both the Nafion and non-Nafion DGT devices concurrently allows accurate measurement of the As^{III} concentration by solving equations 7.1 and 7.2 simultaneously.

9.2.1.2 Effect of pH and cations on the selective accumulation of As^{III} by DGT with a Nafion membrane

It was shown that in the pH range 3 to 7, pH did not significantly affect the diffusion coefficient of As^{III} through the Nafion membrane. However, at pH 3 the diffusion coefficient of As^{V} through the Nafion membrane was significantly increased (relative to pH 5); this was

due to significant amounts of the uncharged H_3AsO_4 species which has a similar diffusion coefficient to H_3AsO_3. Calculations showed that at pH 4.0 for an $[As^V]/[As^{III}]$ ratio of 10, the concentration of As^{III} determined by DGT would be overestimated by ~ 37 % due to H_3AsO_4 present. This would limit the use of the DGT Nafion method to waters above pH 4.0 when using the direct approach to measure As^{III}; therefore it is unlikely that this method could be used to monitor As^{III} concentrations in natural waters affected by acid mine drainage. However, the simultaneous equation DGT approach could be used in theory to calculate the As^{III} concentration at low pH as long as the diffusion coefficients through the Nafion membrane were established.

The presence of cations and anions in solution at concentrations typical of a freshwater had no significant effect on the diffusion of As^{III} through the Nafion membrane at pH 5.0. In contrast, the As^V diffusion coefficient through the Nafion membrane increased by ~ 25 %. This effect was presumably due to cations such as Ca^{2+} and Mg^{2+} associating with the negatively charged sulfonate groups of the Nafion membrane. This would have the effect of shielding the negatively charged As^V species from the negatively charged sulfonate groups and hence increasing the As^V diffusion coefficient. Alternatively, complexation of $H_2AsO_4^-$ by Ca^{2+} and Mg^{2+} may also be occurring which may increase the diffusion coefficient of the As^V species; the effect of complexation increases with pH and therefore this method may be limited at high pH if complexation of the As^V species is significant.

9.2.1.3 Application of DGT to natural waters

DGT was used to determine total As, As^{III} and As^V in two well waters and in a river water that was spiked with two $[As^V]/[As^{III}]$ ratios. Both the simultaneous equation DGT approach and the direct DGT approach were used.

For the two spiked river water samples, good agreement was obtained for the As^{III} and total As concentration measured by both DGT approaches, and the concentration of total As and As^{III} measured by HG-AAS, after filtration. The river water samples were at pH 5.0.

For one well water sample, good agreement was obtained between the total As concentration measured by both DGT approaches and that measured by HG-AAS after filtration. For the other well water sample, the concentration of total As measured by DGT was lower than that measured by HG-AAS. This well water sample showed evidence of colloidal Fe^{III} that had coagulated during storage. It is possible that there was some As adsorbed to fine Fe^{III} colloids

(that passed through the filter) that was not measured by the DGT technique but was measured by HG-AAS. This highlights the advantage of an in-situ technique compared to a method that requires sampling, as it is not always straight forward to maintain the integrity of the sample.

For both well water samples, the concentration of As^{III} measured by both DGT approaches was significantly higher than that measured by HG-AAS. For the well water samples the Ca^{2+} and Mg^{2+} concentrations were 2.0 to 3.5 times higher than that used to prepare synthetic solutions in this thesis, and the pH of the well water samples were > 7 which leads to greater complexation of the As^{V} species by Ca^{2+}. This may have the effect of significantly increasing the As^{V} diffusion coefficient through the Nafion membrane.

9.2.2 Utility of the Nafion DGT method for As speciation and future work

The in-situ, preconcentration, and time-averaged capabilities of DGT offer advantages over other speciation methods currently employed for As. However, when using the direct DGT approach to measure the As^{III} concentration in solution, the usefulness of this method is limited by the $[As^{V}]/[As^{III}]$ ratio, low pH, and the effect that cations such as Ca^{2+} and Mg^{2+} may have on the As^{V} diffusion coefficient. The reason for the overestimation of the As^{III} concentration for the two well waters needs to be investigated further.

It is important to note that if the As^{V} solutions that were used to measure the As^{V} diffusion coefficients through the Nafion membrane contained 1 % As^{III}, this would result in the diffusion coefficient of As^{V} being overestimated by ~ 40 %. Future work may investigate the possibility of adding an oxidizing agent to the As^{V} solution prior to determining the As^{V} diffusion coefficient to convert any As^{III} present to As^{V}.

More work should be carried out with varying concentrations of Ca^{2+} and Mg^{2+}, and a range of pH to examine the effect that complexation of As^{V} has on the As^{V} diffusion coefficient through the Nafion membrane. This would enable the feasibility of the DGT Nafion method to be evaluated for use at high pH.

Additional future work may involve examining the use alternative Nafion membranes. There may be some advantage in using a Nafion membrane with a lower equivalent weight. Lower

equivalent weight Nafion membranes may provide better differentiation between the As^{III} and As^{V} diffusion coefficients than the 60 times difference obtained with a Nafion 112 membrane, which has an equivalent weight of 1100. The equivalent weight is the number of grams of dry Nafion per mol of sulfonic acid groups when the Nafion is in the acid form. A difference of greater than 60 for the As^{III} and As^{V} diffusion coefficients would enable more accurate As^{III} measurements for waters containing $[As^{V}]/[As^{III}]$ ratios > 10. Future work may involve the measurement of As^{III} and As^{V} diffusion coefficients through Nafion membranes of different equivalents weights. Furthermore, various pre-treatments of the Nafion membrane may also affect the As diffusion coefficients, and this could be an avenue for future work.

9.3 ETAAS with a coupled microcolumn

This objective was concerned with the preliminary investigation of a system that consisted of a Chelex-100 microcolumn coupled with the ETAAS instrument for kinetic speciation of metal complexes. This objective involved the investigation of the following issues: Cu adsorption to the microcolumn materials, the background absorbance associated with the use of sodium acetate to buffer the Chelex-100 resin, and uptake of Cd^{2+} by the Chelex-100 microcolumn.

9.3.1 Experimental findings

9.3.1.1 Adsorption of Cu^{II} to microcolumn materials

It was established that Cu^{2+} adsorbed to the surface of both Teflon and polycarbonate microcolumns at pH 5.0. The amount of Cu^{2+} adsorbing to the Teflon microcolumn, from 30 µL of a 10 ppb Cu^{2+} solution, was 28 ± 1 %; for the polycarbonate microcolumn, 31 ± 2 % of Cu^{2+} was adsorbed. The origin of this adsorption was believed to be due to interaction of Cu^{2+} with radicals on the microcolumn surface, which had formed during construction (machining) of the microcolumn.

It was also shown that Cu^{II} adsorbed to the surface of the Teflon and polycarbonate microcolumns in the presence of relatively high concentrations of fulvic acid at pH 5.0. The amount of Cu^{II} adsorbing to the Teflon microcolumn, from 30 µL of a Cu-fulvic acid solution (10 ppb Cu^{II} and 20 ppm fulvic acid), was 26 ± 1 %; for the polycarbonate microcolumn, 34 ± 4 % of Cu^{II} was adsorbed. This adsorption was attributed to a hydrophobic interaction between the fulvic acid and the hydrophobic microcolumn surface.

9.3.1.2 Background absorbance associated with the use of sodium acetate to buffer the Chelex-100 resin

When the Chelex-100 microcolumn was buffered with 0.05 mol L^{-1} sodium acetate (pH 5.0) and eluted with HNO_3 a large background absorbance was obtained. This background was due to the presence of $NaNO_3$ which was formed when Na^+ that was coordinated to the Chelex-100 resin was displaced by $H^+(NO_3^-)$. The presence of $NaNO_3$ significantly affected Cd sensitivity. The problem associated with the background was overcome by using 0.05 mol L^{-1} ammonium acetate (pH 5.0) to buffer the Chelex-100 microcolumn instead of sodium acetate; eluted ammonium acetate showed no significant background in ETAAS.

9.3.1.3 Uptake of Cd^{2+} by Chelex-100 microcolumn

The average uptake efficiency of Cd^{2+} by the Chelex-100 microcolumn was 94 ± 2 % which was in good agreement with the uptake efficiency that was calculated using the SPECIES computer program (96 %). It was established that washing the Chelex-100 resin with Milli-Q water after buffering with ammonium acetate was critical in maintaining high uptake efficiencies of Cd^{2+}. Furthermore, the highest uptake efficiencies were obtained at low ammonium acetate and NH_4NO_3 concentrations in the Cd^{2+} solution. Elution of Cd from the Chelex-100 microcolumn was > 98 % when using 1 mol L^{-1} HNO_3.

9.3.2 Utility of ETAAS with a coupled microcolumn for trace metal speciation and future work

This study was only a preliminary investigation of the use of ETAAS with a coupled microcolumn for trace metal speciation; therefore there is a lot more work that could be carried out to refine this method. A major problem with this current method is the potential adsorption of fulvic acid complexes to the column material. The adsorption of fulvic acid complexes would lead to an underestimation of the inert fraction whilst the labile fraction would be overestimated. Therefore this method would be severely limited when applied to humic waters (which had been an objective of this work). Future work may involve a survey of polymeric materials to identify one that is suitable for applications to humic solutions.

Parameters such as the buffering and washing time of the Chelex-100 microcolumn should be optimized. The 3 min buffering and 3 min washing time of the Chelex-100 microcolumn

utilized in this work were arbitrarily chosen. A reduced washing and buffering time would decrease the measurement time per sample and would also conserve high purity reagents. In addition, decreasing the flow of reagents across the microcolumn would reduce the problems that are generally associated with the use of the Chelex-100 resin such as the compaction of resin to one end of the microcolumn which causes back-pressure and flow problems in the system. The buffering step and washing step may even be able to be carried out using the autosampler system in which the autosampler would pick up an aliquot of buffer and pass it across the Chelex-100 microcolumn followed by an aliquot of water. This would make the system less complex and there would be no need for the peristaltic pump or the 3-way valve which can cause back-pressure in the manifold.

The method should be validated by using a Cd-EDTA system in which a complexation capacity experiment could be carried out and compared with another technique which has a similar timescale, such as flow injection analysis using a microcolumn of adsorbent.

It would also be advantageous for the system to be automated so that all required solutions may be placed in Teflon cups within the autosampler tray of the ETAAS and therefore manual manipulation of the solutions would not be required.